SYSTEMS EVALUATION OF EROSION AND EROSION CONTROL IN A TROPICAL WATERSHED

By

MATTHEW J. COHEN

A DISSERTATION PRESENTED TO THE GRADUATE SCHOOL
OF THE UNIVERSITY OF FLORIDA IN PARTIAL FULFILLMENT
OF THE REQUIREMENTS FOR THE DEGREE OF
DOCTOR OF PHILOSOPHY

UNIVERSITY OF FLORIDA

2003

UMI Number: 3105599

UMI®

UMI Microform 3105599

Copyright 2003 by ProQuest Information and Learning Company.

All rights reserved. This microform edition is protected against unauthorized copying under Title 17, United States Code.

ProQuest Information and Learning Company
300 North Zeeb Road
P.O. Box 1346
Ann Arbor, MI 48106-1346

ACKNOWLEDGMENTS

I am deeply grateful to Dr. Mark Brown for his intellectual and financial support, insight and goodwill. He, along with Dr. Keith Shepherd of ICRAF Kenya, made 10 months of work in Kenya possible. Dr. Shepherd provided extraordinary intellectual and logistical guidance during my time there. Dr. Michael Binford has been a mentor and sounding board for many of the ideas contained herein. Dr. William Wise and Dr. Thomas Crisman graciously filled vacated seats, offering insightful comments despite being unfamiliar with the work. Dr. H.T. Odum originally sat on this committee, but passed away in September 2002. His influence was felt throughout and he remains a source of profound and deeply practical inspiration. I received tremendous input from Dr. Markus Walsh, also at ICRAF, whose own sense of systems science defines the cutting edge. Alex Awiti, Luka Anjeho, Isaac Learamo and a superior field crew made sampling fun and enlightening. Elvis Weullow processed all soil spectra for this work. I am deeply indebted to students at the H.T. Odum Center for Wetlands. Eliana Bardi graciously handled innumerable bureaucratic loose ends while I was in Kenya. I must thank my parents, Jan and Neal Cohen, for their encouragement at the start of this process, and their impatient admonitions at the end. Finally, Leah, my wife and best friend kept this process in perspective for me. She and Safi remain my foundation.

TABLE OF CONTENTS

page

ACKNOWLEDGMENTS ii

LIST OF TABLES ix

LIST OF FIGURES xiv

ABSTRACT xviii

INTRODUCTION 1

Statement of the Problem 1
Review of Literature 3
Soil Loss Globally and Regionally 3
Soil Erosion Models 4
Soil Erosion Costs 7
Watershed Scale Erosion Assessment 8
Watershed Rapid Assessment 10
Diffuse reflectance spectroscopy for soil quality assessment 10
Satellite image processing for spatial erosion risk assessment 12
Landuse Change Models 13
Systems Evaluation 14
Emergy and transformity 15
Energy systems diagrams 17
Description of the Study Site 17
Plan of Study 19

METHODS 22

Emergy Analysis at National, District and Subsystem Scales 22
Emergy Evaluation Protocols 23
Emergy Evaluation Summary Indices 23
Flow aggregation 23
Emergy:money ratio 24
Environmental loading, investment and yield ratios 24
New summary indices 26
National Scale Analysis 27
Data sources 27
Product transformity values 28

Estimates of soil erosion and forest clearing rates 29
District Analysis 31
Data sources 31
Soil loss estimation 32
Awach Basin Landuse Subsystem Analysis 33
Data sources 33
Soil loss estimation 34
Erosion Risk Assessment 34
Quantification of Soil Degradation Factors 36
Field Sampling Protocol 36
Sampling period and sample size 37
Case-control sampling design and additional stratification 37
Spatial site distribution 38
Site protocol 38
Visual degradation classification 40
Soil Sampling 40
Diffuse Reflectance Spectroscopy (DRS) for Rapid Soil Assessment 41
Spectral reflectance signatures 41
Data processing 42
Soil spectral library 42
Spectral outlier analysis 43
Spectral visualization 44
Classification and regression trees (CART) 44
Case-reference definition 47
Soil degradation effects 48
Rainfall Erosivity and Infiltration Methods 48
Rainfall erosivity 49
Infiltration field protocol 49
Data processing 51
Model fitting 51
Spectral reflectance modeling 52
Infiltration transfer function 52
Surface Deflation Estimation 53
Erosion pin sampling 53
Mixed-effects data processing 53
Odds Ratio Analysis of Landuse Degradation and Infiltration 54
Terrain Analysis 55
Digital elevation model development 55
Terrain-based indices 56
Soil Degradation Modeling 56
Standard and Mixed Effects Logistic Regression 57
Graphical Modeling 58
Site Level Risk Factors (SITE) 59

Soil Erodibility Risk Factors 59
Prospective analysis assumption 60
Standard USLE soil erodibility nomograph 60
Local erodibility (SOIL) 61
Hydrologic and Terrain Risk Factors (HYDRO/TERRAIN) 62
Hydrologic variables 62
Terrain variables 63
Model development 63
Overall Risk Model Development 63
Spatial Inventory and Decision Support Modeling 64
Satellite Image Analysis 64
Satellite image acquisition and pre-processing 65
Data extraction 66
Image classifier algorithms 66
Spatial Inventory 67
Change Detection 1986-2001 68
Spatial Model Development 68
Spatial erosion risk inference 69
Landuse scenario development 72
Emergy yield functions 74
Optimality Criteria and Scenario Comparison 74

EMERGY ANALYSES 76

National Emergy Analysis 76
Systems Diagram 76
Spatial Surfaces of Renewable Energy Flows 77
National Emergy Table 79
Emergy Spectra 83
Flow Aggregation 84
Summary Diagram 84
Overview Indices 86
District Emergy Evaluations 87
Systems Diagrams 88
Spatial Surfaces and Data Sources 88
Evaluation Tables and Summary Indices 91
Emergy Spectra 91
Awach Subsystems Analysis 93
Subsistence Agriculture 94
Systems diagrams 94
Emergy table 96
Commercial Agriculture 96
Systems diagrams 96
Emergy tables 98

Livestock Production – Communal and Constrained Systems....99
Systems diagram....100
Emergy table....100
Managed Forest Production....102
Systems diagram....104
Emergy table....104
Communal Unmanaged Forests....105
Systems diagram....106
Emergy table....107
Comparative Summary Indices....108

SOIL EROSION RISK FACTORS....110

Field Sample Sites....110
Digital Elevation Model (DEM) and Terrain Analysis....112
Development of a DEM....112
Terrain Analysis....113
Spectral Analysis....115
Data Visualization and Compression....115
Principal components analysis....115
Outlier analysis....118
Spectral end-member visualization....120
Multivariate Soil Property Models From Reflectance Spectra....121
Definition of Case and Reference Soils....126
Awach Basin Soils Assessment....129
Soil Property Estimation....129
Pairwise Analysis of Degradation Risk....132
Infiltration Data Processing and Assessment....135
Data Sampling....135
Model Fitting....136
Mean Saturated Infiltration Rates....139
Spectral Screening Model....140
Infiltration Transfer Function....142
Pairwise Analysis of Slow Infiltration....143
Soil Surface Deflation Estimation....146
Site Sampling....146
Mixed-Effects Model Results....146
Mixed-effects for deflation by degradation status....146
Mixed-effects for deflation by landuse....147

EROSION RISK MODELS....150

Defining Multivariate Risk Factors....150

Soil Erodibility....151
Soil Erodibility Nomograph....152
Prospective Study Assumption....153
Empirical Soil Erodibility Factor Development....155
Graphical modeling to identify conditional association structure....155
Logistic mixed-effects model development....156
Vegetation, Landuse and Site Characteristics....157
Vegetation Cover....157
Landuse....158
Empirical Site Factor Development....158
Graphical modeling to identify conditional association structure....158
Logistic mixed-effects model development....160
Hydrologic and Terrain Characteristics....161
Terrain Variables....161
Hydrologic Variables....162
Empirical Hydro/Terrain Factor Development....163
Graphical modeling to identify conditional association structure....163
Logistic mixed-effects model development....163
Logistic Regression Model Fit Charts....165
Integrated Risk Model....165
Surface Deflation and Risk Prediction....167

SPATIAL INVENTORY AND RISK ASSESSMENT....169

Spatial Inventory....169
Satellite Image Processing....169
Erosion prevalence assessment....170
Reduced infiltration capacity prevalence assessment....173
Land Cover Classification....175
Land Cover Change....178
Markov Transition Matrix Development....183
Spatial Risk Assessment....184
Hydro/Terrain Factor Interpolation....184
Soil Erodibility Factor Interpolation....185
Site Management Factor Interpolation....188
Overall Risk Model....189
Future Landuse Change Assessment....191
Scenario Assessment Framework....192
Landuse Change Scenarios....194
Change in proportional landuse allocation....194
Spatially targeted landuse allocation....195
Scenario Landuse Proportions....196
Degradation Proportions....196
Watershed Scale Agricultural Benefit Ratio....198

DISCUSSION 200

Summary 200
Principal Conclusions of the Study 201
Discussion of Principal Conclusions 202
Emergy Costs of Soil Erosion 202
National emergy analysis 203
District emergy analysis 205
Awach landuse subsystems analysis 207
Field Protocols, Reflectance Spectra and Infiltration Testing 209
Field sampling protocol 209
Spectral reflectance methods 210
Infiltration assessment 213
Surface deflation estimation 215
Erosion Risk Modeling 215
Site risk factor 217
Soil erodibility risk factor 217
Hydro/terrain risk factor 219
Model suitability and generality 220
Spatial Inventory and Risk 222
Spatial inventory 222
Change detection 225
Spatial risk maps 226
Integrated Assessment of Future Landuse 227
Landuse change scenarios 228
Scenario comparison 230
Landuse recommendations 231
Suggestions for Further Research 232
Emergy Simulation Modeling for Yields and Uncertainty 232
Constrained Landuse Change Modeling 233
Tools to Support Participatory Decision Making 234

APPENDIX

A FOOTNOTES TO EMERGY EVALUATION TABLES 235

B SPECTRAL CALIBRATIONS MODELS 262

C RULE-BASES FOR SATELLITE IMAGE INTERPRETATION 268

LIST OF REFERENCES 280

BIOGRAPHICAL SKETCH 305

LIST OF TABLES

page

2-1 Soil loss rates by landuse for Kenya 31

3-1 Emergy evaluation of resource basis for Kenya (c.1999) 81

3-2 Aggregated emergy flows in Kenya (c.1999)....84

3-3 Summary emergy indices for Kenya (c.1999)....86

3-4 Comparison of Kenyan summary index values with other national economies 87

3-5 Comparison of national and district fuel and electricity use, GDP and population to infer commodity consumption for districts....90

3-6 Summary of annual flows in Kisumu, Kericho and Nyando Districts (c.2000) 91

3-7 Overview indices for district evaluations in comparison to national indices 92

3-8 Emergy evaluation of subsistence maize production in western Kenya 95

3-9 Emergy evaluation table of smallolder sugarcane production for western Kenya 98

3-10 Emergy evaluation table of smallholder tea production for western Kenya 99

3-11 Emergy evaluation table for communal (lowland) livestock production in western Kenya....102

3-12 Emergy evaluation table for constrained (highland) livestock production in western Kenya....103

3-13 Emergy evaluation for farm forest (woodlot) production in western Kenya 105

3-14 Emergy evaluation table for forest/shrubland production in western Kenya....107

3-15 Comparison of Agricultural Benefit Ratio and computed transformity for landuse subsystems for intact and degraded conditions....108

3-16 Summary indices for Kenya and three local districts for comparison with results from sub-systems evaluations....109

4-1 Field sample sites sorted by primary stratification factors (e.g. landuse, elevation/slope, degradation status). Total sampling effort was 420 sites.111

4-2 Extracted sediment transport capacity (Figure 4-4) for field sampling sites by observed erosion severity class 115

4-3 Spectral outliers from Awach Basin soil samples (n = 1260) with reference to principal components ordination of soil spectral library (n = 513). Bolded soils were 3 s.d.-level outliers 119

4-4 Model efficiency for predicting measured soil properties from spectral reflectance signatures 126

4-5 Binary classification efficiency for cross-validated tree models based on reflectance spectra. Screening thresholds are defined based on published soil functional levels (Brady and Weil 2001). 126

4-6 Case-reference definition summary. Given are model fit statistics between soil spectral reflectance and observed degradation 128

4-7 Summary of spectral predictions of degradation for soils at sites where visual designation was confounded 128

4-8 Summary statistics of soil properties by visual soil degradation class 131

4-9 Soil properties by landuse class and categorical degradation status 132

4-10 Correlation matrix for continuous soil properties to determine potential multi-colinearity effects 132

4-11 Summary of field sample sites for infiltration assessment by landuse and binary degradation status 136

4-12 Infiltration model fitting using a bounded quasi-Newton fitting algorithm 137

4-13 Summary of mean and standard deviation of base infiltration rates (mm/hr) organized by degradation status (observed/spectrally defined) and landuse 139

4-14 Nominal infiltration rates for western Kenya (after Wielemaker and Boxem 1982). 140

4-15 Results of screening model to discriminate between rapid and reduced infiltration capacity based on spectral reflectance information 141

4-16 Comparison of soil properties for infiltration classes. Category 1 is sites with saturated infiltration rates less than 60 mm/hr 142

4-17 Conditional association parameters between soil properties and binary soil infiltration from multiple logistic regression model 143

4-18 Summary of sites for which nail data were recovered, organized by landuse and binary degradation status 146

4-19 Summary of mixed effects model of soil deflation rates by spectral case and reference 147

4-20 Summary of mixed effects model of soil surface deflation 149

4-21 Annualized mean and maximum estimates of erosion rates (g/m^2) fitted from mixed effects model. 149

5-1 Summary of field, soil and derived variables assigned to each of three erosion risk components to define risk in the Awach River basin 151

5-2 Mean erodibility for each soil type, along with the proportion of each polygon that showed evidence of degradation (inferred from Figure 6-1a) 154

5-3 Tabular summary of mixed effects logistic regression for risk predicted by soil properties 156

5-4 Tabular summary of mixed effects logistic regression model for erosion risk predicted by soil properties 160

5-5 Nominal land cover parameters for each landuse 161

5-6 Tabular summary of mixed effects logistic regression model for erosion risk predicted by hydrologic and terrain factors 163

5-7 Tabular summary of mixed effects logistic regression model for erosion risk predicted by all composite risk factors 166

5-8 Range and standard deviation of risk factors 167

5-9 Summary of multiple linear regression model relating observed site-level mean deflation rates and erosion risk factors 167

6-1 Summary of classification tree model for calibration and validation accuracy for inference of degradation classes from satellite reflectance data 170

6-2 Cross-tabulation of categorical degradation surfaces between 1986 and 2001 and transition probabilities with change proportions 173

6-3 Classification tree model summary for a) calibration and b) validation accuracy for inference of binary infiltration classes from satellite reflectance data 174

6-4 Cross-tabulation proportions for binary infiltration and degradation maps.....174

6-5 Accuracy assessment for land cover classification tree models in a) calibration and b) cross-validation.....178

6-6 Cross-tabulation of landuse and binary degradation maps. Shown are cell-counts and proportions.....182

6-7 Landuse transition counts and probabilities for 8 classes between 1986 and 2001 in the Awach River basin.....182

6-8 Model results relating soil depth to slope, soil hardsetting and soil degradation 185

6-9 Stepwise deletion multiple regression model relating satellite reflectance data and erodibility values.....186

6-10 Model relating slope and binary depth restriction to site stone cover.....188

6-11 Back-casting (to 1986) accuracy of spatially interpolated overall risk versus direct satellite inference from 1986 imagery.....191

6-12 Agricultural Benefit Ratio (ABR) computed for each landuse for both intact and degraded soil conditions.....193

6-13 Comparison of degradation extent for 1986 and 2001 conditions and expected historic (pre-settlement) and future scenarios.....197

6-14 Comparison of two metrics (percent degraded and Agricultural Benefit Ratio) for each scenario.....199

A-1 Notes to the emergy evaluation of Kenya (Table 3-1).....236

A-2 Emergy evaluation of resource basis for Kisumu District, Kenya (c.2000).....241

A-3 Emergy evaluation of resource basis for Kericho District, Kenya (c.2000).....245

A-4 Emergy evaluation of resource basis for Nyando District, Kenya (c.2000).....249

A-5 Energy and material flows for Awach River basin subsystem evaluation. All analyses were performed for 1 hectare of production.....253

A-6 Transformity values and references for emergy analyses.....259

A-7 Summary of transformity assessment for Kenyan agricultural products.....261

A-8 Summary of dynamic simulation model to predict soil component transformities for tropical soils under two ecosystems.....261

B-1 Soil functional capacity thresholds for local interpretation of soil property observations (adapted from Shepherd and Walsh 2002) 263

B-2 Summary of functional properties for soils in the spectral library (n=513). Mean, 25^{th} and 75^{th} percentile are given 263

B-3 Root mean squared error (RMSE) by quartile for regression tree models in calibration and holdout validation 267

B-4 Summary of soil properties for Awach basin samples. For properties that were assessed using binary screening models proportions of cases are given.....267

LIST OF FIGURES

page

1-1 Typical DRS raw reflectance pattern for a tropical soil 12

1-2 Energy systems symbols with descriptions 16

1-3 Geographic location of the Awach River basin in western Kenya 19

2-1 Standardized economic systems diagram 24

2-2 Land-use map for Kenya ca. 2000 (ILRI 2002) 30

2-3 Site sampling protocol schematic 39

2-4 Conceptual flow chart of spatial model of erosion risk and watershed-scale net benefit indices 75

3-1 Energy systems diagram summarizing the Kenyan national economy and resource basis 78

3-2 Renewable energy surfaces for Kenya 80

3-3 Emergy spectra for Kenyan national economy 83

3-4 Aggregated economic systems diagrams for Kenya (1999) 85

3-5 Map of districts for which emergy evaluations were compiled. 88

3-6 Energy systems diagram depicting the Kisumu district economy 89

3-7 Energy systems diagram depicting the Nyando district economy 89

3-8 Energy systems diagram depicting the Kericho district economy 90

3-9 Empower spectra for district evaluations 93

3-10 Systems diagram of subsistence maize production in the Awach basin 94

3-11 Systems diagram depicting smallholder sugarcane and tea production systems within the Awach basin 97

3-12 Systems diagram depicting communal and constrained animal husbandry systems within the Awach basin 101

3-13 Systems diagram depicting farm forestry systems within the Awach basin. 104

3-14 Systems diagram depicting communal native forest and shrubland systems within the Awach basin 106

4-1 Geologic map of the Awach River basin with overlay of field sampling sites (from Corbett et al. 1997) 110

4-2 Digital elevation model of the Awach River basin showing elevation (in meters) and spatial locations of 420 field sampling sites 112

4-3 Elevation profile between the highlands (Point A in Figure 4-2) and the wetland terminus at Lake Victoria (Point A' in Figure 4-2) 113

4-4 Sediment transport capacity surface inferred from the DEM based on the algorithm proposed by Wilson and Gallant (1996) 114

4-5 Screeplot summarizing principal components analysis of spectral library 116

4-6 Biplot of principal components axes 1 and 2 for spectral library soils, soils from the Awach River basin, and wetland soils from the Awach river terminal wetland at Lake Victoria 118

4-7 Mean and end-member (± 2 s.d.) example raw reflectance spectra for first two principal components 120

4-8 Mean and end-member (± 2 s.d.) example derivative transformed spectra for first two principal components for four spectral regions with large evident spectral separability 122

4-9 Cross-validated regression tree developed for predicting soil organic carbon content of soil from reflectance spectra information 123

4-10 Chart depicting fit between predicted and observed soil organic matter content (in %) 125

4-11 Odds ratios for designation as spectral case conditioned on observed degradation category 129

4-12 Pairwise odds ratios for binary soil physical degradation 133

4-13 Pairwise odds ratios for binary soil physical degradation 134

4-14 Map showing the Awach basin, digitized stream network and location of infiltration assessment sample plots 136

4-15 Infiltration rate over time with three alternative model forms 138

4-16 Marginal odds ratios and 95% confidence intervals for reduced infiltration capacity by landuse types and land cover characteristics 144

4-17 Marginal odds ratios and 95% confidence intervals for reduced infiltration capacity by vegetation cover characteristics and soil physical degradation 145

5-1 Association between computed soil erodibility (from USLE nomograph) and observed grouped degradation probabilities 152

5-2 Soils map for the Awach River basin (after Kenya Soil Survey, 1977) 153

5-3 Correlation between mean erodibility for intact sites for a given soil type versus the proportion of that type that is degraded (using spatial data from Figure 6-1) 154

5-4 Graphical model showing conditional association structure for soil properties and erosion status 155

5-5 Graphical model showing conditional association structure for site properties and erosion status 159

5-6 Graphical model showing conditional association structure for hydrologic and terrain variables and erosion status 162

5-7 Model fit for three logistic regression models describing soil erosion factors 164

5-8 Multivariate regression model between mean site surface deflation observations and Site, Soil and Hydro risk factors 168

6-1 Thematic coverages of soil degradation inferred for the entire Awach River basin from satellite imagery 171

6-2 Degradation maps for inferred from 1986 Landsat imagery 172

6-3 Thematic coverage of binary infiltration classes (< 60 mm/hr and > 60 mm/hr) for the Awach River basin in 2001 175

6-4 Binary infiltration surface predicted for the Awach River basin in 1986 based on classification tree model 176

6-5 Land cover classification of the Awach basin 179

6-6 Land cover pattern inferred from 1986 Landsat imagery based on classification tree model developed for 2001 180

6-7 Changes in land cover proportions between 1986 and 2001 180

6-8 Classes of NDVI difference between 1986 and 2001 181

6-9 Predicted landuse condition for the Awach basin in 2016....183

6-10 Slope shape and slope maps for the Awach River basin as used in defining the hydro-terrain risk factor 184

6-11 Interpolated Hydro/Terrain risk score for the Awach River Basin 186

6-12 Multiple regression model fit between observed and predicted erodibility scores based on satellite reflectance data....187

6-13 Interpolated soil erodibility scores based on satellite reflectance data for 2001..187

6-14 Site management factor degradation score for landuse in 2001 189

6-15 Overall degradation probability map for the Awach River basin in 2001 190

6-16 Inherent risk scores for the Awach Basin 191

6-17 Flow chart of the spatial model as implemented....193

6-18 Distribution of inherent risk scores. Risk classes were designated with centroids at –1.5, -0.5, 0.5, 1.5, 2.5 and 3.5....194

6-19 Example of the effect of risk class (Figure 5-17) on conditional transition probabilities between land uses 195

6-20 Percent change in landuse proportions in 2016 under 5 development scenarios in comparison with landuse proportions under Scerario 1....195

7-1 Schematic depiction of spectral confounding due to within-category variance as it affects linear discriminatory methods....224

B-1 Regression fits between predicted and observed soil performance criteria based on regression tree models from reflectance spectra....264

B-2 Regression fits between predicted and observed soil performance criteria based on regression tree models from reflectance spectra....265

B-3 Regression fits between predicted and observed soil performance based on regression tree models from reflectance spectra 266

Abstract of Dissertation Presented to the Graduate School
of the University of Florida in Partial Fulfillment of the
Requirements for the Degree of Doctor of Philosophy

SYSTEMS EVALUATION OF EROSION AND EROSION CONTROL IN A TROPICAL WATERSHED

By

Matthew J. Cohen

August, 2003

Chair: Mark T. Brown
Department: Environmental Engineering Sciences

Soil erosion represents a significant, often hidden cost of land conversion to human use. It is particularly acute in sub-Saharan Africa, where long-term dependence on soil functional capacity is profound and intervention resources are scarce. This dissertation explores soil erosion, focusing on densely populated regions of western Kenya, in two complimentary ways. First, emergy evaluation, which allows comparison of ecological and economic flows in common units, quantified erosion severity at three scales (national, district and landuse subsystem). Second, probabilistic erosion risk models were calibrated based on empirical observations across the Awach River basin.

Emergy analysis revealed that over 4% of national emergy use is lost topsoil; soil loss severity increases at the district (2.4 to 14.2%) and landuse subsystem scale (14 – 76%). Agricultural benefit (agricultural yields given natural capital costs) ranges from a high 7.6 nationally to 2.25 for Nyando District; landuses ranged between 7.4 and 1.32.

Field observation of potential soil erosion predictors was undertaken at 420 sites distributed throughout the study basin. Tree-based regression models allowed inference of soil properties from visual/near infrared reflectance spectra based on an existing library of laboratory-analyzed samples. Properties successfully delineated included degradation status, infiltration class (<60 mm/h) and 13 soil performance measures.

Erosion risk was conceptually divided into three factors – site protection, detachment resistance and hydrologic/terrain risk – to which observed variables were assigned. Graphical models selected variables conditionally associated with degradation, and multivariate logistic regression quantified effect strength and direction. Resulting models correctly classified 73, 74 and 76% of sites, respectively; an integrated risk model increased accuracy to 84%. The most significant predictors of risk were infiltration class, ground cover and soil organic carbon content.

Satellite imagery facilitated spatial inventory of degradation, infiltration and land use. Over 46% of the basin was classified as degraded (27% severely) by a screening model with 86% accuracy. Infiltration class was classified with 82% accuracy; land use (8 classes) with 73% accuracy. Landuse change trajectories were inferred by comparing a 1986 scene with a 2001 scene. Markov models, both spatially indiscriminate and risk-weighted, were developed to compare landuse change scenarios for erosion attenuation and emergy-based agricultural benefit. Results suggest limited protective effect of moderate changes in landuse change patterns; cattle density reduction and reforestation appear most promising. Extreme changes in landuse were observed to restore the basin, but were highly unrealistic. Spatially targeting low risk landuses to high-risk sites provided small but significant improvement.

INTRODUCTION

Statement of the Problem

Soil is functionally a nonrenewable resource. While soil development occurs over centuries, the world's growing population is actively depleting the resource over decades. As a nonrenewable resource, and the basis for 97% of all food production (Pimentel 1993), strategies to protect soil from depletion at rates faster than replacement are critical for developing sustainable economies.

Concern over soil erosion by water, the primary mechanism for soil degradation on arable land, has existed worldwide for decades (Sanchez 1973, Kirkby 1980, Pimentel 1993, Morgan 1995). While the problem has been documented on every continent, the consequences are especially acute in the semi-humid and humid tropics where poverty, fragile soils, high population densities and intense climatic inputs converge, as is the case in much of sub-Saharan Africa (Lal, 1985). Soil loss has ecological and economic impacts at many scales, ranging from the field scale, where nutrient depletion, degraded soil structure and lost organic matter affect farm livelihoods, to the watershed and national scale, where sediment and nutrient loads adversely affect important waterways and ecosystems (Morgan, 1995). Several studies (Smaling 1993, Sanchez et al. 1997) have documented the crucial role that erosion plays in soil functional degradation throughout sub-Saharan Africa at these varied scales.

Resource allocations to soil conservation strategies by international agencies and national governments have been substantial (Kiome and Stocking 1995, Thompson and

Pretty 1996). However, it must be recognized that allocating resources to attenuate soil losses requires diversion of resources from other sectors of the economy. To what extent is resource diversion justified, and can the magnitude of the problem be quantified to quantify the appropriate degree of diversion? There are cases where local success in controlling and reversing the pattern of soil degradation has been documented (Tiffen and Mortimer 1993), but throughout most of sub-Saharan Africa, the soil resource continues to decline (Sanchez et al. 1997), alarmingly quickly in some areas (Oostwoud and Bryan 2001). Soil clearly provides valuable services (structure, chemostasis, water holding, carbon storage etc.), but without quantifying these values within the context of the larger natural resource basis of the economy, the decision to allocate resources to protect soils or reverse degradation trends is based on frequently exaggerated claims of problem severity (Stocking 1995).

Before resources are targeted to attenuate soil erosion, a clear understanding of mechanisms that elevate erosion risk is necessary (Pimentel 1993). While several universal models exist to quantify risk based on empirical factors, their use can introduce substantial error when applied in regions for which they were not calibrated (Morgan 1995). An alternative approach is to develop local risk models based on rapid reconnaissance and statistical inference. This approach has particular appeal for the rural tropics where mechanisms of degradation are poorly understood, and empirical data sets are less widely available. Furthermore, spatial targeting of intervention resources to areas of critical need and enumerating the association between land management decisions and elevated risk are critically important in tropical areas without significant resources.

Ultimately, a decision support model for land management to control erosion should combine predictions of erosion risk, inference of erosion extent and magnitude, and a cost/benefit comparative framework within which to compare scenarios for future development. This combination of process and context facilitates management solutions to maximize intervention efficiency and system sustainability.

This dissertation explores the costs of soil erosion within the context of the prevailing resource basis, develops statistical models and a rapid assessment framework that enumerates soil degradation risk, and interpolates risk models to a meso-scale study area to compare future land allocation alternatives for controlling natural capital depletion and supporting rural livelihoods.

Review of the Literature

Soil Loss Globally and Regionally

Significant literature exists documenting the magnitude of the soil erosion problem. Pimentel (1993) coalesces evidence from many regions of the world to state that between 30 and 50% of the world's arable land is substantially impacted by soil loss. Soil loss is widely identified as a threat to rural livelihoods (Lal 1985, Kerr 1997, Sanchez et al. 2003) and aquatic resources (Ochumba 1990, Crosson, 1986). Severe problems of soil degradation have been documented world wide, including in the United States (Uri 2001), Spain (Meyer and Martinez-Casasnovas 1999), southeast Asia (Pimentel 1993), Central and South America (Alfsen et al. 1996), Australia (Dregne 1995) and Africa (Morgan 1995, Lal 1985).

The problem is particularly severe in East Africa because of high population densities, fragile soils, intense rainfall and limited soil subsidy. Severe erosion has been

documented throughout the area (Oostwoud and Bryan 1997, Mati et al. 2000, Lufafa et al. 2002, Thomas and Senga 1983), resulting in serious depletion of soil functional capacity (Zobisch et al. 1995, Gachene et al. 1997, Swallow et al. 2002, Smaling 1993).

Clearly, the effects of soil degradation are felt most acutely by the subsistence farmers who populate the region. The marked decrease in soil functional capacity that arises because of erosion and extraction has been illustrated (Sanchez et al 1997), and the cycle of poverty makes long-term solutions difficult to institutionalize (ICRAF 2000). The link between soil erosion and subsistence agricultural yields has been widely cited (Lal 1985, Williams et al. 1983, Mulengera and Payton 1999). While the magnitude of this problem is still disputed (Crosson 1986, Stocking 1995), it is clear that agricultural yields in Africa have failed to keep pace with improvements observed in the rest of the world (World Bank 1996).

Off-farm costs are still poorly documented, but the general concerns of eutrophication and excess turbidity are widely cited (Lindenschmidt et al. 1998, Crul 1995). Lake Victoria, the world's largest tropical freshwater lake, situated in East Africa, has experienced frequent fish kills and algal blooms (Ochumba 1990) and serious destabilization of trophic dynamics (Lehman et al. 1998, Goldschmidt et al. 1993) resulting in unreliable fishery production. One presumed cause, a nutrient-rich sediment plume discharging into Nyanza Gulf, can be seen readily in satellite imagery.

Soil Erosion Models

Measurement of soil loss is an expensive and time-consuming undertaking. While the reliability of recent methods for assessing past erosion has been illustrated (e.g., Cesium^{137}) (Ritchie and McCarty 2003, Bujan et al. 2003), most erosion studies

rely on physical sampling structures to enumerate soil movement. The extremely limited variability in site and management characteristics that can be assessed with these methods given limited research budgets necessitates the use of models that can be extrapolated to a wider range of conditions. Models of the soil loss process can be divided into physically-based and empirical approaches. An alternative to model application is local model development based on direct observation. Each approach is outlined briefly below.

Physically-based models, typified by the Water Erosion Prediction Project (WEPP) (Foster and Lane 1987, Ascough et al. 1996), simulate the processes of sediment detachment, transport and deposition using process equations based on continuity constraints and physical forces (e.g., hydraulic shear stress calculations for modeling soil detachment by flowing water). The WEPP model is a distributed parameter model, which allows spatial patterns of erosion and deposition to be identified. This approach is suited for high temporal resolution studies in small (< 260 ha) (Morgan 1995) basins where sufficient data exist to estimate suitable values for all model parameters. It is also crucial if estimates of sediment yield are to be made. The array of physically-based models is substantial (Dietrich et al. 1993, Moore and Burch 1986, D'Ambrosio et al. 2001, Botterweg et al. 1998), but most suffer from two drawbacks that limit their applicability for this study. First, as discussed, model complexity and need for fine spatial resolution imposes limits for application to small basins. Moreover, the need for high-resolution input data (e.g. rainfall, atmospheric conditions) limits application of WEPP to regions with substantial monitoring infrastructure. Second, they are generally severely over-parameterized for watersheds where significant baseline data collection has

not been undertaken. Model accuracy is compromised when default settings (generally empirically defined) are used as universal settings.

Empirical models range in complexity, but share the characteristic that they are developed for specific regions and can be applied to new regions only with considerable caution (Morgan 1995). The most widely used example of an empirical model is the Universal Soil Loss Equation (USLE) (Wischmeier and Smith 1978) and various revisions of that basic framework (Renard et al. 1991), which statistically relates 5 readily observable factors to soil loss rates. The same factors (rainfall erosivity, soil erodibility, slope, slope length and vegetation cover) are used in the Soil Loss Estimator for Southern Africa (SLEMSA) (Elwell 1981), an empirical counterpart to USLE designed for the specific conditions in Southern Africa. Each factor is computed from standard equations, determined from enormous data sets describing soil loss rates from standardized plots. The advantage of empirical models is that they are conceptually simple and require data that, if unavailable, are relatively easy to collect or estimate. There are several widely cited constraints (Morgan 1995, Jetten et al. 1999). First, as empirical models, their universal application is inadvisable without formal validation. In particular, USLE was developed for the Midwestern USA and application to sub-Saharan Africa (where climate, soil and cropping systems are different) is of questionable utility (Cohen et al., submitted). Despite this constraint, USLE is widely applied around the globe (Millward and Mersey 1999, Chen 1998, Lufafa et al. 2002), usually without any formal ground validation protocol. Second, empirical models are capable of identifying where erosion occurs, but not where eroded material is deposited because there are no physical constraints in the USLE model (i.e. continuity equations).

While estimation of actual erosion rates is frequently desirable, models developed to provide categorical information (e.g., degraded/intact) can offer substantial benefits over a model-based approach (Adinarayana et al. 1999). Limited equipment is necessary to provide categorical erosion models based on visual designation, and each model can be developed for the specific region in which it is applied. This allows specific insight into the effects of local land management on erosion risk, and aids in understanding the kinds of intervention approaches that might provide protective effects. This direct observation approach is the strategy used in this work.

Soil Erosion Costs

Soil erosion represents an externality (Loehman and Randhir 1999); that is, some of the costs of soil erosion are borne by society, now or in the future, rather than entirely by the landowner. Market prices of goods for which there are external costs do not reflect the true cost when all inputs are tallied. The literature is rich with efforts to internalize erosion costs by placing value on eroded soil (Crosson 1986, Bojo 1996).

Soil value can be designated using a variety of methods. The most common puts soil values into economic units so that market and true prices can be compared directly. Specifically, attention focuses on production losses as a result of depleted fertility, off-farm losses (sediment in reservoirs, eutrophication of water bodies, downstream flood problems), and aesthetic losses (Bandara et al. 2001). Where discrepancies occur, tax subsidies or policy instruments are necessary to force market prices higher or encourage better conservation.

Another option is to quantify the value of a resource according to its emergy content. This approach offers several advantages over methods assigning dollar values to

services for which no formal market exists. First, methods are based on biophysical observations of production rather than, as is often the case (Alfsen et al. 1996), basing costs on perception of value (willingness-to-pay survey strategies). Second, emergy allocation of soil value is donor based. As a result, value is embodied in the storage rather than the service that soil provides. The assumption is that, within any self-organizing system, there is a strong link between invested energy and service.

An important issue raised repeatedly in the economic literature on soil degradation (Alfsen et al. 1996) is that erosion represents a cost that may be acceptable given specific tradeoffs to lower soil-loss rates. This study explores emergy-based optimality criteria for mitigation strategy assessment that account for both benefits accrued to society because of soil degradation (i.e., production capacity), and costs of that process.

Watershed Scale Erosion Assessment

Watersheds are widely recognized as the most appropriate biophysical or socioeconomic unit for management and study of water and soil resources (Lal 1999, Brooks et al.1997). Virtually all development organizations (ranging from the World Bank to small local NGOs, along with government agencies) are engaging in watershed management as their primary intervention strategy (ICRAF 2000). The most important aspect of watersheds that make them ideal study units is that all the effects of land management in a watershed accumulate to the same point at the basin outlet, a condition that forces explicit consideration of the linkage between upstream actions and downstream effects (Luitjen 1999). Furthermore, the scale of a watershed is often most

appropriate to bring together the specific concerns of individual farmers and the larger scale issues with which policy makers contend.

However, problems arising from the spatial extent of watersheds in comparison with the scale at which erosion processes are well described. First, many models (i.e., strongly physically based models) are eliminated as potential tools if the basin of interest is substantially larger than 10 km^2 (Morgan 1995). Second, standard empirical models require validation, which can be extremely expensive in a large basin with varied climatic, edaphic and management conditions.

For example, variability in infiltration is a critically important consideration when assessing risk (Jetten et al. 1993), but methods for inferring infiltration rates that are specific to land cover, soil, slope and climate across large areas have only recently been developed (Sullivan et al. 1996). Soil-survey data provide nominal information for soils under generalized conditions. Land use, degradation status, and natural within-class variability are all important components of hydrologic response that are overlooked by using soil survey data (De Roo et al. 1992, Stolte et al. 1997, Ziegler et al. 2001).

Examples abound of studies focusing on soil degradation at the scale of watersheds and larger (Stolte et al. 1997, Kassam et al. 1991, Sutherland and Bryan 1991, Mati et al. 2000). The central theme of these studies is that the physical processes of erosion are abstracted, either statistically or conceptually, to allow analysis at scales that are more meaningful for policy development. The approach taken in this work follows this general protocol by exploring statistical association patterns between risk factors and categories of degradation. Thus, the methods developed in this study are highly scalable but lack physical process constraints.

Watershed Rapid Assessment

Rapid assessment protocols are crucial for assessing land and water dynamics over large areas. Examples of tools used for rapid land assessment are satellite imagery (Hill and Schutt 2000, Dwivedi et al. 1997, Price 1993), cesium-137 radioisotope studies for erosion rate inference (Ritchie and McCarty 2003, Bujan et al. 2003) and diffuse reflectance spectroscopy (DRS) (Ben-Dor and Banin 1995, Shepherd and Walsh 2002, Ludwig et al. 2002, Kooistra et al. 2001). This study made extensive use of satellite image interpretation for interpolating field observations to entire watersheds, and spectral signature analysis for rapid assessment of soil quality.

Diffuse reflectance spectroscopy for soil quality assessment

Conventional methods of soil analysis are well established but limit processing large numbers of samples because of resource-intensive and time-consuming tests. However, for accurate assessment of soil throughout watersheds, large numbers of samples are necessary to capture the significant variability that is widely documented (Burrough 1989). This is particularly true in regions where soil-disturbance regimes are of interest under a variety of land-management options.

DRS is a relatively simple process. A high quality tungsten-filament bulb emits full-spectrum light (between 350 and 2500 nm), and sensors record reflectance characteristics of each material in 1-nm bandwidths (Shepherd and Walsh 2002). Reflectance characteristics have been used widely to differentiate between minerals (Hunt 1977, Clark 1999), plant and animal tissues (Foley et al. 1998, McLellan et al. 1991, Gillon et al. 1999). Newer applications include quantitative inference about soil organic matter (Henderson et al. 1992, Sudduth and Hummel 1993, Ludwig et al. 2002)

and soil properties in general (Ben-Dor and Banin 1995, Shepherd and Walsh 2002, Reeves et al. 1999). A typical soil spectral reflectance curve is given in Figure 1-1. Specific soil properties that have been successfully inferred from these curves include texture, cation exchange capacity, base saturation, pH, organic carbon content, exchangeable P, exchangeable K, nitrogen species and various contaminants (Ben-Dor and Banin 1995, Shepherd and Walsh 2002, Ludwig et al. 2002, Kooistra et al. 2001). Soil physical properties (macroaggregate stability, bulk density) are intuitively less likely to be inferred spectrally than chemical properties, but have not been fully explored. Additional soil chemical properties that are candidates for spectral inference include sodicity, micronutrient concentrations, functional organic matter pools and radioisotope measurements (e.g., Cs-137, Pb-210). An area largely unexplored for application of DRS is integrative metrics. For example, fertility, degradation, infiltration capacity, carbon evolution potential, and structure are composite variables that are impossible to measure using a single standard laboratory technique. In general, these features of soil are dealt with using transfer functions that interpret the relative levels of basic soil properties in comparison with some empirical reference. Since all of basic soil properties are integrated in a single spectral response curve, there is strong potential that composite variables can be inferred directly from spectra, obviating the need for transfer functions. This study addressed two composite variables (degradation and infiltration capacity).

Interpretation methods of spectral response curves vary, but most involve multivariate data mining tools such as Partial Least Squares Regression (PLS – Ludwig et al. 2002), Multivariate Adaptive Regression Splines (MARS – Shepherd and Walsh 2002) or Classification and Regression Trees (CART – Shepherd and Walsh 2002).

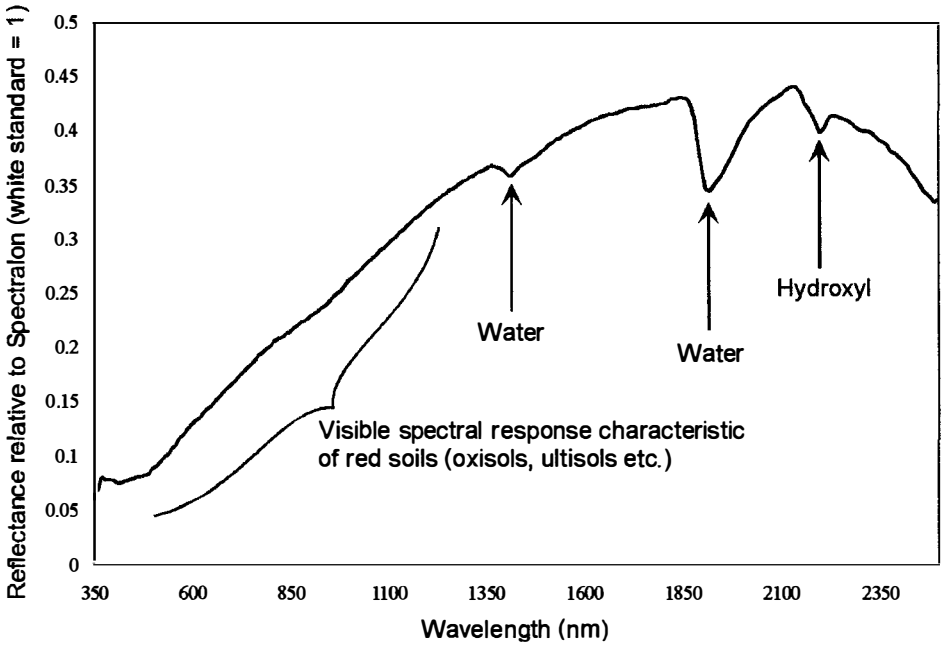

Figure 1-1. Typical DRS raw reflectance pattern for a tropical soil. Shown is relative reflectance versus wavelength. Specific important absorption features are identified.

These newer approaches supplant linear multivariate methods (e.g., multiple regression, discriminant analysis) that were only marginally successful for dealing with the complexities of the soil mixture and the severe co-linearity issues that arise in the analysis of spectral response curves. This work made extensive use of CART (Breiman et al. 1986, Steinberg and Colla 1997) in developing spectral response models, both for DRS data and for satellite image interpretation.

Satellite image processing for spatial erosion risk assessment

Use of satellite imagery to assess ground condition began during the 1970s, displacing conventional survey methods and aerial photographs as the primary tool for land assessment over large areas. While application for inference of land cover patterns is extensive in the literature (Jensen 1996, etc.), less attention has focused on inventories of degraded land (though see Fenton 1982, Pickup and Chewings 1988, Price 1993,

Dwivedi et al. 1997). Even less attention has been given to the potential to infer patterns of infiltration rates from satellite imagery. This is primarily due to issues of spectral confounding: satellites only measure reflectance from the upper-most layer of the landscape; and vegetation may mask soil properties that cause variability in infiltration, necessitating instead a sampling protocol that uses geostatistical inference (Sullivan et al. 1996). Satellite imagery is particularly effective when synoptic data are insufficient. Time series currently available (Landsat imagery is available from 1973) provide a sufficient record to be useful for large-area change detection.

Landuse Change Models

The study of patterns of landuse change and the development of models to forecast it has become central to research in landscape ecology and regional planning (Turner and Gardner 1990, Verburg et al. 1999). Models have been developed to predict changes in water flows (Grove and Harbor 1997, Miller et al. 2002, Calder et al. 1995, Niehoff et al. 2002); biota (Eva and Lambin 2000, Ehrlich et al. 1997, Swenson and Franklin 2000); urban and agricultural growth (Batty and Longley 1989, Clarke and Gaydos 1998, Gilruth et al. 1995); and soil degradation (Feoli et al. 2002, West and Wali 2002, Li and Reynolds 1997) among many other applications.

One particularly flexible model form makes use of Markov transitional probability matrices (Flamm and Turner 1994, Howard et al. 1995, Li and Reynolds 1997). These matrices, calibrated by comparing historical and current landuse maps, allow stochastic prediction of land use patterns in future landscapes. Conditional transition probabilities can be manipulated to reflect effects of alternative land management strategies, allowing future landscapes to be compared. This approach forms

the basis for scenario assessment. While there are substantially more realistic alternatives to this method (e.g., Markov cellular automata – Itami 1994), the Markov method offers the most statistically robust and readily applicable method.

Systems Evaluation

Ecological and human systems self-organize to transform sources of available energy into energy forms with emergent characteristics (Odum 1994). As energy transformations occur, a portion of energy that was previously available loses its ability to do work, increasing entropy at the larger scale, as predicted by the Second Law of Thermodynamics. However, energy retained after adaptive transformations has qualities (e.g., the ability to reinforce and amplify input flows) that distinguish it in form and function from the original energy. A sequence of such transformations results in decreasing quantities of energy, but increasing quality. This organizational property, energy hierarchy, is a readily observable characteristic of many adaptive systems (e.g. food webs, governments, watershed hydrologic convergence), and provides the theoretical basis for emergy analysis (Odum 1996). The maximum power principle (Lotka 1922, Odum 1994), which postulates that, in order to remain competitive, systems select for energy use pathways that maximize the useful dissipation of available energy, suggests that self-organization into energy hierarchies is a means to reinforce exogenous energy flows. Energy invested in higher hierarchical levels, which feeds back control for enhanced overall energy capture, embodies value vastly greater than simply the remaining energy content; emergy analysis is a means to account explicitly for that whole-system value.

Emergy and transformity

Emergy is defined as the energy required, both directly and indirectly throughout a process, to create a product or service (Odum 1996). Since each input to a process is itself the product of energy transformations, emergy is often conceived of as energy memory; that is, the energy, usually expressed using solar energy as the common baseline, that was required throughout the global energy transformation hierarchy. The standard emergy unit is the solar emjoule (sej), which is distinctly different from the joule (J) with which available energy is quantified. The quality of energy in any given product is expressed as transformity and measured as the ratio of emergy (sej) to available energy (J). Systemic analyses (Christensen 1994, Patten 1995) that ignore energy quality inevitably undervalue the contributions of low energy concentrated sources (e.g. human work, information) relative to abundant diffuse ones (e.g., sunlight, wind kinetic energy).

Numerous studies have used emergy accounting to quantify development tradeoffs that must simultaneously consider economic and ecological costs and benefits (Portela 1999, Buenfil 2001, Brown and MacLanahan 1996, Odum et al. 2000). Watershed scale evaluations have focused on water (Romitelli 1997, Brandt-Williams 1999, Howington 1999) and on multi-use functions (Tilley 1999), with significant attention to soil development and loss. Considerable work has been directed at evaluations of agriculture (Brandt-Williams 2001, Doherty et al. 2000, Lagerberg 1999, Odum 1996) with substantial convergence of transformity values for agricultural products (Brandt-Williams 2001, Buranakarn 1997).

Transformity assessments for topsoil are generally based on work presented in Odum (1996). These are based on soil development models for temperate regions where

organic matter accumulation is much more rapid that in the seasonal tropics (Brady and Weil 2001). A model-based approach to soil valuation (Cohen 2001) was used as the basis of this work; a transformity for organic carbon in tropical soils is reported that is 2 times higher (2.2E5 sej/J vs. 1.1E5 sej/J) than previously computed (Odum 1996). Previous valuation ignored soil carbon dynamics (Parton et al. 1994, Bolker et al. 1997), particularly for tropical areas where soil carbon depreciates at substantially faster rates.

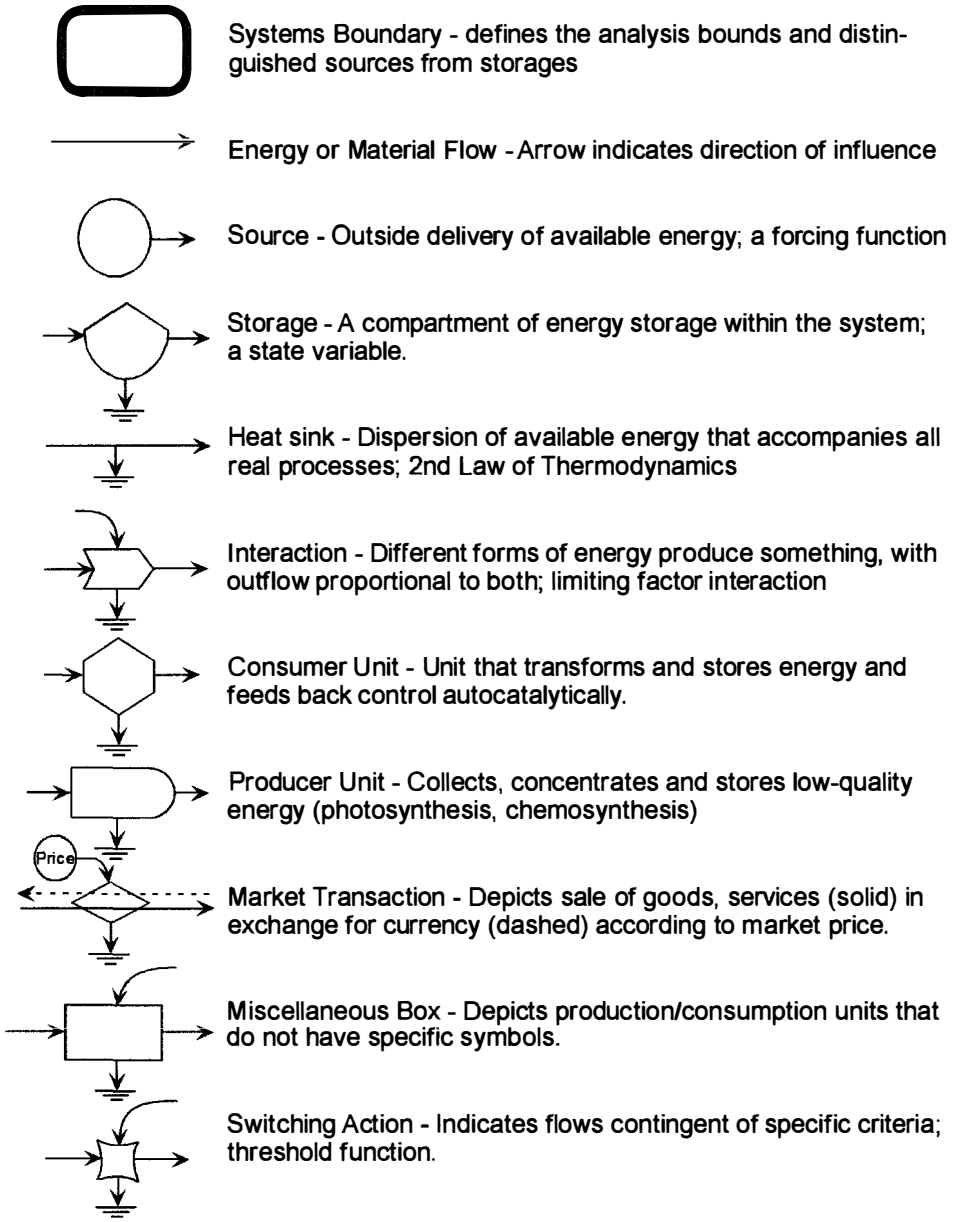

Figure 1-2. Energy systems symbols with descriptions.

Because of the complexity and detail of emergy evaluation, index development is critically important to facilitate interpretation and comparison across production processes or between management alternatives. These indices (presented fully in Odum 1996, Ulgiati and Brown 1998, Ulgiati et al. 1995) summarize system resource use intensity, process efficiency, economic-environment interactions and sustainability. They are described in detail in the methods section of this study.

Energy systems diagrams

Energy systems diagrams were used throughout this work to characterize complex systems, and aid in parametrization of simulation models. While many alternative symbolic languages exist, the energy systems language (Odum 1994) offers a comprehensive modeling language with explicit recognition of the thermodynamic constraints that direct real systems.

Description of the Study Site

The Awach River, which drains a small watershed (330 km^2; centroid 35.1˚E 0.3˚S – Figure 1-3) in the Kenyan portion of the Lake Victoria drainage basin, was chosen as the study site because it exhibits advanced soil degradation (gully formation, prevalent soil hardsetting – ICRAF 2000). The river system drains into a littoral papyrus (*Cyperus papyrus*) wetland before discharging to Nyanza Gulf in eastern Lake Victoria.

Elevations range between 1134 m at the lake edge and 2200 m (mean slope = 6%). The landscape can be divided into lowlands (<1400 m) and highlands (>1400 m), separated by a steep escarpment. The lowlands consist primarily of Pleistocene lake plain deposits (Eutric Leptosols, Planisols and Vertisols) with deep profiles and moderate to low fertility. Shrink/swell potential of these soils is high, as is the prevalence of sodic

soil phases. Highland soils, which overlay Kericho and Kenya-type phonolite sub-strata, are deeply weathered (Humic Nitisols, Humic Cambisols, and Luvic Phaeozems) and structurally stable but with generally low fertility.

Lowland climate is sub-humid tropical (~1100 mm precipitation/yr) with bi-modal rainfall delivery characteristic of equatorial latitudes. Highland climate is humid tropical (~1700 mm precipitation/yr) exhibiting moderated bi-modal rainfall due to continuous subsidized convection from Lake Victoria. Annual solar insolation and temperature are effectively constant.

This area has been settled at low densities for many years. In fact, there are records of settlement on nearby Rusinga Island dating more than 50,000 years b.p. and evidence of proto-hominid habitation as far as 17 million years b.p. (Reader 1997). Recent settlement changed dramatically during the 1950's and 60's during which migration and sedenterization changed land use patterns and regional livelihood strategies. Growing evidence suggests that severe degradation began in the early 1960's in response to the converging circumstances of poor land use planning and a period of intense pluvial activity due to El Nino (M. Walsh, personal communication).

Regional population growth (3.9% per year – Kenya CBS 2000) has forced cultivation of marginal lands on steep slopes; high livestock densities are common throughout the region. Dominant lowland agricultural land-uses are maize, sugarcane and communal rangeland, while tea, maize, sugarcane, woodlots and constrained grazing (using improved breeds) dominate the highlands. Native ecological communities, now extremely rare, include perennial grasslands with interspersed evergreen/semi-deciduous bushland in lowland areas, and evergreen broadleaf forest in the highlands.

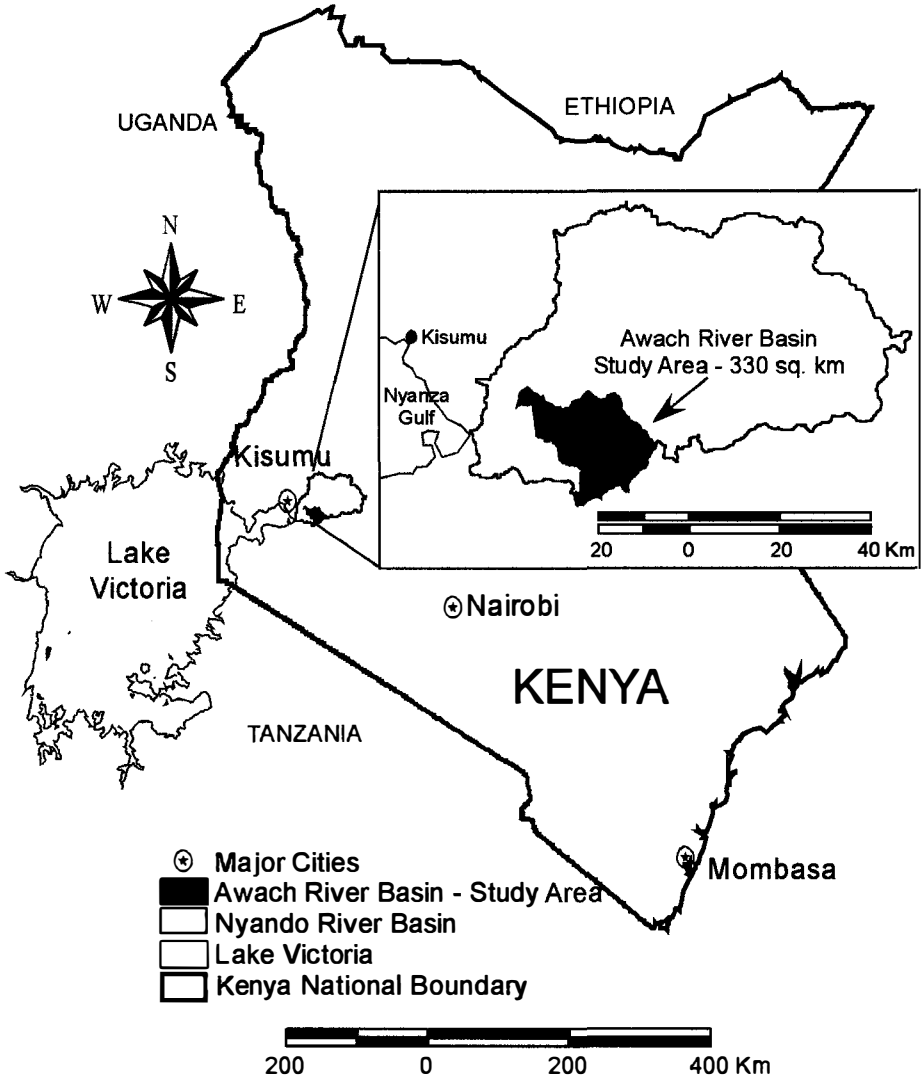

Figure 1-3. Geographic location of the Awach River basin in western Kenya. The centroid of the study area is 35.08˚E and 0.31˚S.

Plan of Study

The problem of soil erosion is addressed in the literature in two general ways. The first is technical: define the factors that lead to elevated erosion risk and describe how can they be managed. The second is decision-oriented: quantify the consequences of soil loss and costs of mitigation so appropriate policy can be developed. This study links these approaches within a systems-based decision support framework. There are three broad objectives for this work:

- Quantify soil erosion costs in the context of the natural resource basis at three scales (national, regional and landuse-specific).
- Delineate factors that elevate erosion risk in the region and develop statistical models to predict degradation probabilities quantitatively.
- Interpolate risk from plot observations to the entire watershed study area to develop a spatial framework to assess alternative land management scenarios.

Within each objective, there are specific essential tasks. For the first component, transformities were computed for a wide range of agricultural products characteristic of Kenya and the study area in particular. Furthermore, two new metrics were defined to quantify the magnitude of local natural capital depletion within the context of the larger resource basis more effectively. Of particular importance was defining reliable transformity values for soil components in tropical ecosystems. Work done tangentially to this study (Cohen 2001) presents transformity calculations for soil organic carbon, soil structure and nutrient exchange capacity for tropical forest and savanna ecosystems.

Tasks specific to the second objective are extensive. In order to define the necessary factors, several layers of analysis were necessary. Calibrations of soil properties to spectral response characteristics were essential. Coupled with a case-control sampling protocol, spectral response was used to delineate degraded from intact soils, distinguish regions of slow infiltration from other areas and develop an empirical composite soil erodibility factor that can be used to assess site risk. Terrain-based indices and field observations of cover and landuse were used to develop two other composite variables that describe erosion risk specific to the study area.

The third objective relied on inferential interpolation of landuse, degradation condition and infiltration capacity from satellite imagery. The spatial extent of soil degradation, coupled with basin-wide sediment yields, provided a benchmark against

which alternative land management schemes can be compared. Land cover change models based on 1986 and 2001 imagery were developed to explore anticipated changes in basin condition, and to quantify risk attenuation for proposed schemes. Specifically, is spatial targeting of specific land uses to regions of low inherent risk effective for maximizing yields while simultaneously minimizing severe natural capital depletion? Which landuse change scenarios are more desirable for degradation rehabilitation, and is there a difference between optimal land allocation for controlling erosion and optimal land allocation when yields are explicitly included in assessment?

METHODS

Two complimentary approaches were used to enumerate the prevalence and magnitude of soil erosion, and while the two methods are quite different, they converged to arrive at recommendations for how to manage the problem in western Kenya. First, methods of emergy analysis were used to compare the magnitude of soil loss with economic benefits on a common basis. Second, watershed-scale field sampling and soil analysis were used to assess erosion risk factors, determine land-use degradation association, and develop a probabilistic spatial model of erosion risk. Finally, the two approaches were coupled to produce comparative assessments of competing regional land-use scenarios. The methods section is organized into three main parts: methods for emergy evaluations of national, regional and landuse subsystems are given first. Then, methods for modeling soil erosion risk are given, which include field data collection protocols, statistical analysis and development of integrated models of degradation risk. Finally, methods for spatial decision support modeling are given.

Emergy Analysis at National, District and Subsystem Scales

Evaluation was performed at three scales, proceeding top-down starting with large-scale considerations that provide local problem context and progressing to assessments of individual land-uses. Emergy evaluations were developed for:

- Kenyan national economy
- Kisumu, Kericho and Nyando district economies (third level of Kenyan governmental hierarchy)

- Specific land-uses that comprise livelihood strategies for people living in the Awach River basin.

Land-uses explored in detail were commercial agricultural (i.e. sugar and tea), subsistence agriculture (i.e. maize and sorghum), timber and fuel woodlots, grazing lands, native forests and shrublands.

Emergy Evaluation Protocols

The standard emergy methods for regional and national analysis (Odum 1996, Brown and McClanahan 1996, Doherty et al. 2002) were followed in this study. This multi-step process includes systems diagram development, compilation of critical cross-boundary flows and internal stock depletion, data collection, and flow aggregation/summary index development.

Emergy Evaluation Summary Indices

Summary indices allow comparison between systems. The suite of standard indices, compiled from aggregated flow data, includes total emergy use, emergy use per capita and per unit area, emergy balance of trade, emergy-money ratio and yield, investment and loading ratios, described below. Two additional metrics were developed for this work specifically to quantify relative costs of soil erosion.

Flow aggregation

Flows are first aggregated into broad categories. Figure 2-1 is a standardized economic systems diagram used to summarize and visualize these aggregate emergy flows and describes the derivation of the standard indices. Aggregated flows include renewable energy flows (R), local non-renewable flows (N), imported goods (G), imported fuels and minerals (F), imported services (S) and exported goods and services (E – also called yield or Y).

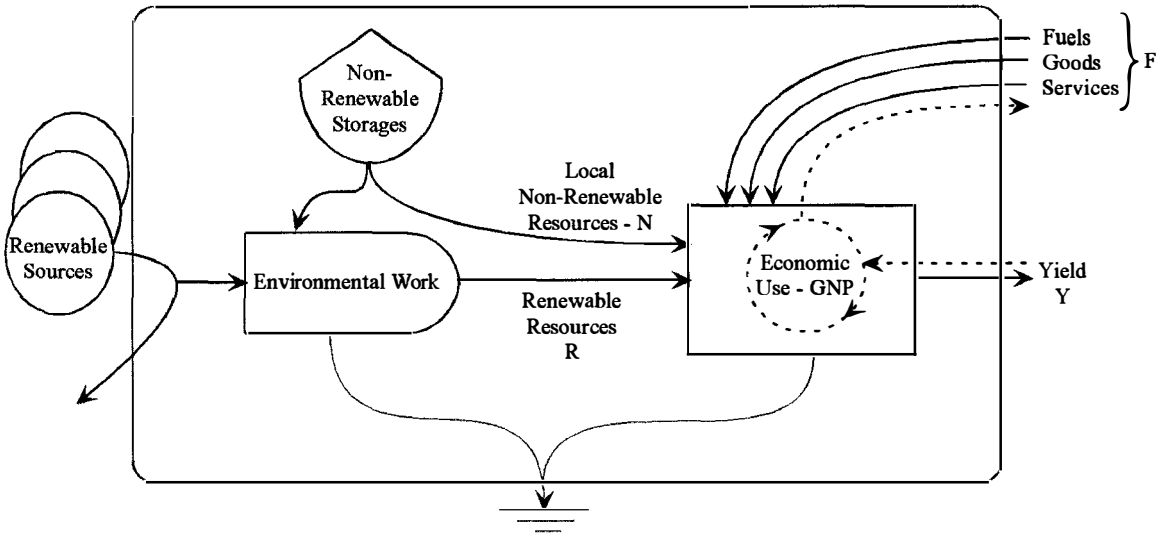

Transformity (for product Y)	=	EMergy of Y / Energy of Y
Emergy:Dollar Ratio (Em$)	=	(R + N + F) / GNP
Emergy Yield Ratio (EYR)	=	Y / F
Emergy Investment Ratio (EIR)	=	F / (N + R)
Environmenatl Loading Ratio (ELR)	=	(N + F) / R
Emergy Sustainability Index (ESI)	=	EIR / ELR
Percent renewable	=	R/ (R + N + F)

Figure 2-1. Standardized economic systems diagram. Shown are aggregated flows and indices that result from these flows.

Emergy:money ratio

The emergy-money ratio (Em$) describes nominal purchasing power, in emergy units, of one unit of currency spent within the local economy. It is computed by dividing total emergy use (R + N + F) by GNP. In order to compare between nations, money is standardized to US dollars via mean currency exchange rates for the year of interest.

This index not only describes purchasing power within a region, it also informs the emergy balance of trade between regions. A detailed discussion of the competitive disadvantage faced by regions with high Em$ ratios with respect to regions with low Em$ ratios is presented in Cohen, Sweeney and Brown (in preparation).

Environmental loading, investment and yield ratios

The environmental loading ratio (ELR), emergy yield ratio (EYR) and emergy investment ratio (EIR) form three critical metrics of system condition. These three

unitless ratios describe development intensity in different ways. The ELR reports the ratio of non-renewable to renewable flows (Figure 2-1):

$$ELR = (N+F) \div R \quad [2\text{-}1]$$

As this metric increases, stress on environmental services is anticipated due to concentrations of non-renewable sources that alter natural energy flow patterns.

The emergy investment ratio (EIR) describes the ratio of purchased inputs to total flows from within the system (Figure 2-1):

$$EIR = F \div (N + R) \quad [2\text{-}2]$$

This index describes investment because it quantifies nominal levels of investment from outside the system boundary to match flows of locally available emergy. A high value indicates that each unit flow of locally available energy has a strong attracting force for outside sources. The investment ratio exhibits non-homogenous spatial patterns in landscapes; cities, deltas, mountain ranges and lakes have higher than average investment ratios because flows converge to these regions. The EIR quantifies development status of nations and regions, with larger values indicating advanced development. The EIR for the United States is roughly 7:1 (Odum et al. 1987), while Thailand has a ratio of 0.46 (Brown and McClanahan 1996).

The emergy yield ratio quantifies net benefit of feedback investment to a nation, region or process; it is the ratio of emergy output to investment to secure that output:

$$EYR = Y \div F \quad [2\text{-}3]$$

where Y = exported goods and services and F indicates all invested inputs (i.e. fuels, goods and services from outside the system). When this metric exceeds 1, investment is

yields net benefit. On a national scale, values less than 1 indicate a nation is a net importer, generally indicative of advanced development status.

All metrics presented above are most useful in comparison with other regions of similar scale. Emergy calculations in this study reflect recent amendments to estimates of tidal momentum absorption (Campbell 1999). To allow common benchmark comparison with older analyses, all flows were divided by 1.68, as proposed by Odum et al. (2000).

New summary indices

Two new metrics were developed specifically to quantify losses of indigenous stocks of natural capital within the context of a regional energy basis. Typically, soil loss is considered non-renewable energy stock depletion (N in Figure 2-1). However, lumping these flows with mined minerals and locally extracted fossil fuels ignores direct ecosystem services that these stocks facilitate. Furthermore, while direct economic benefits of fuel are clear, the benefit of degraded topsoil is not as obvious. It is reasonable to assume that at least a portion of these flows could be prevented given more effective land management policies.

Fraction capital depletion. The Fraction Capital Stock Depletion (FCSD) is computed as the proportion of total emergy use (U) contributed from soil loss:

$$FCSD = N_a \div U \qquad [2\text{-}4]$$

Where N_a is soil loss, a capital stock that economic systems exploit more rapidly than it recovers, making it effectively a non-renewable use. Large values indicate substantial external costs to the economy.

Agricultural benefit ratio. The agricultural benefit ratio (ABR) compares agricultural yields (livestock, subsistence and commercial crops) to emergy flows from natural capital stock depletion:

$$ABR = Y \div N_a \quad [2\text{-}5]$$

where Y is emergy yield and N_a is soil loss costs. Clearly, soil erosion results from urban development, but the predominant tradeoff in Kenya is between rural production decisions and consequent external costs. This ratio is a simple benefit-cost analysis for regional agricultural activity. Because soil erosion is embodied in agricultural yields, a value approaching one indicates increasingly deleterious agricultural effects. The ratio will be generally be substantially greater than 1, indicating agricultural net yields. However, the ABR magnitude will vary considerably within and between regions and cropping systems, identifying which agricultural and/or livestock activities are locally inappropriate. Note that, at the landuse subsystem scale, ABR is inverse of FCSD. This is not the case at larger scales where yields are not entirely agricultural.

The ABR can provide a quantitative objective function, embodying costs and benefits of competing interventions, for evaluating alternative land management scenarios in the agricultural basins such as the Awach River watershed. Methods optimizing land-use decision-making are described in detail in a later section.

National Scale Analysis

Data sources

Data were retrieved primarily from a national statistical abstract published by the Kenyan Central Bureau of Statistics (CBS 2000), which compiled national accounts from 1999. Numerous ancillary data sources were used, both to quantify flows not available

from the statistical abstract and to cross-reference flows to ensure accurate accounting. These sources included United Nations commodity flow data (UN, 2000), Europa World Yearbook (Europa Publications, 2001), World Bank national overview (World Bank, 2002), national tidal amplitude statistics (US Dept. of Commerce 1994), a study of wind power feasibility in Kenya (Chipeta, 1976), global deep-heat flow database (Pollack et al. 1993), and a comprehensive thematic spatial database with precipitation, elevation, runoff and forest coverages (Corbett et al., 1997).

Internal agricultural/fisheries/livestock production, geothermal and hydroelectric power production forest clearing rates and mining data were all compiled from relevant Government of Kenya (GoK) sources, including the Ministry of Agriculture and Rural Development, Ministry of Fisheries, Kenya Power and Lighting Corporation, Ministry of Forestry and the Bureau of Mines.

Product transformity values

The Kenyan national system is highly dependent on rural agricultural production; consequently, reliable local transformity values are essential for accurate assessment. A standard protocol for computing product transformity values (Odum, 2000; Brown et al. 2000; Brandt-Williams 2002) was used for 17 raw agricultural products (e.g. maize, sorghum, sugar cane, tobacco, green tea leaves), 3 protein sources (fish, and highland and lowland cattle) and 2 important processed goods (tea and refined sugar). The results are used throughout this work, particularly for analysis of specific sub-systems within the study watershed; analysis summary data are presented in Appendix A (Table A-1).

Accurate transformity values for soil are of particular importance for this work. Previously, soil organic carbon was considered the sole value-bearer for topsoil, and

relevant calculations were presented for temperate soils that generally accumulate organic matter more rapidly than tropical soils due to reduced annual oxidation (Brady and Weil, 2001). Work associated with this study (Cohen, 2002) employed dynamic systems simulation of topsoil genesis to compute transformity estimates for a suite of potential value-bearers in soil. These include soil organic carbon, soil structure, cation exchange capacity and exchangeable soil nutrients. Since development of these soil functional storages is profoundly coupled, the value of eroded topsoil is reported using only the largest flow to avoid double counting emergy.

A dynamic systems model was calibrated for soils in tropical highland forest and tropical savanna ecosystems that predominate in Kenya. Table A-8 (Appendix A) summarizes select model results. The estimated transformity of soil organic matter in the tropics indicates that it is over twice as valuable as organic material in temperate soils.

Estimates of soil erosion and forest clearing rates

Soil loss is widely considered a major environmental consequence of increased population pressure. In order to quantify erosion costs to the national economy, reliable quantitative estimates of annual soil loss were necessary, but were generally unavailable at the national scale. Two methods were explored: 1) use of soil loss rates on a landuse basis (Table 2-1 based on Barber 1983), adjusted by a sediment delivery ratio (Brooks et al. 1997), and 2) measurements of sediment concentration in rivers (Ministry of Water Development 1992). Typically, the latter would be considered more reliable, but available data are primarily from the 1970's and cover a very limited number of rivers. Therefore, the former was used as the primary method, using river sediment loads to cross-check.

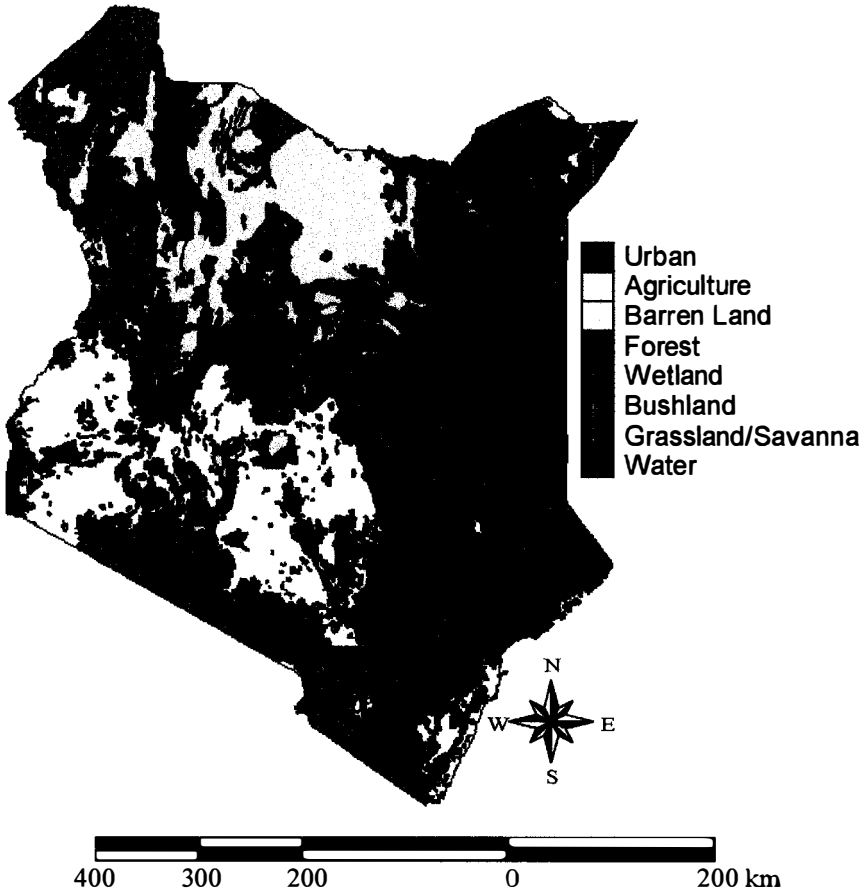

Figure 2-2. Land-use map for Kenya ca. 2000 (Corbett 1997).

National soil loss was computed using average annual erosion rates by landuse (Table 2-1) (Barber 1982). The spatial extent of each land-use was inferred from existing land cover coverages (Corbett et al. 1997 – Figure 2-2, summarized in Table 2-1). To ensure that soil loss estimates did not include eroded material that is subsequently deposited downstream (in wetlands, concave slopes, flow control hedges, etc.), estimated annual soil loss was multiplied by a sediment yield ratio of 5% (Brooks et al. 1997). This approach is exceedingly conservative because costs due to soil loss from a site are not entirely mitigated when eroded material is deposited downstream. Sedimentation in waterways is generally considered detrimental to ecosystem processes, and therefore may constitute a substantial additional cost, not included here, rather than a benefit.

Table 2-1. Soil erosion rates and spatial extent for major land cover classes in Kenya (1999).

Zone	Area(m^2)	Area %	Soil Loss (g/m^2)	Annual Soil Loss (E6 tons)
Barren or Sparsely Vegetated	3.51E+10	6.1%	250	8.77E+00
Broadleaf Deciduous Forest	9.83E+09	1.7%	100	9.83E-01
Cropland/Grassland Mosaic	7.22E+10	12.4%	3000	2.17E+02
Cropland/Woodland Mosaic	2.30E+09	0.4%	2500	5.74E+00
Dry Cropland and Pasture	2.26E+10	3.9%	4500	1.02E+02
Evergreen Broadleaf Forest	1.49E+10	2.6%	100	1.49E+00
Grassland	1.06E+11	18.3%	500	5.30E+01
Savanna	1.64E+11	28.4%	500	8.22E+01
Shrubland	1.39E+11	23.9%	750	1.04E+02
Urban	1.55E+08	0.0%	5000	7.74E-01
Water Bodies	1.40E+10	2.4%	0	0.00E+00
Total	5.80E+11			5.75E+02

Forest clearing is more readily quantifiable. Several sources confirm that clearing rates have average between 1 and 1.7% per year for the last several decades (Kaufman et al. 1996). An existing land-use map (Figure 2-2) allowed all forestlands to be identified, and clearing rates were estimated using an annual forest loss rate of 1.25%.

District Analysis

The next scale of evaluation included districts that define the study area regional context. Figure 2-3 shows Kisumu, Nyando and Kericho districts in relation to Lake Victoria and the Awach River basin. While Kisumu district does not contact the study basin, its importance as a regional trade and manufacturing center warrants its inclusion to understand the regional role in the national economy better. Systems diagrams were first developed for each district to guide concomitant tabular evaluation.

Data sources

Reliable data at the district level were difficult to acquire. Quintennial district development plans report on climate and agricultural production statistics, demographics

and development indicators. However, resource consumption and trade between regions within Kenya are not carefully monitored.

Kenya is serviced by several paristatal agencies, including nationalized electrical power (Kenya Power and Lighting Corporation – KPLC), fuel distribution/refining (Kenya Pipeline Authority – KPA) and tea/sugar production (Kenya Tea Development Authority – KTDA and Kenya Sugar Authority – KSA). These agencies provide a centralized record of regional consumption patterns, and data acquired from them were considered reliable. Records of manufacturing, mining, services and transportation are not comprehensively collected, and the limited data were judged highly suspect.

In order to estimate resource use and trade not documented by paristatal agencies or MoARD (e.g. metals, services, textiles), it was assumed that consumption is directly proportional to utilization of fuels and electricity, using the national analysis as the proportional reference point. This assumption is validated by Hall et al. (2001), who found aggregate economic flows to be highly correlated with fuel use.

Soil loss and forest clearing estimation

Regional soil loss was estimated using data from field observations of erosion rates for each landuse in conjunction with existing landuse maps. A watershed sediment yield ratio of 10% was assumed. This value is larger than the 5% assumed for the national evaluation because the region is dominated by small basins (Brooks et al. 1997). In particular, considerable local drainage occurs via small escarpment streams discharging directly to Lake Victoria and exhibiting signs of extreme sediment load. Sediment delivery values were cross-referenced using mean sediment concentrations for rivers in the area (Kenya National Water Master Plan, 1996). These data were not used

as the primary source because only synoptic measurements, frequently only for the dry season, are available; strongly seasonal local climate and land management patterns necessitate data sets that are more temporally comprehensive.

Awach Basin Landuse Subsystem Analysis

Finally, emergy evaluation was used to compare common land-use subsystems within the Awach River basin. This region of western Kenya has limited livelihood diversity, with most local inhabitants engaged primarily in subsistence farming and animal husbandry. As a result, major land-uses of interest relate to food and fuel production. Land-uses analyzed were:

- Subsistence farming systems (maize, sorghum)
- Commercial farming systems (smallholder production of sugarcane and tea)
- Subsistence woodlots
- Communal and constrained grazing lands for cattle, sheep and goat production
- Existing forests and shrubland, exploited for charcoal production.

Systems diagrams were developed for each land-use as the first step in the standard emergy protocol, followed by tabular evaluation.

Data sources

Data for local cropping system inputs and yields come primarily from a comprehensive study of farm productivity and technique in western Kenya (Jaetzold and Schmidt 1982). These data were used to develop transformities for local agricultural products (Table A-7). Average yields and input regimes were used for these evaluations.

For livestock, woodlot and forest sub-systems, literature data were acquired from Simpson and Evangelou (1984, Raikes (1983), Chavangi and Zimmerman (1987), and

ICRAF (2000) describing activities throughout Kenya. Generalized data, however, may fail to capture specific system details. For example, livestock systems in the basin vary dramatically with altitude, with communal grazing of indigenous (Zebu) cattle and other small ruminants dominating the lowlands and paddock grazing of improved breeds (e.g., Fresian hybrids) characteristic of highland animal husbandry. As such, two separate emergy evaluations were compiled for livestock land-uses.

No effort to modify yields based on soil functional performance measures or degradation status was undertaken. Observational studies like those outlined below for soil erosion assessment would be necessary to establish formal empirical linkage between soil degradation and crop yields.

Soil loss estimation

Soil loss rates were compiled directly from field observations described below (soil deflation estimation) for sites at which soils were judged intact. No sediment yield ratio was necessary because empirical rates were observed at the same scale as individual land-uses. Forest clearing rates were assumed equal to district rates. Total forest area was inferred from land cover classifications developed below.

Erosion Risk Assessment

Emergy analysis quantifies costs and benefits of competing land management scenarios, but relies heavily on estimates of soil erosion. For optimal land-use decision-making, it is critical that effects of alternative interventions to control erosion are correctly anticipated and that models identify regions of high risk accurately. Previous work (Cohen et al. 2003) illustrated critical accuracy limitations when universal models (e.g. USLE – Wischmeier and Smith 1978), which relate generalized site, soil and

management variables to soil degradation, are applied in the Awach River basin. To inform emergy-based decision support tools, models that effectively describe the association between specific land management decisions and soil degradation were necessary. These models are, of necessity, empirical and specific to the region. As a result, emphasis was placed on rapid assessment tools that would facilitate application in other large areas without requiring assumptions of similar degradation associations.

After compiling a list of potential contributing factors, a field sampling protocol was implemented to quantify site factors from direct observations and collect soil samples for subsequent analysis. Potential explanatory factors were grouped into three classes: 1) site characteristics (vegetation, land-use, soil surface descriptions), 2) soil characteristics (physico-chemical properties) and 3) hydrologic/terrain characteristics (infiltration capacity, rainfall, slope and slope length, site profile). For each class, a standardized statistical modeling framework was developed to reveal conditional association patterns between risk factors and soil degradation. The results produced multivariate risk equations describing degradation probabilities for each class.

To assess competing intervention scenarios, risk indices were extrapolated to the entire area and used within a cell-based (raster) stochastic spatial simulation. Calibrated interpretation of satellite imagery allowed interpolation of risk indices. Alternative land management options, presented as thematic spatial data layers, were used in conjunction with risk layers to produce degradation probability surfaces for each scenario.

This provides an estimate of costs; benefits are enumerated from emergy evaluations of each land-use. The Agricultural Benefit Ratio, computed on a cell-by-cell basis, provides one objective function for quantitative comparison of alternatives.

Three sections describe the methods in detail. The first describes data acquisition, sampling and pre-processing. For many variables, direct site-level observation was not possible (e.g. soil properties, hydrologic properties); methods for inference of these factors are presented in this section. Secondary data sources (e.g. terrain indices extracted from digital elevation data) are also described. The second, degradation risk modeling, describes statistical methods used to relate primary data to soil degradation and to enumerate overall degradation probabilities from the suite of predictors. The final section, decision support modeling, describes methods to compare land management scenarios spatially, ultimately linking predicted risk with emergy analysis results. This section includes methods of spatial data layer development from satellite imagery.

Quantification of Soil Degradation Factors

This section describes methods for rapid large area assessment, including observational sampling scheme and spectrometric tools for soil analysis. Results provide factor data necessary to develop statistical risk models and, coupled with digital image processing, provide the empirical framework for spatial decision support tools.

Field Sampling Protocol

Field data collection was undertaken primarily to gather ground observations of degradation and potential explanatory risk factors, controlling for confounding effects from sample points throughout a watershed. Where risk factors where not directly observable during on-site assessment (e.g. soil properties), the field protocol was designed to facilitate sample collection for later analysis. Finally, field data were carefully georeferenced to enable satellite image-based interpolation of each risk factor.

Sampling period and sample size

Field observations took place from February to June of 2001. Sampling coincided with maximum seasonal rainfall, and, consequently, maximum agricultural activity.

To cover the entire study basin adequately and control for variability outside of an experimental setting, a large sample size was required. Overall, 420 sites were sampled using the protocols described below to control for confounding factors.

Case-control sampling design and additional stratification

The field sampling protocol was designed to compare sites with obvious degradation (cases) to those that appear intact (controls). Case-control protocols have been widely used in medical studies where experimental control of risk factors is impossible (Agresti, 1990). The method, also called a retrospective study, approximately fixes marginal response distributions to maximize comparative statistical power. Visual classification of degradation was deemed sufficiently reliable for site selection purposes. It should be noted that, frequently, degraded and intact sites were not explicitly paired. Rather, within clusters and basin-wide, approximately equal proportions of intact and degraded sites were selected, controlling for major confounders.

Field sampling was stratified according to anticipated major confounders. Soil degradation status was the primary stratum, but sampling was further stratified by landuse, elevation and geologic substrate. Additional confounders exist (e.g. specific land management activities, slope, land-use history, distance from roads, hydrologic position), but these were controlled by random sampling within strata.

Land-use stratification was achieved by sorting sites into four main categories representing the fundamental divisions defined in the Land Cover Classification System

(LCCS - United Nations/FAO 1997). These were: 1) agricultural land, 2) rangeland, 3) forest/woodlots/shrublands, and 4) other (e.g. wetlands and severely degraded lands).

Detailed site descriptions and plot measurements further segmented these broad categories. Landuse subsystems of particular interest were subsistence and commercial crops, communal and constrained pasture, and natural/managed woodlands. Wetlands and severely degraded lands (gullies, surface crusting) were also targeted. Sample plots were homogeneous to minimize spectral mixing during satellite image analysis.

Spatial site distribution

The Awach River basin covers 360 square kilometers with limited road access; as a result, dense spatial coverage and evenly spaced sampling were impractical. Instead, a cluster-based sampling scheme was used in which 10-20 sites along a catena were sampled. Maps of geologic substrate and topography were consulted prior to initiating each new cluster to ensure that these confounders were controlled. Land-use and soil degradation stratification took place in the field.

Site protocol

Figure 2-3 gives the site sampling protocol schematic. To conform with the spatial grain of Landsat 7 satellite imagery, each plot was square with 30-meter sides. Differentially corrected GPS measurements were taken at each plot center. A central transect in the direction of steepest slope allowed placement of three within-site sampling positions (5, 15 and 25-m from the upslope plot margin) for sampling topsoil (0 – 20 cm), subsoil (20 – 50 cm), bulk density, infiltration, and for installation of erosion pins for surface deflation rate estimation.

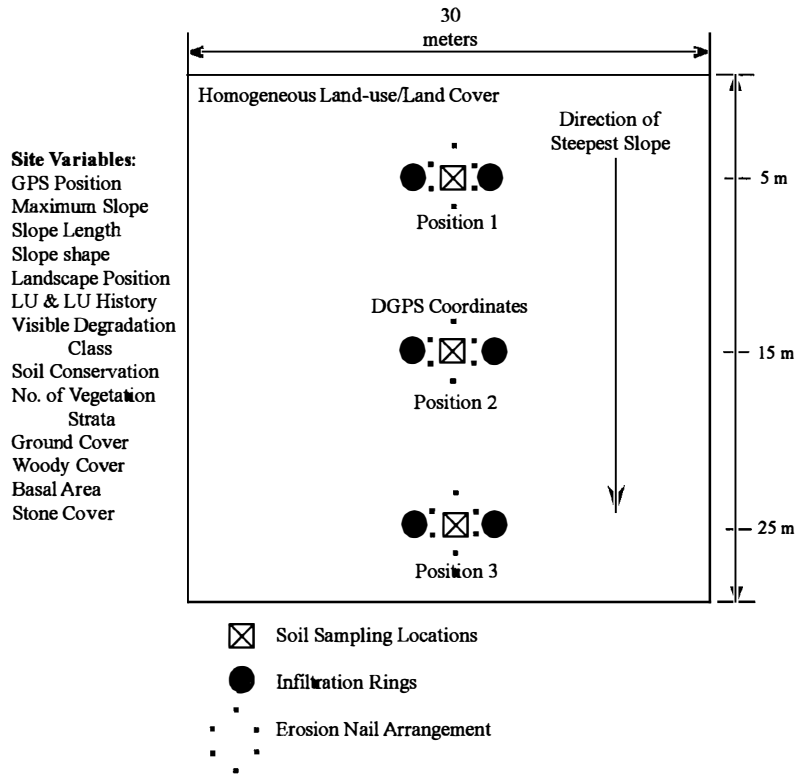

Figure 2-3. Site sampling protocol schematic.

At each site, potential predictors were noted; Table B-1 in Appendix B shows site data collection sheets. Site-level observations were divided into cover characteristics and hydrologic/terrain characteristics. Each terrain characteristic – slope, slope length, slope shape, hydrologic position – was observed directly and the presence and type of soil conservation structures were noted. Detailed cover characteristics included observations of structure (dominant life form, number of strata, basal area/density, ground vegetation height and canopy height), ecology (annual/perennial dominance, dominant leaf morphology, herbaceous/graminoid) and cover (woody vegetation cover, ground vegetation cover). Additional site observations included expected flooding frequency (i.e. dominance of wetland vegetation), land-use, land-ownership and land-use history.

Soil characteristics were divided into site parameters (depth to restriction, stone cover/grade, classes of soil erosion/hardsetting) and laboratory physical-chemical

measurements (pH, organic content, cation exchange capacity, texture etc.), obtained using high resolution visual/near-infrared reflectance signature analysis.

Visual degradation classification

Field designation of soil degradation was based on visual cues including presence of rills or gullies, evidence of root exposure, splash and vegetation pedestals, and evidence of sheet wash. Plots were assigned to five erosion classes: intact, mild sheet erosion, severe sheet erosion, persistent rills, and gullies. Sites where degradation status was not obvious (primarily agricultural sites) were classified as intact. Methods were subsequently developed to delineate degradation status based on spectral reflectance signatures, providing a more reliable and repeatable criterion. Soil hardsetting/crusting, a phenomenon where topsoil becomes impermeable due to particle sorting and organic matter depletion (Graef and Starr 2000), was visually delineated into binary classes.

Soil Sampling

Soil samples were collected at two depths (topsoil: 0-20 cm, and subsoil: 20-50 cm) at each of three within-site sampling locations. Samples were returned to the laboratory where they were air-dried. These were sieved using a 2-mm mesh to remove gravel and analyzed using spectral reflectance procedures outlined below.

In addition to primary soil samples, bulk density cores were taken at each within-site sampling position. A 10-cm core with a diameter of 5-cm with beveled edges was driven into the ground until it was level with the soil surface, and then extracted. The known volume of soil was placed in a plastic bag, weighed to establish approximate water content, then air dried and weighed again to establish dry bulk density.

Diffuse Reflectance Spectroscopy (DRS) for Rapid Soil Assessment

Soils characterization over large areas is expensive because empirical characterization requires substantial data sets. An emerging alternative to expensive laboratory procedures is the use of visible-near infrared reflectance spectroscopy for non-destructive analytical characterization. Extensive use was made of these methods in this work, including spectral regression models of soil properties from existing soil libraries and spectral classification of degraded versus intact soils.

Spectral reflectance signatures

Each soil sample collected during the field protocol (n = 1260 – 420 sites x 3 samples per site – topsoil samples only) was analyzed using a FieldSpec^{TM} FR spectroradiometer (manufactured by Analytical Spectral Devices Inc, Boulder, Colorado). Reflectance spectra were recorded at wavelengths from 0.35 to 2.5 μm with a spectral interval of 1-nm. Light was provided from a tungsten quartz halogen filament lamp (50W bulb; ~3200 K color temperature). Each sample was placed in a 12-mm deep, 55-mm diameter glass petri dish and placed on a platform directly above the light source. Reflected light was collected with a 25° field-of-view foreoptic at a distance of 5 cm from the sample. Reflectance spectra were recorded twice (rotating the sample 90° after the first observation); mean reflectance in each interval was used. Coefficients of variation in average relative reflectance were less than 1% for replicates spectra.

To calibrate the reflectance sensor to pure white prior to batch processing, ten reference spectra were recorded using spectralon (Labsphere®, Sutton, NH). Reflectance in each wavelength band was expressed relative to mean white reference readings.

Data processing

Data compression was necessary to allow manipulation within standard spreadsheet software. Raw reflectance spectra were resampled to 10 nm intervals prior to analysis, retaining the spectral end-points of 0.35 and 2.5 μm. Resampled data were then derivative-transformed using first order differentiation with second order Savitzy-Golay polynomial smoothing at 20 nm intervals (Feam 2000). This reduced variance between samples arising from optical set-up, ambient light conditions and fluctuating battery power conditions. Certain regions of the spectra had low signal-to-noise ratios due to spectrometer sensor splicing and inherent light source characteristics, and these data were omitted. The regions of omission were from 0.35–0.38 μm, 0.97–1.01 μm, and 2.46–2.50 μm. The remaining 198 10-nm spectral reflectance wavebands formed the basis of statistical signature analysis.

Soil spectral library

Soil spectral libraries were used to develop multivariate statistical models to predict laboratory soil characteristics from reflectance spectra. Shepherd and Walsh (2002) formulated the basic techniques used in this study. An extensive library of soils from western Kenya (n = 513), collected prior to this study and analyzed using a suite of standard laboratory methods, was used to develop calibrations between soil properties and spectral reflectance signatures. Standard soil laboratory analysis techniques are outlined in Appendix B, along with spectral regression model results. Soil properties included soil texture (% sand, silt, clay), soil organic matter, cation exchange capacity, pH, and exchangeable ions (P, Ca, Mg, K, Na). Calibrations were developed using classification and regression trees (CART) models.

Spectral outlier analysis

Model development using the spectral library approach is valid for assessment of new soils only if the new data fall with the calibration bounds of the library. For this work, the spectral library was developed for an area much larger than the Awach River basin, increasing the likelihood that the range of mineralogical and management variation was captured. To validate this critical assumption, a screening test based on principal components analysis was developed to identify soils collected from the Awach basin that exceed the calibration bounds of the spectral library.

A standard forward rotation principal components analysis (PCA) was performed on untransformed spectral library data to reduce data dimensionality and identify orthogonal axes that describe maximum soil spectra variance. The analysis was run using a centered variance/covariance cross-products matrix to minimize the effect of outliers on axis definition. In general, only those principal components axes that explain more variance than expected by chance are selected. Using the broken-stick eigenvalue method (PC-ORD – McCune and Mefford, 2000) that compares principal components axis explanatory power with the power expected in a random data set, significant axes were identified for further interpretation.

PCA is sensitive to effects of outliers. Using a standard Euclidean distance measure, outlier analysis identified those spectra from the library falling greater than 3 standard deviations from the mean. Seven (7) soils were identified using this distance criterion; in a data set of n = 513, the expected value for s.d.>3 is approximately 5. Principal components ordination was run with and without these prospective outliers to observe the strength of their effect. Two soils were identified for omission (C1052 and

C838; 6.12 and 5.73 s.d. above mean distance, respectively). All subsequent analyses were performed without these spectra.

After identifying significant ordination axes, the eigenvector matrix was pre-multiplied by reflectance spectra data from the Awach field samples (note that the Awach soils, collected during field sampling, are distinct from the calibration soil library). This process yields principal component scores for each sample, allowing new data to be projected into the spectral library data ordination space. Outliers were identified as Awach basin soils further than three-standard deviations from the spectral library mean.

Spectral visualization

The data compression provided by PCA also facilitates data visualization. To extract average and end-member soils, a sub-sampling protocol of spectra from principal component axes was used. Individual soil spectra were chosen for only the first two principal components. Of interest were spectra that represented component space end-members and average soils. The soil sample with a component score closest to the mean was selected along with soils with component scores closest to 2 standard deviations above and below the mean. In all, 6 spectra were selected in this manner and plotted to observe data set variability, both over the entire bandwidth and for specific spectral regions. All ordination was done using first-derivative transformed data, but graphical depiction was done with both raw reflectance and derivative transformed data.

Classification and regression trees (CART)

Analysis of multivariate soil signatures in this study was done using Classification and Regression Trees, grown using CART™ Version 4.0 (Salford Systems). This

statistical modeling approach was chosen for its strength in handling data sets with high dimensionality, multi-collinearity, and non-standard data structure (Urban 2002).

Classification and regression tree analysis is a non-parametric data-mining tool that uses recursive partitioning to analyze data with complex multivariate structure (Breiman et al. 1984). The result is a sequence of binary rules that form a decision tree by which data are sorted into target classes. The term classification refers to problems with categorical targets, while regression trees model continuous response variables.

One advantage of CART over other statistical classification methods (e.g. linear discriminant analysis, canonical ordination) is that no underlying probability distribution is assumed for either predictors or target variables, and because splitting rules are threshold-based, no normality transformations are required. Furthermore, classification trees are able to uncover contingent data structure and identify salient features of complex data sets without excessive parameter estimation, avoiding statistical power problems often observed with conventional analysis of complex data sets.

Recursive partitioning and splitting criteria. Tree models are developed according to a simple algorithm. Starting with a parent node containing an entire data set, binary questions are developed based on predictor variables – either continuous or categorical – that divide the data into increasingly pure daughter nodes. From the array of potential questions, the most effective is selected using one of several criteria (Siciliano and Mola 2000). Each criterion operates by selecting binary partition criteria that maximize some measure of purity (e.g. entropy, residual error) in the daughter nodes (Breiman et al. 1984). In developing tree-based models for this study, various splitting criteria were compared. In each case, the model with highest cross-validation accuracy was selected.

Tree pruning. Recursive partitioning occurs until each terminal node reaches a minimum specified node size. Frequently, however, the optimal tree is not the most complex. Excessive partitioning generally results in rule-bases that are unstable, and consequently inaccurate, when applied to new data sets. To avoid this overfitting problem, V-fold cross-validation was used, resulting in tree pruning based on trade-offs between complexity and validation misclassification costs.

Calibration using tree committees. To avoid problems introduced by the inherent assumption that local split optimality results in global model optimality (Breiman et al. 1984), committees of trees were grown using data resampling methods. Adaptive resampling procedures (ARCing), which adjust resample probabilities based on previous misclassification, were used instead of conventional bagging (bootstrap aggregation). A committee of exploratory trees (i.e. without pruning) is grown using repeatedly resampled data sets, assigning each datum to an outcome node based on the mean (for regression) or mode (for classification) of the committee.

Spectral calibrations of soil properties. Using the regional spectral library, a committee of trees was grown using spectral reflectance values as predictors, targeting each soil property. Library data were divided into calibration (n = 310) and validation (n = 203) data sets. Calibrations were developed using 200 or more committee trees. CART 4.0 (Salford Systems, 2000) retains splitting rules for each tree and automates rule-base application to new soil spectra, allowing validation accuracy assessment.

Where regression trees were unstable for a given soil property (validation r^2 of less than 0.50), binary screening tests were developed. Functionally significant

thresholds were defined from the literature (e.g. Sanchez 1973), providing a binary target variable for a classification tree grown using spectral reflectance predictors.

Case-reference definition

To discern factors associated with soil degradation reliably, objective measures of degradation status were required. While degradation was readily observed at some sites, human management may have masked visual cues that imply site degradation at others. Most notably, tillage can remove developing rills and vegetation pedestals from the soil surface. Furthermore, degradation mechanisms can be active prior to the emergence of visual symptoms, resulting in loss of soil quality without diagnosis. Since soil integrates physico-chemical indicators of degradation more reliably than site-level diagnostic cues, a soil-based case definition is preferable.

Sites were subjectively categorized according to field classification reliability. All sites (e.g., agriculture plots) for which ambiguity was noted during field sampling were categorized as uncertain (n = 441 soils from 147 sites). The case definition was developed using only samples for which visual classification was deemed reliable (n = 819 soils from 273 sites).

A classification tree was grown using the 198 spectral reflectance values as predictors and binary degradation status as the target variable. Each classification tree model was grown using 10-fold cross-validation. Prior class assignment probabilities were set to sample proportions. This maximizes model balance with respect to commission and omission error rate. For each model, total error in addition to omission (sensitivity) and commission (specificity) error are computed. The odds ratio provides a measure of model effectiveness, with an odds ratio of 1 implying no discriminant ability.

The model rule base was applied to delineate degradation condition of sites that were visually ambiguous and validate designation for sites that were readily classified.

Soil degradation effects

Using a site-level 5-class visual classification, soil properties predicted as described above were compared using standard ANOVA. In addition, hardset and non-hardset sites were compared. Soil properties were transformed, if necessary, to meet normality requirements, and Bonferroni contrasts at the 95% significance level were used to compare soil properties at each level of observed degradation. Similarly, soil properties were compared for the binary hardsetting classification.

This contrast analysis was repeated for soils designated intact or degraded by the spectral case definition. For this comparison, a Students's t-test was sufficient to determine if changes in soil properties were significant at the 95% confidence level.

Rainfall Erosivity and Infiltration Methods

Erosion risk resulting from hydrologic factors is frequently ascertained based on climatic forcing functions alone. However, rainfall erosivity, measured as an index of regional rainfall volume and intensity, is of limited empirical value because it is generally constant over scales characteristic of this study. It is theoretically well established that rainfall intensity is associated with soil particle detachment (Wischmeier and Smith 1978), but subsequent entrainment requires flowing water, which is driven by plot- and catchment-scale soil characteristics in addition to prevailing climate. Therefore, erosion risk may be more accurately estimated using measures of site infiltration rather than indices of prevailing climate. The following section describes methods for erosivity and infiltration measurement. Later sections will their compare predictive power.

Rainfall erosivity

Isoerodent maps that describe climatic contributions to erosion risk are not available for the Awach River region. Typically, rainfall erosivity (R) is computed as total storm energy (E – MJ/m^2) multiplied by the maximum 30-minute intensity (I_{30} – mm/h) (Renard et al., 1997). However, detailed data on storm intensity were also unavailable due to the regions remoteness and lack of monitoring infrastructure, necessitating utilization of proximate methods. One alternative (e.g. Millward and Mersey, 1999) employs a quadratic regression equation based on annual rainfall (see also Morgan 1995). Kassam et al. (1991) used a linear function of annual rainfall for a national erosion risk study for Kenya. Using only annual rainfall ignores strongly seasonal precipitation patterns that exacerbate erosion because of effects on cover. Rowntree (1983) concluded seasonality is a critical consideration for erosivity measurement in Kenya, suggesting the Fournier index as an approximation for local erosivity. This index relates mean annual precipitation to rainfall in the wettest month:

$$F_i = p_i^2 \div P_i \qquad [2\text{-}6]$$

where F_i is the Fournier Index, p_i is wettest month rainfall (mm) and P_i is annual rainfall (mm). The subscript i indicates that calculations were done on a cellular basis using mean annual and mean monthly rainfall (Corbett et al. 1997).

Infiltration field protocol

To quantify site level hydrologic response and explore how local infiltration rates affect erosion risk, a sampling protocol was devised to estimate infiltration rates at numerous sites throughout the landscape. These data are used later to interpolate infiltration behavior to the entire basin based on satellite image interpretation. Infiltration

tests were performed in conjunction with site and soil sampling, ensuring stratified observations by landuse type, degradation status and spatial location (i.e. elevation, etc.).

Infiltration assessment was performed on 61 sites. At each of three within-site sampling positions, two infiltration rings were set in the ground after pre-wetting, resulting in a total of six replicates per site (Figure 2-3). Single-ring design was used to minimize transportation costs between sites. Bouwer (1986) suggests that double-ring infiltrometers are unnecessary for field-testing infiltration rates.

Each infiltration cylinder was 20 cm long of 15 cm in diameter. While Bouwer (1986) recommends that ring diameters exceed 1 meter, these dimensions were deemed adequate given the logistics of field sampling in remote areas. One end of each ring was beveled to facilitate soil penetration. Each ring was set 3-5 cm into the soil surface to avoid leaking; penetration distance was minimized to reduce surface disturbance. Before each ring was set, surface litter, small rocks and woody plant material were cleared, and the site was investigated for macro-pores and cracking. Where possible, these features were avoided, but where cracks or leaks were discovered, they were noted.

Each cylinder was filled completely using water from Kisumu municipality, which was judged free of excessive sediment load, and maintained at ambient air temperature. The time at which the cylinders were filled was noted, and water depth was measured every five minutes for one hour from the cylinder rim. Falling water levels introduce error due to changing gravity head in the infiltration model form, but was necessitated by problems with transporting sufficient water to run constant head tests. After each infiltration test, cylinders were rinsed and dried to avoid rusting.

Data processing

Due to sampling protocol time constraints, antecedent soil moisture conditions were uncontrolled. As a result, high initial infiltration rates were observed, indicating that cumulative infiltration could not be represented as a linear function of time where slope predicts saturated conductivity. The Horton equation (Horton, 1940), which has been widely used to describe the decay behavior of infiltration over time, takes the form:

$$f_p = f_c + f_o \times e^{(\beta \times t)} \quad [2\text{-}7]$$

where f_p is the infiltration capacity, f_c is the saturated infiltration rate (which tends to be slightly smaller than the saturated hydraulic conductivity K_s – Haan et al. 1982), f_o is excess infiltration capacity at $t = 0$ (i.e. rate of infiltration increase above f_c), and β is a soil parameter that controls the rate of decrease in infiltration rate (a negative number).

Data were collected as cumulative infiltration over time. The integral of the Horton equation with respect to time provides the following function of cumulative infiltration (with integration endpoints: time = 0 and time = t):

$$F_p = f_c \times t + (f_o/\beta) \times (1 - e^{\beta \times t}) \quad [2\text{-}8]$$

where F_p is cumulative infiltration. This model form was applied to data from each infiltration replicate to estimate base infiltration rates (f_c) and initial infiltration rates (f_o).

Model fitting

The Horton integral function cannot be transformed to linear form, so a non-linear regression fitting-algorithm (bounded quasi-Newton optimizer –Mathsoft Inc. 1999) was applied to data from each infiltration replicate to estimate parameters using a minimized least squares fit criterion. To ensure that fitted parameters represent the likelihood function global minima, various starting parameter values were used. Model validity was

also checked by visually inspecting each fit, and ensuring that estimated parameters were reasonable given the existing theoretical framework (i.e. $\beta \leq 0$, f_c and $f_0 \geq 0$).

Spectral reflectance modeling

The fitted parameter describing base infiltration rate for a given soil was assigned as the target variable for a regression tree model built in CART. Given the limited precision with which infiltration can be measured using the protocols described, and the inherent uncertainty associated with using soil reflectance to predict a physical property that is strongly dependent on soil macro-structure, classification trees were also grown after sorting the data in functional infiltration classes. A threshold infiltration rate (60 mm/hr – Brooks et al. 1997) was chosen to delineate low infiltration sites expected to generate runoff during an average intensity storm. A screening model based on spectral reflectance was developed targeting this resulting binary variable. To estimate infiltration rates for each site for which infiltration data were not collected (n = 359), the cross-validated spectral models developed for the 61 sample sites were extrapolated.

Infiltration transfer function

Infiltration is a composite variable frequently estimated based on more readily observable soil properties (e.g. texture, soil organic carbon). While spectral calibrations allow direct inference, identifying soil factors that lead to slow infiltration is useful information. Targeting the binary screening classification, standard logistic regression methods were used to identify risk factors that contribute to increased probability of slow infiltration. The resulting fitted model quantifies association effect direction and strength between infiltration and soil properties, providing an empirical transfer function.

Infiltration transfer functions based on soil properties allow regions that might exhibit low infiltration rates if human management were absent to be identified. This is particularly important for agricultural soils that may retain residual hydrologic enhancement from tillage, but in their equilibrium state inhibit infiltration.

Surface Deflation Estimation

Erosion pin sampling

Categorical classification of observed erosion status has limited value for quantifying soil loss rates; quantitative estimates of soil loss, measured as surface deflation over a known period, were achieved using erosion pins. Each pin (a 12 cm steel nail) was hammered into the ground until the nail head was level with the soil surface. At each within-site location, 6 pins were installed in a radial pattern (Figure 2-3), for a total of 18 pins per site. Pins were not installed at sites exhibiting active surface disturbance.

After three months (long rains – March through June), each site with erosion pins was revisited. Pins were relocated using a metal detector, and exposure was measured. Bulk density measurements informed conversion of measured surface deflation to soil mass. Annual loss rates were assumed double measured rates because rainfall during the three-month sampling period is typically half annual rainfall (Corbett et al. 1997).

Mixed-effects data processing

Surface deflation data were used to quantify erosion rates according to landuse and observed degradation status. However, substantial within plot variability was expected due to the scale at which individual rills and splash pedestals form. To account for within-site variance, a linear mixed effects modeling approach was used (MathSoft Inc. 1999). This process is similar to nested analysis of variance with multiple

treatments; it is widely used for modeling grouped data (Venables and Ripley 1999). Rather than using mean nail exposure at each site, raw data are used in a model form that partitions total variance into between plot fixed effects (the objective) and within plot random effects. Fitted fixed effect parameters describe the variance explained by the selected sorting variable (e.g. landuse, erosion status). Significant differences between effects under different sorting variable classes are inferred in the standard way.

Odds Ratio Analysis of Landuse Degradation and Infiltration

While pairwise analysis is generally discouraged when confounder effects can be controlled in a multivariate setting, observed associations between different factors (landuse, cover etc.) were evaluated with respect to binary soil degradation and infiltration classes as a first step in evaluating alternative erosion control scenarios.

Odds ratios (Agresti 1990) were used to relate degradation and infiltration to an array of site-level and landuse factors. They quantify the association between binary variables in a two-way contingency table. Odds are defined as a binomial proportion divided by its complement, and the ratio of odds for a 2x2 table provides information on the extent to which the conditioning variable affects the probability of the outcome. Odds ratios equal to 1 indicate variable independence; values greater than 1 indicate positive association. An asymptotic estimator of standard error allows standard statistical inference. It was impossible to condition on all potential sorting variables using this pairwise approach; statistically controlled evaluation of conditional effects using mixed-effect logistic regression modeling provides substantially more information.

Where a two-way contingency table is insufficient to capture variable associations, or evidence of Simpson's paradox (Agresti 1990) exists, multi-way

contingency tables can be employed. In this situation, two or more sorting variables are used, conditioning the observed effect of one variable on the state of another. In this manner, evidence of interaction between variables can be quantified.

Terrain Analysis

Every model of soil erosion includes some measure of topography as a risk factor. The Universal Soil Loss Equation includes two terrain-based factors: slope and slope length. While direct observations were made of both these quantities during field sampling, and would be sufficient to delineate risk for sampled sites, interpolation of observed associations between terrain and erosion to entire regions required a reliable Digital Elevation Model (DEM). This facet of predicted risk is particularly important because frequently cited works (Desmet and Govers 1996, Wilson and Gallant 1996) indicate that simple GIS-based terrain models can provide effective diagnostic tools for remote erosion risk assessment. For example, Gallant (1999) suggests that terrain-based indices can illustrate dominant spatial patterns without process modeling because terrain directly informs physical hydrologic system behavior.

Digital elevation model development

A DEM was developed for the region using 1:50,000-scale topographic maps (Belgut and Nyakach quadrangles - Survey of Kenya, 1978) with a vertical resolution of 20 meters. Contour lines and river courses were manually digitized, rasterized (to 30 meter cells), and linearly interpolated. Concurrent with field sampling, several thousand spot heights were collected using survey-grade GPS readings of altitude and position, and included during interpolation. Artifacts, depressions and angularity introduced by linear interpolation were removed using a 3x3-kernel smoothing filter. The DEM was projected

into Universal Transverse Mercator coordinates (zone 36 South, Clarke 1880 spheroid) for integration with satellite imagery and ground sampling points.

Terrain-based indices

Through digital terrain analysis, a suite of topographical attributes can be derived to produce maps characterizing landscape morphology. Several simple inferences are automated within geographic information systems, including slope, aspect, slope shape, and watershed accumulation algorithms (Clark Labs 2001). The sediment transport index (Moore et al. 1993) was selected for its simplicity and data parsimony:

$$T_s = [A_s / 22.13]^m \times [\sin \beta / 0.0896]^n \quad [2\text{-}9]$$

where T_s is sediment transport capacity, A_s is the hydrologic contributing area, $\sin \beta$ is the slope gradient and m and n are constants. The equation contains two components: 1) hydrologic accumulation and 2) water velocity. The first is analogous to slope length factors common to many models. The second, using slope as proximate to overland flow velocity, is based on unit stream power theory. Areas with high sediment transport capacity are predicted to be at elevated risk of erosion; where the first derivative of the index is negative, deposition is predicted.

Soil Degradation Modeling

Using primary data collected above, statistical models were developed to relate potential explanatory factors to observed degradation status. Three complimentary models were initially developed, followed by development of an overall risk model:

- Variables characterizing site conditions (SITE)
- Physico-chemical soil properties (SOIL), predicted using regression tree models
- Hydrologic and terrain variables (HYDRO/TERRAIN).

The basic modeling tool is mixed effects logistic regression. However, as with all linear modeling techniques, multi-dimensionality constraints to statistically powerful model development exist. To reduce model dimensionality and eliminate predictors that are conditionally independent of soil degradation, graphical models were used.

Standard and Mixed Effects Logistic Regression

Site condition was not described using a continuous variable. While sites were visually designated into 5 classes, spectral methods were used to classify sites only into binary categories: degraded and intact. Since the spectral case-reference definition provides the most robust assessment of soil condition, all risk factors needed to be statistically related to a binary outcome, necessitating use of logistic regression (Agresti 1990) where continuous and categorical variables are used to predict the probability of a positive outcome. Since probabilities are constrained between 0 – 1, a link function is necessary to allow predictors to remain unconstrained. The most widely used, the logit link, is defined as $\ln (p / 1 - p)$, where p is the proportion of positive outcomes; this link results in the characteristic logistic curve shape. Logistic models are fit using maximum likelihood, and goodness-of-fit assessed using statistical deviance.

The sampling design used in this study results in three soil samples per site. Each was spectrally categorized as intact or degraded, but within-site disagreement was evident. One method to deal with this disagreement is to consider only those sites with two or more soil samples screened positive as degraded. However, this approach fails to recognize the heterogeneity of soil degradation. By assuming within-plot observations are dependent because of nested sampling, a more realistic statistical relationship can be obtained. Mixed effects models use within-site variability as a model component. For

mixed effects logistic regression (both binary and ordinal), specific software was required (MIXOR v. 2.0, D. Hedeker and R.D. Gibbons - Discerning Systems Inc. 2000). MIXOR models are fit using a restricted maximum marginal likelihood solution.

Graphical Modeling

In each model, the number of potential predictors is large. Multi-dimensionality substantially reduces statistical power for estimating conditional effect strength within a logistic regression model. Standard backwards elimination procedures can allow model parsimony to be optimized, but frequently stepwise deletion criteria are not flexible. In particular, use of the Akaike Information Criterion (AIC) for variable deletion often results in more complex model forms than those selected using deviance or Bayesian Information Criterion (Edwards 1995).

To avoid co-linearity issues and provide graphical output that allows rapid interpretation of complex association patterns, graphical modeling, an extension of hierarchical log-linear modeling, was used. A detailed description of this approach can be found in Edwards (1995). Software designed specifically to execute graphical models is called MIM v 3.1 (Edwards 1995). The resulting models list all variables as graph nodes with arcs linking nodes that are conditionally associated. No implication of causal influence is implied, simply statistical association. The results offer rapid and efficient screening of conditionally associated predictors for all subsequent regression analyses.

All graphical models in this study were initialized to homogeneous saturated models (all variables are assumed associated with all others). Stepwise deletion algorithms were used to remove arcs sequentially based on deviance comparison of models with and without a specific arc. Difference of deviance is chi-squared distributed

with degrees of freedom equal to the number of eliminated parameters. The arc with the highest deletion probability is removed, defining a new model, from which the sequential process again attempts to remove non-significant arcs. This proceeds until no arcs have deletion probabilities greater than the critical significance level. Arc deletion at α = 0.001 level of significance throughout this work ensured that only strong conditional associations would be used for predictive modeling. Settings for deletion protocols included coherent backwards selection and restricting models to decomposable forms.

Site Level Risk Factors (SITE)

Graphical models were used to determine conditional associates of observed degradation status among site variables. These include landuse, vegetation and stone cover, and structural characteristics (e.g. leaf morphology, life pattern, height). After relevant associations were identified, association strength and direction estimates were computed using mixed effects logistic regression. Model significance, estimated using the Likelihood Ratio Test (LRT), compares current model deviance to null model (intercept only) deviance to provide a global goodness-of-fit metric. Model residuals were explored to ensure that implicit model assumptions were not violated.

Model sensitivity (correctly predicted yes outcomes), specificity (correctly predicted no outcomes) and predictive odds ratio were computed for each model to provide further indicators of model fit to observed data.

Soil Erodibility Risk Factors

A soils ability to resist detachment, by either raindrops or flowing surface water, is the conceptual quantity that soil erodibility describes. This portion of the study compared existing models of soil erodibility with observed degradation, and, where

universal models were inadequate, developed empirical alternatives using the analytical framework of graphical modeling followed by mixed-effects logistic regression.

Prospective analysis assumption

Soil erodibility affects erosion risk, but the compliment also holds: soil erosion affects a soil's inherent ability to resist erosion. The standard nomograph is based on properties (e.g., soil carbon and silt content) that are expected to diminish due to preferential entrainment as soil erosion proceeds. Therefore, soils with evidence of advanced erosion should exhibit qualities that indicate increasing resistance to erosion.

As such, defining erodibility according to observed conditions at the time of soil sampling may provide incomplete or misleading results. The optimal manner to circumvent this problem is to design a prospective study that first measures soil properties and subsequent erosion rates. The current study could provide such a baseline if observations of post-sampling degradation were made.

In order to make use of the existing data set, the assumption is made that sampled data are prospective: that is, erodibility can be estimated based on observed erosion status during soil sampling. This assumption will be corroborated using linear regression between erosion-pin estimates of erosion rates observed after soil sampling and predicted erodibility. A positive association provided evidence for assumption validity.

Standard USLE soil erodibility nomograph

Extensive experimental data sets (Renard et al. 1991) have shown substantial variation in erodibility between soils; empirical models relating specific soil properties to predicted erodibility have been developed. The most widely used of these is a nomograph (USLE - Wischmeier and Smith 1978) that relates readily measurable soil

properties to experimentally observed erosion rates. This nomograph, common to many soils analysis texts and omitted here, can be summarized in equation form:

$$K_{fact} = (1.29)[2.1E\text{-}6 \times f_p^{1.14} \times (12 - P_{OM}) + 0.033 \times (S_{str} - 2) + 0.025 \times (f_{perm} - 3)] \quad [2\text{-}10]$$

$$f_p = P_{silt}\,(100 - P_{clay}) \quad [2\text{-}11]$$

where K_{fact} is estimated soil erodibility based on P_{OM} = % soil organic matter, P_{silt} = % silt content, P_{clay} = % clay content, S_{str} = soil structure index and f_{perm} = soil permeability index. The latter two are adjustment factors (second estimate factors).

Using soil properties inferred from spectral reflectance, the association between predicted soil erodibility and observed degradation was determined using mixed effects logistic regression with nomograph-predicted erodibility as the only predictor.

A second check of the standard nomograph for predicting erosion in the study basin was based on the following discussion about applicability of concurrent measurement of degradation and soil properties to predict degradation. Using a Kenya Soil Survey 1:250,000 regional soils map (Andriesse and van der Pouw 1985), polygons of distinct soil types were identified. Erodibility estimates at all sites spectrally judged intact and falling in the same soil polygon were averaged. Using satellite image interpolation of degradation (described below), the proportion of each soil polygon predicted as degraded was determined. A linear regression relating the proportion of degraded land in a polygon to mean predicted erodibility of intact sites in that polygon was used to characterize the predictive power of the standard nomograph for this region.

Local erodibility (SOIL)

Given edaphic and climatic differences between where the USLE erodibility calibration was performed and this study area, the predictive ability of standard methods

was uncertain. An alternative to global methods is empirical development of a regional erodibility index given observed soil properties.

The entire suite of soil properties was placed into a graphical model that included soil degradation status. Conditionally dependent predictors were defined using standard graphical model protocols. These predictors were used within a mixed effects logistic regression model to determine association strength and direction. The resulting fitted logit model provides a formula similar, though unitless, to Eq.2-10 and 2-11.

Hydrologic and Terrain Risk Factors (HYDRO/TERRAIN)

The third class of risk factors used to develop regional soil degradation models includes those variables describing local sediment transport capacity. Sediment transport capacity conceptually lumps hydrologic behavior and basin geomorphology. Using Universal Soil Loss Equation terminology, factors R, L and S are combined. A suite of potential variables for estimating each factor was compiled for comparison, and a hydrologic/terrain model of erosion risk developed.

Hydrologic variables

Site-level infiltration, inferred from spectral reflectance modeling. is the primary predictor. Annual rainfall amount and erosivity, estimated using the Fournier Index, were included as factors in this analysis. Soil depth restrictions are assumed to indicate reduced potential to absorb precipitation, and were included as a risk factor. The presence of conservation structures, generally designed to impede or eliminate surface runoff, was used as a predictive variable despite the observed rarity of these efforts in the region. Finally, evidence of frequent flooding, a binary variable, was included.

Terrain variables

Slope, slope length and slope shape were all quantities observed during field sampling. However, there is substantial benefit in models that obviate the need for ground sampling, instead relying on digital elevation data. The sediment transport capacity index presented above is one indicator that has been proposed as a tool to delineate rapidly between high risk and low risk areas over large areas using only a DEM.

Using standard GIS commands (Clark Labs 2001) to define drainage networks and accumulation patterns throughout the basin, estimated hydrologic convergence (A_s in Eq. 2-9) was computed for each cell; this quantity is intended to represent slope length. The slope of the cell (β in Eq. 2-9) was also inferred from the DEM. Model exponents (n and m in Eq. 2-9) were set at 0.6 and 1.3, respectively. Sediment transport capacity estimates at each site were extracted from the coverage resulting from GIS application, providing an additional predictor variable for model development.

Model development

A standardized risk factor modeling framework combining conditional associated variable identification using graphical models, followed by mixed effect logistic regression to quantify effect direction and strength, was followed using all hydrologic and terrain variables available.

Overall Risk Model Development

Each fitted model (site, soil, hydro/terrain) results in an equation that quantifies a continuous risk factor. The combination of these three risk factors into an overall risk model was performed, again using mixed effects logistic regression. This overall risk factor model defines the probability of degradation given all prospective explanatory

variables, and allows conditional odds of degradation to be quantified for each landuse. Conditional degradation odds provide the basis of spatial decision support modeling.

Spatial Inventory and Decision Support Modeling

To define land management strategies that maximize real wealth across an entire landscape required 4 major steps:

- Predict emergy yields for each landuse given climatic data and soil degradation status,
- Define soil degradation risks given a comprehensive list of potential explanatory factors, including land use,
- Interpolate risk models over basin using satellite image processing,
- Compare alternative land-use scenarios, based on inferred change matrices between 1986 and 2001, given computed risk and yields.

Steps 1 and 2 have been presented; steps 3 and 4 are explained below.

Satellite Image Analysis

Plot data were used for spatial decision support after interpolation. An array of geostatistical tools exists for spatial interpolation given certain geographic sampling constraints. The most widely used are simple inverse distance weighting (IDW), kriging and spatial simulation. All rely on the core concept of spatial autocorrelation and make the simplifying assumption that proximity can be used to predict condition. This assumption is hypothesized to be inadequate for the local condition due to fine-grain landscape heterogeneity (resulting in large semi-variogram nugget variance) and distances between sampling locations (resulting in sites being further apart than the range of auto-correlation). Satellite image processing offers the most viable alternative for statistical inference of site characteristics from field observations, and extensive use was made of remotely sensed data to create maps necessary to evaluate land use scenarios.

Satellite image acquisition and pre-processing

Two Landsat 7 ETM scenes (Path 169 Row 60, and Path 170 Row 60) were required for basin coverage. These were obtained for 3 and 10 April, 2001, respectively. The scenes were radiometrically corrected to adjust for sensor drift, solar angle variation and variable atmospheric interference (mean r^2 for band-by-band regression corrections = 0.955), then mosaicked using pseudo-invariant ground features in the region of scene overlap (Jensen, 1996). A spatial subset of the mosaicked scenes covering the Awach Basin was extracted. For both radiometric and geometric correction, the first scene (Path 169, Row 60) represented the reference image because it contained 80% of the basin.

Formal geometric registration, done only for the image subset, was based on 18 identifiable landscape features (e.g. road intersections, quarries, river confluences) that were georeferenced and differentially corrected during field sampling. A first-order affine transformation with nearest neighbor resampling (Clark Labs, 2001) was used, with a root-mean square (RMS) error of 0.34 pixels, or approximately 10 m.

Satellite imagery from February 1986 was also obtained for the region. Radiometric and geometric corrections of the 1986 scene were performed using the 2001 scene as the benchmark. Radiometric correction was done using band-by-band correlation adjustments of gain and offset (Jensen, 1996), determined from regressions between band reflectance from pseudo-invariant targets for 2001 versus 1986. The mean coefficient of determination value for radiometric regression models was 0.96. Geometric registration, using linear interpolation, was achieved using 9 points distributed throughout the study area. Spatial root-mean-square error was 0.65 pixels (~ 20 m).

Data extraction

GPS coordinates from each field plot allowed reflectance data in six Landsat bands (excluding the thermal band) to be extracted to provide classification model predictors. In addition to reflectance data, several standard indices were computed as additional predictors. These included the Normalized Difference Vegetation Index (NDVI – Jensen 1996), a spectral measure of vegetative biomass, and various band ratios (Band3:Band1, Band5:Band3, Band5:Band2, Band 2:Band1, Band4:Band3, and Band3:Band2). These ratios were selected using a t-test to describe the degree to which mean values were different between intact and degraded sites. Only those band ratios showing significant differences at $p = 0.05$ were selected for use in further analysis.

Image classifier algorithms

Standard methods for image supervised classification include linear discriminant analysis (LDA), wherein models are fit to minimize within class variance and maximize between class variance, and a maximum likelihood (ML) algorithm based on Bayesian inference of posterior class probabilities from category means and variance/covariance information. These were explored in this study in comparison with tree-based methods. Tree-based methods have a distinct advantage over linear statistical tools in that predictor collinearity and normality are irrelevant, and contingent data structure can be elucidated. Accuracy assessment is done using standard error matrices for both calibration and validation. Standard summary statistics for model accuracy assessment (Kappa, Chi-squared goodness-of-fit) are computed for each model.

Detailed validation accuracy comparison of the LDA and ML methods with tree-based methods was performed. Trees were grown using CART 4.0 based on the same

predictor data available to LDA and ML. Results indicated that tree-based models outperformed standard supervised classification methods by upto 30%. As a result, decision tree models were used for satellite image processing throughout this work.

To translate rule-bases provided by CART into digital images, the Knowledge Engineer/Expert Classifier module in ERDAS Imagine 8.5 (Leica Geosystems 2001) was used. All other satellite image processing and GIS analysis were done in Idrisi v32 Release 2 (Clark Labs 2001).

Each model was evaluated using several summary indices. Most important was overall accuracy (% correct). Accuracy values were reported for both classification and cross-validation. Also important for binary classifications were sensitivity (correct positives), specificity (correct negatives), and odds ratios. Note, however, that for models predicting binary variables with low case prevalence, odds ratios can be misleading and attention should focus on sensitivity/specificity measures of model fit. For multi-category classification models, a matched pair index called Kappa (Agresti 1990, Jensen 1996) was computed. Kappa ranges from –1 to 1, with values closer to 1 indicating strong convergence of model predicted and observed classes.

Spatial Inventory

Extracted satellite image data were used to develop cross-validated classification tree models to produce spatial layers that provide inventories of current and recent conditions in the Awach basin. Inventory coverages were developed for degradation classes (binary and ordinal), infiltration classes and landuse.

Landuse in particular presented classification challenges. Many land-uses were spectrally similar due to the time of year (early growing season) for which the scenes

were obtained. Specifically, subsistence agriculture appeared similar to bare soil; managed forests could not be distinguished from communal forests; and wetlands, dense pastures and sugarcane had similar reflectance spectra. Field classification of land-use was made regardless of synoptic cover conditions, degradation status, elevation (a proxy for precipitation) or geologic substrate, confounding spectral similarity within land-use classes. To compensate for spectral confounders, ancillary data were added as predictors, including elevation, slope, geologic substrate and reflectance variance (5x5 kernels).

Change Detection 1986-2001

Rule-bases for interpreting satellite imagery to assess degradation, slow infiltration and landuse at each pixel were applied to the 1986 scene. Several direct comparisons between years were performed. First, a comparison of NDVI values (Jensen 1996) provided spatial patterns of vegetation reduction between sample times. Second, proportional changes between 1986 and 2001 were computed to evaluate the direction and magnitude of changes in the basin. Finally, conditional change matrices were developed for landuse, degradation and infiltration class. These matrices, also called Markov matrices (citation), contain pixel counts for each conditional transition (e.g. dense pasture to degraded pasture), which are converted to transition probabilities, describing the likelihood of a pixel becoming any given class in the future given present class membership. A transition probability matrix is essential to formulating future landuse maps under a variety of land allocation scenarios.

Spatial Model Development

Natural resource management requires decision support tools that provide reliable predictions about consequences of competing alternatives. For soil erosion, risk factors

can be divided into two groups: a) variables that can be managed and b) variables that must be accommodated by management. The first group is contingent on the second; certain variables define the context and constraints within which land use decisions are made. The decision support model for this region therefore uses the spatial pattern of these contextual variables so that land management tradeoffs can be quantified. Specifically, the model provides probabilities of soil degradation for various land-uses according the location for which they are proposed. These probabilities can be related to actual soil loss based on surface deflation data, and linked to emergy yields for each proposed alternative landuse to determine the net benefit of that activity. Maximizing agricultural benefit provides the model objective function. This model, linking risk and sub-system environmental accounting, has four main parts:

- Rasterized risk inference conditioned on assigned landuse.
- Maps of proposed landuse scenarios.
- Expected Agricultural Benefit Ratio for each landuse, contingent on degradation status and elevation class.
- Stochastic simulation that links degradation probabilities, landuse change trajectories and anticipated yields.

Spatial erosion risk inference

All three risk factors (site, soil, hydro/terrain), arising from fitted logistic regression models, were spatially interpolated as the foundation of a landuse decision support model. Interpolation procedures were different for each factor. For the hydro/terrain factor, interpolation was done by developing maps for each of the component variables (e.g. infiltration, soil depth, slope, terrain indices, slope shape). In contrast, the soil factor was interpolated directly using satellite image reflectance data. The primary reason for this is that there is limited utility in spatial inference of individual

soil properties from satellite imagery when the target of interest is a composite soil variable. Ideally, geostatistical interpolation would contribute to soil risk surface development, but the spatial extent and heterogeneity of the study area limited application of these tools. Finally, the site management factor included one variable that was interpolated separately (stone cover), with the remainder based directly on landuse, or on inference about characteristics (vegetation cover and height) of each landuse.

Overall risk was computed on a cell-by-cell basis using interpolated risk factor values, applying parameters from the fitted overall risk logistic regression model.

Soil risk interpolation: Soil erodibility is defined as a function of select soil properties, identified using graphical modeling. A model was used to relate erodibility scores, defined by the fitted model containing these select soil properties, to reflectance data. The association between cover and erodibility was assumed sufficiently strong to implement a regression model despite vegetation confounding effects.

Erodibility scores were quantitatively defined by the fitted logistic regression model. Because both predictor (satellite reflectance data) and target (erodibility score) are continuous and unconstrained, linear regression was considered the appropriate method. Stepwise multiple regression with variable deletion based on the Akaike Criterion was the selected protocol.

Site risk interpolation: Site risk is a function of landuse and land cover characteristics. Landuse was inferred directly for 2001 and 1986, and scenarios were developed for 2016, outlined below, for assessing erosion control interventions by landuse transitions. In addition to landuse, the site risk model contained information about cover and structure that can be inferred from satellite imagery. For assessment of

future landuse scenarios, nominal levels of cover and structural characteristics for each landuse were used. This assumption ignores within landuse management variability, which was substantial, particularly as a function of elevation. However, absent of detailed component models, this simplification was necessary.

Hydro/terrain risk interpolation: The hydrologic and terrain indices identified as conditionally associated with degradation were each interpolated separately. Infiltration rate classes were already interpolated using satellite imagery, and many of the factors are derivatives of the DEM that can be produced directly. Slope shape was inferred using a terrain analysis tool in Idrisi (Clark Labs 2001), which classifies pixels into 12 topographic classes. These were aggregated into the four classes used to characterize sites during field sampling: straight, convex, concave and variable. Soil depth was modeled as a function of slope and degradation status.

Overall risk model: The overall risk model is applied directly from the fitted logistic regression model that integrates the three risk factors. The resulting map of logit scores was translated into degradation probabilities and evaluated against existing maps of degradation inferred directly from satellite imagery after classifying the model predicted probability map into binary categories. This was done for 2001, for which the model was developed, and back casted to the 1986 condition as a test of model validity.

Inherent risk: For later analysis it was useful to delineate risk into two categories: management sensitive, or adjustable risk, and management insensitive, or inherent risk. Adjustable risk can be amended by decision makers on the ground, while inherent risk arises from site characteristics that are inflexible. Inherent risk was defined as the weighted sum of soil and hydro/terrain risk factors. While portions of both factors (e.g.

soil organic carbon and infiltration) are sensitive to management decisions, they are treated as fixed variables, primarily because rates of change of these factors are unknown.

Landuse scenario development

Change scenarios were divided into two types. The first explored changes in relative proportions of land use types to improve conditions in the basin. The second change scenario allocated landuse weighted according to landuse degradation probabilities and inherent site degradation risk.

Proportional adjustment scenarios: Forecasting landuse changes was achieved using a stochastic Markov model. The Markov transition matrix, containing conditional probabilities for each landuse transition, was manipulated based on scenarios presented below. Stochastic simulation was applied to the current landuse map based on revised transition probabilities to produce a future landuse map.

This process is automated in Idrisi (Stochastic Choice Module) (Clark Labs 2001). The conditional probabilities for a specific pixel are summed beginning with the first transition and compared with a map of random numbers between 0 and 1. The landuse class at which the cumulative sum exceeds the random threshold is the class to which each pixel is assigned. The resulting image is distinctly less homogeneous than input landuse maps, and different output images result from each module run.

Changes in transition probabilities were constrained by the requirement that transition probabilities from a specific landuse type sum to 1 (transition probabilities to any landuse type could be more or less than 1 depending on whether that landuse was declining or increasing in time). For the scenarios presented below, transition probabilities were changed for a specific landuse, which required adjusting other

transition probabilities to meet this constraint. Each transition probability was adjusted by the same proportion rather than the same absolute value.

Eight different landuse scenarios were developed for comparison within the spatial model, including the scenario where transition probabilities are left unchanged.

- Scenario 1 (Do Nothing) – assess predicted future landscape in the absence of any changes in the transition matrix.
- Scenario 2 (Commercial Agriculture) – change transition probabilities such that the probability of any landuse converting to commercial agriculture doubles.
- Scenario 3 (Reforestation) – increase the transition probability to both forest and shrubland by 50% each.
- Scenario 4 (Reduced Livestock Density) – decrease the transition probability to sparse pasture, and increase the transition probability to dense pasture by 50%.
- Scenario 5 (Active Badland Restoration) – keep transition probabilities constant for active landuse types (pasture, agriculture) but increase transition probability between severely degraded lands and shrublands by 50%.
- Scenario 6 (Combined Efforts) – simultaneously increase commercial agriculture by 50%, increase forest and shrubland cover by 25%, reduce degraded pasture transition probability by 25% and increase transition between severely degraded lands and shrublands by 25%.
- Scenario 7 (Radical Transformation) – deforestation and wetland encroachment stops (transition probabilities go to zero), severely degraded land transitions to shrubland and pasture with a probability of 0.75, sparse pasture is improved to dense pasture and woodland with a probability of 50% and commercial agriculture transition probabilities double.
- Scenario 8 (Historic Condition) – lowlands (>1400 m) entirely shrubland except where wetlands were observed in 1986, highlands (>1400 m) entirely forest. This condition was not implemented by adjusting transition probabilities, but was assessed using the same spatial model framework.

Spatially targeted landuse change scenarios: Using Markov matrix adjustment to explore land cover change ignores spatial constraints by allowing total landuse allocation flexibility. For example, erosion risk is variable across the region, and targeting high-risk

landuse types to regions with low inherent risk of degradation may improve watershed condition without changing the rates and proportions of rural agricultural extensification.

This hypothesis was explored by manipulating Markov transition probabilities according to two factors: site inherent risk, defined above, and degradation proportions for each landuse. Conditional probabilities of conversion to land uses with higher than average degradation prevalence are lowered at sites with high inherent risk; conversely, transition probabilities are raised at sites with lower inherent risk, maintaining landuse proportions and satisfying the constraint that transition probabilities sum to one. The stochastic simulation process for generating landuse maps was applied using risk weighted transition probabilities and evaluated using the same assessment framework.

Emergy yield functions

Harvest yields exhibit substantial variability from both inherent soil functional capacity and climatic inputs. Transformity values and summary indices (including ABR) were computed for nominal yields measured across western Kenya (Jaetzold and Schmidt 1982), adjusted in a simplified manner to account for the documented effects of soil degradation on reduced agricultural yields (Lal 1998, Williams et al. 1983). As previously presented, the assumption was made that for all intact sites, regardless of agroecological zone, yields were constant.

Optimality Criteria and Scenario Comparison

Landuse optimality was defined by maximizing the agricultural benefit ratio across the basin. Maximizing this quantity internalizes costs of soil erosion along with benefits of using land to support humans. A conceptual flowchart of the spatial model to determine expected ABR values under each landuse scenario is presented in Figure 2-4.

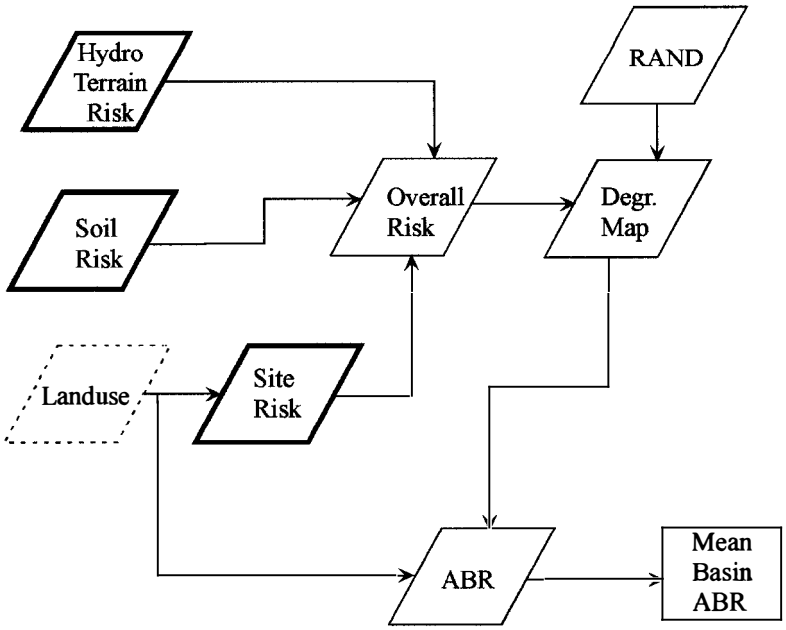

Figure 2-4. Conceptual flow chart of spatial model of erosion risk and watershed-scale net benefit indices.

EMERGY ANALYSES

Emergy evaluations were compiled at three scales. First, a national evaluation was developed, followed by district scale assessments. These analyses provide a regional context for the soil erosion problem. For analysis at the watershed scale, six landuse subsystems were evaluated.

National Emergy Analysis

Systems Diagram

An energy systems diagram synthesizing the Kenyan economy is presented in Figure 3-1. This diagram concentrates on resource flows that cross the system boundary and the organization of major internal components to make use of that energy. Primary renewable flows are sunlight, rainfall, and deep heat; purchased goods, fuels, and services are also shown. The purchased sources are depicted in aggregate to avoid excessive diagram complexity; they were examined in considerable detail for the analysis.

Internal production systems include forests, croplands (commercial and subsistence farming), rangelands, and coastal mangroves and coral reefs. Livestock, fisheries production, and natural fauna are also depicted. In addition to direct harvest from these particular sectors, the associated costs of soil erosion are depicted (storage labeled S in each production symbol represent stocks of soil capital), along with consequent impacts on national aquatic resources.

Major manufacturing sectors include agricultural processing, leather and textile industries, and metal/fuel/mineral processing. These, with tourism, form the core

economic revenue generators. The governments role in protecting wildlife, providing services to urban and rural populations and securing international loans is also shown. International debt, currently 61% of GDP (GDP = $10.4 billion) (World Bank 2002), is repaid as principal (P) and interest (I); the diagram illustrates how that revenue is generated, and how it is spent on importing goods and services from the world market.

Spatial Surfaces of Renewable Energy Flows

Each renewable source of energy is delivered with substantial spatial variability. Spatial characteristics are of interest from a resource allocation perspective, but are also necessary to avoid estimating annual flows based on point estimates biased to certain regions of the country. Renewable energy flow surfaces were interpolated from existing point measurement databases for deep heat, wind and annual precipitation.

Deep heat data were obtained from a global database of point measurements of heat flow in 10^{-3} Watts per square meter (Pollack et al. 1991). The point coverage for Kenya was interpolated using a standard second-order inverse distance-weighting algorithm (Idrisi Release 2) (Clark Labs 2001). The resulting surface is presented in Figure 3-2a. The region of the Rift Valley that is currently used for geothermal can be seen in the western third of the country. A similar map for wind based on surface wind speed observations was developed using the same interpolation method (Figure 3-2b). An existing spatial database (Corbett et al. 1997) of annual precipitation is presented in Figure 3-2c. Other renewable flows were unable to be defined in a spatially explicit manner, which may introduce error into the flow estimates. Additional spatial data of considerable importance included an existing digital elevation model (DEM) of the nation (Corbett et al. 1997), and land-use/land cover maps, previously presented.

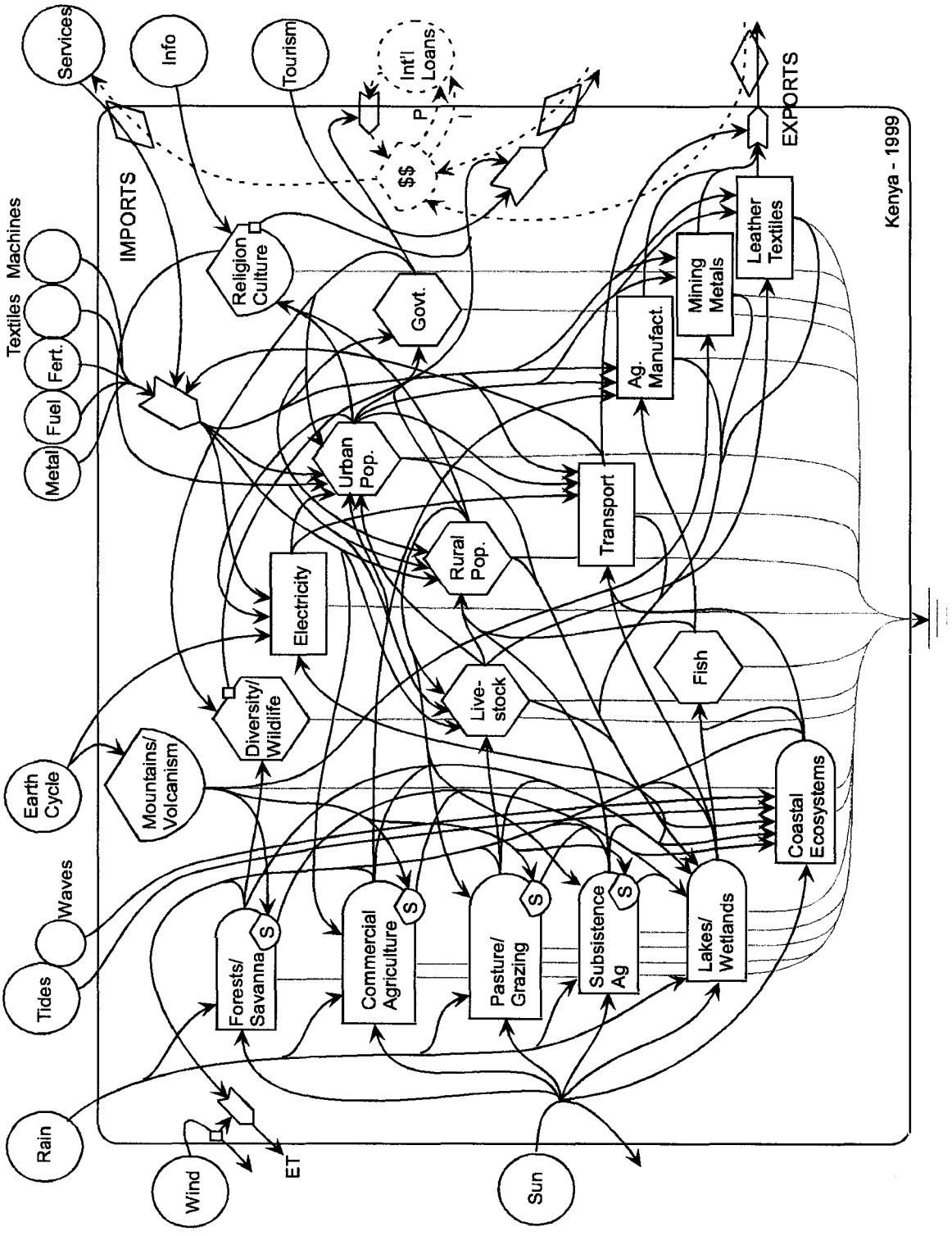

Figure 3-1: Energy systems diagram summarizing the Kenyan national economy and resource basis.

National Emergy Table

Table 3-1 presents annual emergy flows for Kenya in 1999. The table is comprised of renewable flows, indigenous renewable uses, indigenous non-renewable resource extraction, imports and exports. For each item, energy or material flows (J/yr or g/yr) are indicated, followed by the transformity estimate (sej/J or sej/g). The product of these two values is the emergy flow (sej/year), and the ratio of the emergy flow to the emergy:dollar ratio is the estimate of the macroeconomic value of that flow (in units of Em$). Footnotes to the table including raw data and transformity estimates, data sources and energy conversion equations are given in Table A.1 in Appendix A. Following the standard evaluation protocol (Odum 1996), only the largest renewable energy flow is used in delineating the national renewable resource basis.

Within Table 3-1, items 11 and 12 refer to agricultural summary tables that can be found in Table A-3 in Appendix A. Rather than assume a nominal transformity value for agricultural goods, transformities were developed for each specific product. Overall, agriculture and livestock production contribute 5.4E22 and 3.99E22 sej per year.

The major internal sectors listed in the category Indigenous Renewable Energy Use are agriculture and livestock production, followed by managed forest production and fishery yields. Rapidly growing flows of geothermal and hydroelectric electricity generation, the primary national sources of electricity, are minor in comparison, indicating the lack of rural electrification.

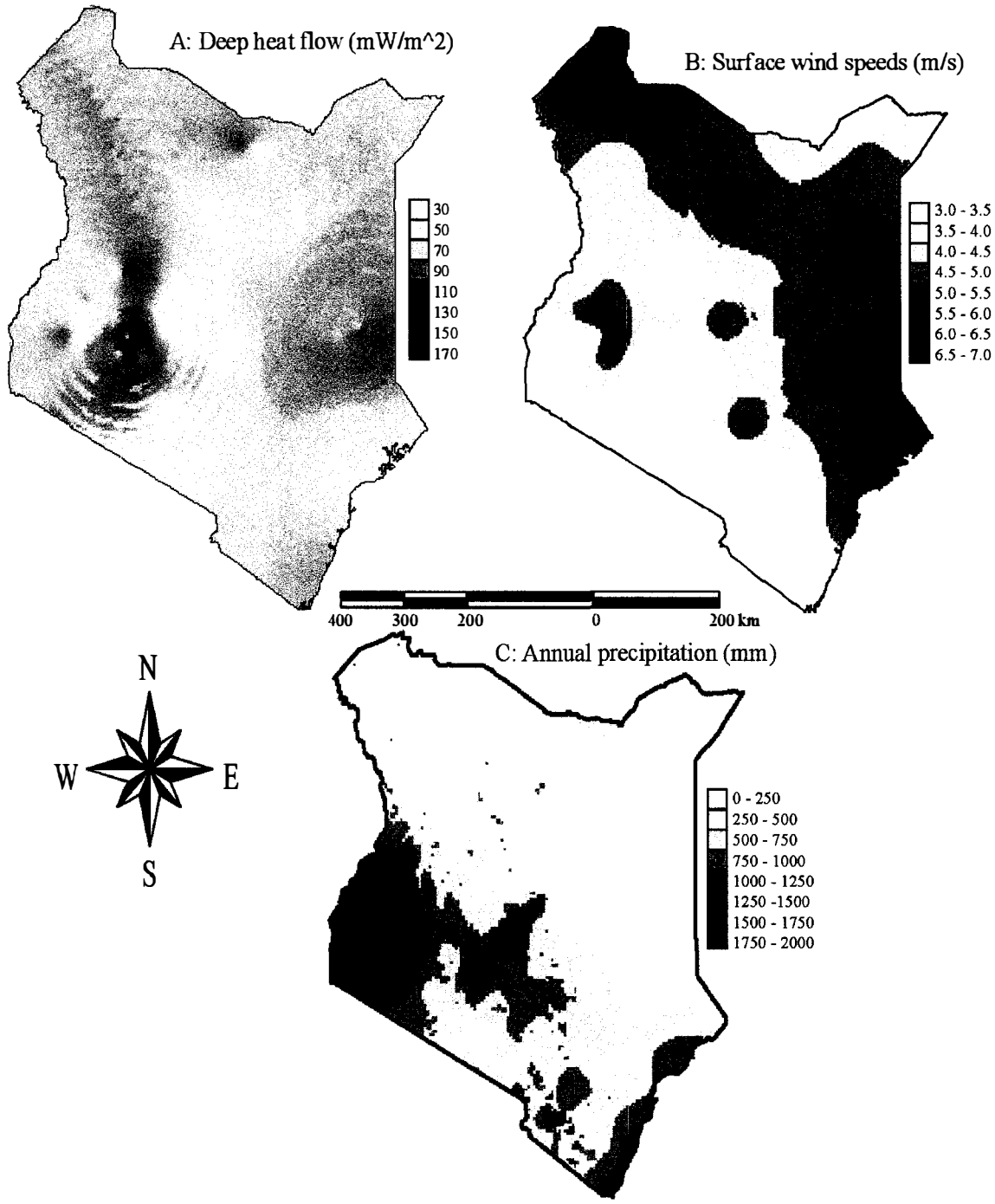

Figure 3-2. Renewable energy surfaces for Kenya: a) deep heat flow ($W/m^2/yr$), b) annual average surface wind speed (m.s) and c) annual precipitation (mm/yr).

Table 3-1. Emergy evaluation of resource basis for Kenya (c.1999).

Note	Item	Raw Units	Transformity (sej/unit)	Solar Emergy (E20 sej)	EmDollars (E9 1997 US$)
Renewable resources					
1	Sunlight	3.70E+21 J	1	36.96	0.32
2	Rain, chemical	1.62E+18 J	31000	503.15	4.30
3	Runoff, geopotential	2.78E+17 J	47000	130.57	1.12
4	Wind, kinetic energy	3.39E+18 J	2450	83.08	0.71
5	Waves	3.34E+17 J	51000	170.49	1.46
6	Tide	5.49E+17 J	73600	404.24	3.45
7	Earth Cycle	1.15E+18 J	58000	665.47	5.69
Indigenous renewable energy use					
8	Hydroelectricity	1.12E+16 J	2.77E+05	31.14	0.27
9	Geothermal Electicity	2.25E+15 J	2.69E+05	6.05	0.05
10	Agriculture Production	1.62E+17 J	see Table A-3	143.21	1.22
11	Livestock Production	1.31E+16 J	see Table A-3	145.42	1.24
12	Fisheries Production	7.47E+14 J	9.42E+06	70.38	0.60
13	Fuelwood Production	1.72E+17 J	3.09E+04	53.10	0.45
Nonrenewable flows from within the systems					
14	Const. Mater. (sand, ballast)	3.69E+12 g	1.69E+09	62.36	0.53
15	Soda Ash	5.81E+11 g	1.69E+09	9.82	0.08
16	Fluorspar, Salt, Limestone	1.72E+11 g	1.69E+09	2.90	0.02
17	Gold	9.90E+05 g	2.00E+13	0.20	0.00
18	Precious/Semi-Precious Gems	4.30E+07 g	1.00E+13	4.30	0.04
19	Forest Clearing	6.18E+16 g	6.72E+04	41.53	0.35
20	Top Soil (OM)	1.92E+16 J	2.35E+05	45.18	0.39
Imports and Outside Sources					
21	Oil derived products	1.41E+17 J		135.45	1.16
	Crude Petroleum	8.20E+16 J	8.90E+04	72.98	
	Refined Petroleum	5.80E+16 J	1.06E+05	61.41	
	Petroleum Products	1.00E+15 J	1.06E+05	1.06	
22	Metals	4.33E+11 g		29.74	0.25
	Ferrous Metals Raw	3.94E+11	2.99E+09	11.79	
	Non-Ferrous Metals	2.50E+10	2.69E+10	6.72	
	Metal Structures and Tools	1.39E+10	8.06E+10	11.23	
23	Minerals	6.87E+10 g		1.16	0.01
	Cement	3.94E+10	1.73E+09	0.68	
	Clay	1.68E+10	2.86E+09	0.48	
	Glass	1.24E+10	1.08E+07	0.00	
24	Food & ag. products	1.48E+16 J	see Table B3	21.36	0.18
25	Livestock, meat, fish	1.27E+14 J	see Table B3	5.33	0.05
26	Plastics & rubber	1.19E+11 g		9.51	0.08
	Rubber	1.19E+11 g	7.22E+09	8.59	
	Plastics	1.45E+11 g	6.38E+08	0.92	
27	Chemicals	5.31E+11 g		28.23	0.24
	Chemical Products, Dyes etc.	1.44E+11	6.38E+08	0.92	
	Fertlizers	3.87E+11	7.06E+09	27.31	
28	Wood, paper,textiles	1.69E+15 J		28.33	0.24
	Wood	3.25E+14	3.09E+04	0.10	
	Paper	9.79E+14	3.61E+05	3.54	
	Textiles	3.87E+14	6.38E+06	24.69	

Table 3-1. (continued)

Note	Item	Raw Units	Transformity (sej/unit)	Solar Emergy (E20 sej)	EmDollars (E9 1997 US$)
29	Mech.& trans equip.	4.45E+10 g	1.13E+11	50.07	0.43
30	Service in imports	2.75E+09 $	2.08E+12	57.28	0.49
Exports					
31	Food & ag. products	1.32E+16 J	see Table B3	49.72	0.42
32	Livestock, meat, fish	4.66E+14 J	see Table B3	15.40	0.13
33	Wood, paper,textiles	4.87E+15 J		33.22	0.28
	Wood	4.15E+15	1.43E+05	5.91	
	Paper	4.01E+14	3.61E+05	1.45	
	Textiles	2.57E+14	6.38E+06	16.43	
	Leather	6.53E+13	1.44E+07	9.43	
34	Oil derived products	1.20E+16 J	1.06E+05	12.69	0.11
35	Metals	1.81E+11 g		21.20	0.18
	Ferrous Metals	1.67E+11 g	2.99E+09	5.01	
	Non-Ferrous Metals	2.57E+09 g	2.69E+10	0.69	
	Metal Structures and Tools	1.14E+10 g	1.35E+11	15.50	
36	Minerals	7.16E+11 g		16.44	0.14
	Cement	6.90E+11 g	1.73E+09	11.94	
	Glass	2.59E+10 g	1.08E+07	0.00	
	Gold and Gems	4.40E+07 g	see above	4.49	
37	Chemicals	7.90E+10 g	6.38E+08	0.50	0.00
38	Mech. & trans equip.	1.48E+09 g	1.13E+11	1.67	0.01
39	Plastics & rubber	5.30E+10 g		0.68	0.01
	Plastics	4.78E+10 g	6.38E+08	0.30	
	Rubber	5.26E+09 g	7.22E+09	0.38	
40	Service in exports	1.98E+09 $	1.17E+13	231.14	1.98
41	Tourism	4.74E+08 $	1.17E+13	55.46	0.47

Note: Table footnotes, and raw data/transformity sources provided in Table A-1 in Appendix A.

The major imports are oil-derived products, followed by embodied services and mechanical and transportation equipment. Major exports are food and agricultural products, wood/paper/textile products and an enormous quantity of embodied services (i.e. the services within the national economy that are necessary both directly and indirectly to facilitate export of goods, measured using money received multiplied by the national emergy:dollar ratio).

Of particular interest is the magnitude of soil erosion (Items 19) in comparison with other national flows. The magnitude (4.5E21 sej/yr) is comparable in magnitude to

total national electricity usage or agricultural exports. Summary metrics, presented below, will further quantify this ongoing loss of natural capital.

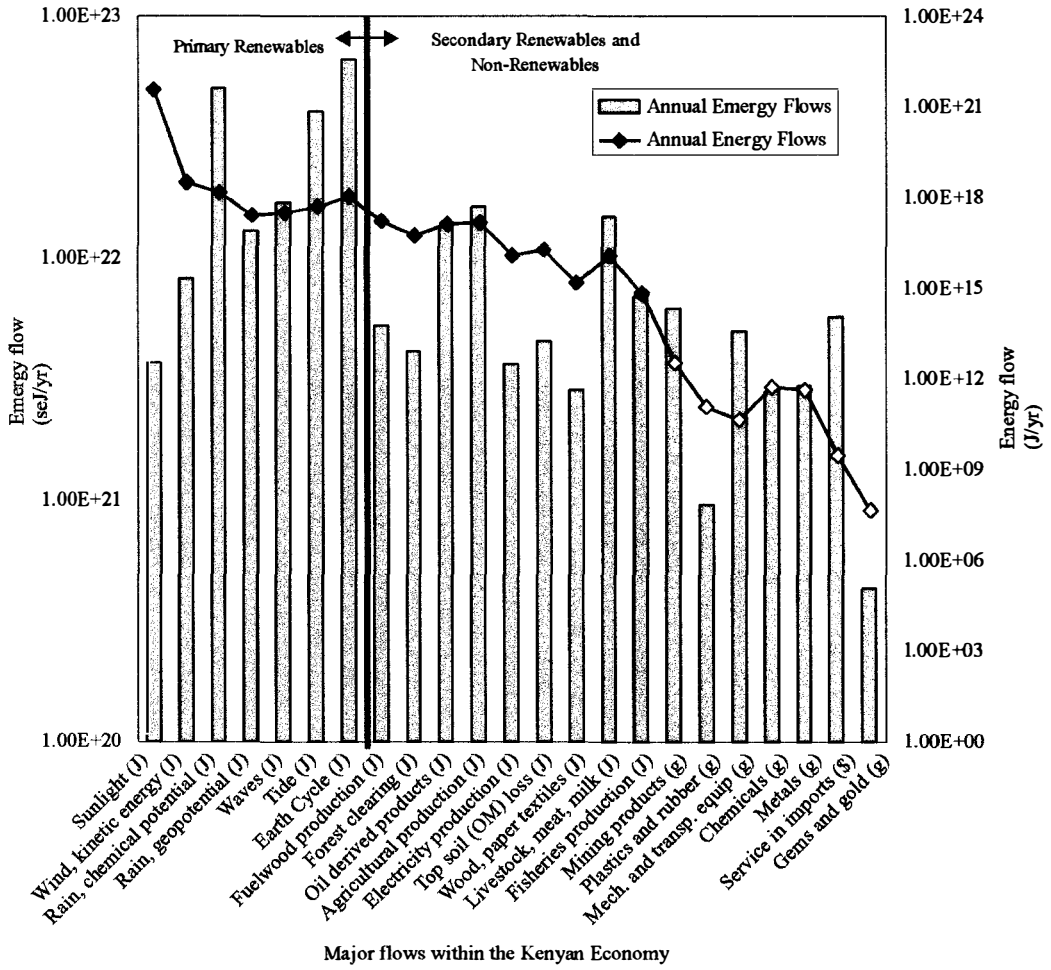

Figure 3-3. Emergy spectra for Kenyan national economy. Shown are annual emergy (seJ/yr), material and energy (J/yr) flows for 1999.

Emergy Spectra

To illustrate the energy basis of the economy further and to reiterate the critical importance of adjusting energy flows according to their quality, the energy and annual empower spectra for Kenya are shown in Figure 3-3. The flows of energy and emergy are ranked from left to right in order of increasing transformity. Note that sunlight represents 99.8% of the energy budget, but only 1.25% of the total emergy flow.

Flow Aggregation

Table 3-2 summarizes the flows into aggregated categories. These categories include renewable, local non-renewable, imported fuels, imported goods, and exported goods. Also included in this table are gross economic data for the nation (GNP, import payments, export revenue).

Table 3-2. Aggregated emergy flows in Kenya, (c.1999)

Variable	Item	Solar Emergy (E20 sej/y)	Dollars
R	Renewable sources (rain chemical and geo-potential)	665.47	
N	Nonrenewable resources from within Kenya	166.29	
N0	Dispersed Rural Source (i.e. not mining products)	86.71	
N0a	Soil Loss	*45.18*	
N0b	Deforestation	*41.53*	
N1	Concentrated Use (mined products)	79.58	
N2	Exported without Use	13.50	
F	Imported Fuels and Minerals	166.35	
G	Imported Goods	142.84	
I	Dollars Paid for Imports		2.75E+09
P2I	Emergy of Services in Imported Goods & Fuels	57.28	
E	Dollars Received for Exports		1.98E+09
P1E	Emergy Value of Goods and Service Exports	437.43	
GNP	Gross National Product		1.02E+10
P2	World emergy/$ ratio (used for imports)	2.08E+12	
P1	Kenya Emergy/$ ratio (used for exports)	1.17E+13	

Summary Diagram

Figure 3-4a is a diagram of the aggregated flows of emergy in the Kenyan economy. Imported services are computed using the world emergy:dollar ratio (Brown and Ulgiati 1999) multiplied by exported currency (P2*I). Similarly, the service embodied in exports is the money paid (E) multiplied by the emergy:dollar ratio computed for Kenya (P1*E).

Figure 3-4b aggregates the flows further to illustrate the national trade balance and indigenous emergy consumption in common energetic units. The Emergy Yield

Ratio (EYR), the Emergy Investment Ratio (EIR) and the Environmental Loading Ratio (ELR) can all be computed based on the numeric flows presented in these diagrams.

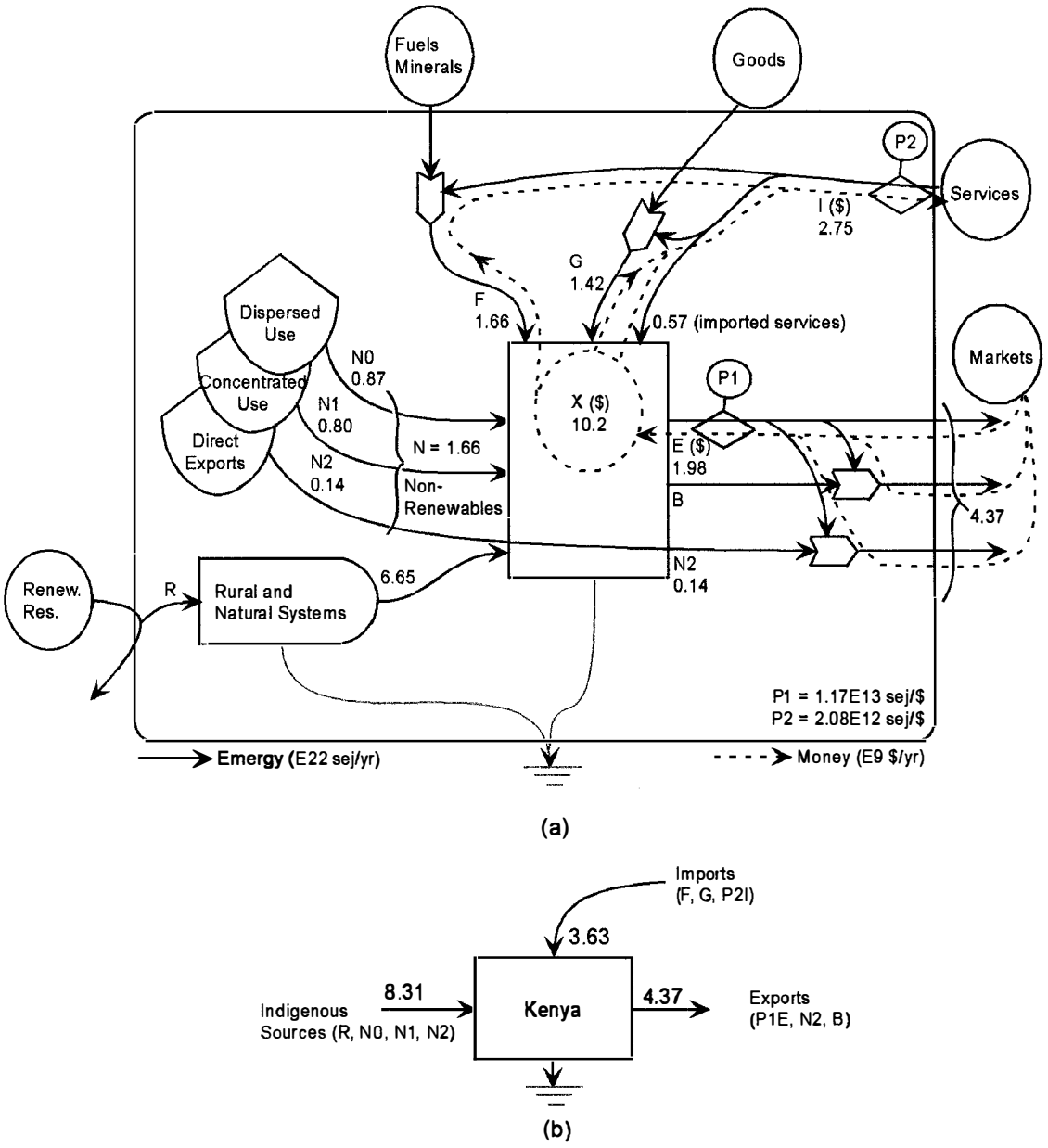

Figure 3-4. Aggregated economic systems diagrams: a) aggregated flows and b) summary of indigenous, imported and exported flows for Kenya (1999)

Table 3-3. Summary emergy indices for Kenya (c.1999)

Item	Name of Index	Expression	Quantity
1	Renewable emergy flow	R	6.65E+22
2	Flow from indigenous nonrenewable reserves	N	1.66E+22
3	Flow of imported emergy	F+G+P2I	3.66E+22
4	Total emergy inflows	R+F+G+P2I	1.03E+23
5	Total emergy used, U	N0+N1+R+F+G+P2I	1.20E+23
6	Total exported emergy	P1E	4.37E+22
7	Fraction emergy use, home sources	(NO+N1+R)/U	0.69
8	Imports minus exports	(F+G+P2I)-(N2+B+P1E)	-8.45E+21
9	Export to Imports	(N2+P1E)/(F+G+P2I)	1.23
10	Fraction used, locally renewable	R/U	0.56
11	Fraction of use purchased	(F+G+P2I)/U	0.31
12	Fraction imported service	P2I/U	0.05
13	Fraction of use that is free	(R+N0)/U	0.69
14	Ratio of concentrated to rural	(F+G+P2I+N1)/(R+N0)	0.59
15	Population	Pop.	3.18E+07
16	Population Density	Pop. / Area (sq. km)	54.8
17	Emergy Density	U / area (sq. m)	2.07E+11
18	Emergy per capita	U / population	3.77E+15
19	Renewable human carrying capacity, present living standard	(R/U)*(population)	1.77E+07
20	Ratio of use to GNP, Emergy/dollar ratio	P1=U/GNP	1.17E+13
21	Ratio of electricity to use	(Electric Use)/U	3%
22	Fuel use per person	Fuel / Population	4.26E+14
23	Emergy Investment Ratio	(F+G+P2I)/(R+N)	0.44
24	Environmental Loading Ratio	(N+F+P2I+G)/R	0.80
25	Emergy Sustainability Index	EYR/ELR	0.55
26	Emergy Yield Ratio	U/ (N+F+G+P2I)	1.23
27	Fraction Capital Stock Depletion	(N0a) / U	3.77%
28	Agricultural Benefit Ratio (ABR)	Agr. Prod. / (N0a)	7.56

Overview Indices

Table 3-3 presents computed emergy indices for Kenya. Included are total emergy use, fraction renewable, ELR/EYR/EIR/ESI, emergy balance of trade, and a suite of other common indices. Of particular interest are the FCSD and ABR ratios that define erosion costs in the context of the national economic system. FCSD indicates that nearly 4% of total flow in the Kenyan economy is soil loss, a figure comparable in magnitude to national electricity consumption or agricultural exports. The ABR figure is 7.56.

Table 3-4 shows several of the most important indices computed for Kenya compared with other national analyses. In order to allow direct comparison, each emergy

flow in Table 3-1 was divided by 1.68 (Odum and Brown, 2001) to account for recent changes in computation of global tidal geomomentum absorption that are propagated through all subsequent energy quality ratios.

Table 3-4: Comparison of Kenyan summary indices with other national economies.

Nation	U	U/P	U/A	U/GNP	R	R+N / U	N + F	ELR	I:E
Netherlands[a]	3702	26	100	2.2	—	23	—	—	4.3
West Germany[a]	17500	28	70.4	2.5	193	10	1730	8.96	4.2
Switzerland[a]	733	12	17.7	0.7	87	19	646	7.43	3.2
USA[b]	66400	29	7	2	8240	77	58160	7.06	2.2
India[a]	6750	1	2.05	6.4	3430	88	3410	0.99	1.45
Sweden[c]	2580	30	6.3	1.5	456	28	2124	4.66	1.21
Taiwan[d]	1340	8	94.6	1.9	—	28	—	—	1.19
Brazil[a]	17820	15	2.08	8.4	10100	91	7600	0.75	0.98
Dominica[a]	7	13	8.8	14.9	2	69	5	2.50	0.84
New Zealand[a]	791	26	2.94	3	438	60	353	0.81	0.76
Thailand[e]	1590	3	2.15	3.7	779	70	811	1.04	0.54
Australia[a]	8850	59	1.42	6.4	4590	92	3960	0.86	0.39
Soviet Union[a]	43150	16	1.71	3.4	9110	97	9100	1.00	0.23
Ecuador[a]	964	10	3.4	—	891	94	483	0.54	0.2
Liberia[a]	465	26	4.1	34.5	427	92	38	0.09	0.15
Papua New Guinea[a]	1216	35	2.63	48	1050	96	166	0.16	0.13
World[a]	299000	4.98	1.99	2.96	94400	—	200460	2.12	—
KENYA[f]	713	2.24	1.23	6.96	396	69	317	0.80	0.81

U = Total Use; P = Population; A = Land area; GNP = Gross Nat'l Product; R = Renewables; N = Non-renewables, F = Purchased inputs; ELR = Env. Loading Ratio; I = Imports; E = Exports

Sources: a – Odum (1996), b – Stachetti (2002), c – Doherty et al. (2002), d – Huang (1997), Brown and McLanahan (1993), f – this study

Note: Values in this table for Kenya are adjusted to reflect recent transformity changes (Odum et al. 2001). All Kenyan flows reported here are divided by a factor of 1.68.

District Emergy Evaluations

Three districts comprise the regional context of the Awach River basin. Kericho and Nyando districts comprise the entire basin area, but the regional importance of Kisumu district as a trading and manufacturing center warranted its inclusion.

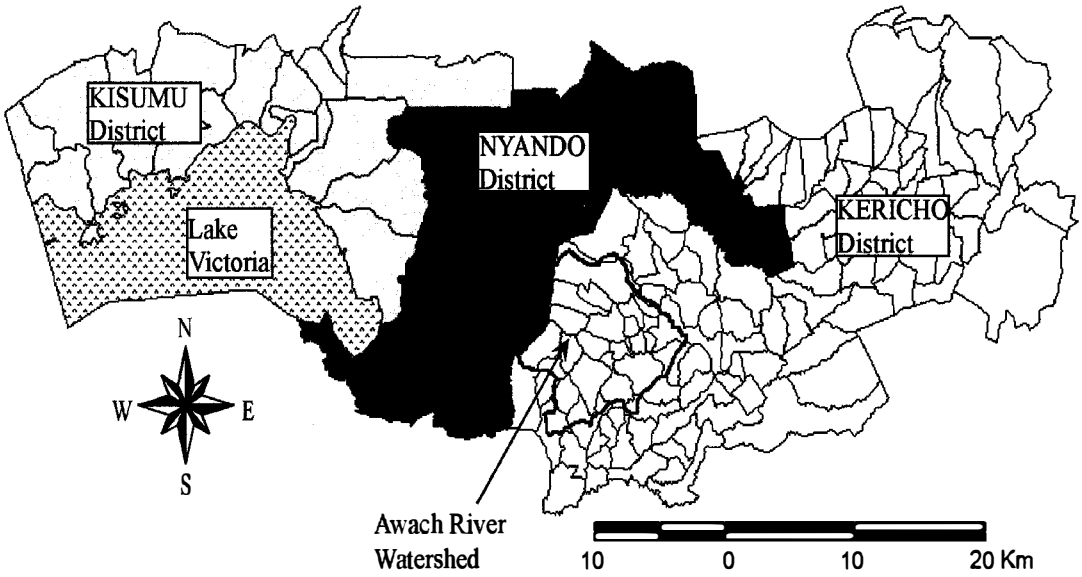

Figure 3-5. Map of districts for which emergy evaluations were compiled. Also shown is the study basin (Awach River) for which landuse subsystems were evaluated.

Systems Diagrams

Systems diagrams were developed for each district (Figure 3-6 through 3-8). In each diagram, stocks of soil capital (S) are shown. Component symbol sizes correspond approximately with relative importance within each system.

Spatial Surfaces and Data Sources

As with the national evaluation, geospatial databases were used to estimate the resource flows driving each district economy. For rainfall, elevation, wind speeds, deep heat, and landuse, spatial coverages were extracted from maps and surfaces presented above. Rainfall, elevation, landuse, deep heat flow and mean annual wind speed surfaces were extracted from national coverages. Soil erosion estimates for given landuse subsystems were based on field observations, presented later. Actual costs were restricted only to sediments crossing the system boundary; overall costs of degradation should be considered conservative. A sediment yield ratio of 10% was assumed.

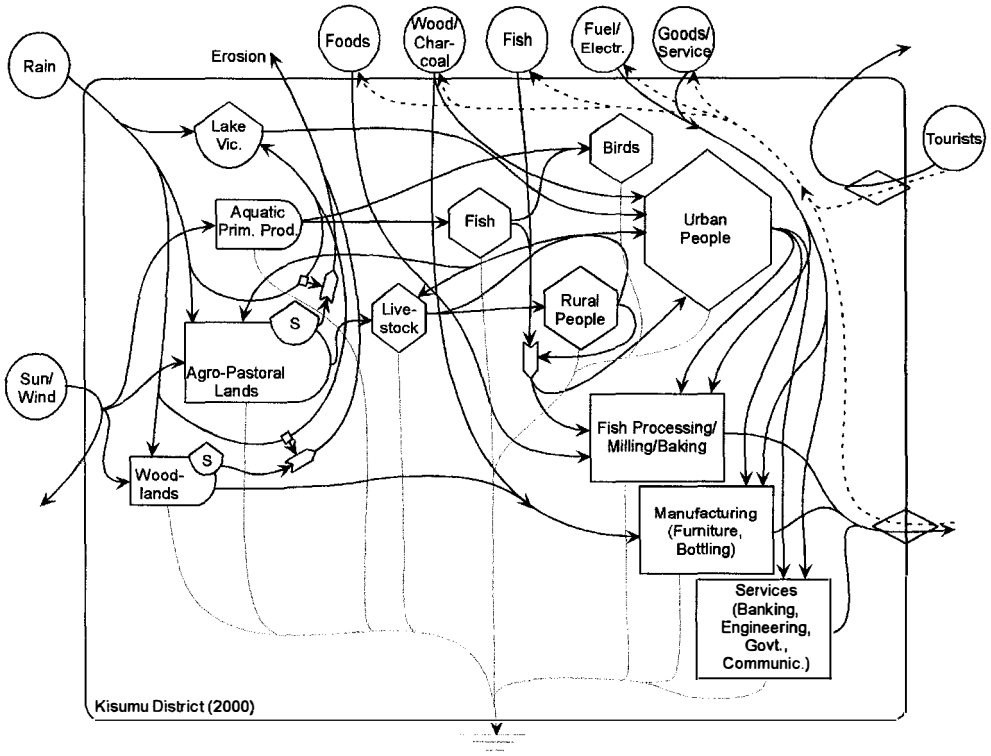

Figure 3-6: Energy systems diagram depicting the Kisumu district economy.

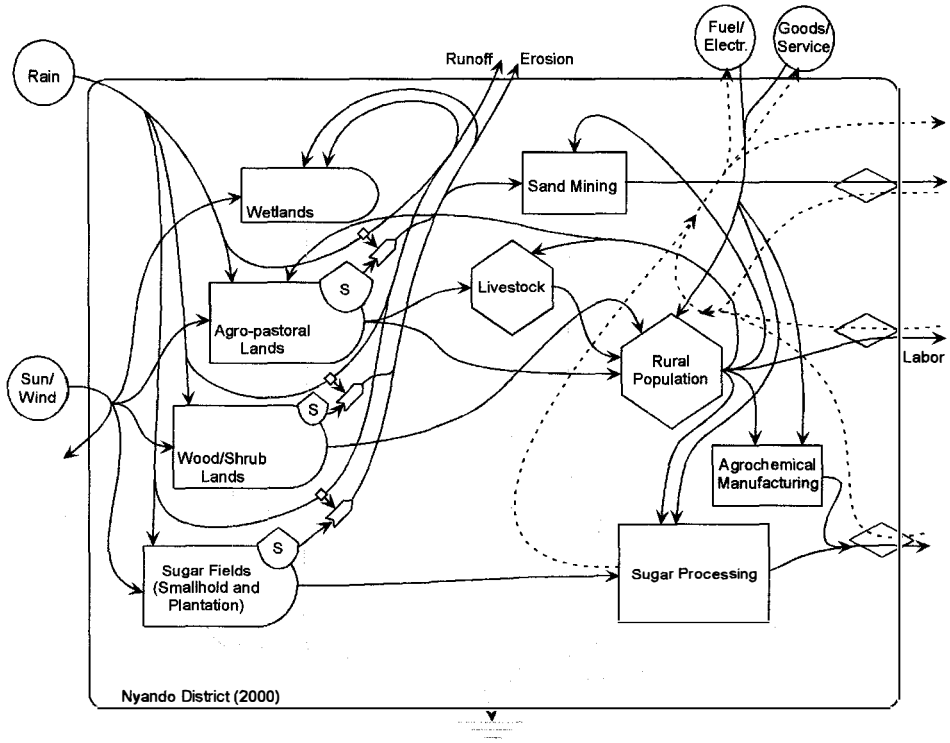

Figure 3-7: Energy systems diagram depicting the Nyando district economy.

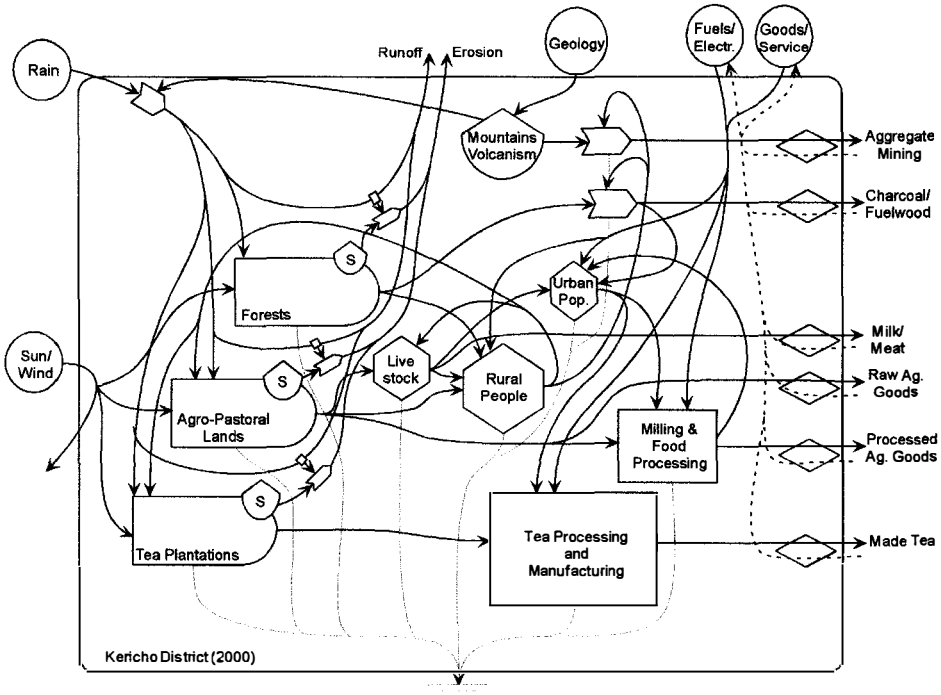

Figure 3-8: Energy systems diagram depicting the Kericho district economy.

Commodity consumption data were unavailable for all goods at this scale of evaluation. To estimate these quantities, use was assumed proportional to the ratio of district fuel consumption to national use. This ratio was extrapolated to the district economies based on reliable fuel and electricity consumption data (KPLC, 2001; KPA, 2001). Where fuel and electricity proportions differed, an average was used. Table 3-5 shows a comparison of national fuel and electricity usage with district level statistics.

Table 3-5. Comparison of national and district fuel and electricity use, GDP and population to infer commodity consumption for districts.

	Nation	Kisumu	Nyando	Kericho
Fuel (J/yr)	1.41E+17	2.58E+15	3.73E+14	1.54E+15
National %	100%	1.83%	0.26%	1.09%
Electricity (J/yr)	1.35E+16	3.07E+14	7.13E+13	2.47E+14
National %	100%	2.27%	0.53%	1.83%
GNP ($/yr)	1.02E+10	2.33E+08	3.30E+07	1.69E+08
National %	100%	2.28%	0.32%	1.66%
Population	3.18E+07	5.04E+05	2.99E+05	5.97E+05
National %	100%	1.58%	0.94%	1.88%

a - Kenya Pipeline Authority (2001), b - Kenya Power and Lighting Corportation (2001), c - Kisumu, Nyando and Kerichi district development plans (Kenya CBS, 2000)

Evaluation Tables and Summary Indices

Detailed emergy evaluation tables are given in Appendix A (Tables A-2 through A-4) along with notes on data sources and energy conversions. Table 3-6 shows aggregated flows for each district. The letters in the first column refer to nomenclature presented in Figure 3-3, a generic diagram of economic systems.

Table 3-6. Summary of annual flows in Kisumu, Kericho and Nyando Districts (c.2000)

		Kisumu		Kericho		Nyando	
Item	Description	Emergy (E19 sej)	Dollars	Emergy (E19 sej)	Dollars	Emergy (E19 sej)	Dollars
R	Renewable sources (rain)	20.68		61.46		27.39	
N	Local non-renewable use	18.40		58.17		22.70	
N0	Dispersed Rural Source	15.04		48.67		19.22	
N1	Concentrated Use	3.36		9.50		9.86	
N2	Exported without Use	0.75		17.67		3.88	
F	Imported Fuels and Minerals	72.38		25.62		11.52	
G	Imported Goods	46.81		18.91		10.62	
I	Dollars Paid for Imports		6.2E+07		2.8E+07		6.1E+06
P2I	Emergy of Services in Imports	78.25		34.90		7.85	
E	Dollars Received for Exports		6.0E+07		2.2E+07		6.3E+06
P1E	Emergy in exports	120.45		100.84		34.31	
GNP	Gross National Product		2.3E+08		1.7E+08		3.3E+07
P2	Kenya Em$ ratio, for imports	1.3E+13		1.3E+13		1.3E+13	
P1	District Emergy/$ ratio	1.0E+13		1.2E+13		2.6E+13	

Table 3-7 gives summary indices for each district and a comparative assessment of districts with index values at the national scale. Total emergy flows are not comparable between nation and district, but flows per capita and per area, in addition to all relativized indices (ELR, EIR, ABR etc), are directly comparable.

Emergy Spectra

Figure 3-9 provides empower spectra for each district. Note that spectra do not adjust for differences in spatial extent or population. Nyando district, where soil degradation is observed as most severe, has the smallest resource basis, and while soil loss is a substantial flow for each of the three districts, it is most significant in Nyando.

In all three districts, the primary renewable flow is chemical potential energy in rainfall. Forest extraction/ production is a significant industry in Kericho District.

Table 3-7. Overview indices for district evaluations in comparison to national indices.

Item	Name of Index	Expression	Kenya	Kisumu	Kericho	Nyando
1	Renewable emergy flow	R	6.65E+22	2.07E+20	6.15E+20	2.74E+20
2	Flow from indigenous nonrenewable reserves	N	1.66E+22	1.84E+20	5.82E+20	2.27E+20
3	Flow of imported emergy	F+G+P2I	3.66E+22	1.97E+21	7.94E+20	3.00E+20
4	Total emergy inflows	R+F+G+P2I	1.03E+23	2.37E+21	1.99E+21	8.01E+20
5	Total emergy used, U	N0+N1+R+F+G+P2I	1.20E+23	2.37E+21	1.99E+21	8.65E+20
6	Total exported emergy	P1E	4.37E+22	1.20E+21	1.01E+21	3.43E+20
7	Fraction emergy use, home sources	(NO+N1+R)/U	0.69	0.17	0.60	0.65
8	Imports minus exports	(F+G+P2I)-(N2+B+P1E)	-8.45E+21	7.62E+20	-3.91E+20	-8.20E+19
9	Export to Imports	(N2+P1E)/(F+G+P2I)	1.23	0.61	1.49	1.27
10	Fraction used, locally renewable	R/U	0.56	0.09	0.31	0.32
11	Fraction of use purchased	(F+G+P2I)/U	0.31	0.83	0.40	0.35
12	Fraction imported service	P2I/U	0.05	0.33	0.18	0.09
13	Fraction of use that is free	(R+N0)/U	0.69	0.15	0.55	0.54
14	Ratio of concentrated to rural	(F+G+P2I+N1)/(R+N0)	0.59	5.62	0.81	0.85
15	Population	Pop.	3.18E+07	5.04E+05	5.97E+05	2.99E+05
16	Population Density	Pop. / Area (sq. km)	54.8	763.64	237.38	209.09
17	Emergy Density	U / area (sq. m)	2.07E+11	3.58E+12	7.91E+11	6.03E+11
18	Emergy per capita	U / population	3.77E+15	4.69E+15	3.32E+15	2.89E+15
19	Renewable human carrying capacity, present living standard	(R/U)*(population)	1.77E+07	4.41E+04	1.85E+05	9.47E+04
20	Ratio of use to GNP, Emergy/dollar ratio	P1=U/GNP	1.17E+13	1.02E+13	1.18E+13	2.62E+13
21	Ratio of electricity to use	(Electric Use)/U	3%	0.05	0.05	0.02
22	Fuel use per person	Fuel / Population	4.26E+14	5.42E+14	4.94E+14	1.32E+14
23	Emergy Investment Ratio	(F+G+P2I)/(R+N)	0.44	5.05	0.66	0.60
24	Environmental Loading Ratio	(N+F+P2I+G)/R	0.8	10.44	2.24	1.92
25	Emergy Sustainability Index	EIR/ELR	0.55	0.48	0.30	0.31
26	Emergy Yield Ratio	See item # 9 above	1.23	0.61	1.49	1.27
27	Fraction Capital Stock Depletion (FCSD)	(N0a) / U	3.8%	2.4%	3.43%	14.2%
28	Agricultural Benefit Ratio (ABR)	Ag. Prod. / (N0a)	7.56	4.37	11.11	2.25

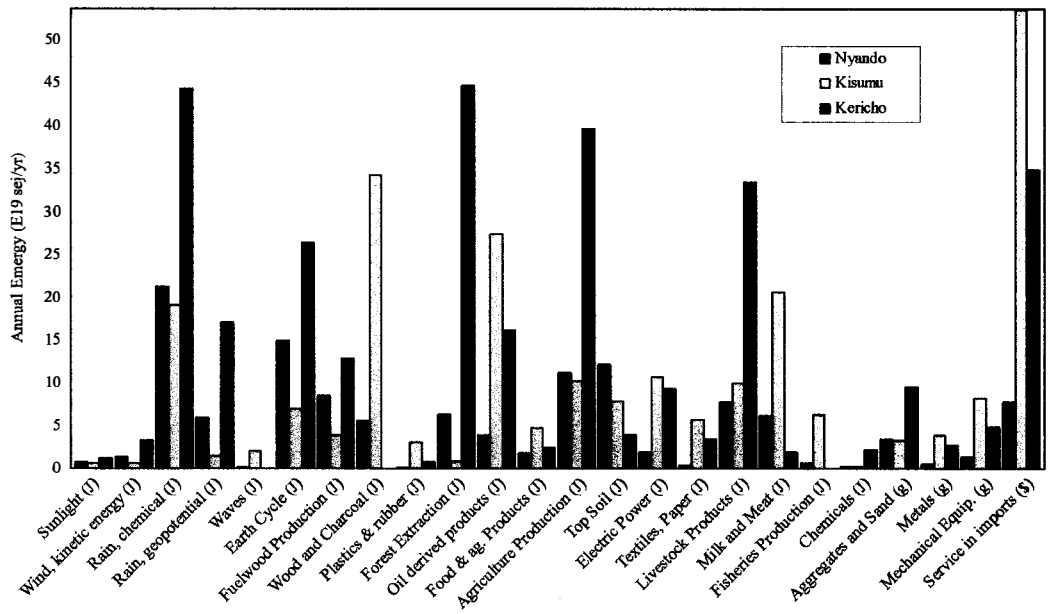

Figure 3-9. Empower spectra for district evaluations. Emergy flows are in E19 sej/yr, and are organized in rank order by increasing transformity.

Awach Subsystems Analysis

Emergy evaluations were developed for six landuse subsystems common in the Awach River watershed: subsistence agriculture, commercial agriculture, lowland pastures, highland pastures, farm forestry and extractive use of native forest/shrubland.

Systems diagrams are given first followed by emergy evaluation tables. Several components are common to all subsystem evaluations. The storage labeled soil function in each sub-system diagram aggregates soil organic carbon, nutrient stocks and soil physical structure into one functional variable. Erosion depletes this stock, and additions of fertilizer, geologic weathering and vegetation processes all increase it. Human labor is shown only partially within the system, indicating that farmers live near their fields, but their labor must be allocated to multiple simultaneous activities. For each transformity and specific emergy (emergy per mass), results are presented computed with and without service inputs (labor, purchased services).

Subsistence Agriculture

Subsistence agriculture is the primary activity within the Awach basin, particularly in the lowlands. Major crops include maize, sorghum, beans, cassava, millet and cooking bananas; maize is by far the most abundant crop. Emergy evaluations to compute transformity values were done for several subsistence cropping systems (maize/bean intercropping, sorghum etc.); results are presented in Appendix A. Given here are the systems diagram and emergy evaluation table for maize only.

Systems diagrams

Figure 3-10 is an energy systems representation of maize production in western Kenya. Inputs and internal dynamics are from Jaetzold and Schmidt (1982). Human labor is allocated to weeding, planting, tillage (seen on the diagram as influencing water infiltration), incorporating soil amendments and harvesting. Total annual labor, after

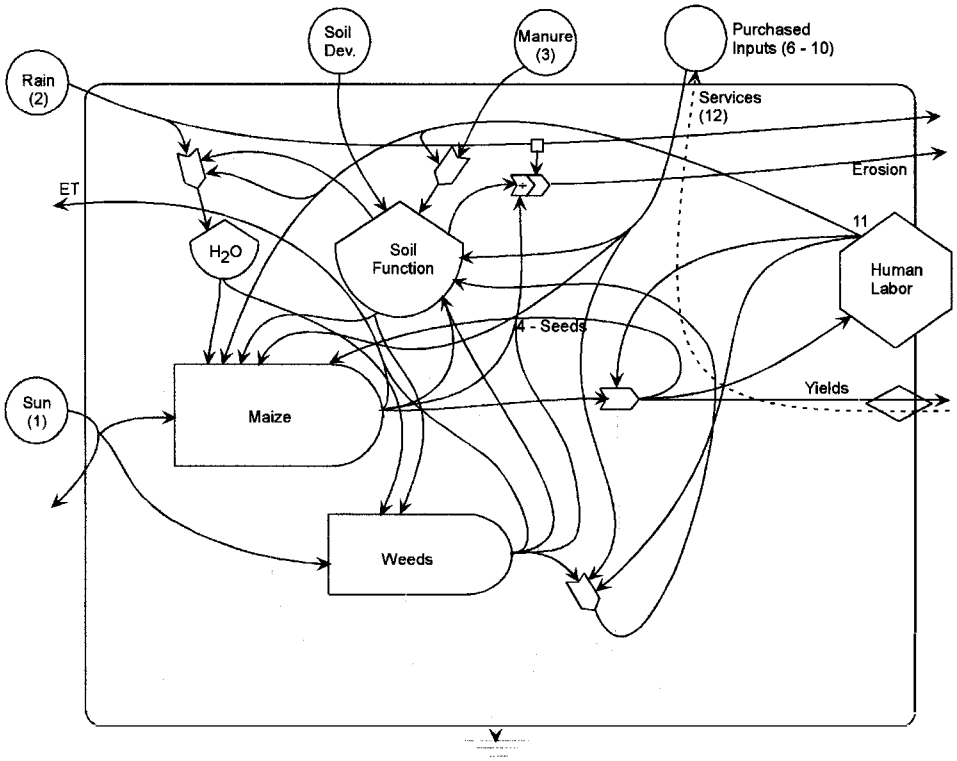

Figure 3-10. Systems diagram of subsistence maize production in the Awach basin.

Rommelse (1999), is estimated at 130 person-days per hectare per year for maize production. Soil erosion is shown as a function of surface runoff and reduced cover. Also shown is the direct competition for nutrient and light resources between weeds and crops. A common problem, particularly in lowland areas not shown on the diagram, is infestation by striga (*Striga hermonthica*), which parasitizes maize and sorghum roots. Though purchased inputs are not included on all farms in the Awach River basin, the evaluation was done assuming average input values for farms throughout western Kenya. This may overestimate the local prevalence of fertilizer and pesticide use.

Table 3-8. Emergy evaluation of subsistence maize production in western Kenya.

Note	Item	Unit	Data (units/yr)	Unit Solar EMERGY (sej/unit)	Solar EMERGY (E13 sej/yr)	Em$ Value (1995 $/yr)
Renewable Inputs						
1	Sun	J	2.64E+13	1	3	1
2	Rain	J	4.47E+10	3.10E+04	139	78
3	Manure	J	4.07E+09	9.25E+04	38	21
4	Native Seeds	J	2.24E+08	7.86E+04	2	1
Nonrenewable Inputs						
5	Net Topsoil Loss	J	4.16E+09	2.24E+05	93	52
	Sum of free inputs (sun omitted to avoid double counting)				271	152
Purchased Inputs						
6	Improved Seeds	J	7.81E+08	1.57E+05	12	7
7	Potash	g K	3.95E+01	1.85E+09	0	0
8	Herbicide/Insecticide	g	1.48E+03	2.52E+10	4	2
9	Phosphate	g P	8.14E+03	3.70E+10	30	17
10	Nitrogen	g N	4.95E+03	4.05E+10	20	11
11	Labor	J	1.36E+09	1.03E+06	140	79
12	Services	$	2.05E+01	1.78E+13	36	20
	Sum of purchased inputs				243	136
Computed Transformities						
13	Total Yield, dry weight	g	2.56E+06	2.00E+09	514	289
	w/out services	g	2.56E+06	1.31E+09		
14	Energy yield	J	4.85E+10	1.06E+05		
	w/out services	J	4.85E+10	6.96E+04		

Notes can be found in Appendix A.

Emergy table

Table 3-8 provides a tabular assessment and summary indices for maize production in western Kenya. Of particular interest are emergy indices that explore the magnitude of soil erosion in the context of agricultural productivity. Specifically, the Agricultural Benefit Ratio (ABR) and fraction avoidable are indices of problem severity. The soil loss figure used for each subsystems evaluation is for intact sites only. Later, costs will be estimated for degraded sites.

Commercial Agriculture

Commercial agriculture in the Awach Basin is exclusively on small farms that provide out-grower inputs to commercial processing factories in the region. Smallholder commercial farming consists primarily of tea (only in the highlands) and sugarcane (throughout the basin). Some cotton is grown in the alluvial lowland soils, but the collapse of the national cotton marketing board hampers market access. A small portion of subsistence crops (maize, vegetables) is sold outside the basin, but this was considered a negligible flow for this analysis. Because sugarcane and tea dominate commercial agriculture, energy systems diagrams and emergy evaluations were developed for both.

Systems diagrams

Energy systems diagrams depicting the production process for sugarcane and tea are presented in Figure 3-11. As with maize, soil loss occurs because of excessive runoff and reduced cover. While this simplifies the erosion process, it should be noted that internal organization of the system is not directly relevant to emergy evaluation, where only sources and stock depletion are considered. Soil loss rates are derived from empirical data in the region.

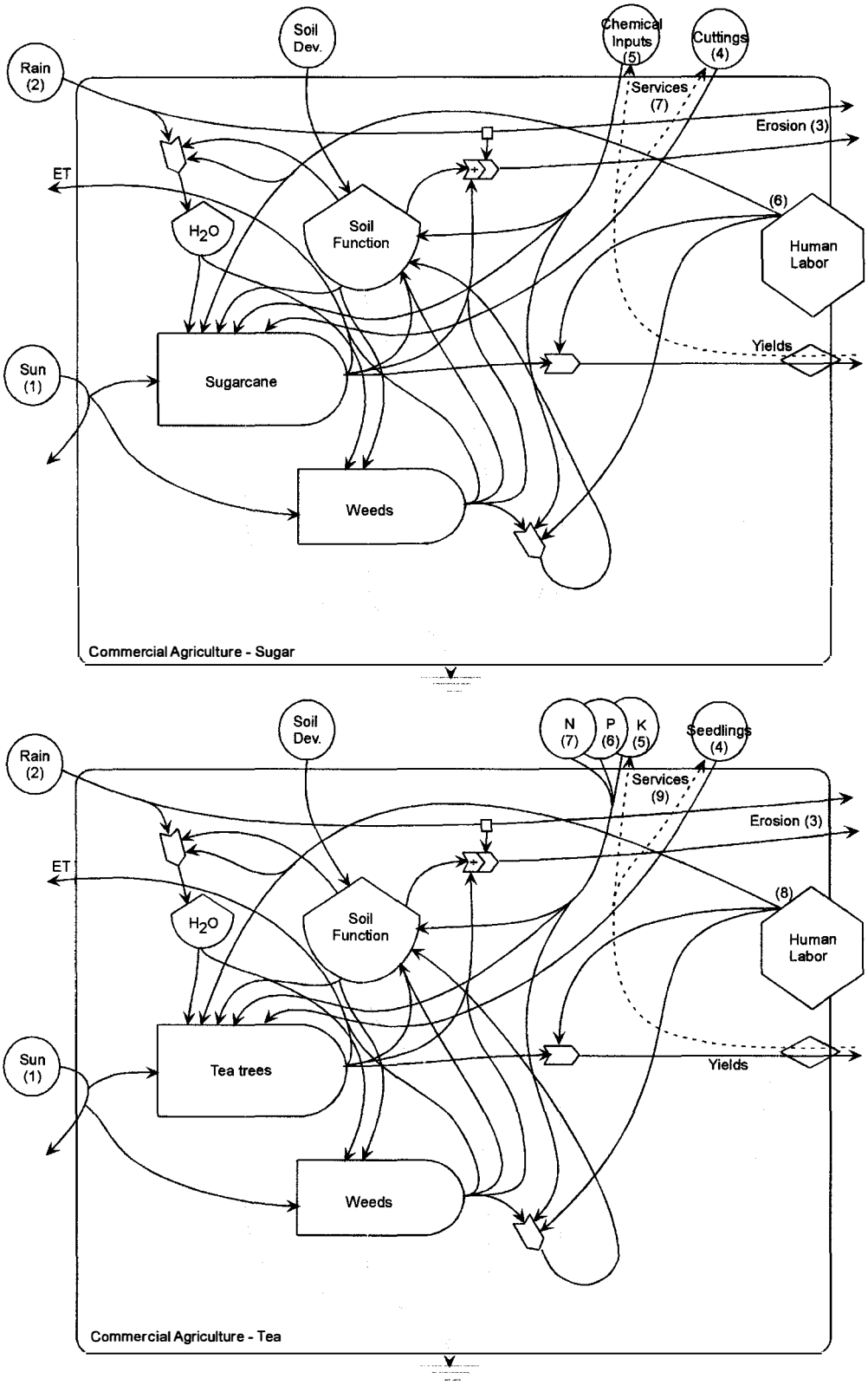

Figure 3-11. Systems diagram depicting smallholder sugarcane and tea production systems within the Awach basin.

Table 3-9. Emergy evaluation table of smallolder sugarcane production for western Kenya.

Note	Item	Unit	Data (units/yr)	Unit Solar EMERGY (sej/unit)	Solar EMERGY (E13 sej/yr)	Em$ Value (1995 $/yr)
Renewable Inputs						
1	Sun	J	6.23E+13	1	6	3
2	Rain	J	6.13E+10	3.10E+04	190	107
Nonrenewable Inputs						
3	Net Topsoil Loss	J	4.99E+09	2.24E+05	112	63
	Sum of free inputs (sun omitted to avoid double counting)				302	170
Purchased Inputs						
4	Cuttings	J	2.79E+09	5.72E+04	16	9
5	Nitrogen	g N	3.14E+03	4.05E+10	13	7
6	Labor	J	1.33E+09	1.03E+06	137	77
7	Services	$	3.02E+00	1.78E+13	5	3
	Sum of purchased inputs				171	96
Computed Transformities						
8	Total Yield, dry weight	g	5.33E+07	8.87E+07	473	266
	w/out services	g	5.33E+07	6.20E+07		
9	Energy yield	J	8.68E+11	5.45E+03		
	w/out services	J	8.68E+11	3.81E+03		

Notes can be found in Appendix A.

An important source for both sugar and tea production is the purchase of improved varieties, usually in the form of cuttings or seedlings. For emergy evaluation, seedlings and cuttings were assumed to have the same transformity as the final product. Chemical inputs, almost exclusively fertilizers, are more widely used for these commercial crops, primarily because of increased access to cash resources from their sale.

Emergy tables

Tables 3-9 and 3-10 summarize detailed emergy evaluations of sugarcane and tea production. In each case, assigned soil loss values are typical of non-degraded sites.

Table 3-10. Emergy evaluation table of smallholder tea production for western Kenya.

Note	Item	Unit	Data (units/yr)	Unit Solar EMERGY (sej/unit)	Solar EMERGY (E13 sej/yr)	Em$ Value (1995 $/yr)
Renewable Inputs						
1	Sun	J	6.23E+13	1	6	3
2	Rain	J	6.04E+10	3.10E+04	187	105
Nonrenewable Inputs						
3	Net Topsoil Loss	J	4.99E+09	2.24E+05	112	63
	Sum of free inputs (sun omitted to avoid double counting)				299	168
Purchased Inputs						
4	Improved Seedlings	J	2.01E+08	1.50E+05	3	2
5	Potash	g K	4.98E+03	1.85E+09	1	1
6	Phosphate	g P	7.75E+03	3.70E+10	29	16
7	Nitrogen	g N	4.30E+04	4.05E+10	174	98
8	Labor	J	1.33E+09	1.03E+06	137	77
9	Services	$	6.06E+01	1.78E+13	108	61
	Sum of purchased inputs				452	254
Computed Transformities						
10	Total Yield, dry weight	g	5.14E+06	1.46E+09	751	422
	w/out services	g	5.14E+06	9.84E+08		
11	Energy yield	J	7.53E+10	9.97E+04		
	w/out services	J	7.53E+10	6.71E+04		

Notes can be found in Appendix A.

Livestock Production – Communal and Constrained Systems

Livestock production is a critical component of livelihood strategies throughout rural Kenya. This is particularly true in sparsely populated semi-arid regions in the north and east of the country. Tribes in the Awach Basin (primarily Luo and Kipsigis) are historically herdsmen in the tradition of the Samburu and Maasai, and cultural vestiges of this tradition are widely evident, particularly in the equation of wealth and herd-size.

In many regions, as population growth has forced agricultural intensification, animal husbandry has shifted from rangeland to pasture. However, in sub-humid lowlands regions of the Awach Basin, despite relatively high population densities,

communal grazing continues to be the dominant herding strategy. Stock animals are primarily Zebu breed cattle, and herds are tended primarily by young boys. Observation suggests that lands under communal grazing are at greatly elevated risk of erosion.

In contrast, the humid highlands are dominated by improved hybrid animals that are paddock-fed. Consequently, highland milk and meat yields are substantially higher than in the lowlands. Emergy evaluations were done for both conditions.

Systems diagram

Figure 3-12 illustrates livestock production systems for the sub-humid lowlands and humid highlands. The primary contrast is food source, which for lowland cattle is grazed from largely unmanaged communal rangeland and for highland cattle is primarily pasture grasses and cultivated napier grass (*Pennisetum pupureum*). Zebu cattle tend to be resistant to the array of diseases that affect ruminants in tropical Africa, and hence preferred where access to medicines and veterinary services are limited. Improved breeds, in contrast, have been selected for their yield potential rather than their disease resistance. This situation has necessitated much greater investment (and incurred risk) among farmers in the humid highlands that keep improved stock. Furthermore, the cost of acquiring an improved breed cow is significantly higher than for native stock.

Emergy table

Emergy tables for both lowland communal (Table 3-11) and highland constrained (Table 3-12) livestock grazing are presented. Transformity estimates for milk and meat are computed for each analysis. It was assumed that these are co-products of the entire livestock management system. As such, emergy required to produce milk and allow a 10-15% (depending on land potential) herd off-take rate for slaughter are the same.

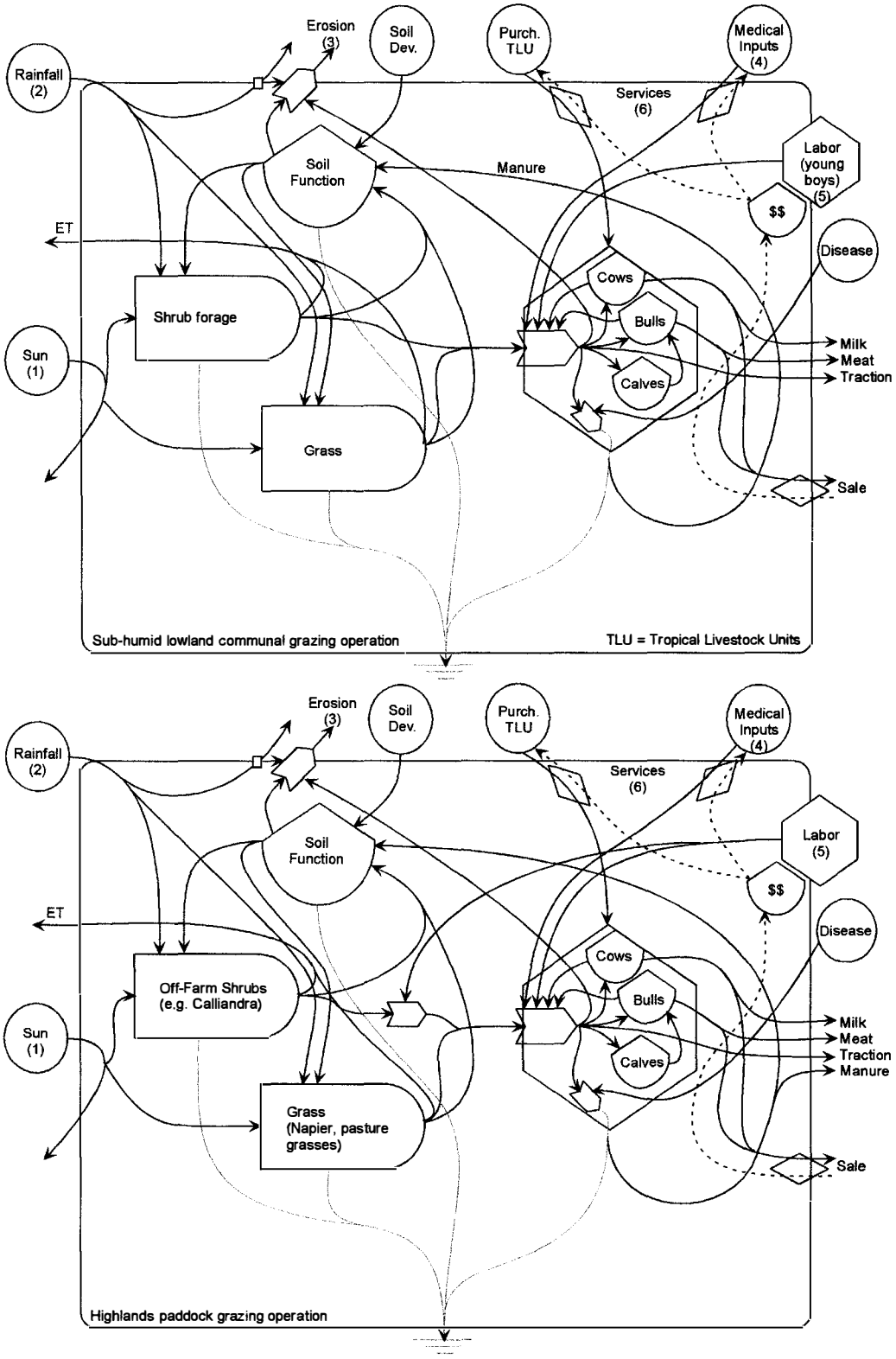

Figure 3-12. Systems diagram depicting communal and constrained animal husbandry systems within the Awach basin.

Table 3-11. Emergy evaluation table for communal (lowland) livestock production in western Kenya

Note	Item	Unit	Data (units/yr)	Unit Solar EMERGY (sej/unit)	Solar EMERGY (E13 sej/yr)	Em$ Value (1995 $/yr)
Renewable Inputs						
1	Sun	J	6.23E+13	1	6	3
2	Rain	J	2.96E+10	3.10E+04	92	52
Nonrenewable Inputs						
3	Net Topsoil Loss	J	6.52E+09	2.24E+05	146	82
Sum of free inputs (sun omitted to avoid double counting)					238	134
Purchased Inputs						
4	Medical Inputs	g	6.50E+02	2.52E+10	2	1
5	Labor	J	7.03E+08	5.00E+05	35	20
6	Services	$	2.60E+00	1.78E+13	5	3
	Sum of purchased inputs				41	23
Computed Transformities						
7	Total Yield, wet weight, milk	g	4.44E+04	6.29E+10	279	157
	w/out services	g	4.44E+04	5.39E+10		
7a	Total Yield, wet weight, meat	g	2.89E+03	9.67E+11		
	w/out services	g	2.89E+03	8.30E+11		
8	Energy yield, milk	J	1.36E+08	2.06E+07		
	w/out services	J	1.36E+08	1.77E+07		
8a	Energy yield, meat	J	2.67E+07	1.05E+08		
	w/out services	J	2.67E+07	8.98E+07		

Notes can be found in Appendix A.

Table 3-12, the emergy table describing highland cattle production also illustrates the yield differences between these two systems. The raw yield data are in Appendix A, but the dramatic differences in transformity (~300%) for comparable emergy flows illustrates the improved potential of highland agro-ecosystems for supporting particularly milk production.

Managed Forest Production

Managed forests are critical in regions like the Awach Basin where supplies of wood for fuel and building has been dwindling. Managed forests are found in both the lowlands and highlands, but the species composition differs dramatically. Lowland farm

Table 3-12. Emergy evaluation table for constrained (highland) livestock production in western Kenya

Note	Item	Unit	Data (units/yr)	Unit Solar EMERGY (sej/unit)	Solar EMERGY (E13 sej/yr)	Em$ Value (1995 $/yr)
Renewable Inputs						
1	Sun	J	6.23E+13	1	6	3
2	Rain	J	6.30E+10	3.10E+04	195	110
Nonrenewable Inputs						
3	Net Topsoil Loss	J	8.29E+09	2.24E+05	186	104
Sum of free inputs (sun omitted to avoid double counting)					381	214
Purchased Inputs						
4	Medical Inputs	g	2.50E+03	2.52E+10	6	4
5	Labor	J	6.72E+08	1.03E+06	69	39
6	Services	$	1.50E+01	1.78E+13	27	15
	Sum of purchased inputs				102	57
Computed Transformities						
7	Total Yield, wet weight, milk	g	2.33E+05	2.07E+10	483	271
	w/out services	g	2.33E+05	1.66E+10		
7a	Total Yield, wet weight, meat	g	7.50E+03	6.44E+11		
	w/out services	g	7.50E+03	5.16E+11		
8	Energy yield, milk	J	7.12E+08	6.79E+06		
	w/out services	J	7.12E+08	5.44E+06		
8a	Energy yield, meat	J	6.93E+07	6.97E+07		
	w/out services	J	6.93E+07	5.59E+07		

Notes can be found in Appendix A.

forests, or woodlots, are comprised primarily of species adapted to ~1000 mm of annual rainfall (e.g., *Acacia* spp., *Terminalia brownii*, *Grevillea robusta*). Highland farm forests are dominated by *Eucalyptus* spp. and *Acacia mearnsii,* in addition to *Grevillea robusta* and other species that coppice readily. A common practice evident throughout the highlands is use of tree leaves (including banana) as subsidized fodder for paddock-grazed animals. Ground cover in these systems is highly variable, and, though largely unmanaged, plays a significant role in controlling erosion. Nurseries exist for acquiring seedlings for exotic plantation trees (*Eucalyptus spp.*, *A. mearnsii* etc.), but availability of native seeds, particularly those species adapted to semi-arid conditions, is poor.

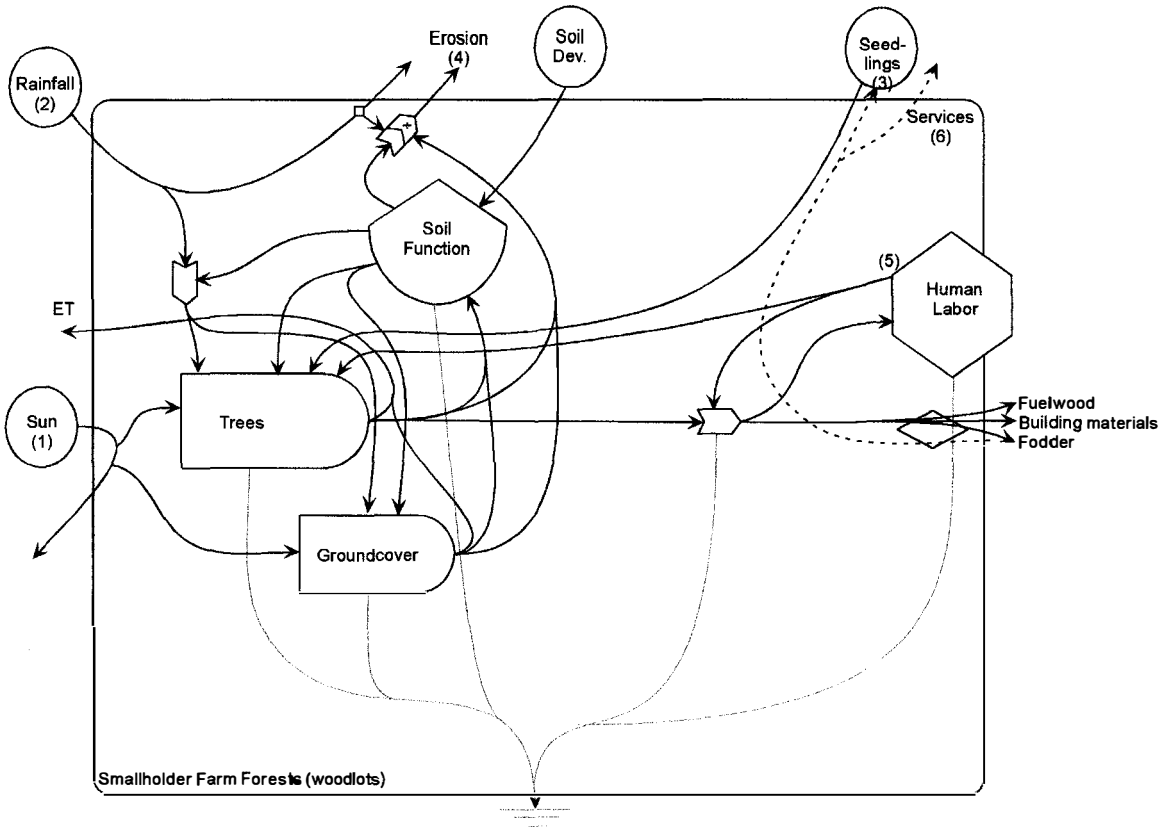

Figure 3-13. Systems diagram depicting farm forestry systems within the Awach basin.

Systems diagram

Figure 3-13 presents a typical farm forestry plot in the Awach Basin. Labor requirements are relatively high during initial planting, but reduce substantially until harvest. Most tree species typical of smallhold woodlots coppice readily so that, after initial establishment, labor and seedling requirements are minimal. Turnover times for maximal woodlot yield are between 8 and 12 years, and each hectare of land produces approximately 100 cubic meters of fuel wood over that period.

Emergy table

Table 3-13 is a tabular summary of the emergy evaluation of a woodlot system in the Awach Basin. For this analysis, no distinction was made between lowland and highland systems. While it is evident that there are moderate differences in yields,

Table 3-13. Emergy evaluation for farm forest (woodlot) production in western Kenya.

Note	Item	Unit	Data (units/yr)	Unit Solar EMERGY (sej/unit)	Solar EMERGY (E13 sej/yr)	Em$ Value (1995 $/yr)
Renewable Inputs						
1	Sun	J	6.23E+13	1	6	3
2	Rain	J	6.04E+10	3.10E+04	187	105
3	Seedlings	J	2.51E+09	7.49E+04	19	11
Nonrenewable Inputs						
4	Net Topsoil Loss	J	1.59E+09	2.24E+05	36	20
	Sum of free inputs (sun omitted to avoid double counting)				241	136
Purchased Inputs						
5	Labor	J	5.23E+08	1.03E+06	54	30
6	Services	$	0.00E+00	1.78E+13	0	0
	Sum of purchased inputs				54	30
Computed Transformities						
7	Total Yield, dry weight	g	8.00E+06	3.69E+08	295	166
	w/out services	g	8.00E+06	3.02E+08		
8	Energy yield	J	1.17E+11	2.52E+04		
	w/out services	J	1.17E+11	2.06E+04		

Notes can be found in Appendix A.

maturation times and coppice potential (Chavangi and Zimmerman, 1987), these were considered minor in comparison with differences between highland and lowland agriculture, for example. In almost all cases, use of herbicides or fertilizers in these systems is extremely limited. Regional data were available for fuel wood yields only Other useful yields would be considered co-products.

Forest/Shrubland Systems

The extent of forest cover has been reduced to remnant patches in the region. These persist primarily on steep escarpment slopes in the northwestern part of the Awach Basin where population densities are low. Charcoal production is the major economic yield from these communal lands. Charcoal is the fuel of choice among rural and urban populations because of reduced smoke content and storage space requirements. Because these forest patches are typically remote from settlement centers, substantial additional

energy is invested in transporting the charcoal product to consumers. This investment is not included in the systems diagram or the emergy table.

Systems diagram

Figure 3-14 shows an energy systems diagram of extractive use of remnant forest patches and dense communal shrublands. Frequently the soils underneath these wooded systems are shallow and stony because of their location on steep escarpments, so limited use is made of post-cleared forestlands. Some multiple-use strategies were observed, with shrublands serving as communal rangeland, but this was not widespread. Human labor is directed at harvesting and then charcoal-firing the wood. Profits reaped are not invested in purchased inputs for the forest system.

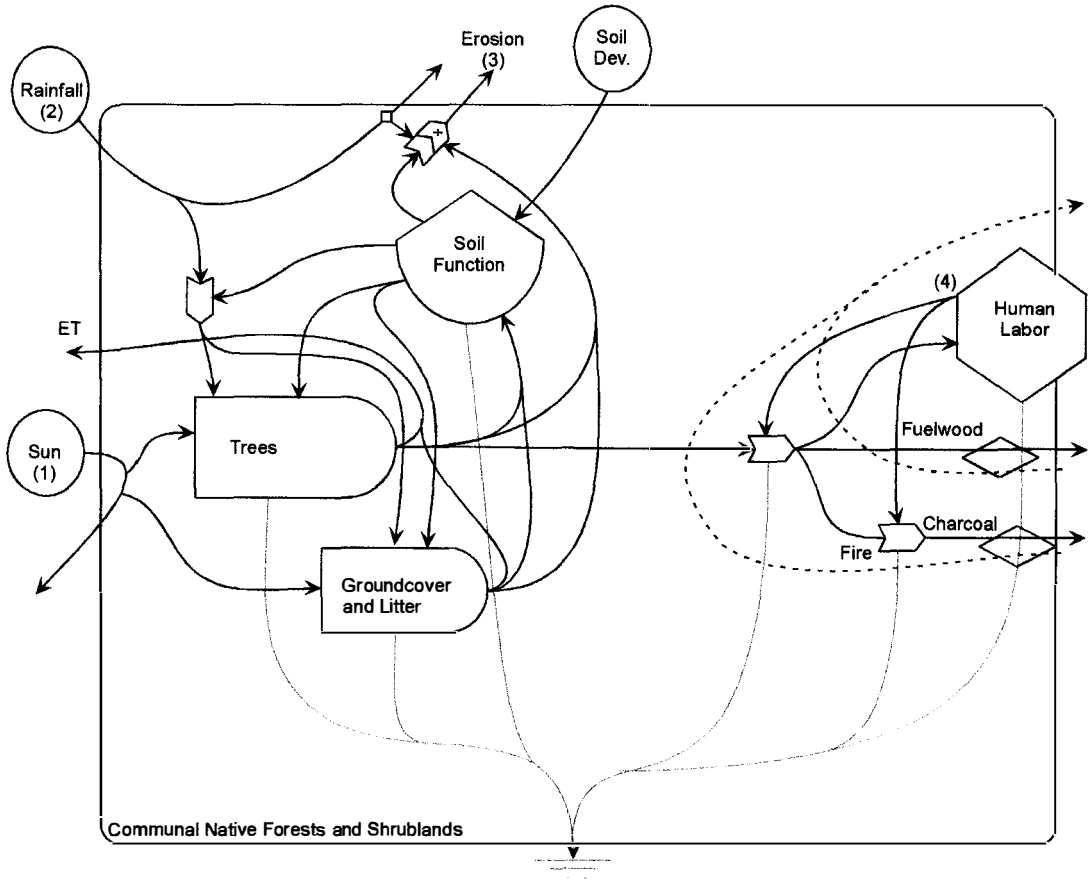

Figure 3-14. Systems diagram depicting communal native forest and shrubland systems within the Awach basin.

Emergy table

Table 3-14 provides a detailed emergy evaluation of forest extraction activities for charcoal production. Typical growth rates for forests in the region suggest that recovery to full canopy cover can take between 15 and 30 years. The latter was used to compute annualized yields from a site left under forest cover, assuming a nominal dry wood yield of 40 tons/ha (Anonymous 1994). This figure represents an average for forest and shrublands that are used for charcoal production. The net dry weight yield of charcoal is approximately 14% of wood inputs (7:1 ratio of input wood to output charcoal). Transformity values are computed for both products, but wood is rarely exported directly.

Table 3-14. Emergy evaluation table for forest/shrubland production in western Kenya.

Note	Item	Unit	Data (units/yr)	Unit Solar EMERGY (sej/unit)	Solar EMERGY (E13 sej/yr)	Em$ Value (1995 $/yr)
Renewable Inputs						
1	Sun	J	6.23E+13	1	6	3
2	Rain	J	6.04E+10	3.10E+04	187	105
Nonrenewable Inputs						
3	Net Topsoil Loss	J	3.73E+09	2.24E+05	84	47
	Sum of free inputs (sun omitted to avoid double counting)				271	152
Purchased Inputs						
4	Labor	J	4.19E+08	1.03E+06	43	24
	Sum of purchased inputs				43	24
Computed Transformities						
5	Total Yield, Wood	g	8.00E+06	3.92E+08	314	176
	w/out services	g	8.00E+06	3.38E+08		
5a	Total Yield, Charcoal	g	1.14E+06	2.75E+09		
	w/out services	g	1.14E+06	2.37E+09		
6	Energy yield, wood	J	1.17E+11	2.68E+04		
	w/out services	J	1.17E+11	2.31E+04		
7a	Energy yield, charcoal	J	1.67E+10	1.87E+05		
	w/out services	J	1.67E+10	1.62E+05		

Notes can be found in Appendix A.

Because most of the inputs are renewable, this land use strategy has the highest % Renewable index (78%) of all the subsystems examined. This also results in extremely high yield ratio and low loading ratio. However, it is critical to illustrate that the Agricultural Benefit Ratio is larger than for other land-use options because yields are small compared with environmental costs. This observation becomes more pronounced when soil loss rates observed under degraded conditions are used (Table 3-15).

Comparative Summary Indices

Table 3-15 gives summary indices for each target subsystem. In addition to providing a comparison of subsystems when soil loss is not evident (i.e. intact conditions), it compiles indices for the degraded condition. Measurement and inference of soil loss rates are presented in a later section. Note that the transformity under livestock systems is for meat production and for charcoal under native forest systems.

Of particular interest is comparison of the ABR between systems. When intact conditions prevail, the largest net benefit comes from farm forestry activities, charcoal

Table 3-15. Comparison of Agricultural Benefit Ratio and computed transformity for landuse subsystems for intact and degraded conditions.

		Landuse Subsystems						
	Summary	Subsistence	Commercial Ag.		Livestock Prod.			
Erosion?	Index	Ag (Maize)	Sugarcane	Tea	Communal	Constrained	Woodlots	Shrubland
Intact	Investment	0.90	0.57	1.51	0.17	0.27	0.22	0.16
	Loading	1.89	1.49	3.01	2.04	1.47	0.46	0.68
	Yield	2.12	2.76	1.66	6.75	4.73	5.57	7.28
	ABR	5.52	6.23	6.72	1.91	2.60	7.41	3.76
	Transformity	1.06E+05	5.45E+03	9.97E+04	2.06E+07	6.79E+06	2.56E+04	2.68E+04
	FCSD	0.18	0.16	0.15	0.52	0.38	0.14	0.27
Degraded	Investment	0.47	0.35	0.93	0.08	0.20	0.08	0.08
	Loading	3.25	2.48	4.02	4.99	2.16	2.43	2.21
	Yield	3.12	3.86	2.08	13.29	6.03	13.11	13.94
	ABR	2.25	2.91	3.13	1.32	1.93	1.58	1.62
	Transformity	1.56E+05	7.61E+03	1.25E+05	4.06E+07	8.66E+06	6.03E+04	5.13E+04
	FCSD	0.44	0.35	0.32	0.76	0.52	0.63	0.62

Note: Transformity values for livestock production are for meat (not milk).

production on shrublands and tea production. Subsistence agriculture and sugarcane production also provide high net benefits. In each case, livestock production has lower ABR values and higher FCSD values. In contrast, when sites are degraded, cropping systems (both subsistence and commercial) provide more net benefit. Table 3-16 summarizes the ABR and FCSD values for Kenya and three local districts to provide a reference point with which to compare sub-systems evaluations.

For each landuse, the transformity of the product increases dramatically under degraded conditions, reflecting the large percentage of the emergy delivered from depleted soil stocks. When degradation occurs in forest systems, it is generally severe. Consequently, net agricultural benefit is reduced dramatically. A more complete discussion of soil loss rates from different landuse subsystems is presented later.

Table 3-16. Summary indices for Kenya and three local districts for comparison with results from sub-systems evaluations.

Index	Kenya	Kisumu	Kericho	Nyando
Emergy Investment Ratio	0.44	5.05	0.66	0.6
Environmental Loading Ratio	0.8	10.44	2.24	1.92
Emergy Yield Ratio	1.23	0.61	1.49	1.27
FCSD	3.8%	2.4%	3.43%	14.2%
ABR	7.56	4.37	11.11	2.25

From Tables 3-11 it is clear that lowland (sub-humid) livestock production in this region is an environmentally costly endeavor. The ABR is 1.91 even for intact sites, suggesting that yields are small relative to erosion costs. The converse of the ABR is the FCSD index, which in this case suggests that over 60% of emergy use in this system occurs via topsoil depletion. It should be noted that the soil loss figure presented in Table 3-11 is the predicted erosion rate under sites that were judged intact. Degraded sites exhibited substantially elevated erosion rates.

SOIL EROSION RISK FACTORS

Field Sample Sites

Field sampling in the Awach River basin took place between February and May 2001. In total, 420 sites were sampled according the basic site protocol described. Of these 420 sites, 61 were selected for measurement of infiltration characteristics, and 180 were selected for surface deflation estimation using erosion pins. Figure 4-1 presents the spatial location of the 420 sample sites overlain on a geological thematic coverage.

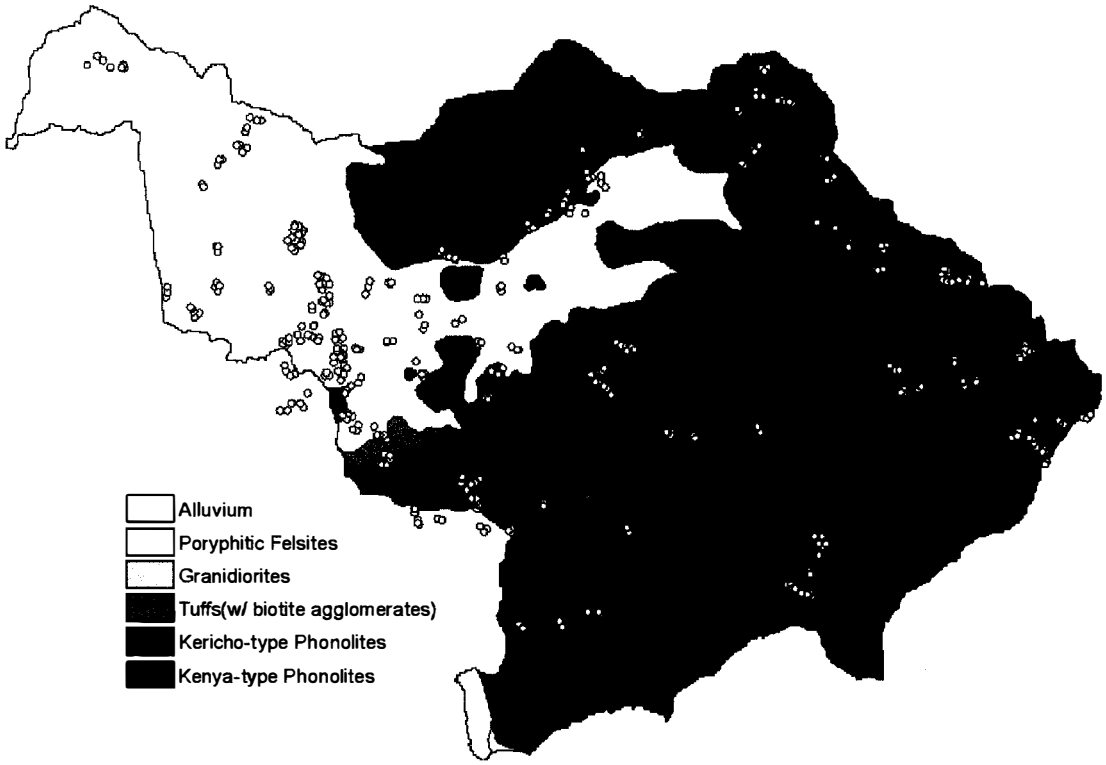

Figure 4-1. Geologic map of the Awach River basin with overlay of field sampling sites (from Corbett et al. 1997).

Dominant geological substrates are recent (Pleistocene) alluvial deposits and Kenya- and Kericho-type phonolites (volcanic alkaline igneous material similar to andesite or rhyolite). Other evidence of regional volcanic origins include granidiorite and tuff deposits. Where possible, clustered sampling was done across geologic boundaries.

In addition to geologic stratification, the most important controlled variables were landuse, elevation and soil degradation. Table 4-1 presents sampling effort for each stratum organized by major category and primary within-category delimiting factors.

Table 4-1. Field sample sites sorted by primary stratification factors (e.g. landuse, elevation/slope, degradation status). Total sampling effort was 420 sites.

	Landuse							
	1 – Agriculture		2 - Rangelands		3 - Forest		4 - Other	
	Subsist.	Comm.	Sparse	Dense	Managed	Unmanaged	Wetland	Sev. Degr.
Count	116	33	95	52	67	11	10	36
Total	149		147		78		46	
							TOTAL	420
	Elevation							
	Lowlands (<1350 m)		Escarpments		Highlands (>1650 m)			
	Steep	Shallow	Steep	Shallow	Steep	Shallow	(Steep is > 8 degrees)	
Count	11	195	58	29	34	93		
Total	206		87		127		TOTAL	420
	Soil Degradation							
	Intact		Moderate		Severe			
	Dense	Sparse	Dense	Sparse	Dense	Sparse	(Dense Cover is > 50%)	
Count	174	68	31	74	6	67		
Total	242		105		73		TOTAL	420

The relative paucity of unmanaged forest sites was a result of their absence from the landscape, not incomplete sampling. The small number of wetland sites, primarily sampled within a large wetland complex at the watershed terminus, does not reflect the total abundance of flooded sites in the basin. Several wetland sites (n = 12) were classified as agricultural lands or pasture despite the presence of hydrophytic vegetation and hydrologic evidence suggesting wetland conditions. The presentation of cover data

as a classifier within degradation status is correlational; no explicit effort was made to stratify within site degradation for vegetative characteristics.

Digital Elevation Model and Terrain Analysis

DEM Development

A digital elevation model was developed for the region as described previously. A complement of spot heights, digitized and rasterized stream networks and 1:50,000 scale topographic contour maps were used to develop the DEM. Figure 4-2 presents the elevation surface with sample site locations and the Awach River basin boundary.

Shown in Figure 4-2 are two end-points (A and A') of an elevation profile, given in Figure 4-3. Spot heights from sample site GPS readings were used to verify DEM

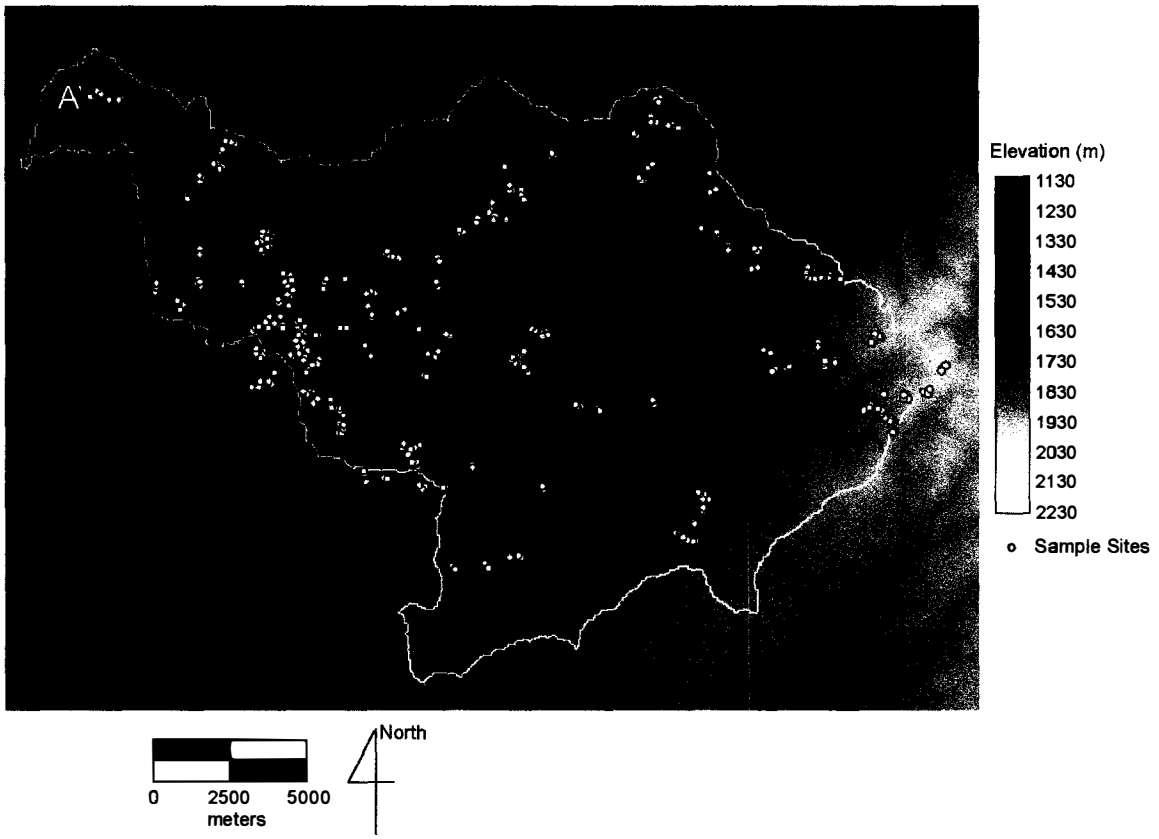

Figure 4-2. Digital elevation model of the Awach River basin showing elevation (in meters) and spatial locations of 420 field sampling sites. Also shown are the end points (A and A') of the profile given in Figure 4-3.

accuracy, yielding a vertical root-mean square error (RMSE) of 8.9 meters. The DEM-based slope map, not shown here, was verified using slope observations; linear regression indicated acceptable accuracy ($r^2 = 0.70$, $P << 0.001$) with no evidence of bias ($\beta = 0.99$).

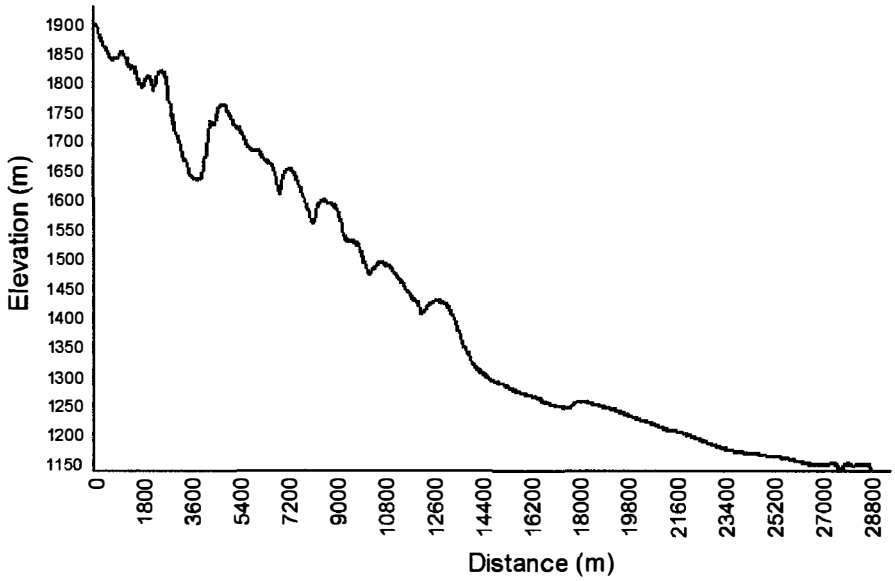

Figure 4-3. Elevation profile between the highlands (Point A in Figure 4-2) and the wetland terminus at Lake Victoria (Point A' in Figure 4-XX). Basin mean slope = 5.3%.

Terrain Analysis

Application of the sediment transport capacity proposed by Wilson and Gallant (1996) was done using a standard watershed accumulation command in Idrisi (Clark Labs, 2001) in concert with the slope surface inferred from the digital elevation model. Figure 4-4 shows the computed index values, truncated for visual interpretability so that all values greater than 6 were assigned the same shade. Maximum values of approximately 80 were found along escarpment walls, but represent an extremely small spatial extent. Large values indicate high potential for sediment movement given no detachment limitation. As such, the map in Figure 4-4 should be interpreted as merely one component of local erosion risk. In addition to displaying the computed index

values, sample sites are presented according to visual designation of erosion status (intact, sheet, severe sheer, rill, gully). Note that degradation was observed throughout the Awach basin, but the majority of severe degradation was observed where transport capacity index values were relatively small.

Computed sediment transport values were extracted for each site, and compiled according to observed degradation status (Table 4-2). Standard analysis of variance (ANOVA) applied to these data result in an F-statistic for significant differences between means of 0.74 (df = 4, $P = 0.57$). Clearly there is insufficient evidence to infer that transport capacity and observed erosion are associated. Moreover, the data in Table 4-2 suggest that as erosion severity increases, predicted site transport capacity is reduced, contrary to expectation.

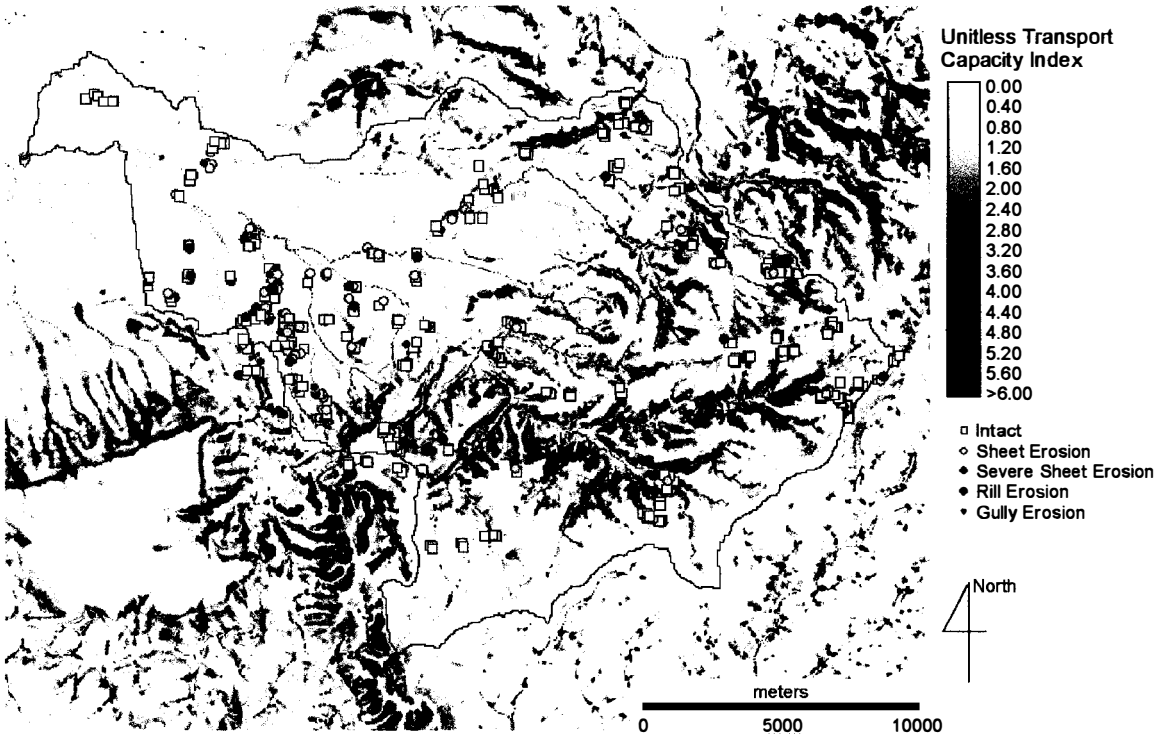

Figure 4-4. Sediment transport capacity surface inferred from the DEM based on the algorithm proposed by Wilson and Gallant (1996). Also shown are field sample sites delineated by field classification of degradation status.

Table 4-2. Extracted sediment transport capacity (Figure 4-4) for field sampling sites by observed erosion severity class.

Erosion Class	Average	Std. Dev.
1	1.20	2.28
2	1.30	2.44
3	1.16	2.41
4	0.84	1.07
5	0.49	0.62
Basin Mean	1.16	2.23

Spectral Analysis

Characterization of soils over large areas at the spatial resolution requires rapid processing of large numbers of soil samples. This work explored using radiometric reflectance signatures to define an array of soils performance measures, ranging from conventional laboratory parameters to binary classifications of degradation status and infiltration capacity. Spectral calibrations were developed using an existing soil library, and subsequently applied to spectra measured from soils collected in the study area.

Data Visualization and Compression

The hyperspectral reflectance library that was used to develop multivariate calibrations of laboratory measured soil properties contained 513 samples collected from throughout western Kenya. Each sample consists of 198 reflectance measurements, derivative transformed to allow direct comparability between samples. In order to visualize variability in this data space, standard linear data compression tools were used. More important than facilitating better data-space visualization, this spectral library allows calibration bounds of the multivariate soil property models to be defined, from which spectra from the Awach basin could be screened for outlier samples.

Principal components analysis

Standard forward-rotation principal components analysis was performed for the 513 soils in the spectral library. Data compression was effective, as shown in the eigen-

value screeplot in Figure 4-5. The 198 bands of reflectance information were reduced to four significant axes, collectively explaining 92.9% of the variance in the original data. The broken-stick comparison method indicates that axes 5 and above explain no more variance than expected by chance, and are therefore disregarded. Furthermore, the explanatory power of the first two axes is substantially larger than axes 3 and 4, allowing axis interpretation and end-member analysis to focus only on these primary axes.

Plotting the 513 soils from the spectral library in principal components space using only the first two axes produces the cross marks in Figure 4-6. Axis 1 is projected on to the abscissa and axis 2 on to the ordinate axis. The variance explained values are for this spectral library PCA. Raw data were left untransformed because none of the standard normalization transformations improved skewness of reflectance across soil samples (mean skewness = -2.25). Furthermore, the observed skewness is a result of deep spectral absorbance features around 1370, 1890 and 2180 nm, which are important

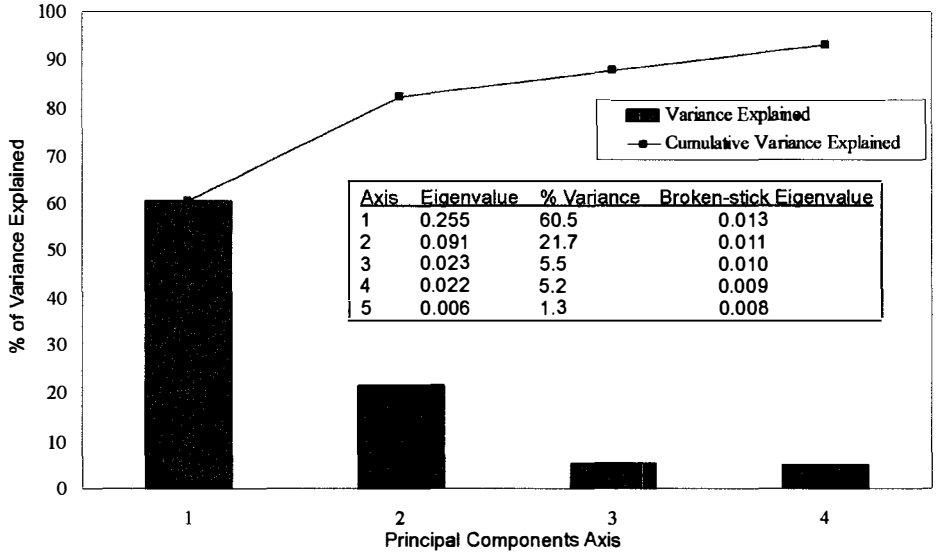

Axis	Eigenvalue	% Variance	Broken-stick Eigenvalue
1	0.255	60.5	0.013
2	0.091	21.7	0.011
3	0.023	5.5	0.010
4	0.022	5.2	0.009
5	0.006	1.3	0.008

Figure 4-5. Screeplot summarizing principal components analysis of spectral library. Variance explained by each of the first four axes is shown in addition to cumulative variance reduction.

physical attributes. Since the PCA approach is robust to moderately skewed normality (McCune and Grace 2001), and the coefficient of variation across samples was relatively small (CV = 35%), no data transformation was performed. Normality assumptions for the data across wavelength band were acceptable (mean skewness = 0.015).

The PCA transformation produced a matrix of eigenvectors that relates each individual wave band reflectance value to the principal components axes. These eigenvectors can be used to project new data into the same multivariate data space. This was done to screen the Awach Basin data to look for soils that fall outside the range of calibration. The gray circles in Figure 4-6 represent the Awach Basin soil samples (n = 1260 – 3 soil samples per plot). The black squares in Figure 4-6 are sediment samples retrieved from the Awach Basin terminal wetland.

Visual analysis qualitatively indicates the extent to which the spectral library bounds the variability in the Awach samples, shown in comparison in Figure 4-6. For example, along principal component 1, the spectral library bounds the entire Awach Basin data set. Along principal component 2, the spectral library fails to encompass the variability displayed by approximately 18 Awach Basin soil samples. Further, there is a region in the lower right quadrant of the bi-plot where additional evidence exists that the spectral library fails to capture the entire scope of variability in the Awach Basin. In the absence of additional laboratory analysis, identification of spectral coverage in this manner is not particularly useful. Within the scope of developing a more comprehensive spectral library, these soils would be analyzed in a laboratory and included in soil property model development, outlined below.

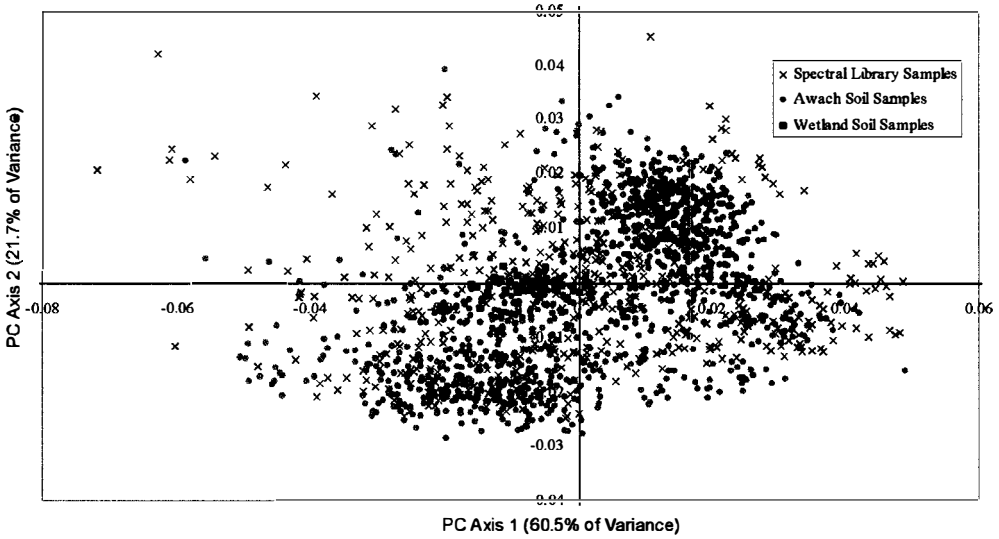

Figure 4-6. Biplot of principal components axes 1 and 2. Shown in the same ordination space are spectral library soils, soils from the Awach River basin, and wetland soils from the Awach river terminal wetland at Lake Victoria.

Outlier analysis

A further application of PCA output data is to identify spectral outliers statistically. Outliers were formally defined as those soils from the Awach Basin that fell more than 2 standard deviations (both criteria were explored) away from the mean for each principal component defined for the spectral library. Table 4-3 presents soils that are defined as spectral outliers. Sample nomenclature is: S – indicates an Awach basin sample, 14 –sample plot number and, B –within-plot sample position.

It is also important to note convergence of outliers to specific locations. For example, all samples from site 14 are outliers (along PC Axis 1 and 4) and all three samples (A, B and C) from site 370 and 345 are outliers along axes 2 and 3. Moreover, outlier sites were clustered spatially. Sites 266, 268 and 272 were proximate and were all classified as significant outliers along axis 1. This convergence suggests that sites designated as outliers may not be so classified because of measurement error.

Given the sample size, a number of sites (n ~ 60) would be expected to fall outside the 2 sd range with a normal probability distribution. As such, only those sites that were more than 3 sd from component means were excluded from further analysis.

Note that outliers defined in this manner are for soil spectra as a whole. However, specific portions of the spectra are information rich for predicting soil functional performance measures. Consequently, outliers for specific soil properties may be quite different from outliers for soil spectra generally.

Table 4-3. Spectral outliers from Awach Basin soil samples (n = 1260) with reference to principal components ordination of soil spectral library (n = 513). Bolded soils were 3 s.d.-level outliers.

	Principal Components Axis			
Sample Soils	1	2	3	4
Outliers (>2 sd)	18	18	29	26
Outliers (>3 sd)	5	0	0	2
Outlier Sites	S14B	S8A	S133C	S14A
(bold sites were	S32B	S8C	S173B	**S14B**
3 s.d. outliers)	S49C	S44A	S241C	S50C
	S102A	S44B	S249C	S55C
	S104B	S44C	S266C	S70B
	S147B	S173B	S268C	S70C
	S232B	S210C	S272C	S86C
	S241C	S284A	S276A	S97C
	S249C	S345A	S277A	S104B
	S260A	S345B	S277C	S128C
	S266C	S345C	S278A	S130A
	S268C	S358B	S285A	S130B
	S272C	S358C	S285B	**S140A**
	S297A	S394A	S293B	S140B
	S323A	S394B	S298A	S152C
	S323B	S394C	S300A	S187B
	S352B	S397C	S301A	S205A
	S372B	S401C	S314B	S231B
			S314C	S301A
			S323A	S318A
			S345A	S318C
			S345B	S322C
			S345C	S324C
			S370A	S332C
			S370B	S368C
			S370C	S383B
			S394A	
			S394B	
			S394C	

Spectral end-member visualization

By projecting new data into principal component space, spectral outliers were identified, allowing visualization of spectral response variability within the data set. Soils with component axis scores closest to the mean and ± 2 standard deviations were selected for only the first two principal components.

Figure 4-7 shows raw reflectance spectra for the entire electromagnetic sampling region for 6 sample soils. These soils represent mean and end-member spectra for the first two principal components. Note that, while Figure 4-7 presents raw reflectance data, PCA and all subsequent analyses were done using derivative-transformed data. This was to allow direct reference to Figure 1-2 that summarizes relevant spectral absorption features. Samples selected for each representative end-member signature are labeled.

It is clear from Figure 4-6 that the general geometry of spectral reflectance curves are remarkably similar. Much of the variability appears to be due to brightness (relative reflectance) and relative intensity of absorption features around 1370, 1850 and 2150 nm. The visible portion of the spectra (350 – 750 nm) exhibits limited discrimination between

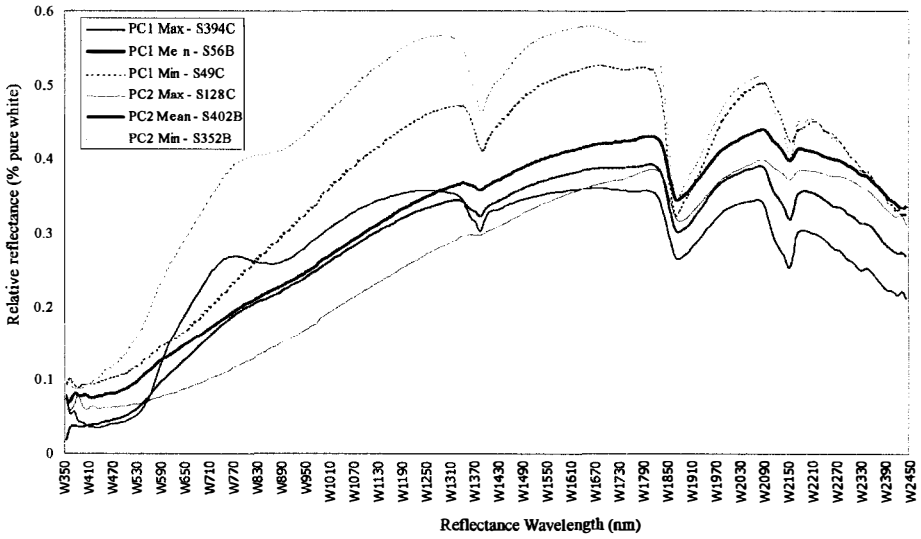

Figure 4-7. Mean and end-member (± 2 s.d.) example raw reflectance spectra for first two principal components.

soils with respect to shape, but shows strong differences in brightness. The mean spectra are similar, as expected given the density of points around the origin in Figure 4-6.

To further visualize reflectance signatures, segments of the spectra containing discriminating features were selected (Figure 4-8). Note that these data are first-derivative transformed data, in contrast to raw reflectance data in Figure 4-7. Also, note that the vertical scale varies between plots. This is particularly important for the segment between 1830 – 1920 nm, which is a consistently deep absorption feature.

Trend consistency offers some insight into spectral regions useful for soil assessment. Specifically, substantial noise is apparent within the visible to near-infrared region (380 – 1360 nm). In contrast, longer wavelength near infrared (1370 – 1470 nm and 1830 – 1920 nm) is more promising for spectral soil inference. Information content in the mid-infrared (1970 – 2450 nm) is evident but the signal is more complex.

Multivariate Soil Property Models from Reflectance Spectra

The technique described previously to allow prediction of standard soil properties from the spectral reflectance data was applied to the spectral library (n = 513 soils). Soil properties that were modeled include soil texture (% sand, silt, clay), soil organic matter, cation exchange capacity, pH, and exchangeable ions (P, Ca, Mg, K). A committee of regression trees was developed for each soil parameter, and the predicted responses for both the calibration data set (n = 310) and the holdout-validation data (n = 203).

Because the regression tree models were developed using tree committees with data resampling, each soil property model cannot be visualized. However, the non-committee approach to model development is to produce a tree which is pruned using V-fold cross validation. The decision tree rule base developed in this manner for predicting

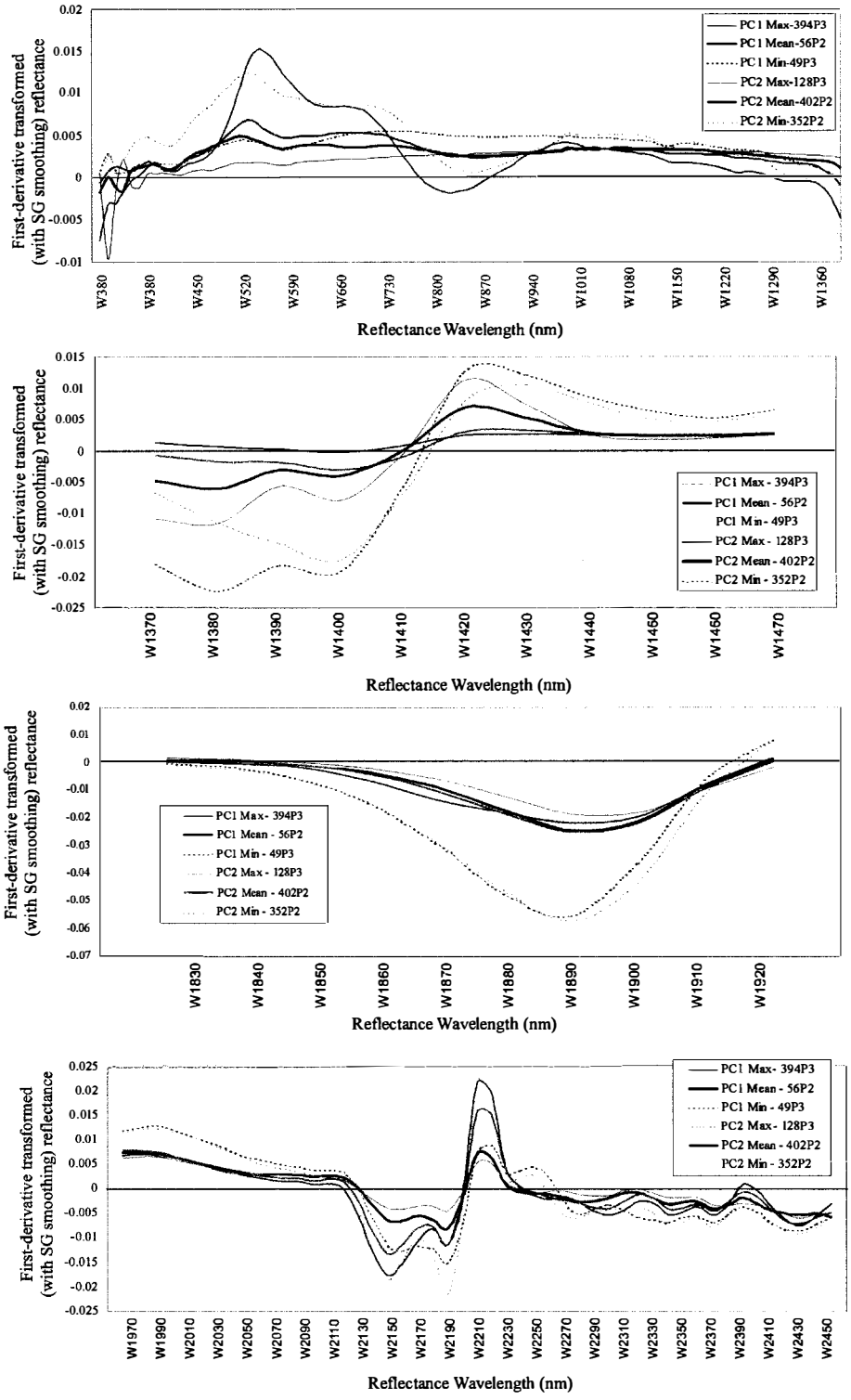

Figure 4-8. Mean and end-member (± 2 s.d.) example derivative transformed spectra for first two principal components for four spectral regions with large evident spectral separability.

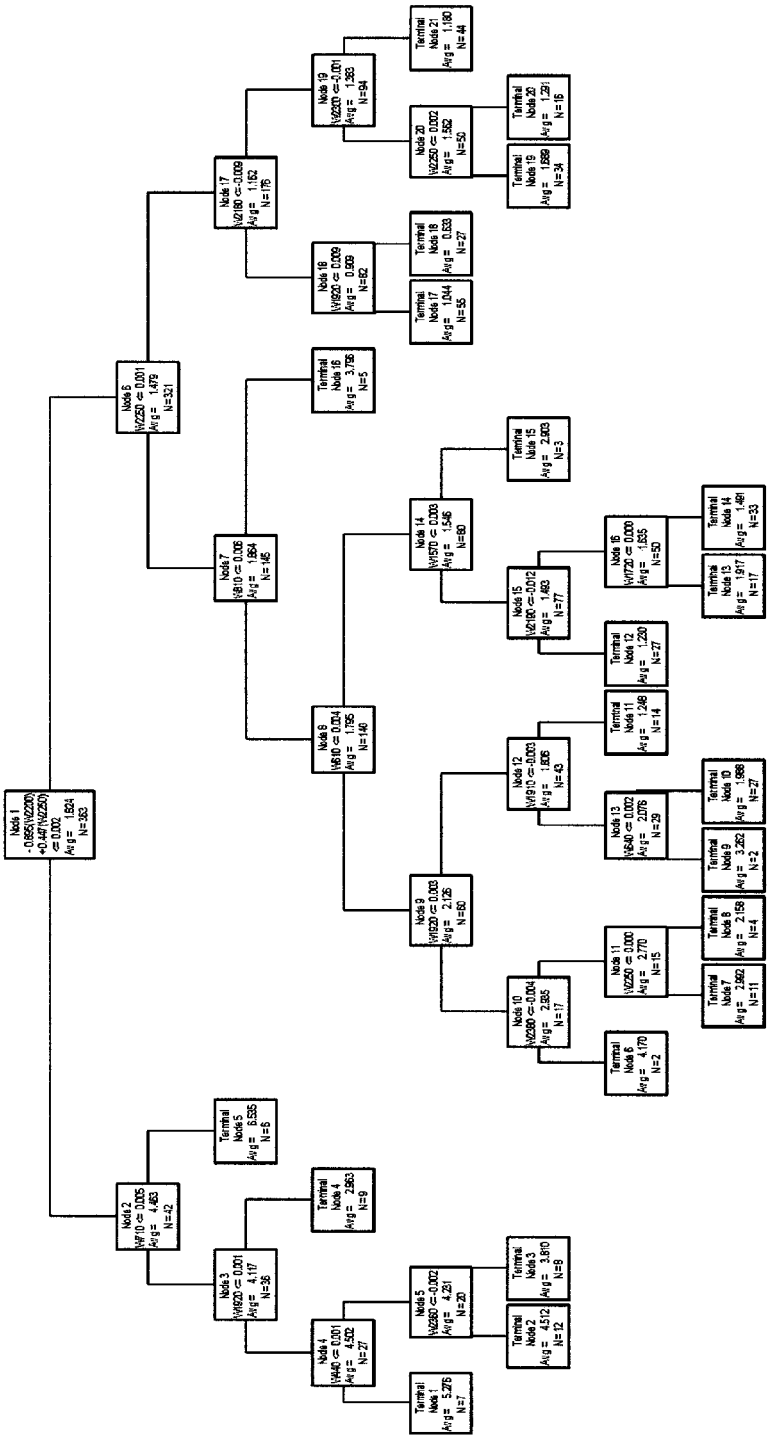

Variable	Importance
W2200	100
W1390	76.04
W1400	48.59
W1430	47.12
W1380	46.81
W2250	19.86
W1920	16
W740	14.03
W750	14.03
W730	13.92
W710	13.92
W760	13.92
W720	13.92
W2050	9.72
W2040	9.23
W810	8.95
W2060	8.39
W2030	8.26
W790	6.79
W800	6.79
W2070	6.33
W610	6.02
W820	5.7
W830	5.7
W840	5.7
W2180	5.32

Figure 4-9. Cross-validated regression tree developed for predicting soil organic carbon content of soil from reflectance spectra information. Also shown are the most important splitting variables.

soil organic carbon (SOC) from spectral reflectance is shown in Figure 4-9. This is presented only as a means to visualize model form. Note that the list of important spectral bands for SOC regression tree development (Figure 4-9) is dominated by bands in the mid- and near-infrared portions (2000 – 2250 nm, 1380-1430 nm and 710-840 nm) of the spectra, with only one important variable falling in the visible portion of the spectrum (W610, or 610 nm). The inclusion of surrogates may result in important spectral bands being absent as primary split criteria.

The tree committee grown for SOC (250 trees grown using adaptive resampling) was evaluated by comparing model predictions with laboratory measurements. This was repeated for each soil property model. Figure 4-10 illustrates the model fit for SOC for calibration soils and those held out to validate the model. Additional model fits are presented along with ancillary model information in Appendix B.

A summary of model fit for each soil property in calibration and validation is presented in Table 4-4a. As shown, models were extremely effective for predicting calibration soil properties (mean $r^2 = 0.97$). More importantly, the validation accuracies are high (mean $r^2 = 0.81$). Of additional interest is the functional relationship (slope and intercept estimates) between observed and predicted values (shown in Table 4-4a for the calibration data). The expected values for the slope and intercept are 1 and 0, respectively. Some deviation from these expected quantities was tolerable because the data range rarely includes the origin, but some evidence of data range compression is observed because almost all slope values are less than 1 (i.e. the range of predicted values is narrower than the range of observed data). Model estimates of soil properties, used in

all subsequent analyses, were adjusted by the model functional form to compensate for this potential problem; correlation between predicted and observed remains unchanged.

Models for two additional soil properties, exchangeable phosphorus and potassium, were unsuccessful, resulting in validation efficiencies of less than 50%. However, by assigning observed data into classes based on functional thresholds for each constituent (e.g., from Brady and Weil 2001), robust screening models were possible

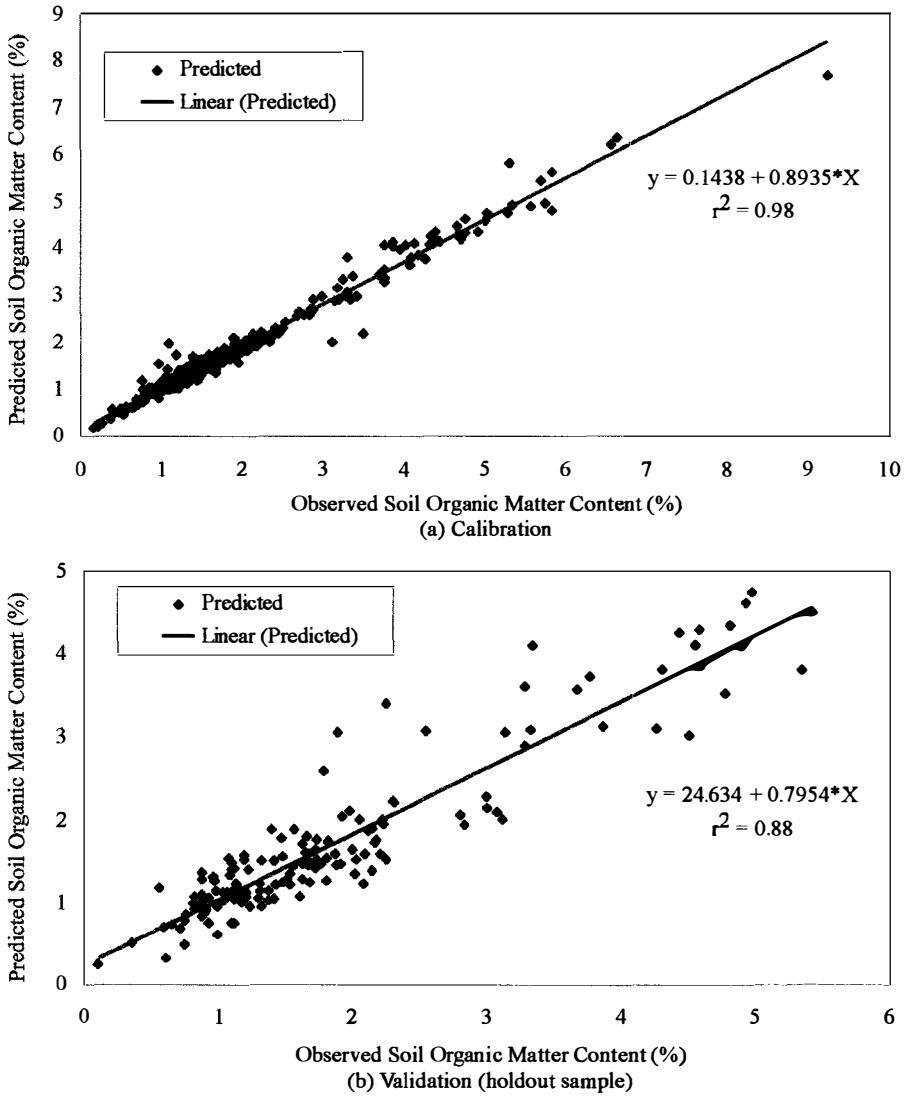

Figure 4-10. Chart depicting fit between predicted and observed soil organic matter content (in %) for a) calibration data set and b) holdout validation data.

using classification trees. The selected threshold for P was 5 ppm (Olsen exchangeable), which is characteristic of soils with severe P limitation. Similarly, the K threshold (0.4 cmol/kg) represents a lower bound for supporting crop production without subsidy.

Table 4-4. Model efficiency for predicting measured soil properties from spectral reflectance signatures.

	Predicted to Actual			
Soil Property	Intercept	Slope	Cal r^2	Val r^2
CEC	2.56	0.845	0.98	0.91
Exch Bases	3.07	0.834	0.98	0.90
CEC-Clay	13.70	0.656	0.98	0.73
Clay	11.70	0.693	0.97	0.82
Silt	-3.42	1.159	0.95	0.72
Sand	15.75	0.621	0.96	0.80
Exch. Mg	1.08	0.749	0.96	0.85
Exch. Ca	3.83	0.789	0.98	0.83
SOC	0.14	0.894	0.98	0.88
pH	3.22	0.516	0.94	0.62

Table 4-5. Binary classification efficiency for cross-validated tree models based on reflectance spectra. Screening thresholds are defined based on published soil functional levels (Brady and Weil, 2001).

	Calibration				Validation			
Binary Soil Parameters	Sens.	Spec.	Total	OR	Sens.	Spec.	Total	OR
P < 5 ppm	0.86	0.88	0.87	43.97	0.73	0.77	0.75	9.31
K < 0.4 cmol/kg	0.86	0.78	0.82	23.14	0.74	0.71	0.72	6.96

Model results are presented in Table 4-5. For each binary model, sensitivity (correct positives), specificity (correct negatives), accuracy and odds ratio are presented for both calibration and cross-validation. For each soil parameter, models are balanced (sensitivity ≈ specificity), and model validation efficiencies are highly significant.

Definition of Case and Reference Soils

A spectral definition of soil degradation based on visual delineation of erosion status was developed using reflectance signatures. This definition was developed using only soils for which degradation status was considered reliably defined during fieldwork. Those soils (e.g. agricultural soils) for which degradation condition is obscured by human

management were omitted from the calibration. This spectral model obviates the need to infer degradation from proximate variables (e.g., texture, SOC). It also facilitates an objective definition of degradation that is repeatable across observers and times, regardless of visual masking (e.g., tillage) or season. After spectral model development, the rule base for discriminating intact from degraded soils was applied to the subset of soils for which site delineation of degradation status was impossible.

Case definitions (i.e. models devised to discriminate between intact and degraded soils) were developed for binary and three-category degradation conditions observed in the Awach Basin, in addition to soil hardsetting and gully soils, using classification tree models. Optimal trees were selected to maximize cross-validation accuracy. Table 4-6 summarizes the model accuracy, both in calibration and cross-validation.

Clearly, discriminating intact from degraded soils using spectral reflectance signatures is effective. For binary classification, calibration accuracy was 95%, with balanced error rates for omission and commission. Three-category models were only slightly less efficient, with classification error primarily in discriminating the middle category (moderate degradation). In each case, cross-validation accuracy was lower than calibration accuracy.

It should be noted that visual designation of hardsetting was confounded by severe erosion. Of the 99 soils that were incorrectly classified as hardset, 88% were severely degraded. This suggests that many sites may have actually been hardset, but that the visual cues for delineating this condition were masked by rill or gully features. The rule-bases developed for discriminating between intact and degraded soils were applied to the remaining soils (n = 445). Table 4-7 summarizes the results.

Table 4-6. Case-reference definition summary. Given are model fit statistics between soil spectral reflectance and observed degradation.

Hardset	Calibration				Validation (V=10)	
(n = 819)	Pred N	Pred Y		(n = 819)	Pred N	Pred Y
Obs N	574	99		Obs N	543	130
Obs Y	6	136		Obs Y	37	105
	Accuracy	Sensitivity	Specificity	Odds-Ratio		
Calibration	87.12%	95.8%	85.3%	131.4		
Validation	79.51%	73.9%	80.7%	11.6		

Gully Soils	Calibration				Validation (V=10)	
(n = 819)	Pred N	Pred Y		(n = 819)	Pred N	Pred Y
Obs N	614	64		Obs N	592	86
Obs Y	24	113		Obs Y	32	105
	Accuracy	Sensitivity	Specificity	Odds-Ratio		
Calibration	89.20%	82.5%	90.6%	45.2		
Validation	85.52%	76.6%	87.3%	22.6		

Binary Erosion	Calibration				Validation (V=10)	
(n = 819)	Pred N	Pred Y		(n = 819)	Pred N	Pred Y
Obs N	374	28		Obs N	300	102
Obs Y	15	402		Obs Y	97	320
	Accuracy	Sensitivity	Specificity	Odds-Ratio		
Calibration	95.0%	93.3%	96.6%	395.7		
Validation	75.7%	76.7%	74.6%	9.70		

Ordinal Erosion	Calibration				Validation (V=10)		
(n = 819)	Pred 1	Pred 2	Pred 3	(n = 819)	Pred 1	Pred 2	Pred 3
Obs 1	334	11	8	Obs 1	273	79	49
Obs 2	31	181	6	Obs 2	57	72	38
Obs 3	26	12	206	Obs 3	21	38	188
	Accuracy	Sensitivity*	Specificity*	Odds-Ratio*			
Calibration	88.5%	93.6%	93.6%	215.7			
Validation	70.6%	84.1%	86.1%	32.6			

* These model summary measures are for discriminating severely degraded soils from other soils.

Table 4-7. Summary of spectral predictions of degradation for soils at sites where visual designation was confounded.

Hardsetting (n = 445)		
	Intact	Hardset
Number	306	129

Binary Degradation (n = 445)		
	Intact	Degraded
Number	227	218

Categorical Degradation (n = 445)			
	Intact	Moderate	Severe
Number	199	120	126

Further indication of the efficacy of the case-reference definition is in assessing the odds of classification as degraded given field observation categorization. Figure 4-11 gives odds ratios of case classification given field assignment of degradation status. Results suggest that the odds ratios of correctly classifying a gully or hardset soil as degraded are over 60. Given intact field designation, the odds ratio of a soil being designated a case are 0.06.

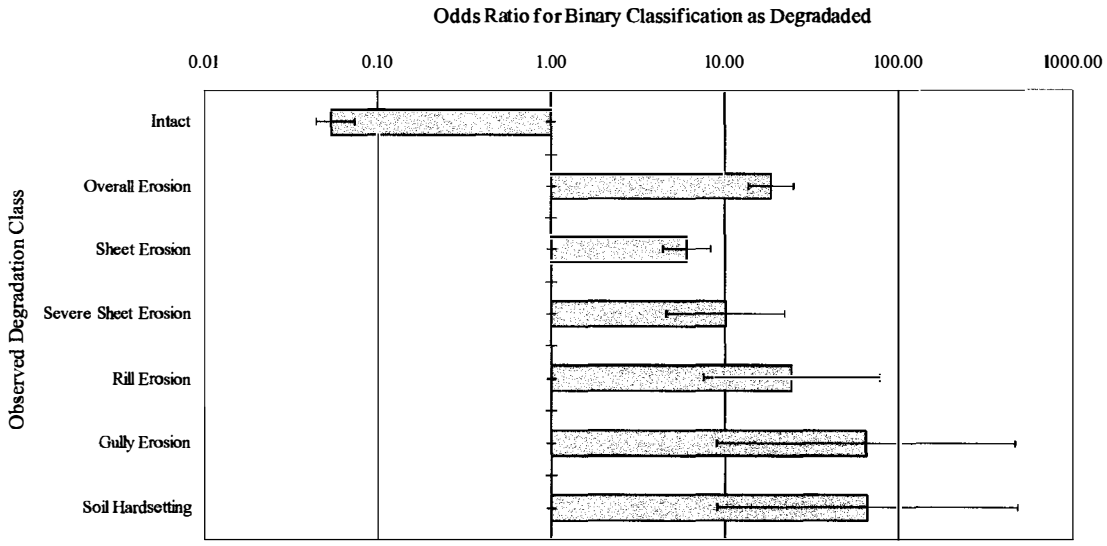

Figure 4-11. Odds ratios for designation as spectral case conditioned on observed degradation category. Also shown are 95% confidence bars for the odds ratio estimate.

Awach Basin Soils Assessment

Soil Property Estimation

The soil property models developed above were applied to soils sampled in the Awach Basin. Table 4-8 summarizes soil properties for the 1260 sample soils according to degradation status (both observed and spectrally-designated). Standard analysis of variance was applied to visual erosion status, and Student t-tests to binary classifications to determine which soil properties responded significantly to changes in degradation status. Where necessary, contrasts were done on transformed data to ensure normality

assumptions were met. Significance levels for ANOVA contrasts were held at 95% (family-wise), while for t-test contrasts, *P*-value classes are reported.

For categorical soil properties (exchangeable P and K) where the comparison is between proportions, these techniques are inappropriate. Instead, pairwise Chi-square tests of independence were performed. Interpretation is similar to continuous analyses: where the result is significant, there is evidence to suggest that the real proportions (Pr) are different between classes. Results conform to expected patterns. Soil organic carbon content, silt and clay content, cation exchange capacity and exchangeable bases decline monotonically with increasing degradation. Similarly, pH and sand increase with degradation. Strongly significant differences ($P<0.001$) between intact and degraded soils were observed for SOC and sand, with silt, clay, pH, CEC and exchangeable bases. For binary soil properties, the sample proportion exhibiting low functional levels increases with degradation for both P and K. Similarly, the sample proportion of strongly P-depleted soils is significantly higher ($P<0.01$) for degraded than for intact soils.

Soil property results were further explored by compiling results according to landuse and degradation class. Table 4-9 summarizes these results. It is clear that within each landuse class, erosion depletes soil of organic carbon, silt, clay, cation exchange capacity, exchangeable bases, and increases the probability of observing P or K depletion. Trends are remarkably similar between landuse classes with regard to effects of degradation. Also clear from this and information in Table 4-8 is that moderate degradation leaves soil largely unchanged with respect to most soil quality parameters. In contrast, severe erosion (severe sheet, rill, gully) radically alters soil composition, particularly for variables (silt, SOC, CEC, P) considered critical for agricultural function.

Table 4-8. Summary statistics of soil properties by visual soil degradation class.

		Visual Erosion Classification					Hardsetting			Spectral Case		
Soil Property		Intact	Sheet	Severe	Rill	Gully	No	Yes	Sig.	Intact	Degr.	Sig.
Number of Samples		726	315	78	75	66	1101	159		597	663	
SOC		3.02a	2.69b	1.93c	1.77cd	1.47d	2.89	1.50	***	3.26	2.03	***
	Std. Dev	1.34	1.23	1.05	0.96	0.74	1.33	0.53		1.31	1.34	
Silt (%)		24.57a	23.90a	20.93b	20.84b	20.46	24.18	20.72	**	25.38	21.67	**
	Std. Dev	4.17	4.26	3.70	4.00	3.93	4.22	4.13		3.84	4.79	
Sand (%)		34.92a	37.55a	44.00b	43.51b	45.14b	37.97	46.48	**	34.21	42.22	***
	Std. Dev	6.20	6.89	7.19	7.65	6.29	6.43	7.44		5.50	7.14	
Clay (%)		40.61a	39.10a	37.35ab	35.50b	34.85b	38.05	33.67	***	40.97	37.11	**
	Std. Dev	8.41	9.16	7.92	6.90	6.19	8.63	6.33		7.59	9.35	
pH		6.57a	6.67a	6.89b	6.70b	7.07b	6.60	6.98	**	6.49	6.79	**
	Std. Dev	0.45	0.47	0.57	0.61	0.67	0.50	0.42		0.45	0.51	
CEC		20.01a	18.76a	19.21a	17.4b	16.95b	20.27	17.37	**	19.18	16.12	**
	Std. Dev	6.26	6.55	6.81	6.13	7.00	6.52	5.56		6.37	6.22	
Exch. Bases		19.46a	18.39a	18.80a	17.07b	16.53b	19.95	16.94	**	18.81	15.67	**
	Std. Dev	6.35	6.63	6.77	6.24	6.90	6.59	5.47		6.41	6.29	
Exch. Mg		4.85a	4.41a	4.06ab	3.76b	3.68b	4.26	3.92	*	4.46	3.96	**
	Std. Dev	1.45	1.51	1.56	1.28	1.07	1.47	1.32		1.32	1.54	
Exch. Ca		18.04a	17.16a	17.14a	14.82b	16.80ab	15.46	13.82	**	17.50	13.89	**
	Std. Dev	7.18	7.13	7.13	6.45	5.89	7.23	5.82		7.39	6.41	
Pr (Extr. P < 10 mg/kg)		0.71a	0.78b	0.80b	0.88c	0.89c	0.81	0.85	-	0.78	0.84	*
	Std. Dev	0.21	0.17	0.16	0.11	0.09	0.15	0.13		0.17	0.13	
Pr (Extr. P < 5 mg/kg)		0.46a	0.48a	0.65b	0.81c	0.79c	0.56	0.80	***	0.49	0.64	**
	Std. Dev	0.25	0.25	0.23	0.15	0.17	0.25	0.16		0.25	0.23	
Pr (Exch. K < 0.2 cmol/kg)		0.12a	0.20b	0.23b	0.20b	0.24b	0.22	0.19	-	0.18	0.23	*
	Std. Dev	0.11	0.16	0.18	0.16	0.18	0.17	0.15		0.15	0.18	
Pr (Exch. K > 0.4 cmol/kg)		0.80a	0.77a	0.54b	0.36c	0.35c	0.76	0.53	**	0.76	0.45	*
	Std. Dev	0.16	0.18	0.25	0.23	0.23	0.18	0.25		0.18	0.25	

Note: Mean values with different subscripts are significantly different at the 95% confidence level based on standard ANOVA (for categorical comparison) and t-tests (for binary comparison). The binomial proportions were compared using pairwise Chi-squared tests of independence. The following raw data required normalizing transformation before ANOVA was performed: SOC (ln), CEC (√), Exch. Bases (√), Exch. Mg (√), and Exch. Ca (√). For binary comparisons, significance levels are *** - $P < 0.001$, ** - $P < 0.01$, * - $P < 0.05$. ANOVA was performed with a family-wise error rate of 0.05 using Bonferroni contrasts.

Table 4-9. Soil properties by landuse class and categorical degradation status.

	Landuse											
	1 – Agriculture			2 - Rangeland			3 - Woodland			4 - Other		
	Spectral Degr. Class			Spectral Degr. Class			Spectral Degr. Class			Spectral Degr. Class		
Soil Property	1	2	3	1	2	3	1	2	3	1	2	3
SOC (%)	3.38	3.10	1.66	2.97	2.97	1.54	3.74	3.33	1.75	3.18	3.19	1.46
Silt (%)	26.25	24.85	19.58	25.12	23.70	19.85	27.03	24.50	19.88	25.56	24.81	19.81
Sand (%)	35.93	37.22	43.03	36.49	37.92	40.36	34.19	42.72	45.32	34.48	39.02	42.44
Clay (%)	39.89	37.06	36.32	39.91	39.21	39.05	40.89	33.27	34.60	40.29	36.82	37.40
CEC (cmol/kg)	20.84	15.66	15.38	20.39	17.20	17.20	20.14	18.13	17.54	19.04	17.32	15.46
Ex. Bases (cmol/kg)	20.33	15.33	15.07	19.99	16.96	16.78	19.56	17.83	17.06	18.57	17.28	14.75
Exch. Ca (cmol/kg)	13.40	13.91	18.61	18.10	15.65	15.44	18.02	17.26	15.97	16.08	16.31	13.71
Exch. Mg (cmol/kg)	4.16	4.19	4.05	4.50	4.29	3.98	4.78	4.75	4.10	4.51	4.17	3.64
pH	6.51	6.40	6.93	6.56	6.49	6.93	6.63	6.65	6.70	6.38	6.47	6.92
Pr (P<5 ppm)	0.49	0.56	0.60	0.48	0.60	0.62	0.39	0.36	0.53	0.66	0.50	0.84
Pr (K>0.4 cmol/kg)	0.84	0.91	0.45	0.89	0.85	0.49	0.87	0.83	0.53	0.93	0.88	0.28

Table 4-10 summarizes the correlation structure between continuous soil parameters. Except for the correlation between base nutrient measures (CEC, base saturation, exchangeable Ca and Mg), there is only limited evidence of strong collinearity between soil samples. Interestingly, soil organic carbon is inversely proportional to soil clay content, but positively associated with silt content.

Table 4-10. Correlation matrix for continuous soil properties to determine potential multi-collinearity effects.

	SOC	Silt (%)	Sand (%)	Clay (%)	pH	CEC	ExBases	ExMg	ExCa
SOC	1.00								
Silt (%)	0.46	1.00							
Sand (%)	0.46	0.20	1.00						
Clay (%)	-0.61	-0.61	-0.80	1.00					
pH	-0.24	-0.30	0.01	0.32	1.00				
CEC	-0.24	-0.27	-0.24	0.55	0.76	1.00			
ExBases	-0.24	-0.26	-0.23	0.54	0.76	1.00	1.00		
ExMg	0.23	0.01	0.04	0.18	0.47	0.76	0.77	1.00	
ExCa	-0.21	-0.22	-0.19	0.48	0.73	0.95	0.95	0.80	1.00

Pairwise Analysis of Degradation Risk

While risk assessment for predictive purposes will be made within a multivariate framework, it is instructive to summarize marginal effects of site-level characteristics on observing degradation. Figures 4-12 and 4-13 show marginal odds ratios of observing

degradation given specific site characteristics. Included are 95% confidence intervals for estimates of these odds. An odds ratio of one indicates that degradation is independent of the given specific site characteristics over the probability of observing degradation at sites without those characteristics. Odds larger than 1 indicate increased risk.

Figure 4-12a shows odds ratios for degradation based on general land-use categories. Subsistence agriculture has a non-significant detrimental effect, whereas commercial agriculture has a significant protective effect. Active landuse (range, crop, wood production) does not significantly increase risk, but passive land cover classed forests and wetlands appear to substantially reduce risk of degradation.

Figure 4-12b illustrates marginal odds of degradation given specific information about land cover. Specifically, there is a strong protective effect of perennial vegetation

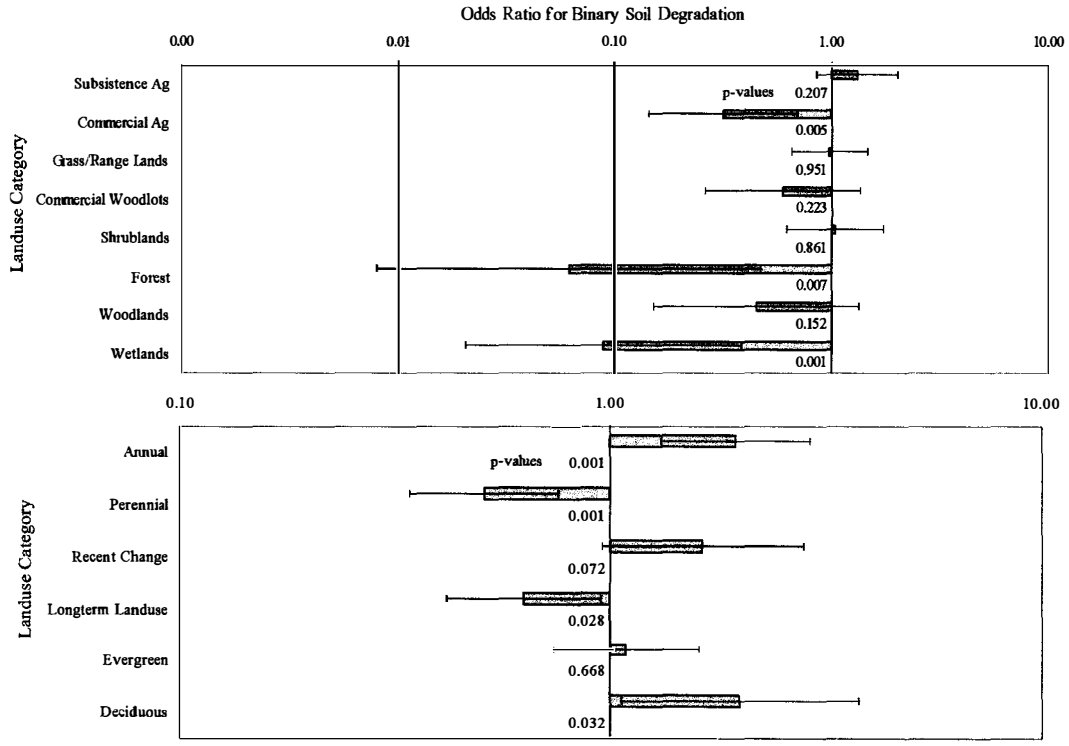

Figure 4-12. Pairwise odds ratios for binary soil physical degradation. Shown are odds ratios and 95% confidence intervals of observing degradation given a) general and b) specific land-use information.

and a moderate protective effect where sites have been maintained under the same land use for greater than 5 years. Annual vegetation appears to have a detrimental effect, and recent changes appear to increase risk non-significantly. Curiously, deciduous vegetation also appears to have a detrimental effect, though the sample size is small (n = 48).

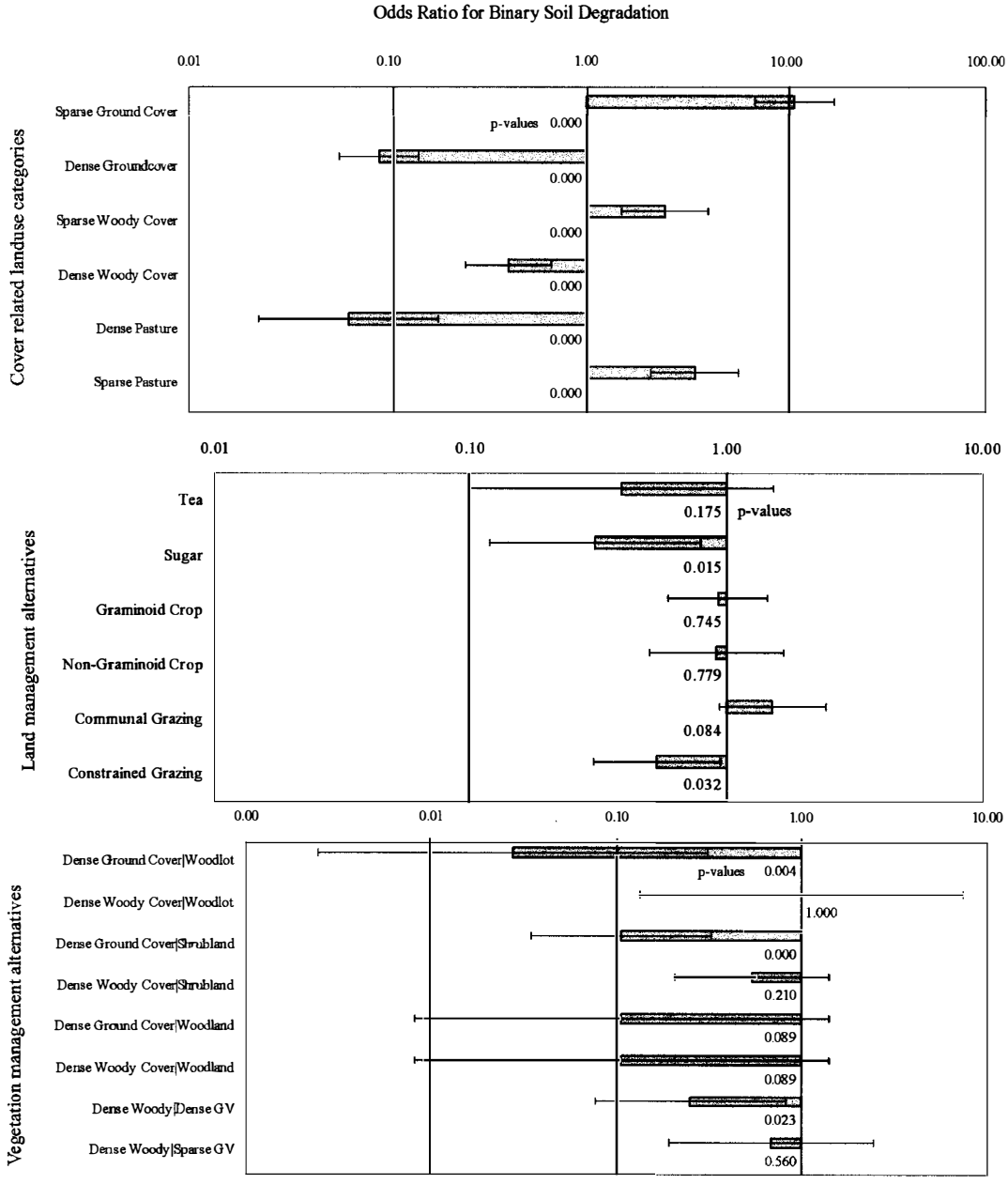

Figure 4-13. Pairwise odds ratios for binary soil physical degradation. Shown are odds ratios and 95% confidence intervals of observing degradation given a) general and b) specific management, and c) cover characteristics.

Figure 4-13 provides much more detail about odds of observing degradation given site-level characteristics. The effect of vegetative cover is summarized in Figure 4-13a. The protective effect of dense ground cover is the most significant pairwise effect observed, whereas the protective effect of dense woody cover is less persuasive. For pasturelands, the protective effect of cover is even more pronounced. Figure 4-13b illustrates that sugar has a significant protective effect while tea plantations provide non-significant protection. There was no effect of subsistence crop choice between graminoid and non-graminoid species. Finally, livestock management appears to affect risk substantially, with communal grazing increasing and paddock grazing decreasing risk.

Figure 4-13c shows conditional odds ratios for ground versus woody vegetation protection against soil degradation. Results indicate that woody vegetation has negligible effect for risk attenuation. For woodlot systems, the effect of dense woody vegetation is negligible, whereas the effect of dense groundcover is highly protective. Shrub lands exhibit similar behavior. Summarizing this effect over all sites (lowest two odds ratios) indicates that dense woody cover has a protective effect only when dense ground cover is present. With sparse ground cover, the protective effect is convincingly non-significant.

Infiltration Data Processing and Assessment

Erosion is fundamentally a hydrologic process. To measure the hydrologic component of increased erosion risk, an infiltration assessment protocol was developed. The following section gives results from site-level processing of infiltration tests.

Data Sampling

Figure 4-14 shows a digitized stream network and all infiltration sampling plots(n = 61). Sampling effort was stratified by landuse type and degradation status. Table 4-11

summarizes sampling stratification. Infiltration tests were performed at 3 wetland sites and 3 gully sites, labeled "Other".

Table 4-11. Summary of field sample sites for infiltration assessment by landuse and binary degradation status.

		Landuse				
Binary Erosion		1 - Croplands	2 - Rangelands	3 - Woodlands	4 - Other	Total
	0	12	11	8	3	36
	1	9	10	5	3	25
Total		21	21	13	6	61

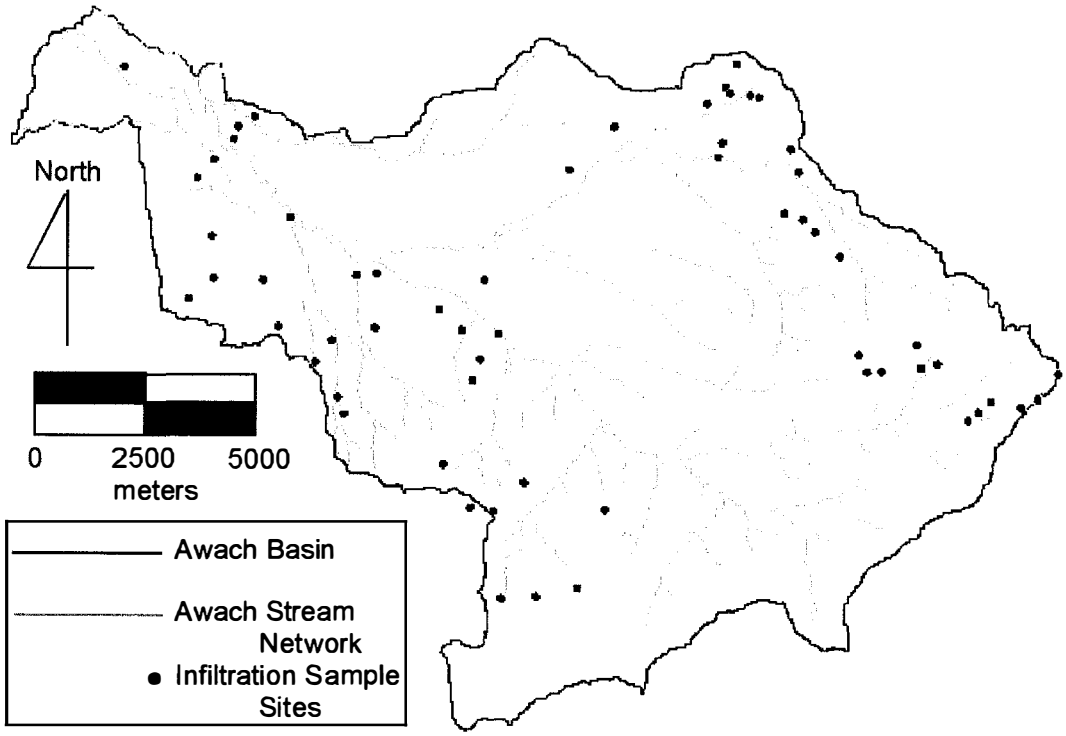

Figure 4-14. Map showing the Awach basin, digitized stream network and location of infiltration assessment sample plots.

Model Fitting

Bounded non-linear optimization techniques used to fit the integrated Horton equation (Eq. 2-8) required development of simple S (MathSoft, 2000) code. Table 4-12 gives the code along with a description of each code section. Central to the model fit routine is use of nlminb, which allows bounded parameter optimization in S. The fit

criterion is the sum of squared residual error (RSS) between predicted and observed values. Parameters were bounded to ensure real solutions (i.e. infiltration rates less than 0 are undefined). To avoid complications arising from local minima in the RSS surface, multiple reasonable initial "guesses" for q (see Table 4-12) were tried until a solution was found that yielded a repeatable global minimum. The specified lower bound (0.00001 – units of cm/sec, equal to 0.36 cm/h) artificially constrains parameters to be positive. In some cases, the best fit was observed when parameters were set to this lower bound. While this suggests that the bounded fit is non-optimal, it was considered justifiable to assign sites with such low infiltration rates to this minimum rather than permit physically meaningless parameter values. Predicted parameter values for each model fit were written to a file for later interpretation. Of specific interest was the parameter describing steady state infiltration rate (q[1] in Table 4-12).

This approach to handling infiltration observations introduces considerable complexity. However, the alternative of using mean infiltration rate grossly

Table 4-12. Infiltration model fitting using a bounded quasi-Newton fitting algorithm.

Code Notes:	S-Plus 2000 Code:
Define integrated Horton infiltration function with 3 parameters and one variable, time (x0). Compute RSS of current parameter estimate vector (q) vs. observed data for sample replicate i.	sscomplex_function(q,x0=inf.data[2*i],y=inf.data[2*i-1]){ y0 <- q[1] * x0 + q[2]/q[3]*(1 - exp(- q[3] * x0)) sum((y - y0)^2)}
For each infiltration test, find parameters that minimize the sscomplex function output (i.e. RSS). Parameter values are lower bounded to a minimum of 0.00001. Results are written to a parameter files and SSE file.	for (i in 1:366){ loopsscomp_nlminb(q,sscomplex,lower = 0.00001, max.fcal=300,max.iter=300) Param[i,1]_loopsscomp$parameters[1] Param[i,2]_loopsscomp$parameters[2] Param[i,3]_loopsscomp$parameters[3] Sscomp.est[i]_sscomplex(Param[i,])

overestimates the saturated infiltration capacity. Figure 4-15 summarizes model fit for one infiltration replicate. Shown are two Horton models. The first (Horton Standard Fit) resulted from transforming the observed data on cumulative infiltration into infiltration rates and fitting the standard Horton Equation. The second procedure fits the Horton Equation directly to cumulative infiltration data. The third method shown uses mean infiltration over the sampling period as the infiltration estimate. Note that model fit is comparable for the two Horton Equation-based methods (suggesting no advantage of selecting one over the other) but that considerable error is introduced by ignoring temporal dynamics of infiltration.

The average RMSE for model fit was 1.13 cm. Those samples for which the best fit resulted in RMSE greater than 10 cm were regarded as outliers and discarded. In addition, sites at which cracks or leaks were observed during the sample period were removed from further analysis.

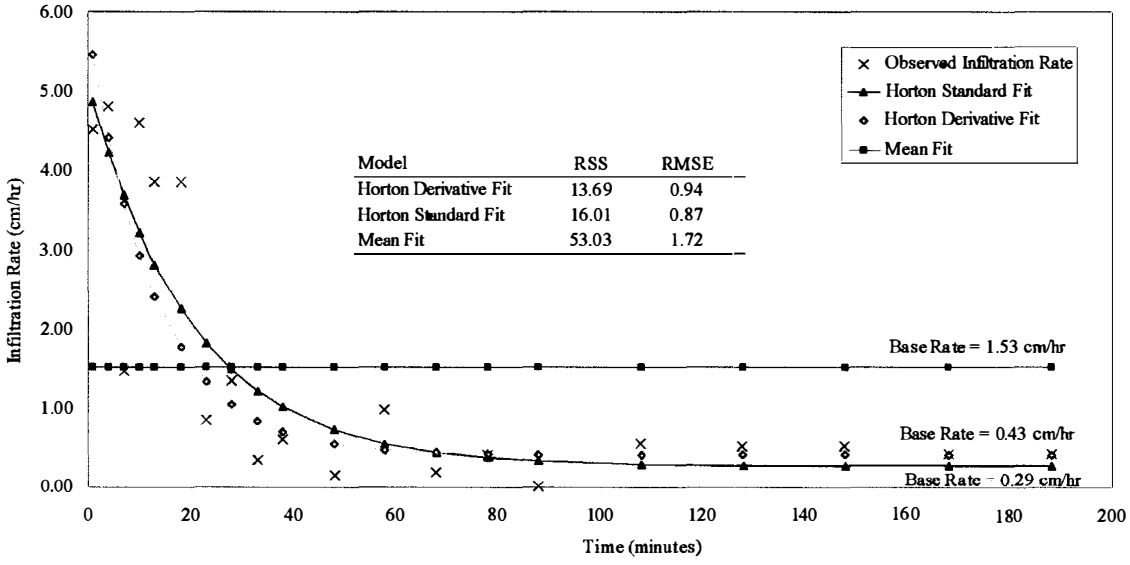

Figure 4-15. Infiltration rate over time with three alternative model forms. Shown are raw data, non-linear best fit line and model residual error (RSS), root mean square error (RMSE) and the predicted base infiltration rate.

Mean Saturated Infiltration Rates

Base parameter fits were compiled for all non-outlier samples according to landuse and degradation status. Table 4-13 summarizes the results, with base infiltration rates reported in mm/hr. Note that contrast strengths are substantially weakened by the small sample size (n = 61). Despite the limited statistical power, there are clear differences in infiltration between intact and degraded sites. Using observed degradation classes, there appears to be a strong effect of severe degradation on reducing infiltration.

When data are organized according to landuse, results suggest that agricultural lands have the highest mean infiltration rates. However, substantial variability within landuse class is evident. Woodlands (woodlots, shrublands and forests) also exhibit high infiltration. Rangeland has significantly lower infiltration rates. "Other" includes wetland and gully sites, both of which exhibit exceptionally low infiltration rates.

While rangelands have low nominal infiltration rates, an important distinction between intact and degraded sites was observed. Intact sites (n = 8, based on spectral

Table 4-13. Summary of mean and standard deviation of base infiltration rates (mm/h) organized by degradation status (observed/spectrally defined) and landuse.

	Spectral Case/Reference			
Base Infiltration	Intact	Degraded	Grand Total	
Mean	273.4a	102.1b	189.1	
Std. Dev	212.9	340.5	293.5	
	Observed Degradation Condition			
Base Infiltration	Intact	Sheet	Severe Sheet	Rill/Gully
Mean	233.3a	116.0a	20.4b	13.1b
Std. Dev.	315.5	245.2	1.2	5.9
	Landuse			
Base Infiltration	Agriculture	Range	Woodland	Other
Mean	341.9a	57.2b	237.1a	12.4b
Std. Dev	404.6	82.6	239.0	8.2

Note: Mean levels accompanied by the same letter were not significantly different at 95% confidence level based on ANOVA using Tukey contrasts. For spectral case/reference contrast, a t-test was used ($P = 0.02$).

classification) had an mean rate of 129 mm/h, while degraded sites (n = 13) had an mean rate of 28 mm/h. This distinction is more pronounced for woodland sites, where intact sites (n = 9) averaged 316 mm/h compared with 60 mm/h at degraded sites (n = 6).

Table 4-14 summarizes model findings from previous work in western Kenya (Wielemaker and Boxem 1982) for nominal infiltration rates under different land-uses and across soils typical of the Awach highland areas. Correspondence between these published figures and field observations is excellent, illustrating the need for Horton model inference as described herein for direct physical comparison.

Table 4-14. Nominal infiltration rates for western Kenya (after Wielemaker and Boxem 1982).

Soil Type	Land-Use	Infiltration Rate (mm/h)
Mollic nitosol	pasture	36
Mollic nitosol	maize	662.4
Mollic nitosol	millet	374.4
Lithosol	pasture	18
Humic acrisol	maize	190.8
Humic acrisol	maize	489.6
Humic nitosol	maize	511.2
Gleyic phaeozem	sorghum	140.4
Ferralitic cambisol	maize	471.6
Eutric planosol	pasture	43.2

Spectral Screening Model

The ideal spectral transfer function would allow infiltration along a continuous gradient to be described by reflectance characteristics. A regression tree model was developed for this purpose, but while calibration model fit was tolerable ($r^2 = 0.78$), the hold-out validation accuracy was extremely poor ($r^2 = 0.27$). This may result from limited data, or from inherent physical confounders resulting from the substantial impacts of human management on surface infiltration rates.

Infiltration is a risk factor for soil degradation when surface runoff occurs. Sanchez (1973) reports a range of minimum infiltration rates for tropical soils between 2 and 10 cm/h. Jetten et al. (1993) report critical infiltration rates in the range of mean rainfall intensity, which for the region is between 50 and 80 mm/h. Infiltration rates slower than average rainfall intensity would result in surface runoff during most rainfall events, which provides a useful functional threshold for delineating hydrologic risk.

Results of the classification tree model to delineate soils exhibiting slow (< 60 mm/h) infiltration from those with higher infiltration rates are presented in Table 4-15.

Table 4-15. Results of screening model to discriminate between rapid and reduced infiltration capacity based on spectral reflectance information.

A: Binary Classification Tree -- 0 = Infiltration > 60 mm/h

Calibration			10-fold Cross Validation		
	Predicted			Predicted	
Actual	No	Yes	Actual	No	Yes
No	88	11	No	75	24
Yes	9	72	Yes	21	60
Accuracy		0.89	Accuracy		0.75
Sensitivity		0.89	Sensitivity		0.74
Specificity		0.89	Specificity		0.76
Odds Ratio		64.00	Odds Ratio		8.93

B: Categorical Classification Tree -- 1 = Infiltration < 30 mm/hr, 2 = Infiltration < 60 mm/h, 3 = Infiltration > 60 mm/h

Calibration				10-fold Cross Validation			
		Predicted				Predicted	
Actual	1	2	3	Actual	1	2	3
1	45	0	3	1	30	8	10
2	7	18	8	2	11	12	10
3	9	2	88	3	9	10	80
Accuracy		0.84		Accuracy		0.68	

Also shown are results of a categorical model, with three classes (< 30 mm/h, 30-60 mm/hr and > 60 mm/h). Model sensitivity is 90% in calibration, declining to 75% in cross-validation. Model balance, as indicated by comparable sensitivity and specificity in

both calibration and cross-validation, is adequate. Overall accuracy declines for the three-category model, with 68% of samples correctly classified in validation.

Infiltration Transfer Function

Predicting infiltration from soil properties that are more readily quantified is a standard practice in soil survey work. Functional forms have been empirically developed to relate texture and soil carbon content information. The potential for using soil properties to predict infiltration class is evident in Table 4-16, which summarizes soil properties for the entire Awach soils data set (n = 1260) according to predicted infiltration class. Simple mean comparisons were done according to infiltration class, and every soil property showed significant differences. Particularly strong contrasts were observed for soil carbon, clay content, CEC, exchangeable Mg, and exchangeable P class.

Table 4-16. Comparison of soil properties for infiltration classes. Category 1 is sites with saturated infiltration rates less than 60 mm/h.

	Infiltration Category		
Soil Property	0	1	*P*-value
SOC	3.13	2.35	<0.001
Clay	37.53	39.85	0.003
Silt	24.24	23.30	0.017
Sand	38.98	36.73	<0.001
pH	6.73	6.57	<0.001
CEC	19.11	16.52	<0.001
ExBases	18.73	16.07	<0.001
Ca	17.56	14.23	<0.001
Mg	4.79	3.71	<0.001
Pr (P<5)	0.47	0.64	<0.001
Pr (K>0.4)	0.83	0.67	<0.001

Note: The p-value refers to the probability that mean soil property values are the same at two levels of infiltration (i.e. high = 0 and low = 1)

To predict infiltration class from soil properties in a multivariate framework, a multiple logistic regression model was developed (Table 4-17). The fitted model is

similar in principle to empirical transfer functions that are common in the literature. The model is highly significant, and produces a model that correctly classifies over 75% of the samples into infiltration classes. It suggests that infiltration is conditionally associated with soil organic carbon content, percent clay, pH and exchangeable magnesium. As SOC, pH and exchangeable magnesium increase, the probability of observing slow infiltration decreases; inverse association is estimated for clay. Because of strong co-linearity between texture measures, only clay was significantly associated despite each component exhibiting significant pairwise effect. Similarly, the effect of magnesium is strongly correlated with CEC, exchangeable bases and exchangeable calcium. Neither binary variable (P and K) was significant after stepwise deletion.

Table 4-17: Conditional association parameters between soil properties and binary soil infiltration from multiple logistic regression model.

	Range		Binary Logistic Regression			
Soil Parameter	+2s	-2s	Param. Estimate	S.E.	*P*-value	Cond. Odds Ratio
SOC	5.39	0.04	-0.518	0.085	< 0.001	0.65
%Sand	50.95	24.62	-	-	-	-
%Silt	32.47	15.01	-	-	-	-
%Clay	55.92	21.60	0.084	0.013	< 0.001	1.05
pH	7.66	5.64	-0.778	0.180	< 0.001	0.50
CEC	30.68	4.79	-	-	-	-
ExBases	30.40	4.25	-	-	-	-
ExCa	30.03	1.55	-	-	-	-
ExMg	7.14	1.30	-0.862	0.086	<0.001	0.52
P<5 mg/kg	Binary		-	-	-	-
K> 0.6 cmol/kg	Binary		-	-	-	-

Note: Cells with no parameter estimates indicate those soil properties that were conditionally independent of the target variable, and were eliminated during step-wise variable removal (using AIC deletion). The intercept estimate was 5.74. Model residual deviance for the logistic regression model 1200.0, with a null deviance of 1612.2 (df = 4, $P << 0.001$). The odds ratio for correct classification by the binary model is 9.90 (7.50, 13.06).

Pairwise Analysis of Slow Infiltration

As presented for binary soil degradation, marginal odds ratios can be computed for observations of slow infiltration (< 60 mm/h). This allows bi-variate exploration of

land use, cover and management effects on infiltration. Figure 4-16 summarizes marginal odds for slow infiltration according to general landuse and specific land cover parameters. Results are generally non-significant at 95% confidence, primarily because of substantial variability within classes due to soil degradation status (Figure 4-17).

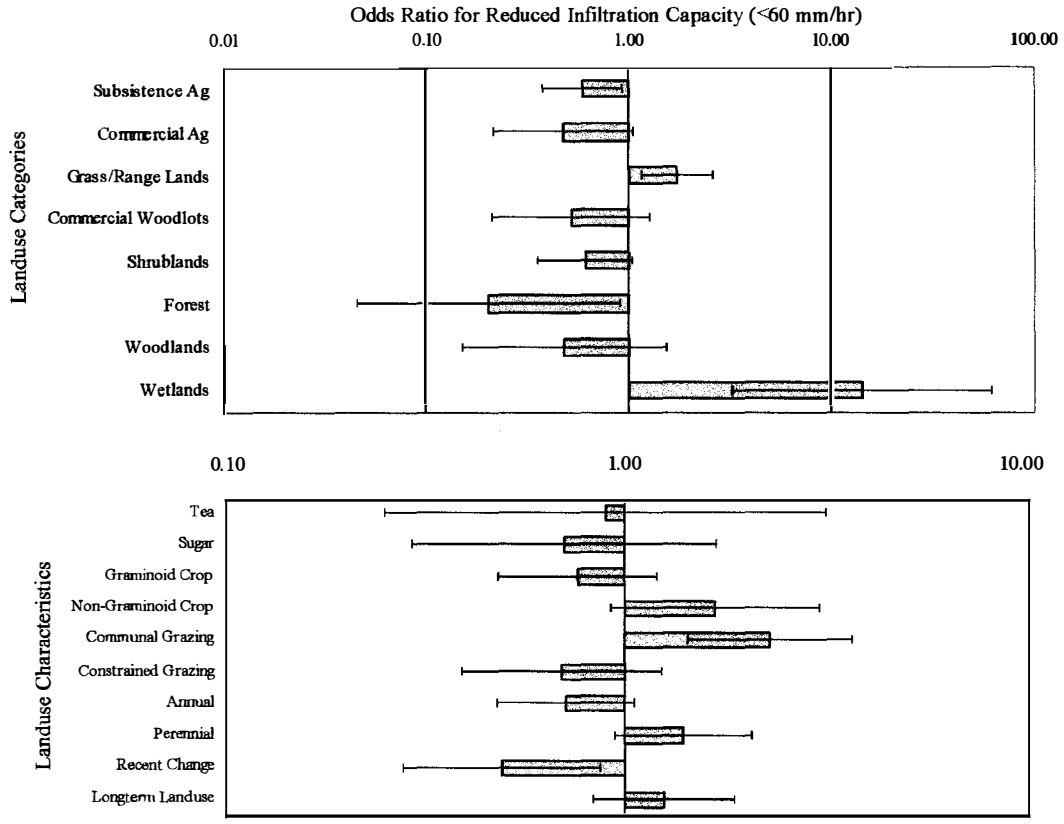

Figure 4-16. Marginal odds ratios and 95% confidence intervals for reduced infiltration capacity by landuse types and land cover characteristics.

The significant protective effect of agriculture, particularly subsistence cropping, and wooded land covers (forests in particular) can be inferred from Figure 4-16. Only wetlands and rangelands are significantly associated with slow infiltration.

Figure 4-16 also shows the marginal effect of various specific land cover and management features. There is a general detrimental effect of non-graminoid crops and communal grazing to contrast protective effects of graminoid cropping systems and

constrained grazing operations. Similarly, annual vegetation appears to provide a protective effect, whereas perennial vegetation increases the probability of a site exhibiting slow infiltration; both effects are non-significant at the 95% level.

Figure 4-17 shows further marginal odds analysis. Contrasting dense vs. sparse vegetative cover reveals that dense cover is strongly protective regardless of strata.

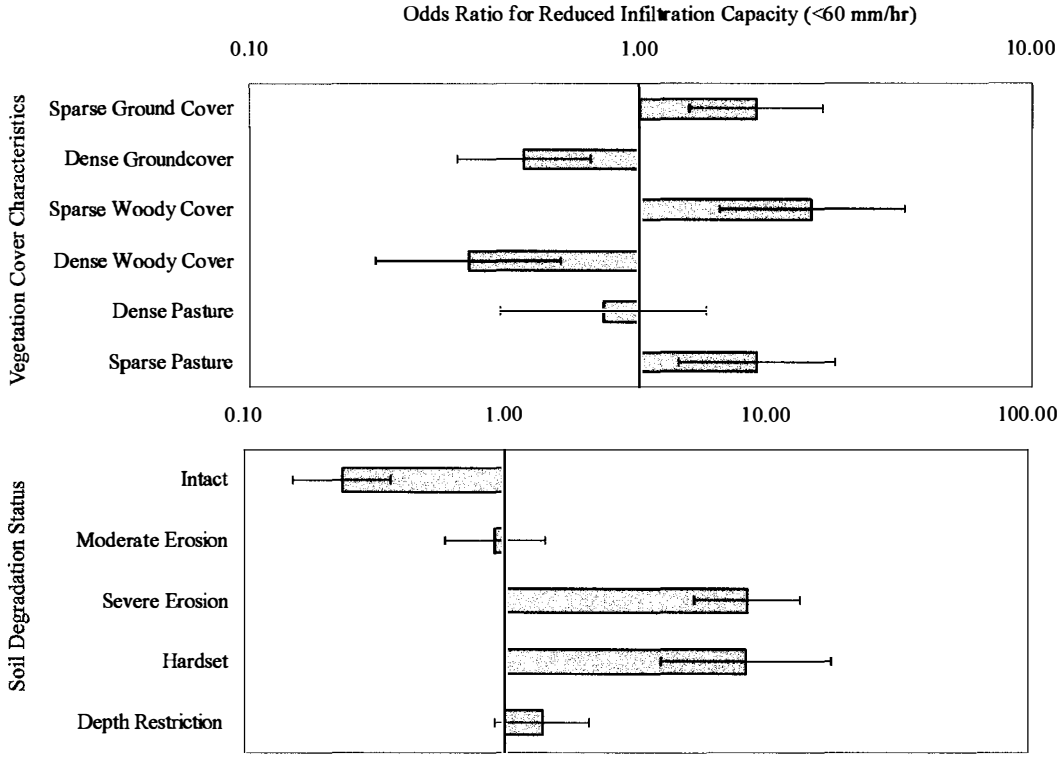

Figure 4-17. Marginal odds ratios and 95% confidence intervals for reduced infiltration capacity by vegetation cover characteristics and soil physical degradation.

Sparse pasture shows a strong detrimental effect, but dense pasture is not significantly protective. Figure 4-17 also illustrates an association between observed soil degradation status and slow infiltration rates. Effects are strong, with intact sites exhibiting low prevalence of slow infiltration. Severe degradation and soil hardsetting are equally strongly associated with low infiltration rates. Moderate degradation appears to have little effect on infiltration, while the presence of a depth restriction within 50 cm of the soil surface is non-significantly associated with reduced infiltration.

Soil Surface Deflation Estimation

Site Sampling

To establish physical rates of erosion without detailed runoff sampling, nails were used to demarcate the soil surface at 181 sites. Surface deflation was measured at each site where they were recovered after approximately 3 months, including the long annual rainy season. Table 4-18 summarizes nail recovery information according to landuse. Nail recovery varied between 3 and 18 per site; mean recovery was 14 nails (75%). As presented, recovery at agricultural sites was poor due to tillage and weeding activity.

Table 4-18. Summary of sites for which nail data were recovered, organized by landuse and binary degradation status.

# Sites	Landuse				
Spectral Case	Agriculture	Range	Woodland	Other	Total
0	6	24	14	5	49
1	8	32	13	18	71
Total	14	56	27	23	120

Mixed Effects Model Results

A substantial portion of variance in exposure was observed within plots, particularly for severely degraded sites. Using mean nail exposure to characterize plot surface deflation incorrectly assumes that rates are spatially constant. To account for within-plot variance appropriately, a linear mixed effects model was employed.

Mixed effects for deflation by degradation status

The first mixed effects model explores the hypothesis that erosion rates are higher at sites judged degraded. Results of this model, summarized in Table 4-19, suggest a strongly significant difference (P-value = 1.07E-6 to reject null hypothesis) in deflation rates between intact and degraded sites. However, there is substantial within plot and within position variance. Variance observed between plots (effect of interest – labeled residual variance in Table 4-19) is less than total nested variance, suggesting that some

degree of spatial autocorrelation exists, but the range of autocorrelation is confounded by the fine spatial scale over which erosion can vary. This demonstrates the danger of extrapolating from plot scale data sets to large areas. Parameter estimates provided above are in centimeters. Using a standard bulk density of 1 g/cm^3, the implied erosion rates are 430 grams/m^2 for intact sites and 2420 grams/m^2 for degraded sites. Also, this surface deflation occurred over a 3 month period. Actual erosion rates are assumed twice a large.

Table 4-19. Summary of mixed effects model of soil deflation rates by spectral case and reference

Fixed Effects	Parameter Estimate	Standard Error
Intercept	0.043	0.033
SPD	0.199	0.042
Random Effects	**Standard Deviation**	
Nail w/in Position	0.191	
Position w/in Plot	0.329	
Residual	0.391	

Mixed effects for deflation by landuse

A similar model comparing deflation rates across plot-level landuse designations produced the results shown in Table 4-20. Two model results are presented. First, a mixed effects model of surface deflation as a function of landuse only is presented. Second, a model of surface deflation accounting for both landuse and soil degradation status is developed. Estimated rates of soil loss can be inferred as follows: for model A (landuse only), predicted deflation is simply the intercept plus parameter estimate for each landuse. The model intercept describes estimated deflation rates for agricultural lands. Conversion to eroded mass per unit area is simply the estimate multiplied by 10,000, yielding 1750 g/m^2 for agricultural activities and 2600 g/m^2 for degraded lands.

These data were originally intended to provide the quantitative basis necessary to make empirical judgments about various land practices. However, field logistics made this intended use impossible. First, all sites where tillage was recent or imminent were

not sampled, reducing substantially representation of agricultural land-uses. Second, nails were not recovered for all sites, presumably due use in local building construction. The data were used, therefore, primarily to corroborate categorical probability models.

Substantial within position and within plot variability lowers the power of parameter estimation (Table 4-20). The result suggests that there are no significant differences in surface deflation among agricultural, pasture and woodlands. Only sites classified as "other" were significantly different ($P < 0.001$). In Table 4-20b, results of an interaction mixed effects model are reported. These results suggest a significant effect of observed soil degradation (SPD) on deflation rates. The effect of landuse is non-significant across all categories at intact sites (there are 5 intact "Other" sites that were wetlands), yielding an erosion rate of between 140 and 530 g/m^2 for the sample period.

There are three marginally significant interaction terms. The interaction effect of soil degradation and "Other" is highly significant, providing a surface deflation estimate of 3890 g/m^2 for the sample period. Parameter estimates for rangelands and woodlands are significant with 90% confidence; both tend to erode more rapidly than agricultural lands under degraded conditions. Variance partitioning presented in Table 4-20 illustrates substantial variability both within site and within position that confounds efforts to generalize fixed effects. In both cases, nearly 60% of total variance is observed at smaller than plot scales, leaving only 40% to discriminate between fixed effect classes.

Table 4-21 summarizes annual soil loss rates. Table 4-21a shows mixed effect model estimates of loss rates and 4-21b shows maximum observed rates (g/m^2) for each landuse and degradation status. For each, values reflect loss rates for only the sampling period (3 months). Because approximately half of annual precipitation falls from March-

June, the values reported in Table 4-21 are double the observed surface deflation. These annualized values were used in emergy evaluations of Awach basin landuse subsystems.

Table 4-20. Summary of mixed effects model of soil surface deflation.

A: LU Fixed Effects	Parameter Estimate	Standard Error	*P*-value
Intercept (LU = Agriculture)	0.175	0.023	<0.001
LU = Rangeland	0.019	0.034	0.545
LU = Woodland	-0.012	0.018	0.493
LU = Other	0.085	0.013	<0.001
Random Effects	**Standard Deviation**		
Nail w/in Position	0.235		
Position w/in Plot	0.235		
Residual	0.361		
B: LU x SPD Fixed Effects	**Parameter Estimate**	**Standard Error**	***P*-value**
Intercept (LU = Ag, SPD = No)	0.031	0.041	0.456
SPD (Yes = 1)	0.085	0.029	<0.001
LU1 = Rangeland	0.022	0.062	0.730
LU2 = Woodland	-0.017	0.028	0.538
LU3 = Other	-0.005	0.026	0.837
SPD*LU1	0.069	0.043	0.055
SPD*LU2	0.049	0.036	0.087
SPD*LU3	0.271	0.029	<0.001
Random Effects	**Standard Deviation**		
Nail w/in Position	0.223		
Position w/in Plot	0.224		
Residual	0.361		

Table 4-21. Annualized mean and maximum estimates of erosion rates (g/m^2) fitted from mixed effects model.

Degradation Status	Landuse			
Case/Reference	Agriculture	Rangeland	Woodland	Other
0	613	1043	267	508
1	2307	4122	2934	7624
Degradation Status	**Landuse**			
Case/Reference	**Agriculture**	**Rangeland**	**Woodland**	**Other**
0	1600	1820	1200	1444
1	12857	9667	10400	35412

Next, multivariate risk models results are presented for three classes of erosion risk factors (site factors, soil factors and hydrologic and terrain factors). Models will be developed targeting binary degradation, but will be cross-checked with information on actual soil erosion rates gleaned from these surface deflation data.

EROSION RISK MODELS

Defining Multivariate Risk Factors

Defining soil erosion risk in the Awach River basin required consolidating the suite of measured and inferred variables presented in the previous chapter into aggregate factors using multivariate statistical modeling. The conceptual framework of the Universal Soil Loss Equation provides a template for this despite evidence that the specific USLE formulation is inappropriate for the region (Cohen et al. submitted 2003). In USLE, erosion is formalized as the product of 5 factors (assumed independent) describing aspects of physical, chemical and biological erosion controls. The USLE model (Renard et al. 1991) can be further distilled into three components of the erosion process (Morgan 1995):

- Soil particle detachment
- Impact protection
- Transport potential

The first is directly comparable with K (soil erodibility) in USLE and is solely a function of soil physical-chemical characteristics. Soil texture, sodicity, and organic carbon content are among the variables that will be considered in developing this factor (Table 5-1). Values of these soil parameters were inferred from spectral models.

The second component relates risk with site-level characteristics. This category integrates site management decisions, though these decisions can have profound implications on other aspects of risk. This component is comparable with C and P in

USLE. Variables included descriptors of cover (e.g. ground cover, annual vs. perennial), structure (canopy height, strata) and management (e.g. landuse, conservation measures).

The third component describes hydrologic and geomorphologic contributions to sediment transport after detachment. This component lumps USLE factors R, L and S. Variables selected to define this component included slope, slope length, infiltration class, soil depth and rainfall. Table 5-1 presents variables that were candidates for quantifying each aggregate factor. For each model, the target variable was binary erosion status, inferred spectrally.

Table 5-1. Summary of field, soil and derived variables assigned to each of three erosion risk components to define risk in the Awach River basin.

A: Soil Erodibility	B: Site/Vegetation Characteristics	C: Terrain/Hydrologic Factors
Soil Organic Carbon	Ground Vegetation Cover	Slope
Silt Content	Woody Vegetation Cover	Slope Length (categorical)
Clay Content	Rock/Stone Cover	Slope Shape (nominal)
Sand Content	Tree Basal Area/Density	Site Infiltration Class (binary)
pH	Ground Vegetation Height	Annual Rainfall
CEC	Woody Vegetation Height	Fournier Index
Exch. Bases	Annual/Perennial (binary)	LS – Function
Exch. Ca	Land Use (nominal)	Evidence of Flooding (binary)
Exch. Mg		Conservation Structures (binary)
Exch. Na (binary)		Soil Restriction (binary)
Exch. P (binary)		
Exch. K(binary)		

Soil Erodibility

Erodibility is the inherent capacity of soil to resist detachment from raindrop impacts or flowing water. Physical models generally include aspects of shear stress susceptibility and flow pattern persistence, but empirical models delineate erodibility based strictly on statistical associations between degradation and soil properties. An existing model (USLE) is compared with an empirical model developed based on direct observation in the Awach River basin.

Standard Erodibility Nomograph

Soil erodibility was first computed for each soil sample in the Awach basin according to Equations 2-6 and 2-7. Adjustment factors (S_{struct} and S_{perm}) were omitted because they were not observed during field sampling. Logistic regression was used to assess the association between the continuous erodibility prediction and a binary condition of soil degradation (i.e. spectral case definition).

Figure 5-1 gives a logit model describing the probability of observing degradation given computed soil erodibility values. Sample proportions observed for groups along the erodibility continuum, along with 95% confidence intervals, are also shown.

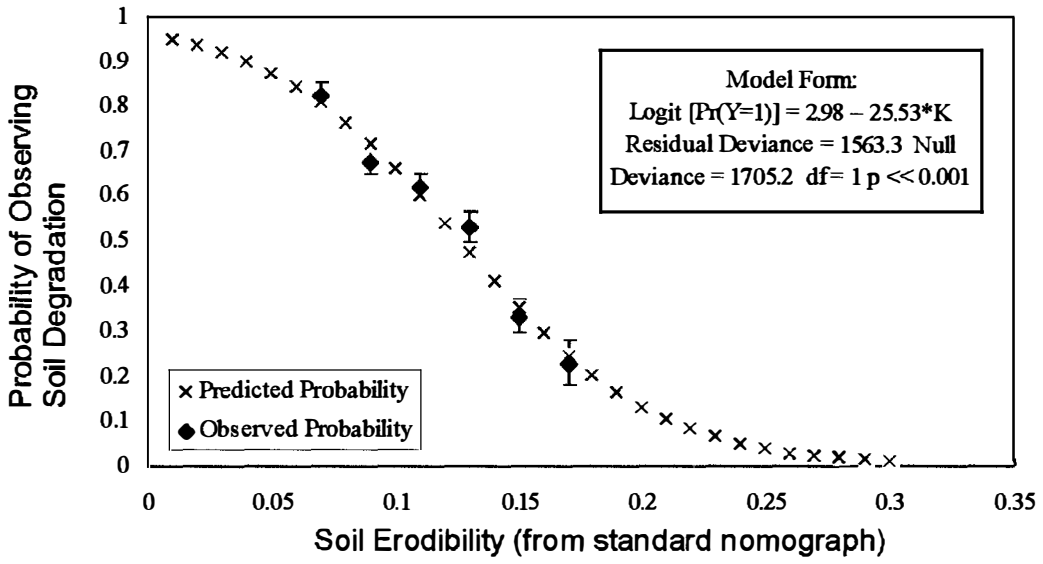

Figure 5-1. Association between computed soil erodibility (from USLE nomograph) and observed grouped degradation probabilities with binomial 95% confidence intervals.

Several important results from Figure 5-1 should be noted. First, the model is highly significant ($p << 0.0001$) as are both parameter estimates. Estimated standard error for the parameter describing the effect of soil erodibility is 2.27; this suggests a 95% confidence interval for the parameter of {-21.1, -30.0}. A parameter estimate of -25.5

implies that, for each 0.01 unit change in erodibility, the odds of observing degradation decrease 0.77 times. Second, this odds ratio implies that the effect direction is opposite to expected; increased erodibility should increase observed degradation probability.

Prospective Study Assumption

The above analysis assumes that soils exhibiting degradation during sampling will continue to erode. This assumption is partially validated by surface deflation results, which indicate that degraded sites exhibit significantly higher erosion rates than intact sites. However, without a prospective study to compute erodibility values for intact soils and only later observing the degree to which those soils degrade, it is not possible to establish causality. As a result, an assumption that erosion and erodibility can be observed simultaneously (i.e. assume that sample data can provide prospective information about erodibility) was required.

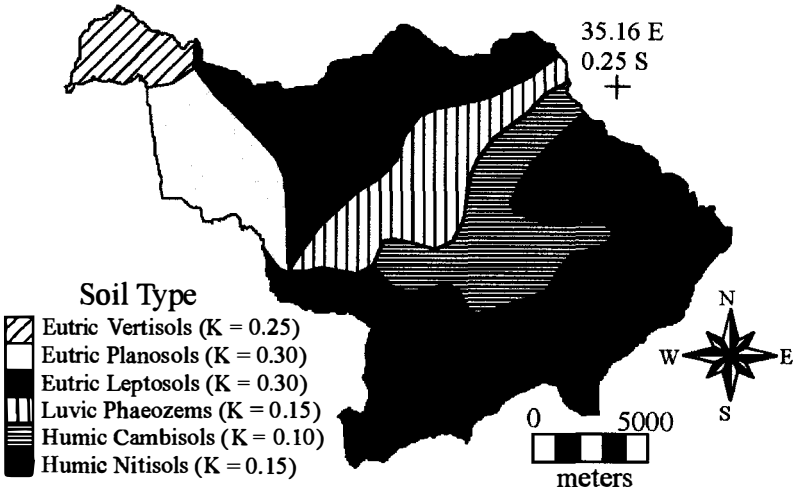

Figure 5-2. Soils map for the Awach River basin (after Kenya Soil Survey, 1977)

Based on a degradation surface for the entire basin, interpolated from sample plots to the entire basin (presented in the next chapter), it was possible to explore erodibility from another perspective. Mean erodibility values were computed for each

soil type, delineated using the existing soil map shown in Figure 5-2, using only those samples judged intact. For each soil-type polygon shown in Figure 5-2, the proportion degraded was computed from the degradation map (Figure 6-1).

Table 5-2 shows these data with mean erodibility estimates for intact sites in each polygon. The plot of mean erodibility versus proportion degraded is given in Figure 5-3. The association direction between computed erodibility and the extent of degradation in that soil type is inverse to expected direction (Figure 5-3). While the regression model is significant, it provides limited predictive power so was not used in subsequent analyses.

Table 5-2. Mean erodibility for each soil type, along with the proportion of each polygon that showed evidence of degradation (inferred from Figure 6-1a).

Soil Type	Mean Intact Site Erodibility	Proportion Degraded
Cambisol	0.11	0.38
Leptisol	0.12	0.45
Nitisol	0.10	0.30
Phaeozem	0.12	0.37
Planosol	0.08	0.66
Vertisol	0.13	0.24

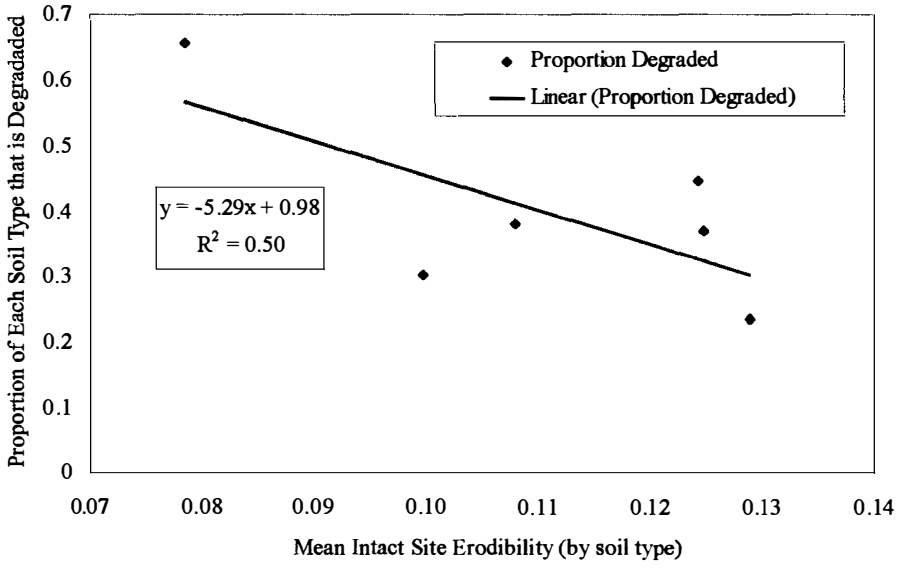

Figure 5-3. Correlation between mean erodibility for intact sites for a given soil type versus the proportion of that type that is degraded (using spatial data from Figure 6-1).

Empirical Soil Erodibility Factor Development

Graphical modeling to identify conditional association structure

Conditional association patterns between degradation and the list of variables in Table 5-1 for soil erodibility were elucidated using graphical models. Strong collinearity between variables necessitates this approach: association within a multivariate framework needs to be conditioned on correlations with all other variables. Starting with a saturated

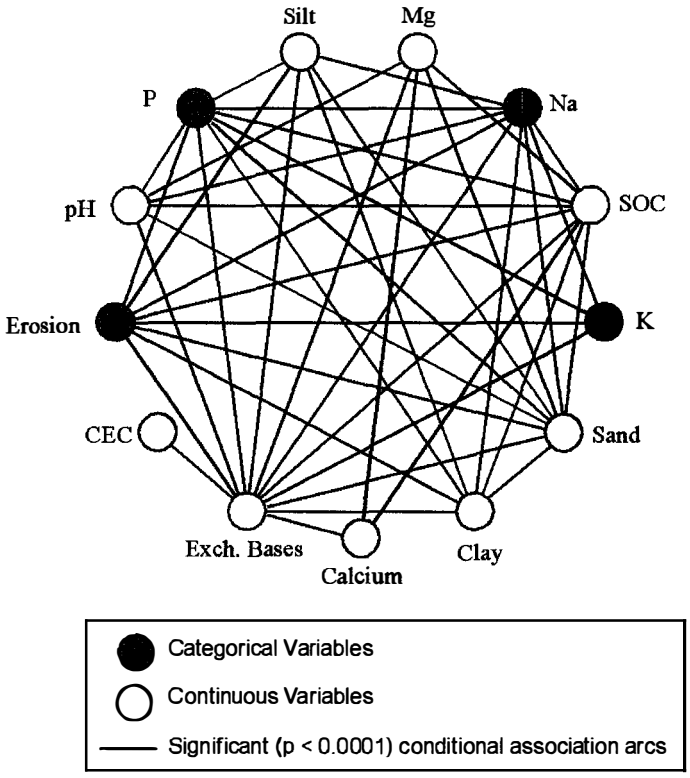

Figure 5-4. Graphical model showing conditional association structure for soil properties and erosion status. All categorical variables are binary. Arcs between nodes indicate conditional association significant at the $\alpha = 0.0001$ level.

model (i.e. arcs connecting each node), variable deletion was performed using the deviance criteria at $\alpha = 0.0001$ significance. This restrictive threshold was chosen because the sample size ($n = 1260$) returned conditional associations judged to spurious.

The resulting graphical model (Figure 5-4), has the following characteristics: it is collapsible onto the discrete variables, mean linear, homogeneous graphical and decomposable. It implies that erosion is strongly associated with P (binary), silt content, sodic phase (binary), soil organic carbon, K (binary), sand content, clay content and exchangeable base concentration. Effect strength and direction were quantified within the context of mixed effects logistic regression below.

Logistic mixed-effects model development

Selecting only those variables observed to be conditionally associated with degradation as predictors (Figure 5-4), a mixed-effects logistic regression model was developed. The marginal maximum likelihood parameter estimates are presented in Table 5-3, along with asymptotic standard error estimates and parameter interpretation. Model fit is summarized by residual deviance of 1245.2 with df = 1249. The null model deviance was 1416.6 with df = 1259, yielding a model *P*-value of 7.2E-31.

Table 5-3. Tabular summary of mixed effects logistic regression for risk predicted by soil properties.

Variable	± 2 σ Range	Parameter Estimate	Std. Error Estimate	*P*-value	Unit Cond. Odds Ratio	OR 95% Conf. Int.
Intercept	-	0.45	0.14	0.0018	-	-
SOC	0.04 - 5.39	-0.83	0.13	0.0000	0.44	(0.34, 0.56)
Silt	15.01 - 32.47	-0.05	0.03	0.0683	0.95	(0.90, 1.00)
Sand	24.62 - 50.95	0.10	0.02	0.0000	1.11	(1.07, 1.15)
Bases	4.25 - 30.4	0.12	0.03	0.0000	1.24	(1.17, 1.32)
Clay	21.6 - 55.92	-0.26	0.02	0.0000	0.85	(0.82, 0.88)
P – (0: P > 5 ppm)	Binary	-0.51	0.25	0.0458	0.60	(0.37, 0.99)
K – (0: K > 0.4 cmol/kg)	Binary	-1.01	0.29	0.0005	0.37	(0.21, 0.64)
Na – (0 : Na < 4 ppm)	Binary	0.68	0.25	0.0395	1.98	(1.22, 3.21)
Random Effects	-	1.28	0.13	0.0000	-	-

Model Accuracy	Predicted			
Actual	No	Yes		
No	436	160	Specificity	73.2%
Yes	171	493	Odds Ratio	7.86

As shown, the predicted probability of degradation decreases with increased SOC, silt and clay content. For the binary screening variables (P, K and Na), the model predicts increased risk under low P and K conditions and high Na conditions. The probability of observing degradation increases with increased sand content and base saturation. Random effects are highly significant, indicating substantial variability within plots, and validating the need for mixed effect modeling.

The strongest effects were observed for SOC, sand, clay and exchangeable bases. Parameters describing each conditional effect on degradation probability can be interpreted using odds ratios and confidence intervals. For example, the odds of degradation decrease by more than a factor of 2 with each unit increase in SOC content. For binary predictors, the odds ratio describes conditional effects of positive classification (i.e. low P and K or high Na).

Table 5-3 presents a summary of model discriminatory power. Of 1260 samples, 929 were correctly classified (with a probability threshold of 0.5). Model sensitivity and specificity are balanced. Odds of correctly classifying a soil with this model are 7.9:1.

Vegetation Cover, Landuse and Site Characteristics

Vegetation Cover

Vegetative cover is an important predictor in all soil erosion models. However, specific characteristics of cover are often overlooked. The effect of woody cover appears to be weak compared with the effect of ground cover (Figure 4-12). Similarly, there appears to be a substantial protective effect of perennial vegetation over annual vegetation. Observed vegetative characteristics, including ground and woody cover,

cover height, strata, basal area, annual/perennial etc., were assessed for their conditional association with degradation using graphical models.

Landuse

Specific land management decisions for a parcel of land affects the probability of degradation. Eight land-uses were defined based on field sample data:

1. Subsistence Agriculture
2. Commercial Agriculture
3. Sparse Pasture
4. Dense Pasture
5. Woodlands (forest, woodlots)
6. Shrublands
7. Wetlands
8. Severely Degraded Lands

It was expected that landuse would exhibit association patterns with all of the site descriptors because of the effects of human management on site characteristics.

Empirical Site Factor Development

Graphical modeling to identify conditional association structure

Figure 5-5 shows the conditional association patterns between site level variables, landuse and erosion status; all arcs are significant at the 0.0001 level of significance to reduce the chance of spurious association. Several notable inferences are evident. First, landuse, as expected, is conditionally associated with all site variables, indicating the strong effect of human decision making on these factors. Second, the variables determined to be conditionally independent of erosion are woody cover and tree basal area. Woody vegetation height is significantly associated, but given observations of woody height, ground cover and landuse, erosion is conditionally independent of tree canopy cover, a result strongly at odds with conventional wisdom.

Further inference from graphical model in Figure 5-5 includes the observation that erosion can be linked to stone cover, annual/perennial dominance, ground vegetation height and cover, and woody vegetation height. These factors alone were used in a mixed effects logistic regression model, presented below.

Note that categorical landuse is nominal, requiring 7 dummy variables to describe effects. All other variables are either binary or ordinal, reducing model dimensionality. While observations of cover and height were ordinal, they are given linear scores to allow them to be modeled as continuous variables (e.g. 0-5% cover = 1, 5-25% cover = 2, 25-50% cover = 3, 50-75% cover = 4, 75-95% cover = 5 and 95-100% cover = 6).

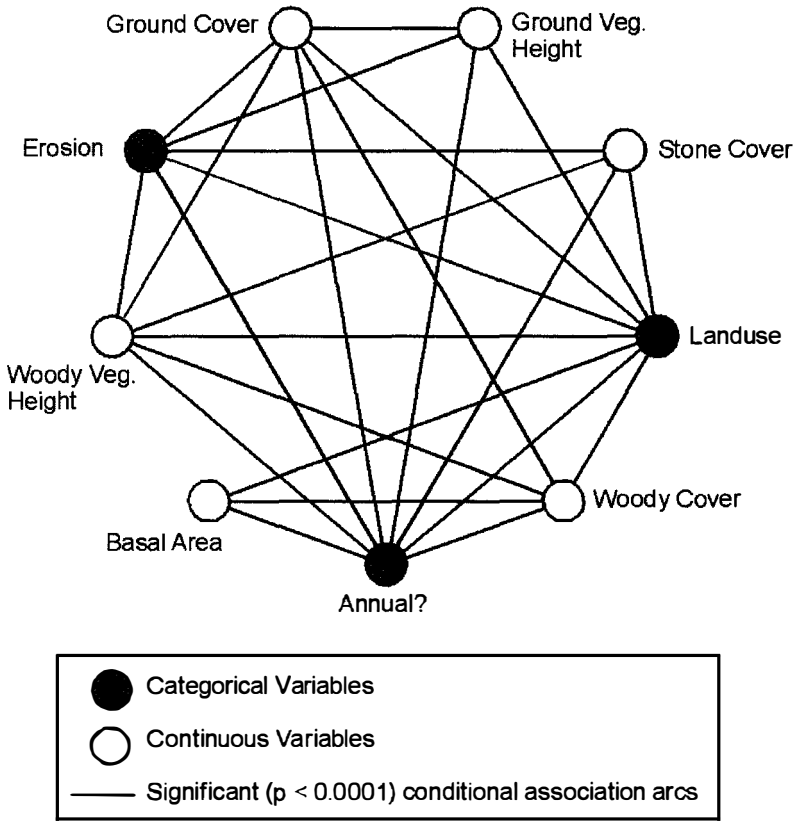

Figure 5-5. Graphical model showing conditional association structure for site properties and erosion status. All categorical variables are binary. Arcs between nodes indicate conditional association significant at $\alpha = 0.0001$.

Logistic mixed-effects model development

Using variables previously identified, a mixed-effects logistic regression model was developed targeting erosion. Table 5-4 summarizes model fit. Overall goodness-of-fit is strong, with model residual deviance = 1233.4 with df = 1246 compared with null deviance of 1416.6 with df = 1259. The resulting *P*-value is effectively zero.

Table 5-4. Tabular summary of mixed effects logistic regression model for erosion risk predicted by soil properties.

Variable	Parameter Estimate	Std. Error Estimate	*P* -value	Unit Conditional Odds Ratio	OR 95% Confidence Interval
Intercept	4.27	0.52	0.0000	-	-
Ground Cover	-0.62	0.07	0.0000	0.54	(0.46, 0.61)
Stone Cover	0.15	0.05	0.0011	1.17	(1.05, 1.28)
Ground Height	-0.12	0.07	0.0439	0.89	(0.77, 1.01)
Woody Height	-0.17	0.09	0.0229	0.84	(0.71, 0.99)
Annual	0.75	0.18	0.0000	2.12	(1.49, 2.99)
LU - SubAg	-3.16	0.50	0.0000	0.04	(0.01, 0.11)
LU - ComAg	-2.55	0.53	0.0000	0.08	(0.02, 0.21)
LU - SpaPast	-1.64	0.47	0.0003	0.19	(0.07, 0.49)
LU - DenPast	-2.25	0.50	0.0000	0.11	(0.03, 0.28)
LU - Shrubland	-2.48	0.50	0.0000	0.08	(0.03, 0.22)
LU - Woodland	-2.83	0.51	0.0000	0.06	(0.02, 0.16)
LU - Wetland	-8.27	3.80	0.0147	0.01	(0.01, 0.43)
Random Effects	1.18	0.12	0.0000	-	-

Model Accuracy	Predicted			
Actual	No	Yes		
No	413	154	Specificity	72.8%
Yes	184	509	OR	7.42
			Overall	73.2%
			Sensitivity	73.4%

The probability of observing degradation decreases with increased ground cover, ground vegetation height, and woody vegetation height. Degradation probabilities increase with increased stone cover and annual vegetation dominance.

Interpretation of landuse (LU) parameters is made with respect to the condition of dummy variables set to 0; that is, for severe soil degradation. Notably, all land-uses are protective in comparison with severe degradation; sparse pasture (LU – SpaPast), dense pasture (LU – DenPas) and shrublands (LU – Shrubland) exhibit the weakest effects.

Being under subsistence agriculture (LU – SubAg) has a strong protective effect. The effect for commercial agriculture (LU – ComAg) is weaker. However, since information about both landuse and land cover is included in this model, interpretation requires consideration of land cover characteristics as well and LU parameters. Nominal values by landuse are presented in Table 5-5. Note that annual dominance, while binary, is reported as a proportion, with high values indicating dominance of annual vegetation. Ground cover, ground height, woody height and annual dominance are all lower risk for commercial agriculture than for subsistence agriculture, making inference about landuse from LU parameters alone inappropriate. Likewise, small differences in LU parameters for dense and sparse pasture are modified by large differences in nominal ground cover.

Overall, the model performs well. Assuming a cutoff probability of 0.5 for assigning samples to either intact or degraded classes, the model has an accuracy of 73%. The odds of correctly classifying samples based on this model are over 7.4:1.

Table 5-5. Nominal land cover parameters for each landuse.

Landuse	Ground Cover	Ground Height	Woody Height	Annual Dominance
SubAg	2.75	2.09	0.37	0.84
ComAg	3.85	2.21	0.55	0.18
DenPas	4.50	1.46	0.74	0.15
SpaPas	3.60	1.36	1.21	0.14
Shrub	3.74	1.63	2.11	0.46
Wood	4.02	1.53	2.60	0.53
Wetland	5.70	2.40	0.30	0.10
SevDegr	1.76	1.00	1.32	0.19

Hydrologic and Terrain Characteristics

Terrain Variables

Terrain variables that contribute to detachment and transport capacity are slope, slope length, terrain factor/transport capacity index (previously presented), slope profile (straight, concave, convex, variable) and presence of conservation structures. Very few

sites in the region (n = 20) had conservation structures. These included contour stone lines, hedge rows, *fanya juu* (contour ditching) and terracing.

Hydrologic Variables

In addition to infiltration (inferred spectrally), hydrologic variables included mean annual rainfall (mm), Fournier Index of rainfall erosivity, evidence of site flooding and presence of soil depth restrictions. Soil depth could have been included in the site model, but was selected here because shallow soils can function as effective impervious surface.

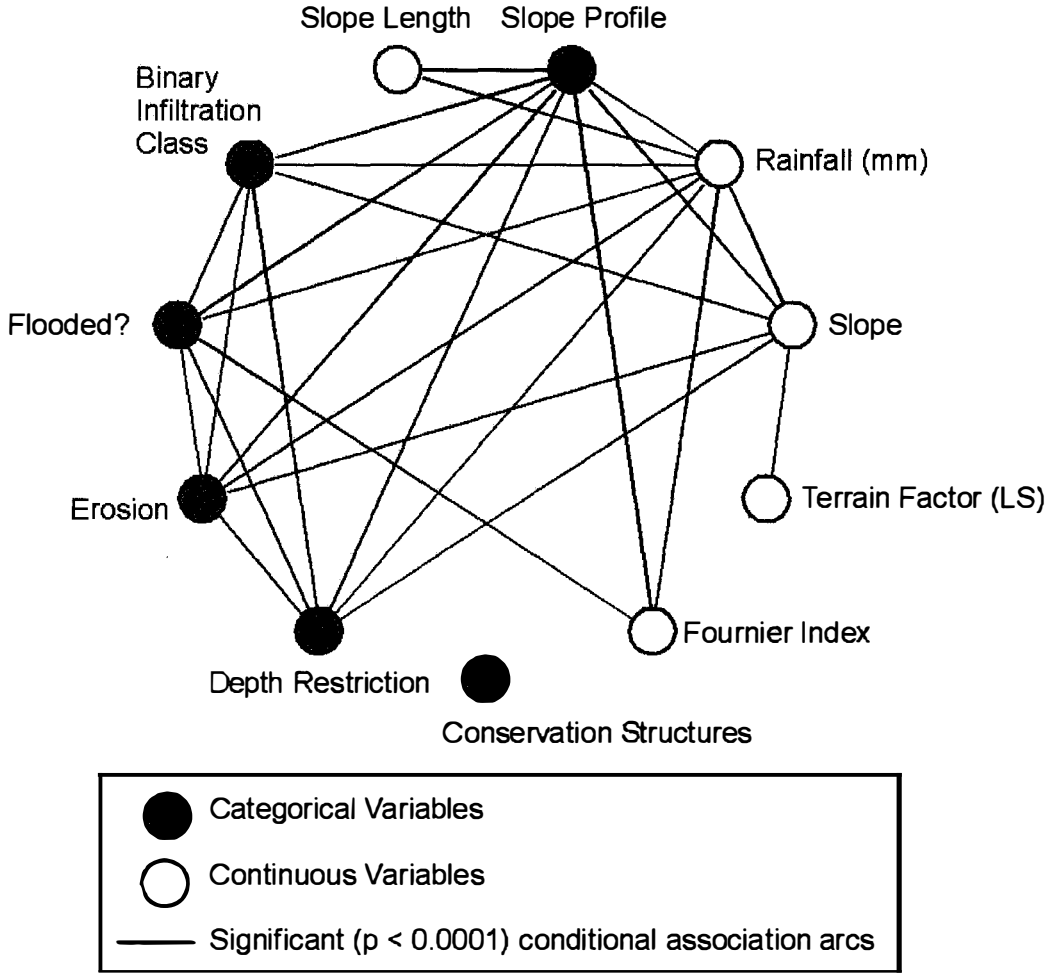

Figure 5-6. Graphical model showing conditional association structure for hydrologic and terrain-based measures and erosion status. All categorical variables are binary. Arcs between nodes indicates conditional association significant at the $\alpha = 0.0001$ level.

Empirical Hydro/Terrain Factor Development

Graphical modeling to identify conditional association structure

As before, graphical modeling identified conditional association patterns between these variables and soil erosion status. Figure 5-6 presents the graphical model output after arc-deletion at $\alpha = 0.0001$ significance. Notably, erosion appears to be conditionally independent of slope length, terrain index, Fournier Index and conservation structures. Rainfall, infiltration, depth restriction, evidence of flooding, slope, and slope profile are conditionally significant predictors of erosion status. Note that slope profile is a nominal variable, requiring 3 binary variables for statistical description.

Logistic mixed-effects model development

Application of logistic mixed effects modeling produced the model summarized in Table 5-6. Fitted residual deviance of 1099.7 with df = 1250; this is compared with null deviance of 1416.6 with df = 1259 to yield a goodness-of-fit *P*-value of effectively 0.

Table 5-6. Tabular summary of mixed effects logistic regression model for erosion risk predicted by hydrologic and terrain factors.

Variable	Parameter Estimate	Std. Error Estimate	*P* -value	Unit Conditional Odds Ratio	OR 95% Confidence Interval
Intercept	0.47	0.15	0.0021	1.61	-
Infilt. (binary)	3.68	0.33	0.0001	39.51	(20.89, 74.71)
Depth (binary)	1.98	0.25	0.0001	7.27	(4.43, 11.9)
Slope	0.07	0.02	0.0001	1.07	(1.03, 1.12)
ProfStraight (binary)	-0.65	0.41	0.1148	0.52	(0.23, 1.17)
ProfConvex (binary)	-0.73	0.51	0.1506	0.48	(0.17, 1.3)
ProfConcave (binary)	-0.49	0.42	0.2445	0.61	(0.26, 1.39)
Flood (binary)	-1.85	0.72	0.0099	0.16	(0.03, 0.64)
Rainfall*	-0.28	0.03	0.0001	0.76	(0.71, 0.8)
Random Effects	1.38	0.14	0.0000	-	-

Model Accuracy	Predicted			
Actual	No	Yes		
No	443	154	Specificity	74.2%
Yes	151	512	OR	9.75

* - Rainfall was modeled in units of 100 mm (e.g. 1200 mm annual rainfall = 12)

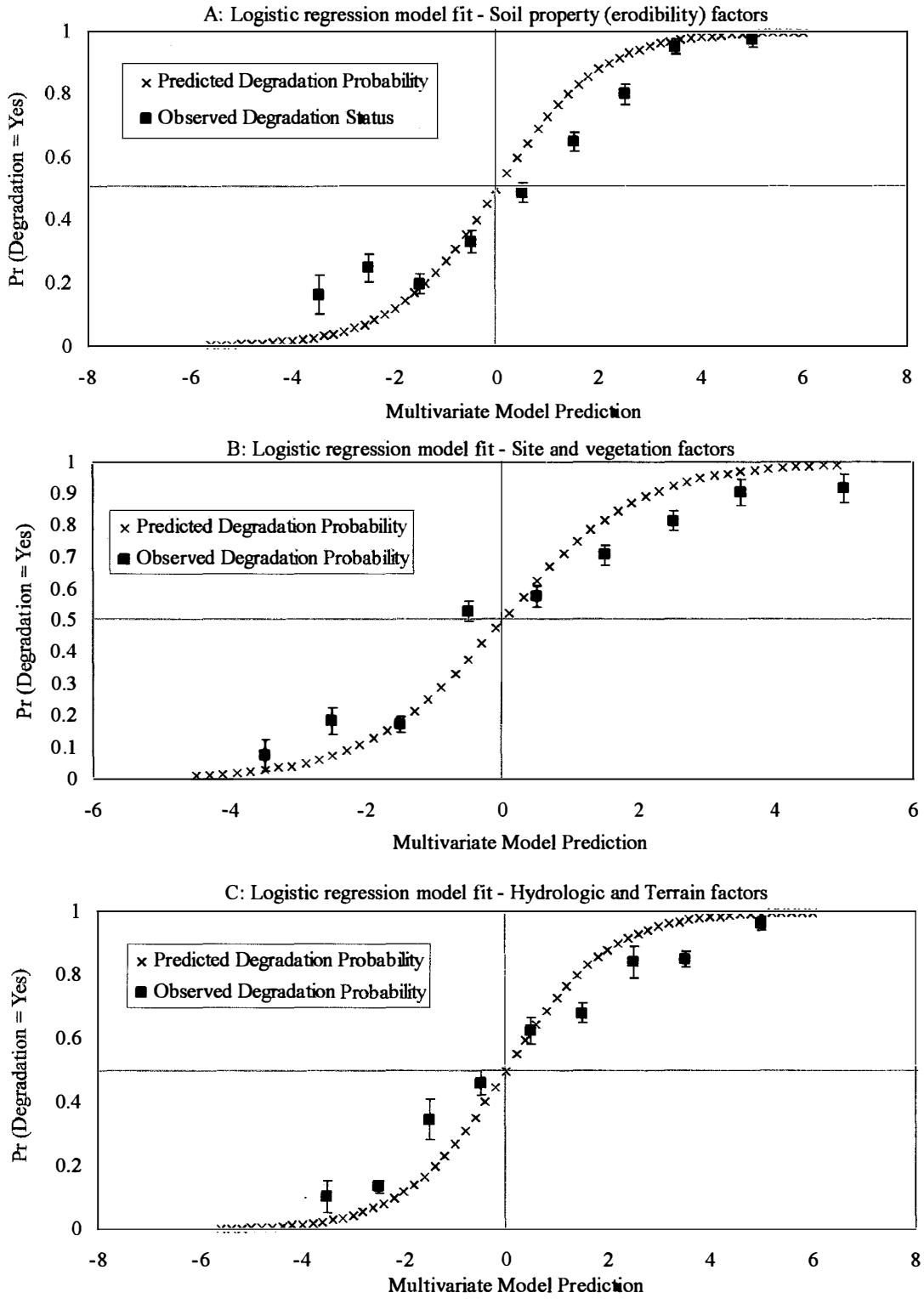

Figure 5-7. Model fit for three logistic regression models describing soil erosion factors a) soil properties (erodibility), b) site and vegetation characteristics and c) hydrologic and terrain variables. Shown are maximum marginal likelihood model fit and observed group proportions (with 95% binomial error bars).

The best-fit model predicts an increase in degradation probability with slope, slow infiltration (Infilt. = 1), and depth restriction (Depth = 1). Erosion probability decreases with evidence of flooding, and rainfall. The effect of the 4-category nominal variable slope profile is summarized in three dummy variables labeled ProfStr, ProfConvex and ProfConcave. This indicates elevated risk when the profile is highly variable (condition when each dummy variable is set to 0). Convex and straight slopes appear to provide greater protective effect than concave slopes, though each effect is non-significant. This result conflicts with other studies that suggest that convex slopes are subject to substantially increased erosion rates (Morgan 1995) over other profile shapes.

This model exhibits greater accuracy than the previous two models, with almost 76% of samples correctly assigned (assuming a probability threshold of 0.5).

Logistic Regression Model Fit Charts

Summarizing model goodness-of-fit using deviance and class-assignment accuracy was complimented by plotting predicted degradation probability values versus model functional form. Grouped binomial proportions are given to compare predicted and observed values. Figure 5-7 presents these plots. For each grouped proportion, binomial 95% confidence intervals for actual proportions are shown.

Integrated Risk Model

Using the functional formulas predicted by each of the three models presented above, an integrated risk model was developed to assess overall erosion risk, again using a mixed effects logistic regression model of the form:

$$\text{Logit}\,[\Pr(\text{Degr} = \text{Yes})] = \beta_1 \times \text{Site} + \beta_2 \times \text{Soil} + \beta_3 \times \text{Hydro}$$

The mixed-effects approach, again, avoided pseudo-replication issues. The model form is summarized in Table 5-7. Each factor is strongly conditionally associated with risk, and the direction of the effect is uniformly positive. It is important to note that, while the factors are correlated (mean r = 0.44), they are sufficiently independent for each to retain substantial predictive power with respect to site risk delineation.

Table 5-7. Tabular summary of mixed effects logistic regression model for erosion risk predicted by all composite risk factors.

Variable	Parameter Estimate	Std. Error Estimate	*P*-value	Unit Conditional Odds Ratio	OR 95% Confidence Interval
Intercept	0.083	0.077	0.0004	-	-
Site (σ = 1.86)	0.481	0.048	<0.0001	1.62	(1.47, 1.78)
Hydro (σ = 2.42)	0.487	0.038	<0.0001	1.63	(1.51, 1.75)
Soil (σ = 1.85)	0.342	0.061	<0.0001	1.41	(1.25, 1.57)
Random Effects	1.042	0.109	<0.0001	-	-
Model Accuracy	Predicted			Overall	83.7%
Actual	No	Yes		Sensitivity	83.4%
No	458	86		Specificity	84.2%
Yes	119	597		OR	26.72

Exploration of interaction effects revealed no significant terms (α = 0.05), so the main effects model presented (Table 5-7) was selected. Model deviance is 987.5 with df = 1257 versus null model residual deviance of 1416.6 with df = 1259. The likelihood ratio test (deviance comparison) yields a goodness-of-fit p-value of effectively zero.

Parameter interpretation indicates that the strongest effect is due to the hydrologic and terrain factor. The other two factors (Site and Soil) are equally strongly associated with erosion. The odds ratios describing the effect of unit changes in each factor should be interpreted while considering the range and standard deviation of those factors (Table 5-8). For each unit increase in the Hydro factor, the conditional odds of observing degradation increase by a factor of more than 2. Given the range for this factor (-5.53,

6.01), the inference is that the odds of observing degradation change by a factor of over 20 between the lowest and highest samples.

Overall model accuracy is improved over each factor treated separately. Overall accuracy was 84% with an odds ratio for correct classification of 26.7.

Table 5-8. Range and standard deviation of risk factors.

	Minimum Value	Maximum Value	Std. Deviation
Site Factor	-4.44	4.78	1.79
Hydro/Terrain Factor	-5.53	6.01	2.42
Soil Factor	-4.73	5.55	1.85

Surface Deflation and Risk Prediction

Surface deflation data offer a second mode of assessing the efficacy of the three composite risk factors for predicting erosion. A multiple linear regression model was developed to relate site mean observed surface deflation rates with the previously developed risk factors. Table 5-9 summarizes the model fit. Overall fit is significant ($P << 0.001$), but the model efficiency is low (adjusted multiple $r^2 = 0.382$). The Site factor was highly significant as a predictor of surface deflation, Hydro was marginally significant, while the Soil factor was non-significant. The model fit is presented graphically in Figure 5-8 along with the model equation and adjusted r^2-value.

Table 5-9. Summary of multiple linear regression model relating observed site-level mean deflation rates and erosion risk factors.

Variable	Parameter Estimate	Standard Error	P-value
Intercept	0.1588	0.0185	0.0000
Soil	0.0109	0.0117	0.3508
Hydro	0.0218	0.0123	0.0803
Site	0.0641	0.0142	0.0000
	Multiple R-squared	0.385	
	F-statistic	24.23	
	df (model, residual)	3, 116	
	P-value	3.03E-12	

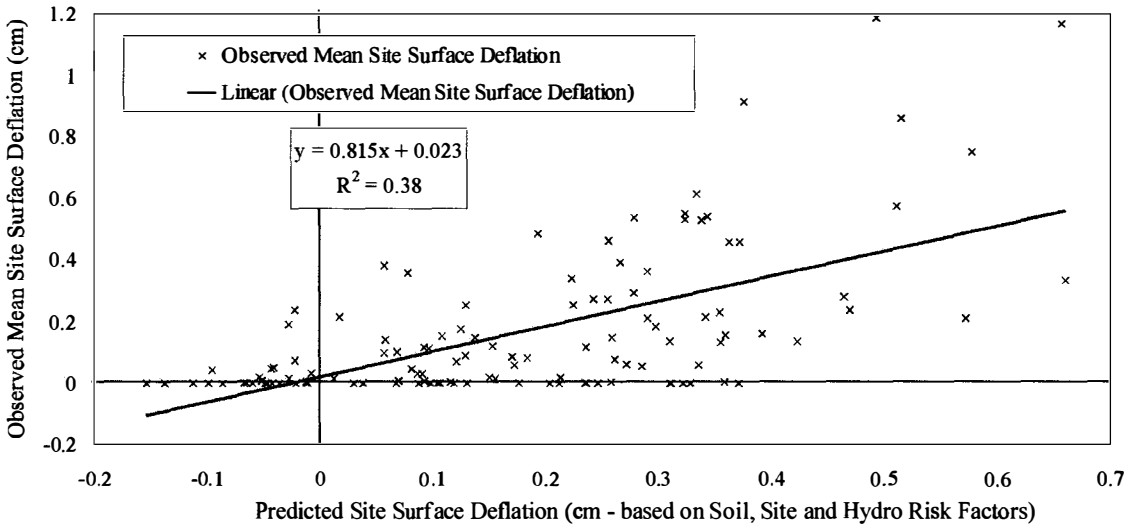

Figure 5-8. Multivariate regression model between mean site surface deflation observations and Site, Soil and Hydro risk factors. Model F-statistic = 24.2, df = 3, 116, $P << 0.001$.

SPATIAL INVENTORY AND RISK ASSESSMENT

Preceding work enumerated erosion risk at the plot-scale based on observations of soil, vegetation, hydrology and terrain. However, effective intervention to control erosion requires spatial tools for assessment of erosion risk over large areas. The first section below presents results of interpolation from field samples to watershed-scale predictions of degradation, infiltration and landuse. The second section couples the statistical predictive framework presented previously with emergy-based cost/benefit data to compare land development scenarios for large-scale erosion control intervention.

Spatial Inventory

Geospatial statistical models (e.g. kriging) were explored for variable interpolation. Results are omitted because they failed to discern spatial pattern in soil degradation or infiltration data. Specifically, semi-variograms were characterized by pure-nugget variance, indicating that variables were uncorrelated at the spatial resolution characteristic of this sampling protocol. Ascertaining spatial pattern statistically over large areas would require sampling at a scale and intensity that is prohibitive.

Satellite Image Processing

Satellite imagery from 2001 was processed to extrapolate various factors from field sampling locations to the entire basin. Of interest were maps of degradation (binary and categorical classifications), infiltration rates, landuse, and site characteristics (e.g. vegetative cover, soil erodibility). In addition to inference about 2001 imagery, rule-bases for each classification model were applied to imagery from 1986.

Table 6-1. Summary of classification tree model for calibration and validation accuracy for inference of degradation classes from satellite reflectance data.

a) Binary Degradation Model

Calibration	Predicted Degradation Class			
Actual Class	Intact	Degraded	Overall Accuracy	85.5%
Intact	176	26	Sensitivity	87.1%
Degraded	35	183	Specificity	83.9%
			Odds Ratio	35.4

Validation	Predicted Degradation Class			
Actual Class	Intact	Degraded	Overall Accuracy	77.5%
Intact	159	44	Sensitivity	78.2%
Degraded	51	167	Specificity	76.6%
			Odds Ratio	11.8

b) Ordinal Degradation Model

Calibration	Predicted Degradation Class				
Actual Class	Intact	Mod. Degr.	Sev. Degr.	Overall Accuracy	77.1%
Intact	158	20	10	Sens.(severe)	92.1%
Mod. Degr.	37	75	15	Spec. (severe)	86.7%
Severe. Degr.	6	8	91	OR (severe)	75.4
				Kappa	0.64

Validation	Predicted Degradation Class				
Actual Class	Intact	Mod. Degr.	Sev. Degr.	Overall Accuracy	65.0%
Intact	132	36	20	Sens.(severe)	87.0%
Mod. Degr.	44	62	21	Spec. (severe)	75.2%
Severe. Degr.	11	15	79	OR (severe)	20.3
				Kappa	0.46

Erosion prevalence assessment

Satellite interpolation was performed for soil degradation using both binary and ordinal classes. Table 6-1 summarizes classification tree model fit for both targets. The model rule-bases, containing 13 and 17 nodes, respectively, are given in Appendix C.

Thematic surfaces for binary and ordinal degradation are shown in Figure 6-1 after application of the model rule-base using the ERDAS Imagine Knowledge Engineer (Leica Geosystems 2000). Binary classification indicates that over 46% of the basin exhibits evidence of degradation. For ordinal classification, degradation (moderate and severe) represents almost 52% of the basin, with 26% severely degraded.

There is strong spatial agreement between the models, with over 75% of pixels appropriately allocated (intact or degraded in both). Disagreement between the themes appears for the moderate degradation category, with about 33% incorrectly assigned. Image cross-tabulation is presented in Table 6-2 for categorical proportions.

a) Binary Degradation Status

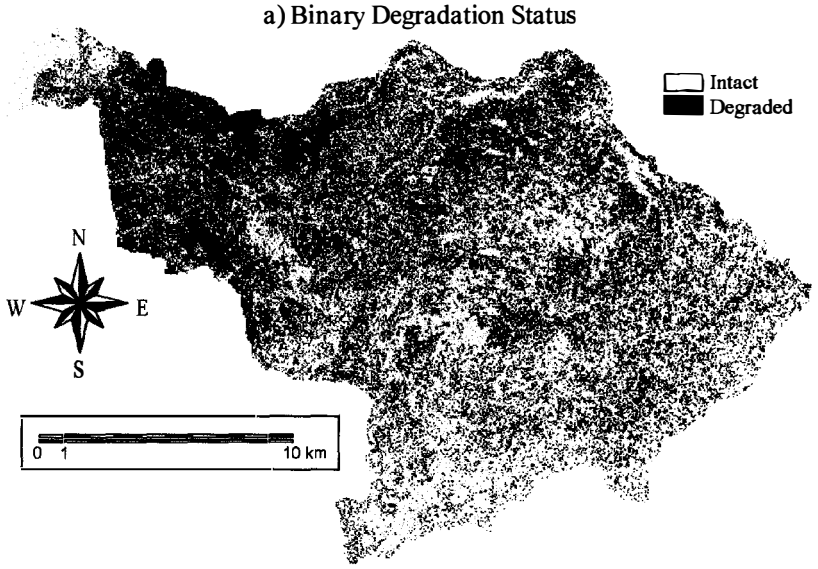

b) Ordinal Degradation Status

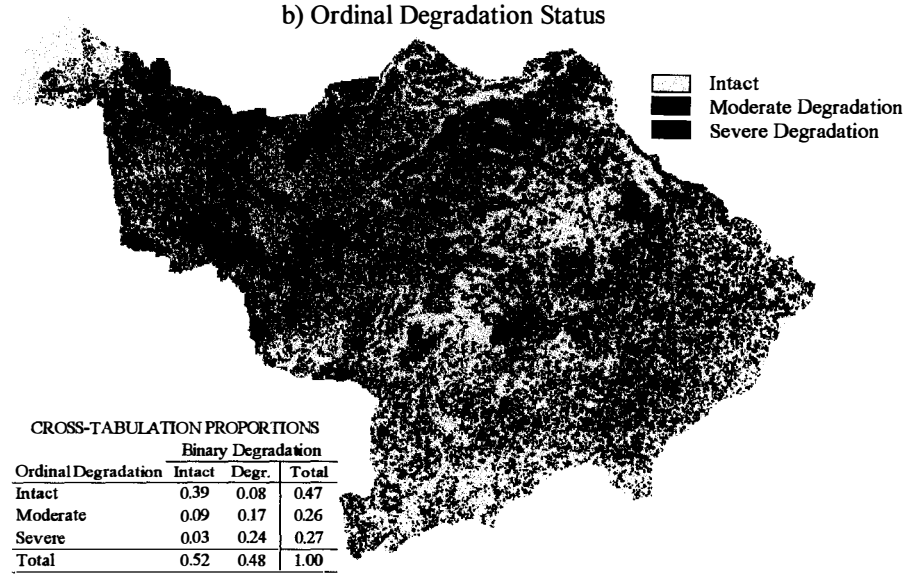

CROSS-TABULATION PROPORTIONS

	Binary Degradation		
Ordinal Degradation	Intact	Degr.	Total
Intact	0.39	0.08	0.47
Moderate	0.09	0.17	0.26
Severe	0.03	0.24	0.27
Total	0.52	0.48	1.00

Figure 6-1. Thematic coverages of soil degradation inferred for the entire Awach River basin from satellite imagery. Classification and cross-validation accuracy for each model are presented in Table 6-2.

The same decision tree algorithm was applied to satellite spectral data from the 1986 scene, yielding maps given in Figure 6-2. Cross-tabulation of 1986 and 2001 map of erosion prevalence indicates a strong degradation trend (Table 6-2). Specifically, severely degraded lands more than doubled in extent, while intact lands fell by over 25%.

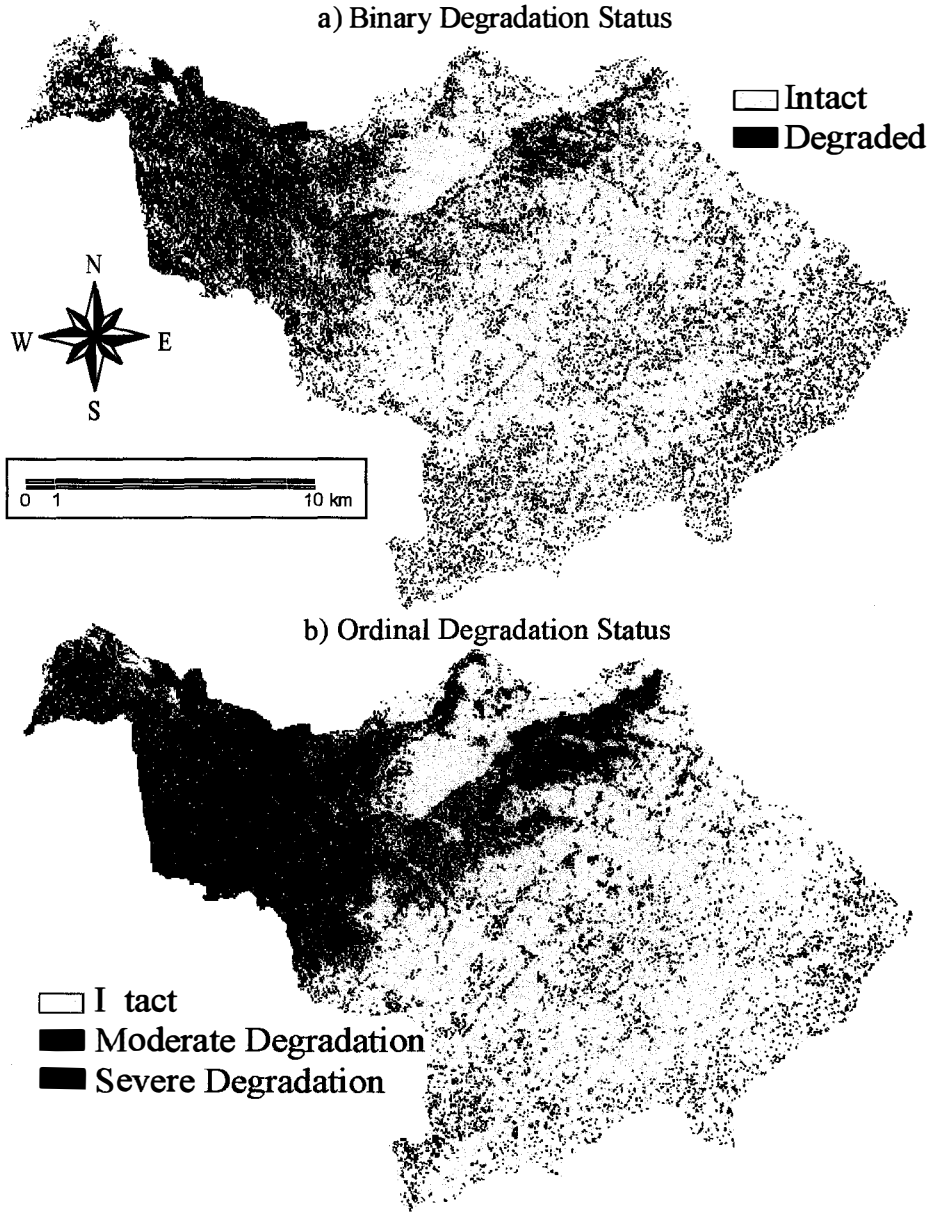

Figure 6-2. Degradation maps for a) binary erosion status and b) ordinal erosion status inferred from 1986 Landsat imagery using classification tree models.

Reduced infiltration capacity prevalence assessment

Based on application of the binary screening model for slow infiltration (<60 mm/hr) to the entire soil database, a classification was developed for the entire watershed into those binary classes. Table 6-3 summarizes model calibration and validation accuracy. The rule-base for this classification model is given in Appendix C. Overall accuracy expected for the thematic surface inferred from the model is above 75%. Site misclassification was independent of land use. Shrubland and pasture sites had a slightly higher proportion (~25%) misclassified than the overall rate (~18%). No other inherent biases (e.g. elevation, proximity, slope) were evident.

Table 6-2. Cross-tabulation of categorical degradation surfaces between 1986 and 2001 and transition probabilities with change proportions.

	From 1986			
To 2001	1	2	3	Total
1	162574	26541	4927	194042
2	57800	40376	10807	108983
3	47229	35809	30171	113209
Total	267603	102726	45905	416234

	From 1986			
To 2001	1	2	3	Proportional Change: 1986 to 2001
1	0.61	0.26	0.11	0.73
2	0.22	0.39	0.24	1.06
3	0.18	0.35	0.66	2.47

Note: Class 1 = Intact, Class 2 = Moderately Degraded and Class 3 = Severely Degraded

An important inference from Figure 6-4 is that lowlands (western basin) are particularly susceptible to the impaired infiltration condition. Almost the entire upper basin, and particularly steep-sloped, forested regions of the basin, are categorized into

Table 6-3. Classification tree model summary for a) calibration and b) validation accuracy for inference of binary infiltration classes from satellite reflectance data.

A) Calibration	Predicted Infiltration Class			
Actual Class	> 60 mm/h	< 60mm/h	Overall Accuracy	82.4%
> 60 mm/h	207	34	Sensitivity	85.9%
< 60 mm/h	40	139	Specificity	77.7%
			Odds Ratio	21.2

B) Validation	Predicted Infiltration Class			
Actual Class	> 60 mm/h	< 60mm/h	Overall Accuracy	76.9%
> 60 mm/h	196	45	Sensitivity	81.3%
< 60 mm/h	52	127	Specificity	70.9%
			Odds Ratio	10.6

the high infiltration class. The model appears to capture the two conditions under which slow infiltration is manifest adequately: lands with degraded or inherently poor soil structure, and wetlands. Linear statistical methods encounter problems with simultaneous classification of multiple spectrally-distinct nodes displaying similar attributes. Linear Discriminant Analysis (LDA) was performed using the same reflectance data, resulting in a calibration classification accuracy of 75.5%, with reduced sensitivity (72.6%).

Table 6-4. Cross-tabulation proportions for binary infiltration and degradation maps.

	Degradation			
Infiltration	0	1	Chi-Sq (df=1)	34055
0	0.42	0.26	*P*-value	<0.0001
1	0.10	0.22	Odds Ratio	3.55

Cross-tabulation between Figure 6-3 (binary infiltration) and Figure 6-1a (binary degradation) demonstrates further the importance of surface hydrologic condition on degradation. Table 6-4 summarizes the cross-tabulation, giving proportions of the classified image falling into each cell of a 2x2 contingency table. The Chi-Squared statistic illustrates strong dependence between the variables, and the strength of that

effect is summarized by the odds ratio, showing that the odds of observing degradation increase 3.55 times when a site is classified as exhibiting slow infiltration.

As with soil degradation, the decision tree algorithm for interpreting the 2001 scene was applied to 1986 data. Figure 6-4 shows the infiltration surface for 1986. One notable conclusion from the cross-tabulation between 1986 and 2001 imagery is the relative consistency of this measure between periods. Specifically, at each time 33% of the basin was expected to exhibit slow infiltration, with strong probability that a site remains in the same category (odds ratio = 34.3 that class association is retained).

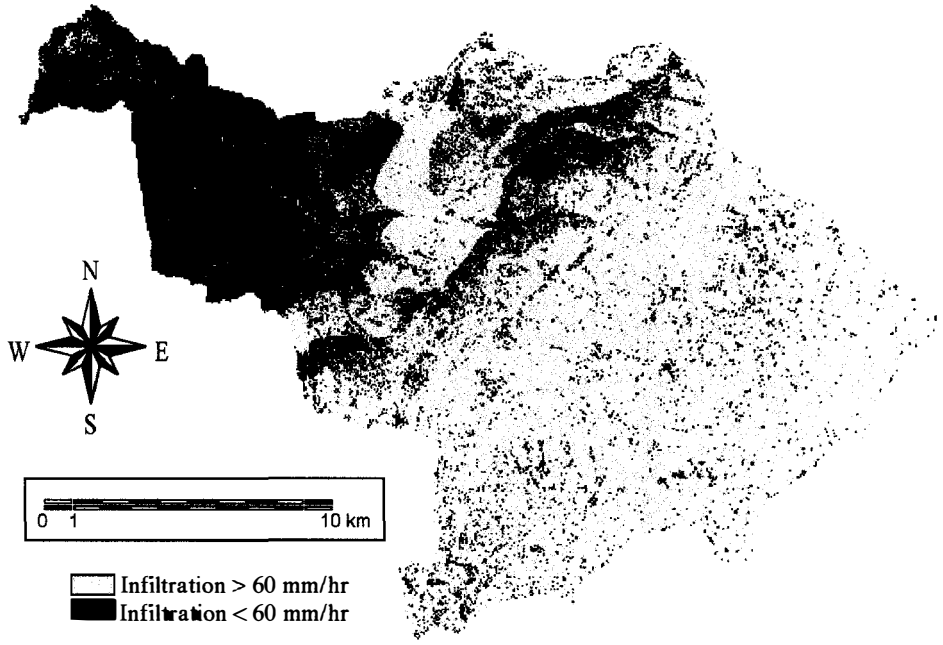

Figure 6-3. Thematic coverage of binary infiltration classes (< 60 mm/h and > 60 mm/h) for the Awach River basin in 2001.

Land Cover Classification

Delineating land cover in the Awach Basin was crucial for risk assessment. Of central consideration was deciding the necessary categorical resolution to allow accurate classification and sufficient detail. During field sampling, land use/land cover at each site was assigned to 4 basic classes (agriculture, pasture, woodland, other). Further

delineation was made between commercial (CA) and subsistence (SA) agriculture, woodland (WL) and shrubland (SL), dense (DP) and sparse (SP) pasture (corresponding

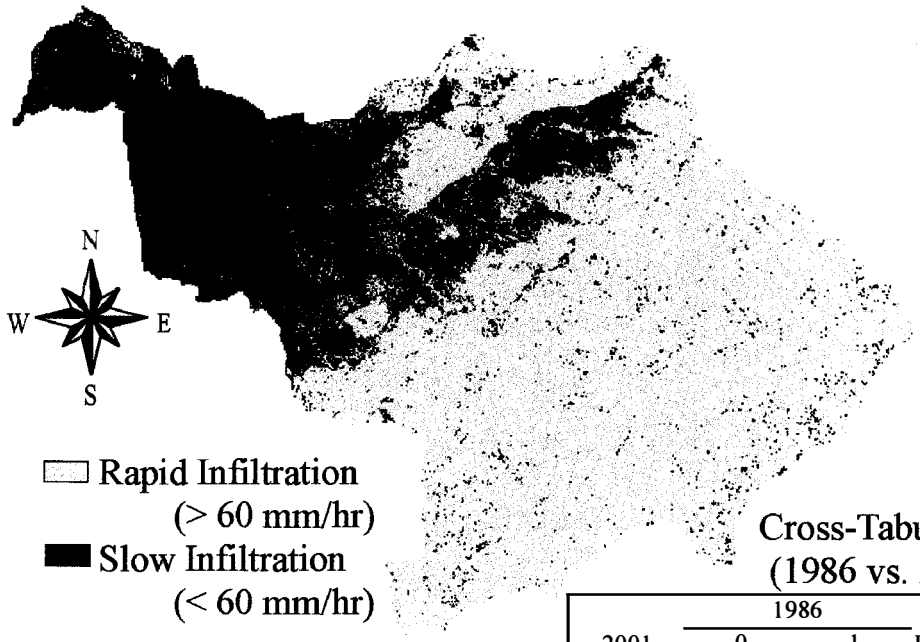

Cross-Tabulation
(1986 vs. 2001)

	1986		
2001	0	1	Pr (2001)
0	250555	29943	0.67
1	26635	109101	0.33
Pr (1986)	0.67	0.33	

Figure 6-4. Binary infiltration surface predicted for the Awach River basin in 1986 based on classification tree model. Also given is the cross-tabulation table for binary infiltration classes compared between 1986 and 2001.

to constrained and communal grazing lands for which emergy evaluations were performed), wetlands (WT) and severe degradation (SD). These 8 classes, also used in the site risk model, were chosen as target categories for land cover classification.

Model predictors included reflectance data (Bands 1 –5 and 7, and band ratios) in addition to slope and elevation. Additional predictors that were explored but proved ineffective were reflectance variance measures (in 3x3 and 5x5 kernels) and pattern indices based on 8-class unsupervised classification (using a k-means clustering algorithm). The optimal tree, as measured by cost-complexity metrics determined in

cross-validation, had 51 terminal nodes. The rule base is given in Appendix C. A tabular summary of model fit for both classification and validation is given in Table 6-5.

There is a significant decrease in accuracy in validation, which suggests spectral confounding between classes. This was particularly strong (>10% commission error) between CA and SA, CA and SL, SL and DP, and SP and SD. While classification accuracy for SA and DP was relatively poor, there were no obvious confounding classes, suggesting that the primary problem with remote classification of these categories is substantial within-class variability.

A comparison of conventional classification methods and the CART approach was made for classifying landuse at the 420 sample sites. Maximum likelihood classification accuracy was moderate (overall accuracy = 55%, Kappa = 0.47). However, this result compares poorly with the classification and cross-validation accuracy from tree-based models (72.9% and 45.2% respectively, Kappa = 0.68 and 0.36). The accuracy within specific classes is particularly informative. Those classes that might be expected to be spectrally consistent (e.g. wetlands, woodlands, severely degraded areas) were effectively classified by both methods. For classes that are expected to vary considerably with elevation, degree of degradation, and moisture regime (subsistence and commercial agriculture and pasture lands), classification is observably more effective using the contingent non-linear approach of recursive data partitioning.

Application of the tree model rule-base to the entire scene yields a land cover map (Figure 6-5). While raw classification (Figure 6-5a) is used for all analyses, a 5x5 kernel model filter (Figure 6-5b) allows better visual interpretation. Prevalence values shown in Figure 6-5 are for the raw classification map.

Table 6-5. Accuracy assessment for land cover classification tree models in a) calibration and b) cross-validation.

Calibration Accuracy	Predicted Landuse									CART	ML Model
Actual Landuse	SA	CA	DP	SP	SL	WL	WT	SD	Total	% Correct	% Correct
Subsistence Ag (SA)	73	2	10	6	4	3	3	7	108	67.6%	46.6%
Commercial Ag. (CA)	4	25	1	3	4	0	2	0	39	64.1%	60.6%
Dense Pasture (DP)	4	5	48	4	5	3	1	0	70	68.6%	48.6%
Sparse Pasture (SP)	2	0	3	56	4	1	0	8	74	75.7%	46.7%
Shrubland (SL)	2	0	6	3	29	3	0	0	43	67.4%	43.2%
Woodland (WL)	2	0	1	2	2	29	0	1	37	78.4%	80.0%
Wetland (WT)	0	0	0	0	0	0	11	0	11	100.0%	90.9%
Severe Degradation (SD)	0	0	0	3	0	0	0	35	38	92.1%	80.6%
Total	87	32	69	77	48	39	17	51	420	72.9%	54.5%
									Kappa	0.68	0.47

Validation Accuracy	Predicted Landuse									
Actual Landuse	SA	CA	DP	SP	SL	WL	WT	SD	Total	% Correct
Subsistence Ag (SA)	55	3	8	19	5	10	3	5	108	50.9%
Commercial Ag. (CA)	5	18	4	0	4	3	4	1	39	46.2%
Dense Pasture (DP)	9	7	26	9	8	9	2	0	70	37.1%
Sparse Pasture (SP)	13	3	12	26	5	3	0	12	74	35.1%
Shrubland (SL)	6	5	3	5	18	6	0	0	43	41.9%
Woodland (WL)	5	2	4	6	3	16	0	1	37	43.2%
Wetland (WT)	0	2	1	0	0	0	8	0	11	72.7%
Severe Degradation (SD)	6	0	0	8	1	0	0	23	38	60.5%
Total	99	40	58	73	44	47	17	42	420	45.2%
									Kappa	0.36

Land Cover Change

The classification tree rule-base was applied to 1986 imagery to determine patterns and proportions of landuse change in the area. Figure 6-6 gives the landuse map for 1986. Results of this map indicate substantial changes in landuse in the basin. These are summarized in Figure 6-7, which shows current landuse conditions (2001), 1986 landuse conditions and predictions of future landuse proportions for 2016, described in detail below. Between 1986 and 2001, nearly 50% of woodlands were lost to encroachment, and a substantial increase in sparse pasture (resulting from higher local cattle densities), severe degradation and shrubland was observed. There also appears to have been a decline in the area of subsistence and commercial agriculture.

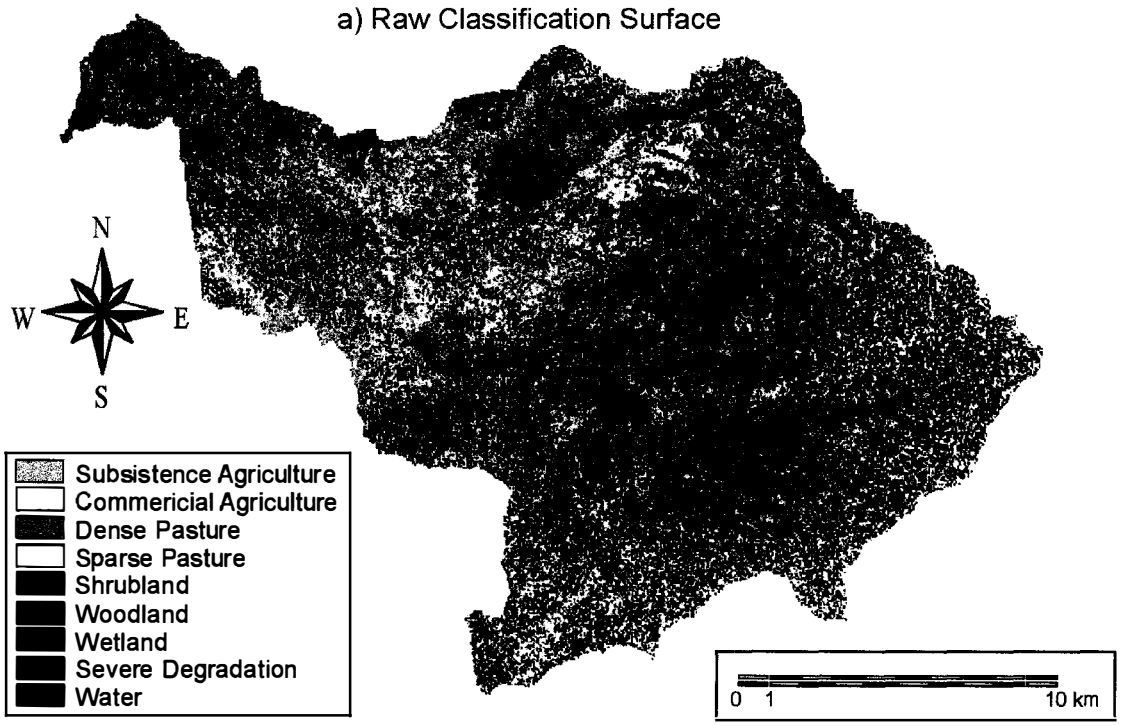

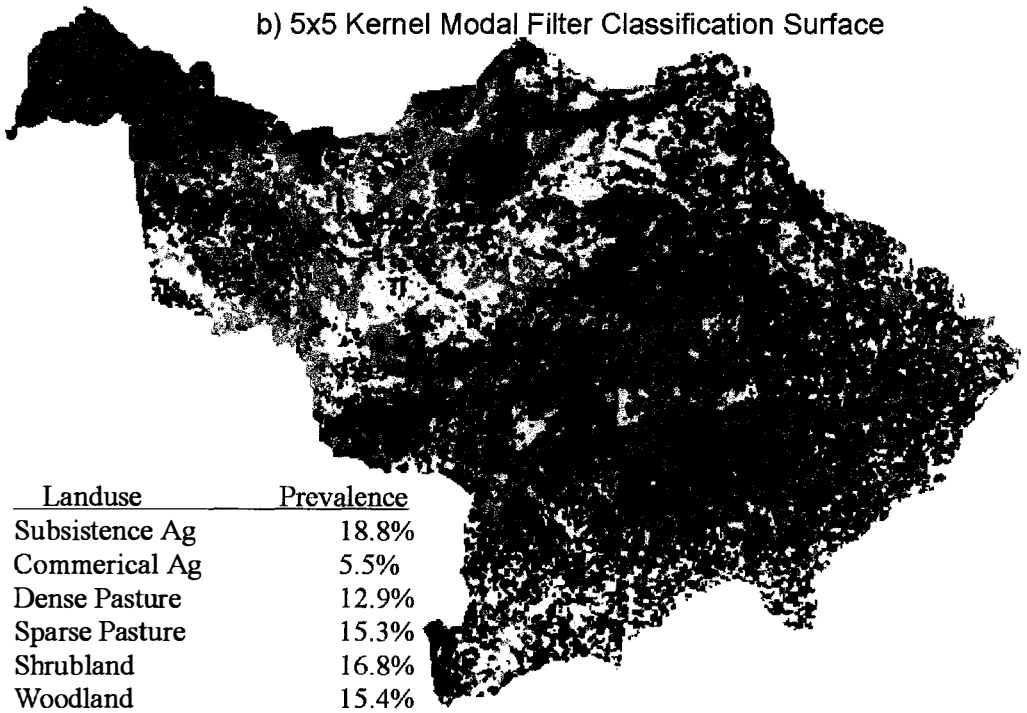

Landuse	Prevalence
Subsistence Ag	18.8%
Commerical Ag	5.5%
Dense Pasture	12.9%
Sparse Pasture	15.3%
Shrubland	16.8%
Woodland	15.4%
Wetland/Water	6.2%
Severe Degradation	9.1%

Figure 6-5. Land cover classification of the Awach basin. Shown are a) raw thematic surface inferred directly from CART model and b) 5x5 kernel modal smoothing filtered theme.

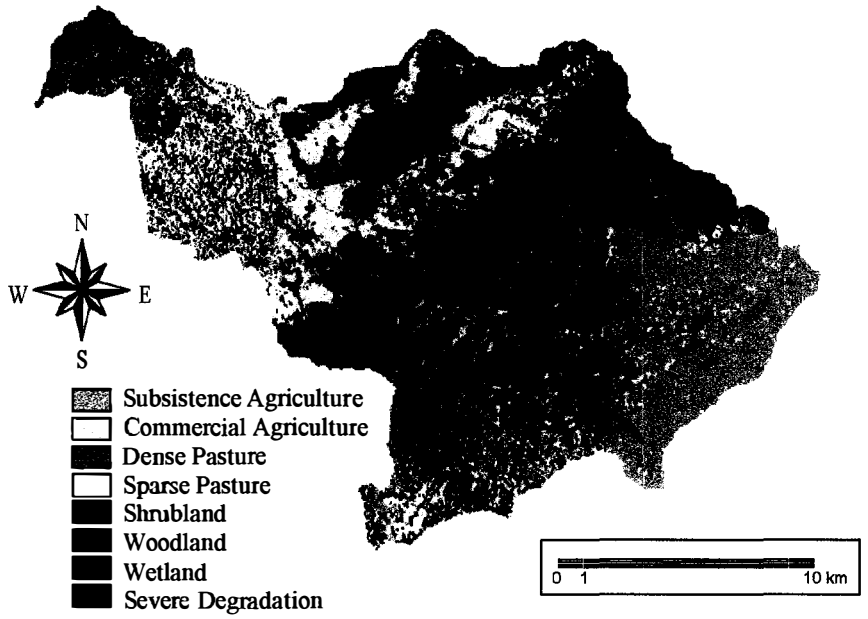

Figure 6-6. Land cover pattern inferred from 1986 Landsat imagery based on classification tree model developed for 2001. Shown is land cover classification after application of 5x5 kernel modal filter.

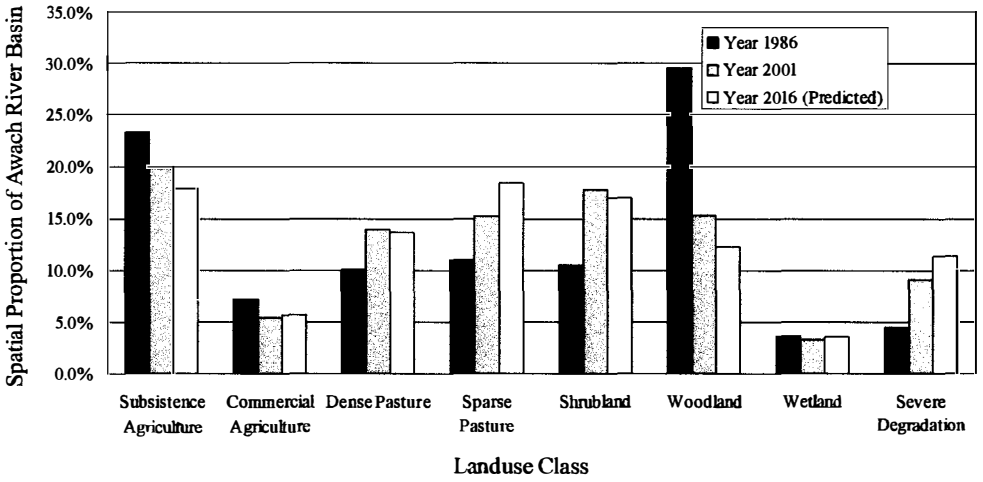

Figure 6-7. Changes in land cover proportions between 1986 and 2001.

The loss of commercial agricultural use is realistic, given the decline in outgrower (independent farms) services for tea, cotton and sugarcane (Biamah et al. 1999). However, there is no evidence that subsistence agricultural activities have decreased in the region; indeed, there is substantial documentation (e.g. Kenya Central Bureau of Statistics, 2001) of increased regional population densities. Extreme within-class

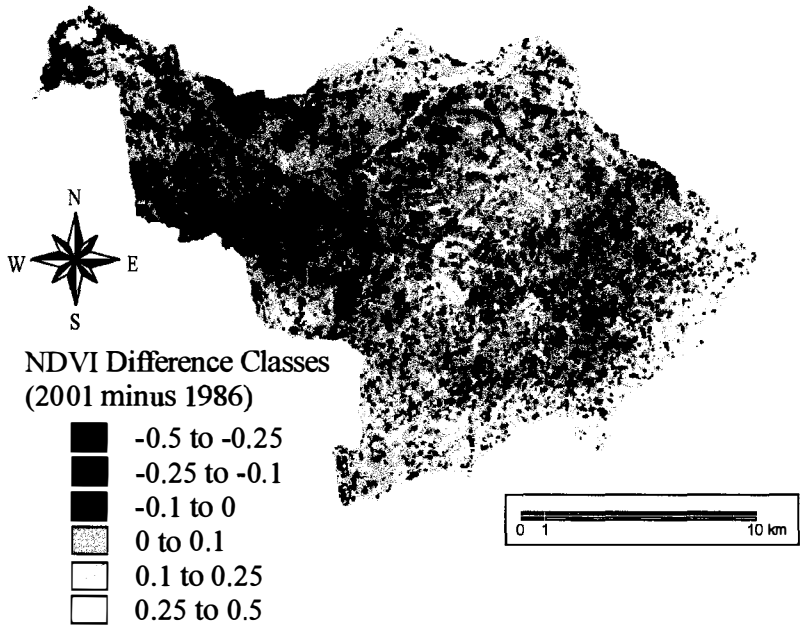

Figure 6-8. Classes of NDVI difference between 1986 and 2001. Classes represent the result of $NDVI_{2001} - NDVI_{1986}$.

variability of subsistence agricultural land cover category was already determined to contribute to lowered classification accuracy, and may explain the unexpected change.

Land cover change can be related to biomass as well as landuse. Figure 6-8 gives changes in NDVI between 1986 and 2001. Negative values indicate decreased vegetative cover. Overall, values fell by an average of only 0.02 units, but in certain areas, the decrease was as much as 0.54 units. Note that 1986 imagery was obtained in late February, while the 2001 imagery was from early April. This period corresponds with "green-up" due to rain onset. As such, the expected condition is increased NDVI.

Table 6-6 gives a cross-tabulation of degradation and landuse for 2001. These data are used as part of an algorithm that assigns low-risk landuse types to high areas and high risk uses to low risk areas. Table 6-6 illustrates that subsistence agriculture is more likely to be classified as degraded than commercial agriculture, sparse pasture is over 75% degraded and woodlands and wetlands are rarely classified as degraded.

Table 6-6. Cross-tabulation of landuse and binary degradation maps. Shown are cell-counts and proportions.

Counts	Erosion Status			Proportion	Erosion Status	
Landuse	Intact	Degraded	Total	Landuse	Intact	Degraded
SA	39944	42612	82556	SA	48.4%	51.6%
CA	15478	7283	22761	CA	68.0%	32.0%
DP	43309	14475	57784	DP	74.9%	25.1%
SP	13836	49689	63525	SP	21.8%	78.2%
SL	34530	39593	74123	SL	46.6%	53.4%
WL	56255	7637	63892	WL	88.0%	12.0%
WT	12820	790	13610	WT	94.2%	5.8%
SD	589	37394	37983	SD	1.6%	98.4%
Total	216761	199473	416234	Total	52.1%	47.9%

Note: SA - subsistence agriculture, CA - commercial agriculture, DP - dense pasture, SP - sparse pasture, SL - shrubland, WL - woodland, WT - wetland, SD - severe degradation

Table 6-7. Landuse transition counts and probabilities for 8 classes between 1986 and 2001 in the Awach River basin.

Transition Counts

	From Landuse								
To Landuse	SA	CA	IP	DP	SL	WL	WT	SD	Total 2001
SA	37076	6625	8058	3045	6624	17911	1762	1455	82556
CA	6823	11178	2801	201	375	1177	0	206	22761
IP	15993	2865	15231	9565	3878	9301	196	755	57784
DP	13403	1915	6918	19290	9375	9944	191	2489	63525
SL	12074	3245	3023	4973	15741	33400	43	1624	74123
WL	2919	2520	3586	256	5087	49365	137	22	63892
WT	430	100	109	185	6	75	12619	86	13610
SD	8573	1875	2224	8352	2671	1785	194	12309	37983
Total 1986	97291	30323	41950	45867	43757	122958	15142	18946	416234

Transition Probabilities

	From Landuse								% Change
To Landuse	SA	CA	IP	DP	SL	WL	WT	SD	1986 to 2001
SA	**0.38**	0.22	0.19	0.07	0.15	0.15	0.12	0.08	0.85
CA	0.07	**0.37**	0.07	0.00	0.01	0.01	0.00	0.01	0.75
IP	0.16	0.09	**0.36**	0.21	0.09	0.08	0.01	0.04	1.38
DP	0.14	0.06	0.16	**0.42**	0.21	0.08	0.01	0.13	1.38
SL	0.12	0.11	0.07	0.11	**0.36**	0.27	0.00	0.09	1.69
WL	0.03	0.08	0.09	0.01	0.12	**0.40**	0.01	0.00	0.52
WT	0.00	0.00	0.00	0.00	0.00	0.00	**0.83**	0.00	0.90
SD	0.09	0.06	0.05	0.18	0.06	0.01	0.01	**0.65**	2.00

Class definitions are SA = subsistence agriculture, CA = commercial agriculture, IP = intact pasture, DP = degraded pasture, SL = shrubland, WL = woodland, WT = wetland and SD = severe degradation

Markov Transition Matrix Development

Cross-tabulation of 1986 and 2001 landuse maps (Figures 6-5a and 6-6) yields counts of pixels that meet each landuse transition (e.g. forest to commercial agriculture). From this change matrix, global Markov transition probabilities (i.e. not spatially explicit) were computed for the 15-year period between scenes. Table 6-7 summarizes both the pixel counts of each transition and the resulting transition probabilities. Also shown in Table 6-7 are the proportional changes in each landuse in the basin from 1986 to 2001. Stochastic simulation was applied based on computed conditional probabilities to forecast land use patterns 15 years into the future (2016). Figure 6-7 shows 2016 predicted landuse proportions without any changes in transition probabilities. A map of predicted landuse is given in Figure 6-9; note that this presents predicted landuse after a 5x5 kernel modal filter was applied to improve visual clarity.

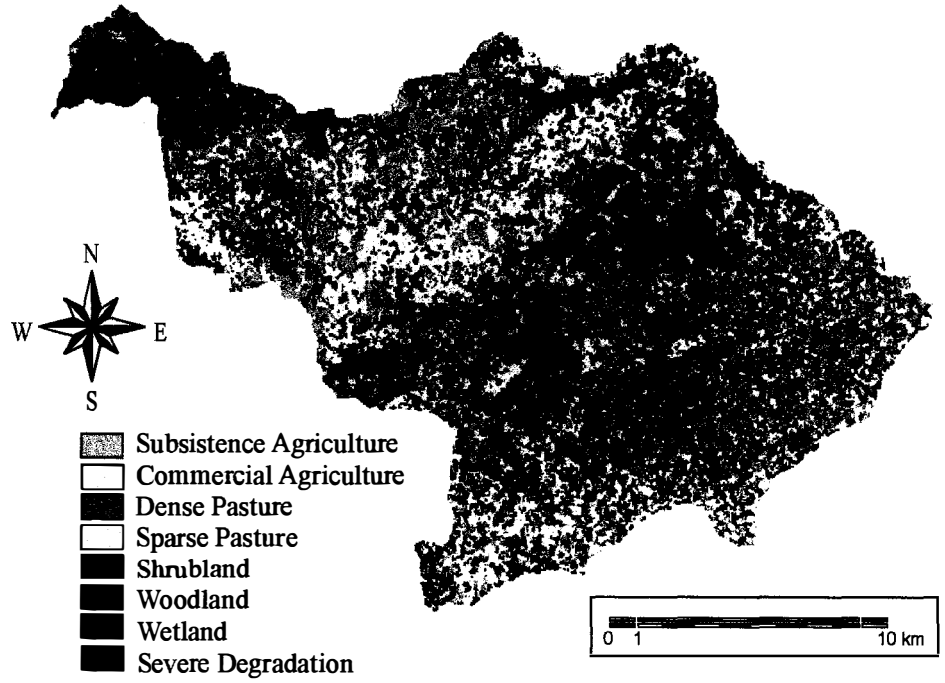

Figure 6-9. Predicted landuse condition for the Awach basin in 2016. Predicted landuse was smoothed using a 5x5 kernel modal filter to improve clarity.

Spatial Risk Assessment

Statistical models previously developed to predict probabilities of degradation were applied to the entire basin using a variety of interpolation methods. Each factor (site, soil and hydro/terrain) was interpolated separately, and then coupled using the overall risk model equation. Interpolation of each factor was different.

Hydro/Terrain Factor Interpolation

Several variables were required to delineate hydro-terrain risk across the entire basin. These included infiltration class (binary), depth restriction class (binary), slope, slope shape, flooding and rainfall. Infiltration data were previously presented (Figure 6-3), and slope and slope shape were inferred directly from the regional digital elevation

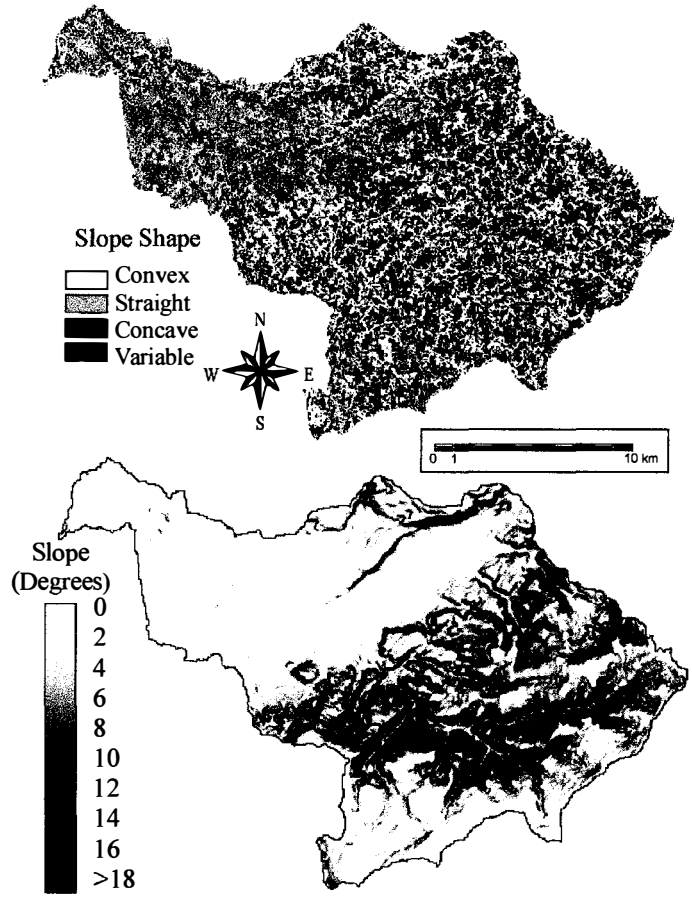

Figure 6-10. Slope shape and slope maps for the Awach River basin as used in defining the hydro-terrain risk factor.

model (Figure 6-10 derived from Figure 4-2); the map slope shape was developed using a standard topographic algorithm available in Idrisi (Clark Labs 2001). Rainfall was determined based on an existing climate database (Corbett et al. 1997, Figure 3-2c), and flooded regions were delineated based on the landuse classification (WT – wetlands in Figure 6-5). Soil depth was effectively modeled as a function of slope, soil hardsetting and degradation (Table 6-8). These coverages were incorporated into the model presented in Table 5-6 to yield the hydro/terrain risk map given in Figure 6-11.

Table 6-8. Model results relating soil depth to slope, soil hardsetting and soil degradation.

Parameter	Estimate	Std. Error	p-value
Intercept	-2.27	0.31	<0.0001
Slope	0.15	0.03	<0.0002
Hardsetting	1.27	0.41	<0.0003
Degradation	0.76	0.17	<0.0004

Null Deviance = 580.1 Residual Deviance = 477.0
df = 3 $P << 0.0001$

	Predicted		Model Summary	
Observed	0	1	Accuracy	70.5%
0	162	63	Sensitivity	68.7%
1	61	134	Specificity	72.0%
			Odds Ratio	5.65

Soil Erodibility Factor Interpolation

Soil erodibility was inferred directly from satellite imagery based on reflectance characteristics using backwards stepwise multiple regression targeting sample site erodibility, determined from the soil logistic regression model previously presented. While satellite sensors generally do not directly measure soil reflectance characteristics, model results (Table 6-9) indicate a strong fit between predicted and observed erodibility scores, presumably due to strong association between erodible soils and degraded vegetative cover. Overall model fit is summarized with an adjusted multiple-r^2 value of

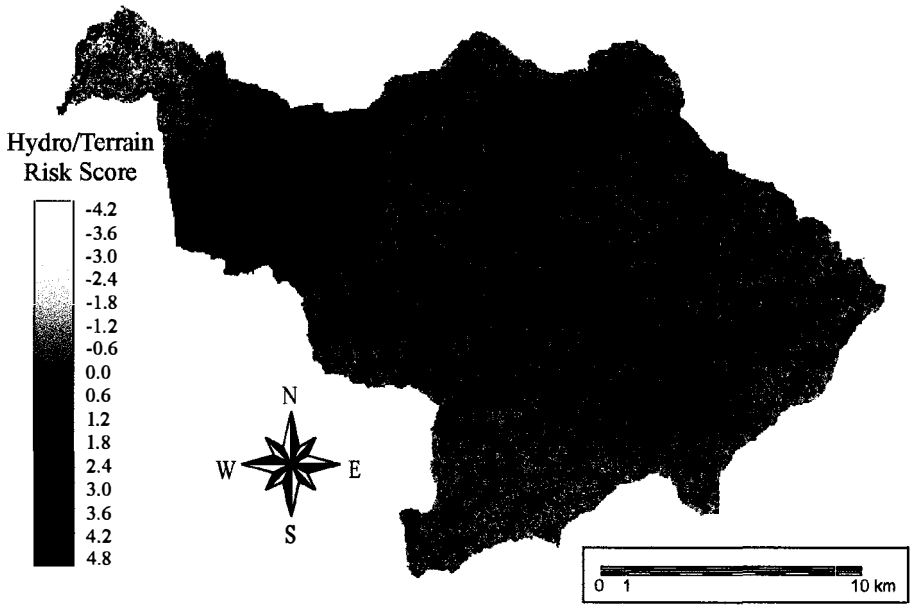

Figure 6-11. Interpolated Hydro/Terrain risk score for the Awach River Basin. Values are logit model scores.

0.68; the model fit is shown in Figure 6-12. This model was applied basinwide to yield a map of soil erodibility (Figure 6-13). Overlaying this is a thematic coverage showing soil survey unit boundaries. Little association between risk and soil type is evident; the resolution and reliability of using soil survey data are questionable given these findings.

Table 6-9. Stepwise deletion multiple regression model relating satellite reflectance data and erodibility values.

Variable	Parameter Estimate	Std. Error	p-value
Intercept	24.39	11.33	0.03
B1	0.06	0.03	0.05
B2	-0.29	0.14	0.04
B3	0.21	0.11	0.05
B4	0.07	0.04	0.08
B7	0.02	0.01	0.03
Elev	-0.02	0.00	0.00
NDVI	-0.20	0.09	0.02
B3B4	-0.03	0.02	0.15
B3B2	-0.17	0.09	0.06
B7B5	-0.08	0.02	0.00
	Residual Std. Error	0.89	df = 409
	Multiple Adj. R-Sq.	0.683	
	F-Statistic	76.2	df = 10, 409
			P-value <<0.001

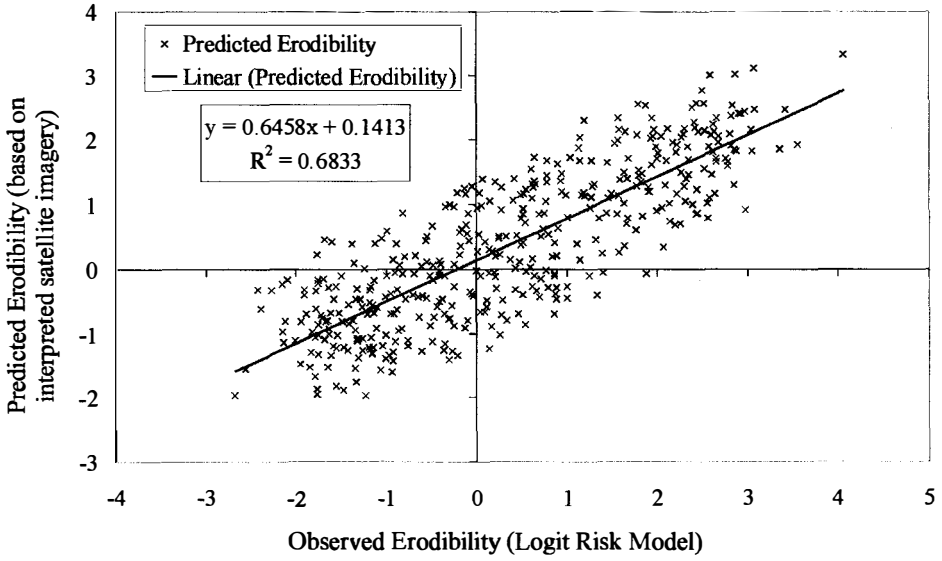

Figure 6-12. Multiple regression model fit between observed and predicted erodibility scores based on satellite reflectance data.

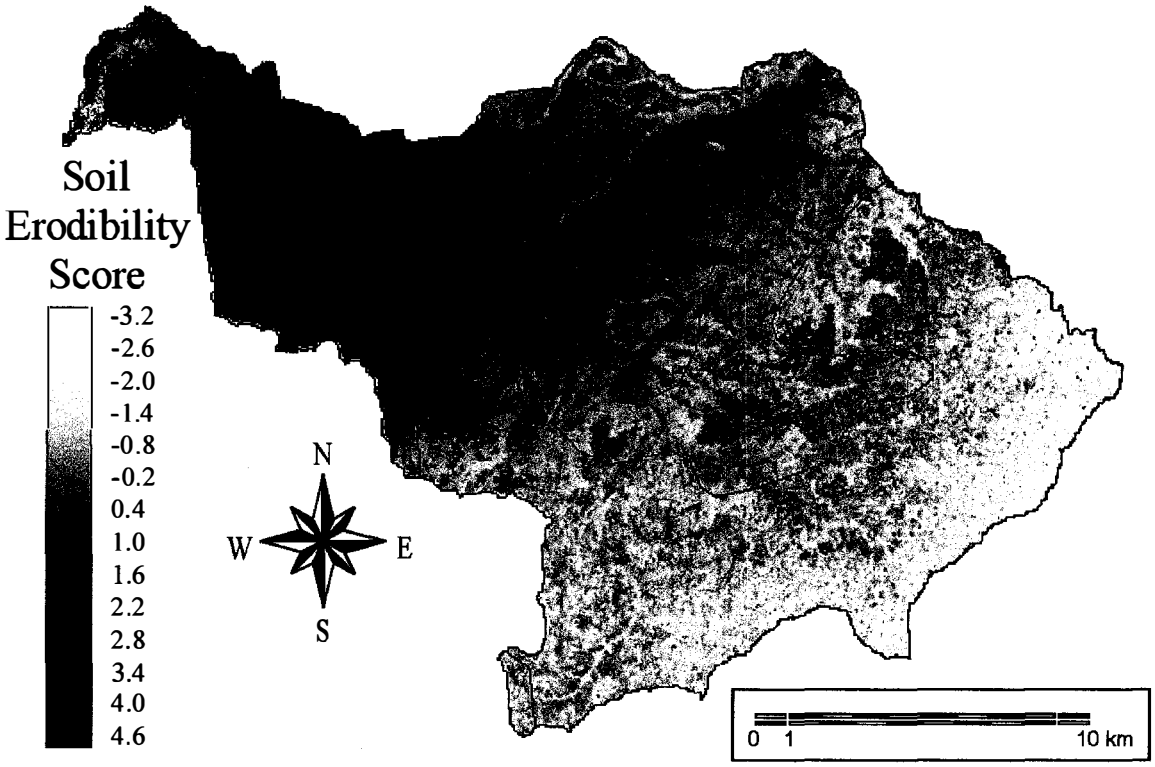

Figure 6-13. Interpolated soil erodibility scores based on satellite reflectance data for 2001. Also shown are soil polygons for the region (see Figure 5-2).

Site Management Factor Interpolation

Site management risk was defined based on landuse and vegetative cover characteristics. Thematic landuse coverages have been presented (Figure 6-5). Other significant risk factors (see Table 5-4) include stone cover, ground cover and height, woody cover and annual/perennial dominance.

Cover class and dominant vegetation type prediction from satellite imagery was poor (accuracy < 45%). Given the need to include cover information in landuse scenario forecasts, the assumption was made that site cover characteristics were equal to mean levels for each landuse (see Table 5-5). This assumption ignores within landuse management variability, which was substantial, particularly with regard to variability as a function of elevation. That graphical models of site risk (Figure 5-5) include both landuse and cover characteristics as significant degradation associates indicates the extent to which this assumption is a simplification. Based on the risk model, a site management risk surface was interpolated based on the 2001 landuse condition (Figure 6-14).

Stone cover was interpolated as a function of slope and soil depth (Table 6-10), resulting in a model that predicts stone cover at 67% of the sites correctly. The resulting coverage is not presented here. The site risk factor surface is presented in Figure 6-14.

Table 6-10. Model relating slope and binary depth restriction to site stone cover.

Variable	Par. Estimate	Std. Error	P-Value
Intercept	-0.082	0.129	0.524
Slope (Degr.)	0.098	0.009	<0.001
Soil Depth (< 50 cm)	1.48	0.118	<0.001

	Predicted Class		
Observed Class	0	1	2
0: 0 - 5%	214	85	11
1: 5 - 25%	5	61	37
2: 25-100%	0	0	7

Overall Risk Model

The multivariate model (Table 5-7) that includes all three risk factors was extrapolated to the entire basin based on the three risk maps presented (Figs. 6-11, 6-13 and 6-14) for the 2001 condition, and degradation probabilities computed (Figure 6-15). After reclassifying this map to a binary image (intact-degraded), a cross-tabulation was performed with the satellite inference map of binary degradation (Figure 6-1a) to determine overlap between the two maps. This cross-tabulation is summarized in Figure 6-15. Recall that overall risk model accuracy was 82% (Table 5-7) indicating only a minor decrease in accuracy across the whole basin (accuracy = 78%).

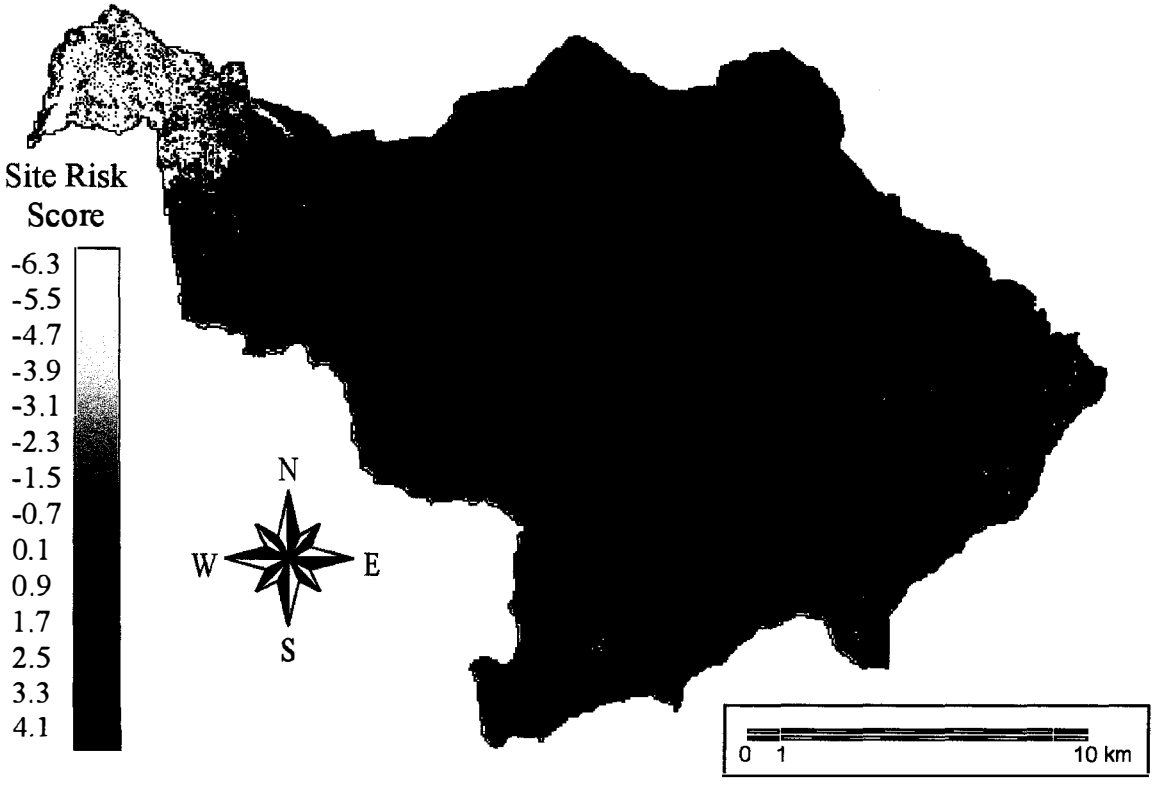

Figure 6-14. Site management factor degradation score for landuse in 2001.

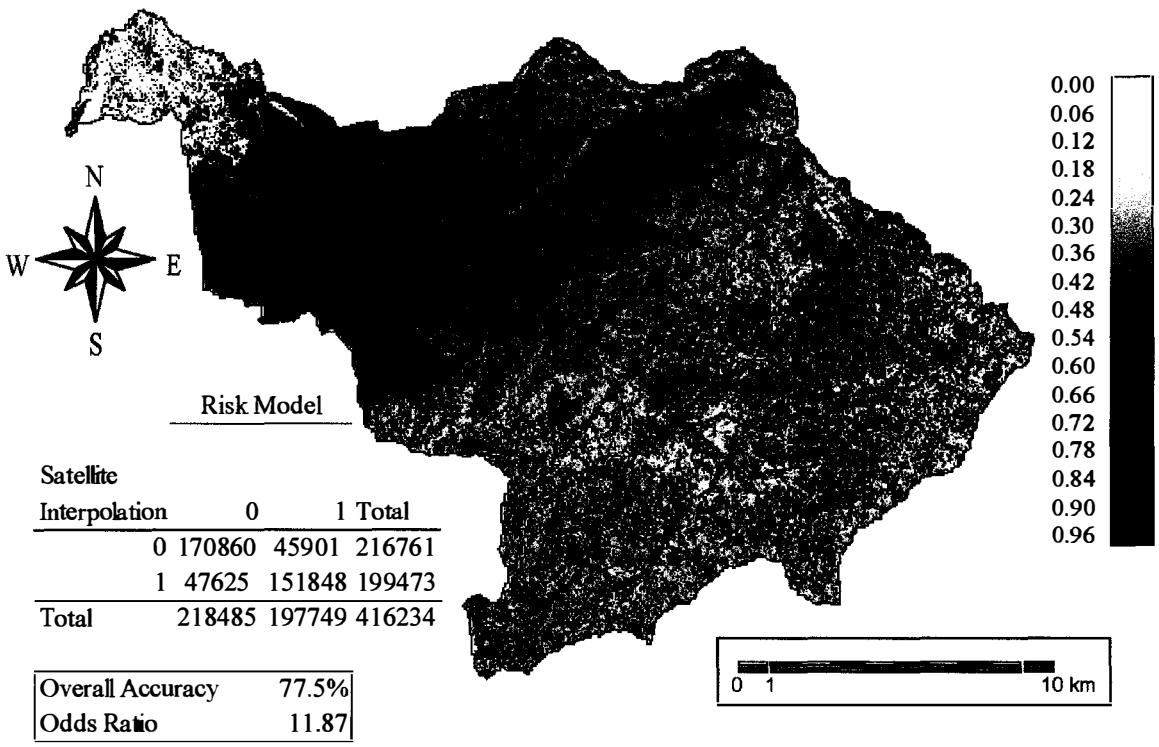

Risk Model

Satellite Interpolation	0	1	Total
0	170860	45901	216761
1	47625	151848	199473
Total	218485	197749	416234

Overall Accuracy	77.5%
Odds Ratio	11.87

Figure 6-15. Overall degradation probability map for the Awach River basin in 2001.

Inherent risk defines site degradation propensity before land management decisions are made. It is the weighted sum of soil and hydro/terrain risk. Weighting was defined by overall risk (Table 4-7); the inherent risk map is given in Figure 6-16.

The overall risk model was also applied to the 1986 land cover condition (assuming that there has been no change in inherent risk), and predictions of intact and degraded lands were compared with direct satellite inference (Figure 6-2). Table 6-11 summarizes back-casting accuracy in the same manner as presented for the 2001 risk map in Figure 6-15. Notably, the risk model overestimates the total area degraded by nearly 40%, indicating the extent to which inherent risk may be responding to human management. Despite this simplification, the result indicates a relatively accurate, if somewhat conservative, model for forecasting effects of future landuse changes.

Figure 6-16. Inherent risk scores for the Awach Basin.

Table 6-11. Back-casting (to 1986) accuracy of spatially interpolated overall risk versus direct satellite inference from 1986 imagery.

	Overall Risk Model		
Satellite Interpolation	0	1	Total
0	224608	79160	303768
1	34598	77868	112466
Total	259206	157028	416234
% Accuracy	72.7%		
Odds Ratio	6.39		

Future Landuse Change Assessment

Spatial risk assessment models allow comparison of various large-scale intervention strategies. While most intervention takes place at the farm scale, the scope of the problem warrants decision support intervention at the regional scale. Future landuse scenarios were developed based on adjustments made to the Markov transition matrix, and assessed within a standardized framework that includes proportional degradation and projected agricultural benefits. A flow chart of the assessment

framework is presented first, followed by explication of scenario development, and finally, results comparing each landuse scenario are presented.

Scenario Assessment Framework

An assessment framework was developed to compare each alternative based on two criteria: first, reduction in degraded lands and second, maximized basin-wide agricultural benefit. The former, required to quantify the latter, was assessed using the spatial-statistical modeling framework presented in flow-chart form in Figure 6-17. Each landuse scenario map is manipulated to produce a prediction of site risk based on nominal levels of cover characteristics for each landuse type. The other two risk factors (soil and hydro/terrain) are derived products previously presented, and are considered the inherent component of overall risk. The overall risk model is implemented for each landuse scenario, producing maps of degradation probabilities and eventually binary degradation classes. This product is developed by comparing a map containing random numbers (0 to 1), labeling a site degraded if the random value is less than the degradation probability.

This risk assessment model is coupled with emergy accounting analyses that indicate yields expected under specific land uses to provide an index that, when maximized, optimizes the trade-offs between soil protection and resource extraction. Specifically, computed values of the Agricultural Benefit Ratio (ABR) under both intact and degraded soil conditions for the Awach basin (Table 6-12 summarizing Table 3-15) were applied based on landuse and degradation coverages. The module "ABR Recl" in Figure 6-17 applies information in Table 6-12 to cross-tabulations of landuse and resulting degradation maps for each scenario. ABR values for wetlands were not computed in this study; consequently, they were omitted from scenario assessment.

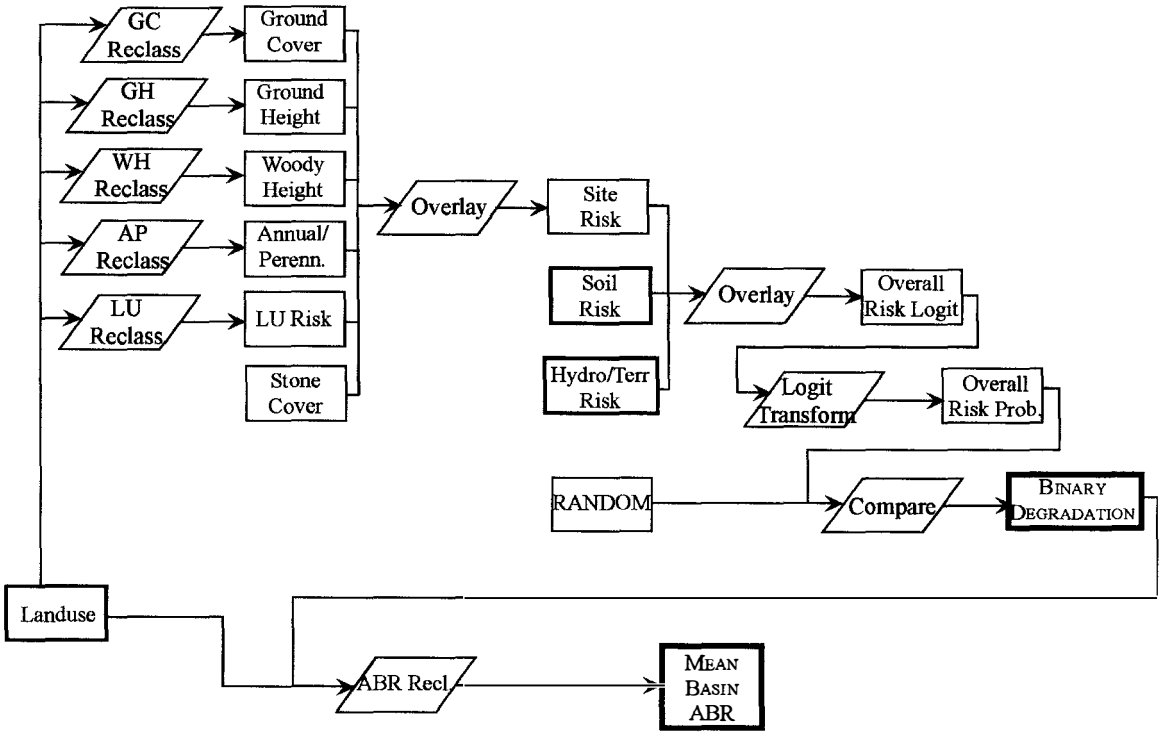

Figure 6-17. Flow chart of the spatial model as implemented. Note that Soil Risk and Hydro/Terr risk surfaces are also derived, but these details are omitted.

.

Table 6-12. Agricultural Benefit Ratio (ABR) computed for each landuse for both intact and degraded soil conditions.

	Degradation Status	
Landuse	Intact	Degraded
Subsistence Agriculture	5.52	2.25
Commercial Agriculture	6.42	3.01
Dense Pasture	2.60	1.93
Sparse Pasture	1.91	1.32
Shrublands	3.76	1.62
Woodlands	7.41	1.58
Wetlands	-	-
Severe Degradation	0.00	0.00

This assessment framework provides two numbers with which to compare alternatives. The first is the proportion of the basin predicted to be degraded under each. The other, which encompasses that information as well as predictions of rural livelihood support, is the basin mean ABR value.

Landuse Change Scenarios

A suite of alternatives exists for erosion intervention. The majority of them are on-farm solutions that are best assessed at that scale. However, the information presented in Figure 6-16 (inherent risk) and Table 6-12 (Agricultural Benefit Ratio) indicates that there may be leverage to improve livelihoods and reduce natural capital depletion by exploring basin-wide land cover changes. It should be noted, however, that this assumes that recovery is possible, and that degradation, once started, is reversible.

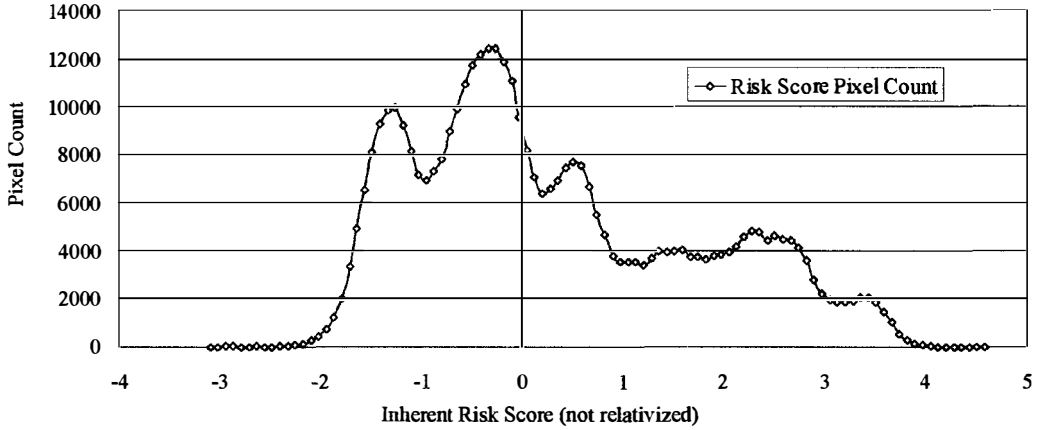

Figure 6-18. Distribution of inherent risk scores. Risk classes were designated with centroids at –1.5, -0.5, 0.5, 1.5, 2.5 and 3.5. Mean and median risk are 0.35 and 0.08.

Changes in proportional landuse allocation

All eight landuse change scenarios were explored using this technique: 1) do nothing, 2) commercial agriculture, 3) reforestation, 4) reduced livestock densities, 5) active badland restoration, 6) combined efforts, 7) radical transformation and 8) historic condition. Specific description of how the Markov matrix was amended for each landuse scenario was previously presented. Transition matrices, modified from Table 6-7 for each scenario, are given in Table C-1 (Appendix C).

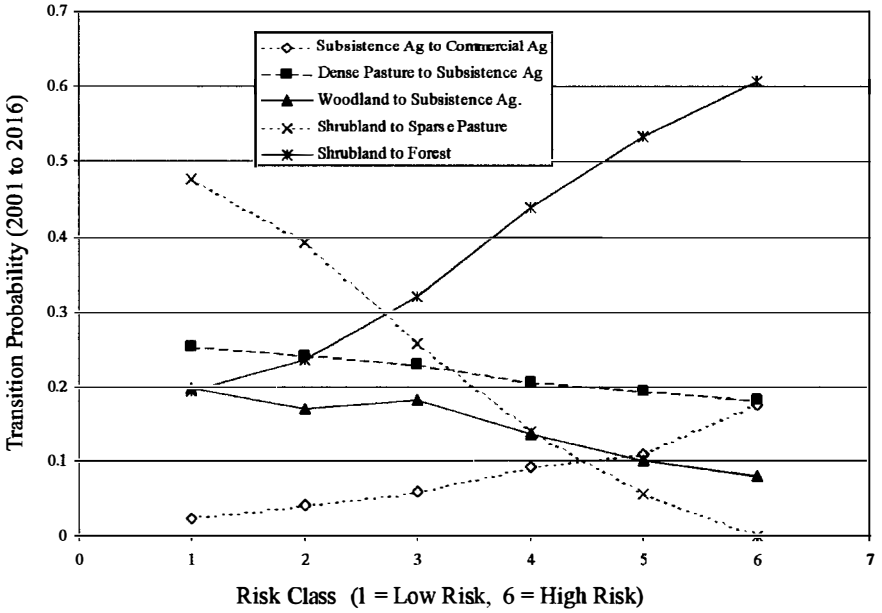

Figure 6-19. Example of the effect of risk class (Figure 5-17) on conditional transition probabilities between land uses. Note that effect on transition probability is proportional to difference in degradation risk between land uses.

Spatially targeted landuse allocation

Inherent degradation classes were defined based on frequency counts of inherent risk scores (Figure 6-18) derived from Figure 6-16. Original transition probabilities

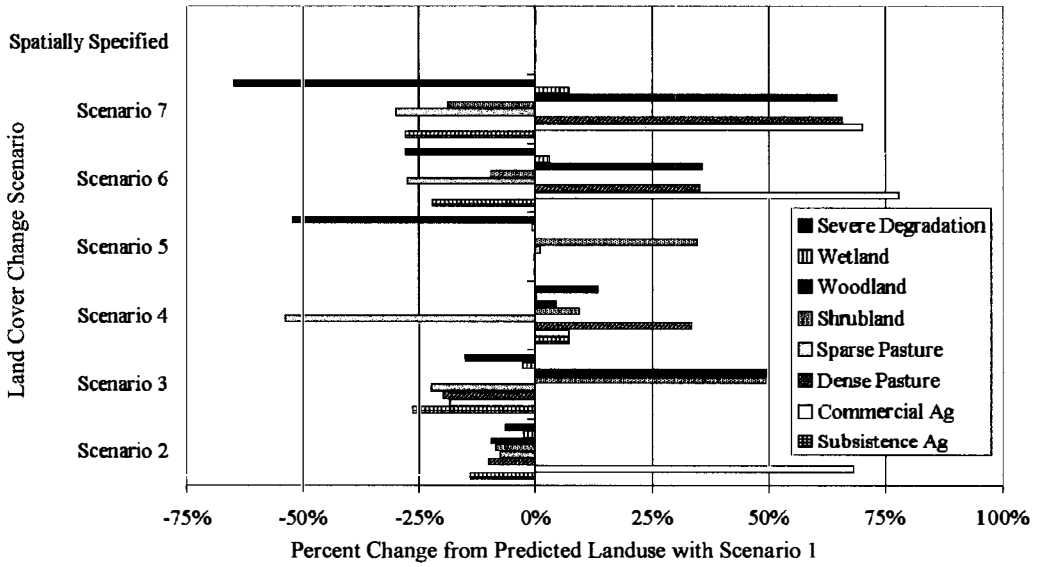

Figure 6-20. Percent change in landuse proportions in 2016 under 5 development scenarios in comparison with landuse proportions under Scerario 1 - predicted landuse in 2016 without adjustment of Markov matrix.

(Table 6-7) were amended so that each landuse had transition probabilities defined contingent on pixel inherent risk. Figure 6-19 shows five of the 64 transition probability trajectories. Uneven lines result from the constraint that transition probabilities for each pixel sum to one. The line slope corresponds to the difference in proportion of total area that is degraded between the given landuse and landuse to which it is transitioning.

Scenario Landuse Proportions

The results of proportional allocation to each landuse are given in Figure 6-20 relative to Scenario 1. Scenario 1 is the condition for which transition probabilities inferred between 1986 and 2001 are unchanged. It is important to note, particularly for assessing comparative risk presented later, that the "Spatially Specified" scenario maintained landuse proportions as nearly identical to Scenario 1 as possible.

The transitional steady-state condition occurs after approximately 6 iterations. While little evidence suggests that landuse change patterns are linear with time, resulting steady state proportions further illustrate change trends: at steady-state, over 20% of the basin is severely degraded, 25% is under sparse pasture and only 7% of forest remains.

Degradation Proportions

Application of the risk protocol described for each landuse change scenario allowed tabulation of predicted spatial degradation prevalence. Table 6-13 summarizes these data, showing for each scenario cell counts and proportions for intact and degraded condition. Since degradation is defined stochastically, standard errors associated with each parameter value were estimated. Standard error of proportions was defined for only Scenario 1, based on 10 different random surfaces, and assumed to generalize to each other scenario. Standard errors were computed as 0.06%, indicating that each estimate of

degradation is relatively precise. While there is limited basis for assessing statistical significance in comparing scenarios, the small estimated standard errors indicate that even small differences observed between landuse scenarios cannot be attributed to the stochastic component of this analysis. For historic conditions (pre-settlement – scenario 8), it should be noted that, while it is unlikely that degradation rates were as high as 30%, this figure provides a benchmark against which various scenarios can be assessed. High degradation prevalence is due to assuming invariant inherent risk.

Table 6-13 suggests that relatively significant changes in land use decision-making may have a relatively small effect on degradation prevalence. Specifically, doubling the number of sites under commercial agriculture only reduces basin wide degradation by 0.7%. Under scenarios 2 through 5, conditional probability values were changed to target one landuse; this model suggests that cattle density reduction, active restoration of severely degraded lands and reforestation offer comparably effective tactics for controlling degradation, though cattle density reduction appears most successful.

When activities are implemented in combination (though with smaller proportional changes in Markov probabilities), as in Scenario 6, the result is a moderate

Table 6-13. Comparison of degradation extent for 1986 and 2001 conditions and expected historic (pre-settlement) and future scenarios.

	Cell Counts		Proportions	
Scenario	Intact	Degraded	Intact	Degraded
Historic Condition (scenario 8)	293454	122780	70.5%	29.5%
1986	259206	157028	62.3%	37.7%
2001	214573	201661	51.6%	48.4%
2016 Scenario 1	195264	220970	46.9%	53.1%
2016 Scenario 2	197938	218296	47.6%	52.4%
2016 Scenario 3	202348	213886	48.6%	51.4%
2016 Scenario 4	208381	207853	50.1%	49.9%
2016 Scenario 5	204093	212141	49.0%	51.0%
2016 Scenario 6	208811	207423	50.2%	49.8%
2016 Scenario 7	254475	161759	61.1%	38.9%
2016 - Spatially Targeted	199882	216352	48.0%	52.0%

decrease in erosion risk. However, substantial recovery of the basin is not observed until the unrealistic transition conditions of Scenario 7 are implemented, and even then, the basin condition does not recover fully to 1986 levels.

Of particular interest is exploration of the ability to adjust basin degradation rates by simply reallocating lands to uses based on inherent risk. The results suggest that even while keeping identical landuse proportions, degradation extent can be reduced over 1%. While this result is not exceptionally encouraging, presumably due to the dominance of inherent risk components in the overall risk model, it does suggest some leverage for basin-wide management. Additionally, results suggest that the combined effect of spatial targeting and changes in transition probabilities can improve conditions.

Watershed Scale Agricultural Benefit Ratio

Table 6-14 summarizes mean ABR scores for the basin under landuse and degradation conditions inferred for 1986 and 2001. The table indicates that mean ABR fell from 3.80 to 3.44 over the 15-year period, and is predicted to fall to 3.18 in 2016. Interestingly, while reducing cattle densities reduces degradation rates most, the reforestation alternative (Scenario 3 – provided ground cover is carefully managed) provides the most improved agricultural benefit. When landuse changes are applied in combination (Scenario 6), mean ABR rises to 3.39, which is still lower than in 2001. However, under dramatic changes (Scenario 7), mean basin benefit levels are higher than 1986. Application of spatial targeting without changing overall landuse proportions results in improved mean ABR levels, but offers limited hope that better allocation can substantially improve rural livelihoods and decrease natural capital depletion.

Table 6-14. Two metrics (percent degraded and Agricultural Benefit Ratio) to compare scenarios.

Scenario	% Degraded	Basin Mean ABR
Historic Condition (scenario 8)	29.5%	3.99
1986	37.7%	3.80
2001	48.4%	3.44
2016 Scenario 1	53.1%	3.18
2016 Scenario 2	52.4%	3.23
2016 Scenario 3	51.4%	3.36
2016 Scenario 4	49.9%	3.30
2016 Scenario 5	51.0%	3.26
2016 Scenario 6	49.8%	3.39
2016 Scenario 7	38.9%	3.93
2016 - Spatially Targeted	52.0%	3.26

DISCUSSION

Summary

Soil erosion represents a significant cost of rural and urban development. Substantial evidence suggests that, while largely hidden from contemporaneous land use decision-making, these costs accrue to society in general and rural farmers in particular over time. The problem has been documented worldwide, but the conditions in sub-Saharan Africa of severe disease burden, rural poverty, and explosive population growth make reliance on rapidly depleting natural capital an acutely pressing concern (Sanchez et al. 1999). Soil degradation is compounded by the lagging pace of agricultural intensification (e.g. improved varieties, nutrient subsidies) in sub-Saharan Africa (Bojo 1996). Resulting agricultural extensification has occurred into marginal lands that yield less and are more vulnerable to degradation. This dissertation explored the causes and costs of soil degradation at the regional scale with the intent to assist breaking this cycle.

Effective decision support requires a framework for internalizing costs of natural resource depletion. That erosion is a social cost is widely acknowledged, but precisely how serious a cost remains unknown, with a multitude of proposed means to internalize these costs. The selected protocol for including soil depletion in decision-making was environmental accounting using emergy. Emergy offers one means to put natural capital depletion costs in units common to the whole system for meaningful comparison.

Whole-cost accounting is critical for sustainable decision-making, but in the absence of accurate physical estimates of risk, such analyses are not sufficiently specific to be of local intervention value. A portion of this work involved developing rapid assessment protocols and developing analytical tools to process the data. Considerable emphasis was placed on using reflectance spectra for rapid, non-destructive soil analysis.

Enumeration of potential risk variables allowed development of risk factor models that integrate these variables. Three risk models were developed for each of three aspects of the erosion process (energy dissipation, detachment resistance and transport).

Erosion prevalence assessment and regional erosion control require that patterns of degradation be defined at the landscape scale. Using the Awach River basin as the analysis bounds, these risk models were interpolated to produce maps that form the basis of a spatial model. Concurrently, satellite image processing facilitated spatial inventory of landuse and degradation and parameterized change matrices necessary for forecasting future landuse conditions. These coverages provided the foundation for an assessment framework that links risk and emergy yields to assess a compliment of alternative land management scenarios for intervention effectiveness.

Principal Conclusions of This Study

- Erosion represents a substantial cost of production in Kenya. Erosion costs at the national scale are comparable in magnitude to total agricultural exports. The study region is even more severely impacted by soil loss than the national economy. At the landuse subsystem scale, soil loss ranged from 14 to 76% of total emergy use. Indices of agricultural benefit ranged from 7.4 to 1.3.
- Observational field protocols coupled with spectral analysis of soil samples allows detailed data sets characterizing variability over large areas to be collected rapidly and cheaply. Sample density implications for regional studies are profound.
- Detailed characterization of regional variability obviates the need for generalized models of erosion risk, which were shown to be ineffective for local risk

assessment. Development of locally calibrated multivariate risk factors limits model generality but significantly enhances predictive accuracy. Aggregated risk factors were developed for protective cover, soil erodibility and sediment transport capacity based on direct observations.

- Spatial inventory assessment, calibrated by ground observations and interpolated using satellite imagery, displays high prevalence of soil degradation in the study area; comparison with 1986 imagery indicates high incidence rates. Landuse change trajectories include forest clearing and rapid incidence of badlands.

- An assessment framework that links emergy costs and benefits with land management risk provides evidence that, in the absence of dramatic changes in landuse patterns, degradation incidence will not reverse. However, results suggest that preventative actions may be taken to preempt degradation. This is the proposed strategy for overall management. However, land management strategies that are most likely to reverse advancing degradation include, in order of efficacy, cattle density reduction, reforestation and active restoration of badlands. Targeting landuse allocation based on inherent site risk offers comparable improvement in agricultural benefit and degradation prevalence without changing landuse subsystem proportions.

Discussion of Principal Conclusions

Emergy Costs of Soil Erosion

An important conceptual issue about the valuation of soil and quantification of costs emerged from this work. Soil loss represents costs at several scales. There are clearly long-term costs to farm productivity as the high quality components of topsoil are selectively removed, but there are also costs that accrue off-site. For this dissertation, these latter costs are ignored. There are certainly areas where erosion is considered a benefit (e.g. Nile delta), and documenting whether sediment delivery is a cost or a benefit requires excessively specific data for aggregated analysis. Therefore, only sediment that is lost from the system (i.e. crosses the boundary) is included as a cost. For watersheds, sediment yield ratios provide a means to translate from *in situ* erosion rates to total loss.

The implication of using sediment yield ratios for cross-scale evaluation is important. Specifically, analyses at the farm scale will tend to have higher erosion costs

because no sediment deposition on-site is assumed. In contrast, at the national scale, sediment delivery ratios can range between 0.1 and 10% and even lower for large river systems indicating that a large proportion of on-site costs are hidden at larger scales. Consequently, comparison of index values across scales was done cautiously.

Emergy analyses documented the substantial costs of soil erosion at three scales. In previous emergy evaluations, soil loss was lumped together with other locally depleted natural capital (e.g. minerals, groundwater). There is a strong conceptual difference, however, in that soil is not a traded commodity and not an intended input. This distinction is critical because, in assessing the emergy basis of a regional economic system, soil erosion is usually counted as an input, where it is really an undesirable by-product of production. While it is valid to include erosion costs in loading, investment and yield ratios because it represents a capital stock depletion that may be as necessary as any other intentional input, it is also useful to quantify the extent of these non-market losses separately. The indices Fraction Capital Stock Depletion (FCSD) and Agricultural Benefit Ratio (ABR) were attempts to do this. Each scale of evaluation is discussed below with regard to general aspects of resource base assessment and specific considerations of soil erosion.

National emergy analysis

Several specific insights about the Kenyan national economy were identified. Unsurprisingly, Kenya has low emergy use per capita (3.77E15 vs. a world average of 8.37E15 sej/person). The relatively low fraction of total use that is electricity (3%) suggests that the emergy that is available for each person is not compatible with modern

economic activity. This results in agriculture and other natural-resource based economic sectors (e.g. tourism) representing over 50% of national economic activity.

Kenya maintains an emergy trade deficit: that is, more emergy is exported annually than is imported. The magnitude of this deficit (Exports:Imports = 1.23) is relatively small compared to other developing countries (e.g. Thailand = 2, Ecuador = 5). However, coupled with observations that Kenya is also in fiscal deficit ($2.75E9 paid for imports, $1.98E9 received for exports) and carries a significant international debt (over 60% of GNP – World Bank 2001), the emergy deficit suggests that future development will continue to rely on exported natural capital to generate foreign exchange. Future reliance on dwindling natural capital stocks warrants long-term policy concern.

Among the most important indicators of Kenya's reliance on raw resources (soil, mineral, forest products) are the emergy money and environmental loading ratios. The emergy money ratio of 1.17E13 sej/$ is nearly five times larger than the world value (2.08E12 sej/$), which results in Kenya selling substantially more environmental service per fiscal unit of international trade than it receives. Among other reasons, this explains a relatively low ESI (sustainability) of 0.55 (Ulgiati and Brown 1998). The environmental load is characteristic of developing countries (ELR = 0.8); a large component of that load is, in this case, soil loss. Overall, Kenya continues to rely substantially on renewable energy flows. The aggregated economic diagram (Figure 3-4) summarizes this condition.

Focusing on indices that document the scope of soil degradation within the national context further illustrates the severity of Kenya's reliance on declining natural capital stocks. The FCSD data for the national economy suggest that almost 4% of emergy driving the national economy comes from flows that are not directly tradable and

have substantial long term consequences for on-farm productivity and off-farm water quality. The national ABR value was 7.56. The same index computed for the United States in 1985 (Odum 1996) was 60.38. The Kenyan National FCSD and ABR values provide a benchmark against which evaluations at smaller scales can be assessed, and against which the effect of national policy instruments can be evaluated.

Another means to assess the scope of erosion nationally is to compare the magnitude of these flows to other more familiar aspects of the economy. This is only made physically meaningful because of the common energetic basis of the evaluation. That soil loss (45.5E20 sej/yr) rivals total national electricity consumption (37.2E20 sej/yr) or agricultural exports (49.7E20 sej/yr) strongly reinforces the need for a coherent and well-funded national policy for erosion control.

District emergy analysis

The national evaluation does not show the degree to which summary indices are spatially uneven. The major manufacturing centers (primarily Nairobi and Mombasa) exhibit significantly higher emergy per capita, loading and investment ratios, and lower emergy:money and sustainability ratios. Comparing results for each of the three district-scale evaluations with summary index values for the nation clarifies this point.

The three districts represent a gradient of development status that can be observed nationally. Kisumu, a regionally important manufacturing and trading center, exhibits characteristics of enhanced development (e.g. larger reliance on imported emergy, lower emergy money ratio, substantially higher investment ratio) compared to Kericho and Nyando; also note the substantially higher population density in Kisumu district. Of the three, Nyando district is clearly the least developed, with lower than national levels of all

indices, including emergy per capita, fraction electricity, emergy-to-money ratio and environmental loading ratio. Only Kisumu is consistently higher than the national average in most indices, and only Kisumu (exports:imports = 0.61) is a net importer of emergy. Nyando district (1.27), a sugarcane producer, and Kericho (1.49), a tea and dairy producer, are both major export districts within the national system.

For different reasons, each district exhibits very low sustainability index scores. All three are lower than the national level; Kisumu because it is largely a fossil fuel driven system, and Kericho and Nyando because they are reliant on rapidly depleting natural capital stocks. Similarly, all three have loading ratios much higher than the national average. Kisumu in particular has high empower density and environmental loading. This is confirmed by reports of extremely degraded water quality in Kisumu Bay (Lake Victoria) because of untreated sewage discharge and urban runoff (Crul 1995).

Comparison of indices specific to natural capital depletion illustrates the severity of erosion is this region of the country. Kisumu district is impacted to a similar extent as the nation, with an ABR of 4.37 and an FCSD of 2.4%. While soil loss rates per area are very high, the small size of the district and the degree of external resource subsidy (typical for urban areas) mask these costs. The findings contrast with results from Nyando and Kericho districts. Kericho district exhibits relatively low levels of soil loss due to comparatively large areas of remnant forest, well-drained and stable soils and abundant rainfall, resulting in a high ABR value (11.11) and average FCSD (3.4%). There are, however, substantial natural resource management concerns in this district. Specifically, deforestation of legally protected forest represents 22% of total emergy use.

This has implications for soil loss, but wider implications on biodiversity protection, carbon sequestration and a growing fuelwood crisis in rural western Kenya.

Nyando district also has the lowest ABR (2.25) and highest FCSD (14.2%) due to severe erosion, particularly in lowland regions around the Awach and Nyando rivers. That 15% of total emergy use flows from stocks of natural capital that must be treated as a non-renewable resource explains why the Nyando area has received international attention as a degraded landscape (e.g., Journey to Planet Earth, April 2nd, 2003 on PBS).

Awach landuse subsystems analyses

Emergy evaluation at the scale of the landuse subsystem is effectively an exploration of the magnitude of erosion under each. In general, use of subsidies for production (e.g., fertilizers, pesticides, improved seeds) is limited, so the major components of each evaluation are renewable flows, soil loss and labor. In each case, rainfall represented the primary renewable input. Soil loss rates, estimated from the mixed effects model results presented in Table 4-21, were input for both intact and degraded conditions (yielding data in Table 3-15). This analysis assumes no effect on physical yields from degradation, which would serve to amplify the observed differences in benefit indices between intact and degraded sites.

Table 3-15 provided several indices that document the effect of increased soil degradation. For each product, transformities go up in degraded sites. In this case, transformity is indicative more of inefficiency than of location in the energy hierarchy. Accordingly, the loading ratio increases substantially under degraded conditions, as does, perhaps counter to expectations, the yield ratio. The latter simply reflects the fact,

mentioned before, that treating soil loss as an input (similar to seeds and labor) is confounding.

To address this problem, the ABR and FCSD indices, which at this scale of analysis are precisely inverted, are useful. For intact conditions, farm forests (woodlots) yield the greatest benefit, followed by commercial and subsistence agriculture. Shrublands used for charcoal production and all rangelands, regardless of management scheme, are of limited benefit. The order of landuse desirability changes under degraded conditions. Woodlots were observed to have extremely high soil loss rates when managed or situated in a way that allowed degradation to occur, which is manifest in the dramatic change in ABR between intact and degraded sites (7.41 vs. 1.58, respectively).

Commercial and subsistence agriculture are the best landuse subsystems for agricultural benefit when a site is degraded. This is because soil loss estimates at sites judged spectrally degraded are less dramatically elevated under agricultural use. This may be because of more active infiltration capacity management at these sites or it may arise from the limited number of observations at agricultural sites. Future iterations of surface deflation estimation will concentrate on ensuring sufficient sample size for agricultural sites to avoid this.

Finally, it was expected, and confirmed, that ABR levels for landuse subsystems are higher than for entire districts. This is due to sediment yield considerations for adjusting soil loss costs across scales. Specifically, soil loss for large areas is adjusted so that only material that actually leaves the region is counted. Sediment that is redistributed within the area is not counted as a cost. This is not the case for individual landuse evaluations, where all eroded material is included as a cost.

Field Protocols, Reflectance Spectra and Infiltration Testing

The basis of empirical assessment of erosion risk is the ability to discern risk factors across the range of study area variability in a rapid manner. While the assessment protocol described and implemented for this work required 6 weeks of field time which may be prohibitive for each meso-scale study area, lessons learned during both field sampling and subsequent data analysis suggest that sampling time could be shortened substantially. Foremost amongst these is the conclusion that 420 sample sites is probably more than adequate to describe the 360 square kilometer basin. More samples would only increase statistical power, and, in some analyses (e.g., graphical models), significance criteria more stringent than conventional were necessary to avoid excessively complex models. Sample limitation was only observed for surface deflation analysis because of the physical removal of nails from croplands during tillage and weeding. Furthermore, given a sampling strategy that is cognizant of confounding factors, and with extensive use of satellite image-based interpolation procedures, large areas can be statistically described without excessive density. The limited effectiveness of geostatistical methods in this highly heterogeneous environment simply reinforces the conclusion that the main geographic sample considerations are geology, elevation and population. Several components of a rapid assessment protocol for large areas warrant further discussion and exploration. Each is discussed in brief below.

Field sampling protocol

First, observational sampling protocols maximize statistical power with regard to the main sorting variable (in this case soil degradation). The strategy herein to stratify only informally by other factors (landuse, geology) offered a flexible protocol that

allowed an average of 18 plots to be sampled each day. Informal stratification runs the risk of poor statistical power post-sampling if data are imbalanced with regard to conditioning variables, but this was not a problem in this study. Field protocol efficiency could be significantly improved by collecting only topsoil samples (subsoil samples were collected but never analyzed) and streamlining variable selection to only those variables that exhibit early promise as relevant predictors.

Spectral reflectance methods

Second, spectral methods for rapid soil assessment are an indispensable component of large area characterization. Not only was the analysis of 1200 soils for a suite of standard soil properties made possible, but calibrations to non-conventional properties were also feasible. Binary screening tests for sodium, phosphorus and potassium, screening diagnostics for soil degradation and infiltration class, and direct inference of erodibility were developed using the information rich reflectance data, in addition to continuous regression models for organic carbon, texture and cation parameters. Mean hold-out validation efficiency for 10 soil properties is over 80% with proportional RMSE of less than 8%, which for many standard methods is within the tolerance limits for observation variability. Most of the residual error in the regression models is consistently observed for higher sample values, suggesting that laboratory variability may contribute to model error.

Case/reference definition and degradation odds: Of particular importance were models to discriminate between intact and degraded soils. High model efficiencies, with over 95% of samples correctly classified by the optimal cross-validated tree were observed. This is well within the anticipated range of variability introduced by observer

error and temporal dynamics alone. The latter error is introduced at sites where degradation is just initiating, so the topsoil has not been significantly depleted, but visible cues such as splash pedestals have emerged. On several cleared steep sites where maize was planted for the first (and likely only) time, this was the situation.

The case-reference definition based on spectral reflectance has this distinct advantage of providing early warning indicators of degradation, prior to the onset of visual diagnostic cues. This allows application in monitoring as well as assessment of large areas, with strategic spatial soil sampling offering the potential to engage in whole-basin adaptive management in these remote regions.

The three-category case definition model (Table 4-6) illustrates the power of the spectral screening model to identify severely degraded soils. Over 93% of severe sites were discriminated, even from moderately degraded soils, a result which offers similar monitoring opportunities.

A spectral classification for degradation allowed all soils to be assigned based on the same algorithm. From the degradation status of each soil, binary odds ratios were presented that offer a glimpse at the marginal effects of various cover and landuse descriptors. Several notable conclusions from these figures (Fig. 4-11 and 4-12) include:

- Significant protective effects were observed for commercial agriculture, forest and wetlands. While none of the active landuses appears significantly detrimental, subsistence agriculture has an odds ratio of 1.5, which, while quite weak, indicates an elevated risk of degradation.
- There is a strong protective effect of perennial vegetation and long-term landuse. This may be an effect rather than a cause (only annual vegetation can persist at highly degraded sites, for example).
- Dense groundcover has the strongest protective effect; woody cover has a pairwise effect but is substantially weaker.

- Specific landuses that offer protection are sugarcane and constrained pasture (paddock grazing). Communal pasture has a large, non-significant detrimental effect.

- The effect of woody cover disappears when the odds are conditioned on ground cover. This is particularly true for farm forests. This result suggests that extensive tree planting proposed for the basin to control erosion is of limited utility.

Spectral inference of soil properties: Spectral calibrations of soil properties allowed inference of the effect of degradation on soil quality. Most observations were as expected: soil carbon declined, sand content rose while clay and silt were depleted, and the probability of observing depletions of P or K increased. Strong trends in ANOVA significance were observed along the 5-category degradation gradient. There were few differences observed among intact soils under different landuse types. Only soil organic carbon showed a pattern, with lowest stocks under intact rangeland and highest under forest. This result suggests that selecting sites for specific landuse subsystems is not based on soil quality: landuses start with relatively similar soil functional capacities, but erode that capacity at different rates.

In delineating soil properties for a large number of samples, a benchmark for long-term intervention assessment has been established. After 5 - 10 years, a similar sampling scheme could quantify the efficacy of selected activities. This is particularly true where specific sites are being observed through time.

Spectral analysis for environmental characterization: Spectral reflectance characterization of materials is emerging as a useful tool for environmental analysis. Limiting most ecological or edaphic inventories is sample processing costs; the feasibility of spectral calibrations to predict standard analytical properties, as well as infer more complex composite metrics, should facilitate detailed spatial inventory and analysis.

While the methods herein have been confined to assessments of soil, spectral calibrations to vegetation properties (lignin content, ethylene stress, turgor pressure) have been demonstrated (Foley et al. 1998, Gillon et al. 1999, McClellan et al. 1991).

One component of spectral analysis that is critically important is screening new samples for calibration bound outliers. By compressing the data, using PCA or other ordination tools, and projecting new samples into primary axes ordination space (in this case two axes were sufficient), outlier samples can be identified. These outliers can be analyzed for the suite of target properties and included in the library, ensuring that model generality grows, and spectral predictions never exceed calibration bounds.

Infiltration assessment

One conclusion of this study (shown in the model fit for hydro/terrain risk factors) is that infiltration capacity is a fundamental control of the erosion process (see Figure 4-16 for graphical indication of this). While physical models explicitly account for infiltration mechanisms, often in exceptional detail, most empirical models simply allocate uniform infiltration capacity to all sites in a landscape and assume that rainfall erosivity adequately describes site hydrology. This study indicates that, at least for the local condition in the Awach basin, this is an inadequate assumption.

Assessment of infiltration capacity is most commonly done based on soil type. This has serious limitations that the approach developed herein only partially addresses. Most importantly, different landuse and land management dramatically alters inherent infiltration rates. Figure 4-15 documents this conclusion, illustrating variability in infiltration conditioned only on site characteristics (i.e., lumping all soil types together). Among the indications that human management affects infiltration is the finding that sites

that recently changed landuse have a significantly lower risk of exhibiting slow infiltration than other sites. Cover characteristics also appear to significantly impact infiltration, perhaps because of root facilitation of water inflow, which will vary substantially within soil types. The spatial and categorical resolution of soil maps available for the region (Figure 5-2) is insufficient for characterization at the pixel scale.

The methods developed to process infiltration data are complex, primarily because of sampling logistics. Each test was done for less than one hour, which was often insufficient time to reach saturated infiltration rates. Furthermore, tests were run with a variable hydrologic head (to minimize water hauling). The bounded non-linear parameter fitting routine was generally functional, but for some replicates, particularly those with infiltration rates that approached measurement resolution (approximately 1 mm), the existence of local minima and global minima that violate physical parameter boundaries made model fitting tedious. However, a previous study of infiltration rates in western Kenya (Table 4-14) (Wielemaker and Boxem 1982) reported infiltration rates that correspond extremely well to observations in this study.

Future iterations of infiltration assessment over large areas will incorporate procedural and sampling changes. First, constant-head tests will be used, and infiltration rates will be assessed for a longer period. Second, an effort to quantify spatial variance will be incorporated via a more strategic nested spatial sampling design. While there appears to be substantial spatial autocorrelation, the lack of paired observations at moderate distances (distances are either 10 m or much larger) complicates semi-variogram development.

Surface deflation estimation

Finally, use of surface deflation measurements facilitates physical quantification of erosion while the remainder of this study dealt only with categorical erosion classes. While surface deflation data are characterized by substantial within plot variability, and were unavailable for all landuse types in sufficient quantity, the method proved extremely cost effective. In the absence of deflation data, values for soil loss to inform subsystem emergy evaluations would have been literature derived, and for every landuse, observed values deviated substantially from published rates. For example, subsistence agriculture in Kenya is usually assigned loss rates between 1200 and 1500 $g/m^2/yr$ (Barber 1982). Under intact conditions, the observed value was substantially less (600 $g/m^2/yr$), while rates at degraded sites were much higher (2307 $g/m^2/yr$). Another notable discrepancy between the literature and observations was for woodlot systems. Under intact conditions, loss rates were comparable to literature values (~300 $g/m^2/yr$) (Barber 1983), but if degraded conditions persist, that value jumps to nearly 3000 $g/m^2/yr$, much higher than published values. While high loss rates were expected for severely degraded lands, the observed values (mean 7600 $g/m^2/yr$ and maximum 35,000 $g/m^2/yr$) are alarming. Recall that these are model estimates after accounting for within-plot and within-position variability; localized rates within sites are therefore expected to be even higher.

Erosion Risk Modeling

The physical process of erosion is well understood and has been modeled extensively. Unfortunately, physical process models often require detailed information about soil or hydrologic properties that are difficult to estimate, particularly in regions like western Kenya where thematic spatial data are largely unavailable. Empirical

models of erosion are more flexible, but suffer from a lack of generality, particularly when models developed for temperate-zone field-scale conditions are applied to tropical watersheds. While it would be consistent with much of the current literature to use existing erosion prediction models to delineate risk, evidence interpreted during this study suggests that application of such models has serious limitations. Specifically, GIS-based application of the Universal Soil Loss Equation correctly allocated only 58% of sample sites to binary degradation classes (Cohen et al. submitted 2003). Contrasted with accuracy of over 82% for the empirical model developed herein, this suggests that rapid assessment methods and statistical inference may be more useful, if slower, for effective risk assessment and subsequent management.

While application of USLE to the basin may not be suitable, the conceptual framework of the model proved useful for developing risk models. Erosion was conceptualized as a three-factor process, and for each (protective cover, inherent erodibility and sediment transport) a multivariate risk factor was defined.

The analysis framework adopted is robust to variation in sampling protocol. A compliment of variables observed in the field is allocated as potential predictors from which extrapolative models are derived. It is at this stage that the conceptual overlap between this approach and USLE ends. Where other models assume full statistical interaction, this approach maximizes model parsimony by allowing the model functional form to be flexible. By delineating variables of interest for each factor and deleting those that are conditionally independent (using graphical modeling), simpler models were achieved. Each integrated risk factor exhibited features that warrant further attention.

Site risk factor

The site factor links general landuse information with specific data on protective cover from trees, stones or ground vegetation. The variables selected for the multivariate parameter are generally as expected, but there were some notable omissions, discussed below. Landuse is a strongly significant predictor even after controlling for cover characteristics. Wetlands, forests and cropping systems exhibit the strongest protective effect, while shrublands and pasture appear to be at greater risk.

Inherent landuse risk is modified substantially by site cover characteristics, illustrating the critical importance of within-landuse management practices for mitigating erosion. The most important recommendation for within-landuse management is maintenance of ground cover, which might be maintained via conservation tillage, perennial cropping systems, more effective intercropping schedules or mulching. A single unit increase in ground cover score (ranging from 0 to 6) cuts the odds of degradation in half. Ground and woody cover height are both significant variables, but do not have strong effects. Woody vegetation cover was conditionally independent of degradation risk, reinforcing the pairwise analysis findings of Figure 4-12 that suggest that trees by themselves do little to mitigate soil degradation. Annual vegetation dominance also has a strong impact.

Soil erodibility risk factor

Soil erodibility links soil properties and detachment capacity. The first conclusion is that the USLE nomograph does an exceedingly poor job of describing local erodibility. The result that K computed from the nomograph inversely predicts erosion risk in the Awach basin was cross-checked two ways. The first and most convincing is a

logistic regression relating K to binary degradation. The model is highly significant, with the direction of association implying that as K rises, the risk of degradation falls. A second way was devised to avoid making the prospective analysis assumption (page 63). Mean erodibility scores for intact sites only in each soil polygon were compiled and related to proportional degradation Figure 6-1. That the direction of association is negative (higher polygon mean erodibility implies lower proportional degradation) reinforces the conclusion that a locally calibrated erodibility function is necessary even though the model fit is not exceptional.

Development of such an empirical erodibility function allowed conditional associations between soil properties and degradation to be quantified. The strong inverse association inferred between soil organic carbon and erodibility was expected, as was the direction of association for sand and clay. The binary variable screening sodic content (Na) affected erodibility as expected. However, the direction of association for exchangeable bases and silt was inverse to expectation, and the effect of P and K on erodibility has limited precedence. As exchangeable base saturation rises, erodibility rises, which contradicts the pairwise findings (Table 4-7) that suggest that base saturation decreases with degradation. However, in controlling for clay and organic content, where bases are bound, the shifted effect direction may be due to higher base saturations and 2:1 clay mineralogy in lowland soils (Vertisols, Leptosols). The same explanation can be offered for the inverted effect of silt on erodibility. Silt, sand and clay are substantially correlated (Table 4-10), so while the pairwise effect of silt on degradation is positive, controlling for sand and clay causes the direction of influence to reverse.

The effect of P and K on erodibility is likely to be an effect of inherent fertility on cover. Soils with abundant nutrients will tend to support denser vegetation, which provides physical detachment protection. As such, inclusion of these variables might be considered an artifact. Controlling for cover in future efforts to quantify erodibility may reduce sensitivity to this kind of effect. However, retaining this effect in the absence of additional site information significantly improves predictive accuracy.

Hydro/terrain risk factor

Risk conditioned on hydrologic and terrain variables was overwhelmingly dominated by site infiltration, which in turn is strongly dependent on landuse and management. Strong conditional effects were also observed for soil depth and evidence of flooding, but contrasted with the odds of degradation given slow infiltration (O.R. = 39.5), these are of limited importance. Notably, while infiltration was the core variable, other hydrologic variables were retained. Mean annual rainfall was a significant predictor, but the Fournier Index of erosivity was not. Increased rainfall reduces degradation risk, contrary to conventional application (e.g., Kassam et al. 1991), which suggests a strong link between rainfall and site cover. When this effect is controlled, the expected association direction may be revealed.

Terrain factors were of less importance in this model. Slope is only a marginally significant predictor, slope length and sediment transport index were omitted, and slope shape was of limited importance despite the finding that variable slope shapes increase risk. The clear reason that terrain measures were of limited importance is the prevalence of highly susceptible soils on shallow slopes, and rarely on steep slopes. Furthermore, active landuse systems were generally not found on steep slopes; the limited remnants of

intact forests remaining in the area are found there instead, and these lands are generally intact. As a result, there is a statistical tendency for steep slopes to be intact. Anecdotal observation during field sampling indicates that active landuse, particularly by farmers leasing land, is advancing on steep slopes. As a result, the statistical model form may be changing to include increased risk on steep sloping lands.

Model suitability and generality

A major difference between physical models and the approach taken herein concerns the form of the degradation target variable. Most models predict physical rates of soil loss (either physically or statistically), but the data required to calibrate such models is prohibitively expensive to collect, involving standardized plot experiments that require considerable replication to capture the range of factor variability. For rapid observational assessment over large areas, a more effective target is categorical erosion (e.g. intact/degraded or finer class resolution). This also lends itself more readily to monitoring applications over time.

Centrally, a categorical target simplifies data collection, allowing much more comprehensive data sets to be collected. There are other advantages, however, including making risk (based on probabilities) the focal point of research, invoking use of logistic regression modeling. A further advantage is the demonstrated feasibility of using soil spectral reflectance to characterize condition, obviating the need for extensive runoff sampling and allowing collection of substantially larger, and statistically more powerful data sets.

An alternative to runoff sampling is use of surface deflation estimation. The regression relating overall erosion risk at each plot with observed nail exposure is highly

significant, but reduces observed variance only approximately 40%. For accurate delineation of erosion, this may be insufficient accuracy. However, the entire analysis of surface deflation data illustrates the considerable variability that exists, even within-plot, for physical rates of soil loss. This observed variability reinforces the conclusion that categorical degradation designations are an improvement for large area assessment.

The risk modeling approach adopted has several clear benefits and limitations. The foremost benefit is model accuracy, which is substantially improved using local empirical modeling. Specifically, application of USLE in the region was accurate in 58% of the cells (for binary classes), while the empirical model was 82% accurate. This has implications for effective spatial targeting of interventions, but most importantly for providing reliable predictions of which management actions are likely to provide enhanced protection of the soil resource. It is a significant finding of this work that locally developed calibrations are suitable for assessment.

A clear limitation of highly data driven empirical modeling is that the calibrations are subject to extrapolation concerns. In the absence of physical process modeling, the results of each study will be of questionable general value, even in nearby areas, without some formal validation process that requires further field sampling. For generic assessment, particularly over extremely large areas, this poses logistical constraints. However, carefully designed spatial sampling protocols (e.g. targeting geologic and agroecological zone variability) with appropriate sampling intensity, coupled with satellite image-based interpolation, will allow model development applied within calibration bounds rather than extrapolated without validation.

Spatial Inventory and Risk

Scaling observation from the plot scale to the watershed scale was necessary to begin evaluating and comparing land management scenarios. Satellite image interpretation figured prominently in this process, and proved, given appropriate analytical tools, extremely effective at spatial interpolation of degradation, infiltration, landuse, and erosion risk. Model accuracies were all acceptably high, primarily due to the use of non-linear statistical classification methods that can simultaneously delineate classes comprised of spectrally distinct groups. This is discussed further below.

Spatial inventory

Degradation: Spatial inventory indicates that almost half the watershed exhibits characteristics of soil degradation (46% in 2001). Maps of degradation inferred from satellite imagery illustrate a spatial pattern to degradation prevalence. Specifically, the lowlands (<1400 m) were over 75% degraded. High rates of degradation incidence were also evident, with degradation observed in 36% of the basin in 1986. During that same interval (1986 to 2001), the extent of severely degraded land more than doubled. At nominal erosion rates across landuse types (Table 4-19) this corresponds to an additional 70,000 tons of soil lost from the basin each year, which is equivalent to more than 1% of total annual emergy use in Nyando District. Given extreme soil loss rates from severely degraded lands (the most rapidly expanding class) this estimate is likely to be conservative. Some anecdotal evidence from the region suggests that severe degradation began in earnest in the early 1960's in response to the converging circumstances of a major El Niño (which delivers substantially increased rainfall to the region) and population influx. However, other evidence from Lake Victoria sediment coring studies

suggests that degradation began earlier (M. Walsh and K. Shepherd, ICRAF – personal communication). If it is assumed that, prior to 1960, there was only limited degradation prevalence, the mean incidence rate is 1.2% annually, or 4 sq. km degraded per year.

Infiltration: The map of infiltration classes for 2001 suggests that 33% of the basin infiltrates at less than 60 mm per hour. The majority of slow infiltration sites are in the lowlands, where soils are primarily alluvial and susceptible to surface crusting. It was shown (Table 5-6) that on-site infiltration is the primary hydrologic predictor of degradation. The spatial pattern of slow infiltration rates in the lowlands partially explains degraded site spatial patter, particularly for those classified severely degraded.

Notably, the proportion of pixels classified as slow infiltration did not change between 1986 and 2001. The degree of overlap between 1986 and 2001 is over 86%, suggesting that infiltration responds to land management more slowly than degradation.

It should be noted that, while the classification model selected was accurate, even in cross-validation, there is evidence that selected model partitioning rules overly emphasize static features of the landscape (e.g., slope and elevation) over reflectance characteristics that would change over this period (see Appendix C for model rule-base).

Landuse classification with CART: Landuse classification was done using 8 categories with relatively limited spectral separability. The results indicate strong advantages of this data analysis approach, particularly given the spectral confounding observed between subsistence agriculture and all other landuse classes.

Standard methods for statistical analysis of satellite reflectance data are well established, but they do not perform as well as classification tree models. For some classes (severe degradation, forest, wetlands) maximum likelihood classification accuracy

is comparable, but for others, CART, a non-parametric model wherein assumptions of continuous covariance are relaxed, performs by as much as 30% better.

Figure 7-1 offers a rationale for this dramatic improvement given identical predictor data. Two distinctly different clouds of sample points in feature space (axes of wetness and greenness) comprise a class (subsistence agriculture), with a second sample class (pasture) also shown. Standard linear methods lump the two subsistence agriculture clouds to form a central cloud, which exhibits both expanded variance and reduced spectral separability from the second class.

Threshold-based recursive partitioning can circumvent this problem. The characteristics of the contrived example (Figure 7-1) provide an explanation. CART readily assigns each cloud of subsistence agricultural plots to the same class based on entirely different partitioning criteria. In this case, low wetness plus low greenness and

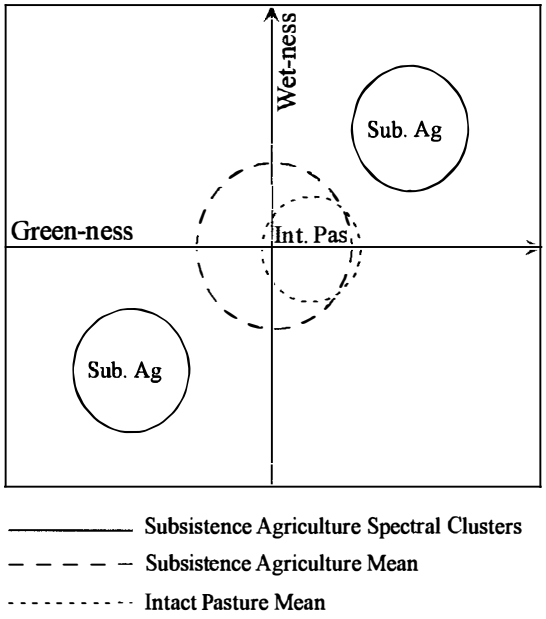

Figure 7-1. Schematic depiction of spectral confounding due to within-category variance as it affects linear discriminatory methods. Circle size reflects variance in class means for two imaginary axes (greenness and wetness).

high wetness plus high greenness would allocate a site to subsistence agriculture, while moderate wetness plus moderate greenness would be reserved for pasture sites. The particular condition of spectrally distinct areas categorized to the same functional class was observed in this study where wetlands and severely degraded lands were both classified to the slow infiltration category. The success of CART (82.5% accuracy) is contrasted with linear discriminant analysis (71.5% accuracy) to illustrate this issue.

Change detection

The change detection results for degradation, infiltration and landuse assume that images from the two periods are directly comparable. While every effort was made to ensure strong statistical association between reflectance from pseudo-invariant ground features in the two scenes, the fact that the 1986 scene is from earlier in the year (February) than 2001 (April) confounds interpretation. However, the expected effect of this seasonal shift is to inflate the extent of degradation in 1986 because unvegetated areas prior to the onset of the rainy season in March/April will appear degraded. Furthermore, the expected trend in NDVI values is to observe an increase in 2001 (see Figure 6-8). Neither effect was observed. This does not suggest that spectral confounding was not present, simply that the direction of that confounding effect would be to make estimates of degradation rates between 1986 and 2001 more conservative.

Rates of landuse change between 1986 and 2001 align with observations of changing degradation patterns. While there is a substantial uncertainty in inferring a landuse change matrix from 15-year intervals, the results suggests a dramatic decrease in forest cover and a concomitant increase in severe degradation and sparse pasture.

Transition probabilities for conditional transformation from one landuse to another were presented; these formed the foundation of landuse scenario development.

Spatial risk maps

Defining risk across the entire basin offers the ability to assess modifications to land management for the region. Interpolating the multivariate risk models (site, soil and hydro/terrain) required a variety of tools, but the results show that the process is readily accomplished given some simplifying assumptions.

Site risk map: The most important assumption for spatial risk assessment is that cover characteristics for a pixel, critical for site risk computation, are assumed inherited from basin-wide nominal values for the landuse in each pixel. The logistic regression risk model contains both landuse effects and within-landuse effects of cover; this assumption creates the condition where there is no variability in cover within landuse type. Clearly, this is not the case. However, since within-landuse cover management is the focus of on-farm interventions, results produced after making this assumption reflect the potential to change basin-wide degradation conditions in the absence of on-farm intervention. Consequently, site risk maps for scenario assessment are almost entirely driven by landuse, with a variety of reclassification tables for delineating cover characteristics from pixel use. The exception is the map of stone cover, inferred spatially from soil depth and degradation maps.

Soil risk map: Using satellite imagery to discern erodibility is a pure statistical relationship. Most of this basin is vegetated, so the inference is contingent on a strong association between erodibility and vegetative cover. The results indicate that there is variance in the regression model, but overall this approach seems tenable even if

conceptually problematic. When existing soil polygons are overlain on the map of erodibility, the loss of accuracy introduced by using soil survey data instead of this approach is clear (Figure 6-13). There is no pattern evident to support existing polygon topology with regard to erodibility. Further, this map illustrates the significant within-polygon variability in erodibility scores that would be lost assigning a single score to each soil type.

Hydro/terrain risk map: Rather than infer this risk factor from satellite imagery as a single function, each of the component variables was interpolated separately then integrated. Since infiltration so dominates this equation, the finding that infiltration class can be effectively inferred from satellite imagery aids model reliability. The other factors were extracted from existing databases (rainfall) or DEM inference (slope, slope shape, soil depth). The necessity of a high quality DEM is clear in this regard, and the DEM developed for this study appears more than adequate.

Inherent risk: Inherent risk is defined as that risk assumed insensitive to landuse decision-making (soil + hydro/terrain). The concept was useful primarily for landuse allocation devised by modifying transition probabilities according to nominal degradation proportions under each landuse. Sites with high inherent risk should be limited to low-risk landuses; the methods and results of spatially specific landuse allocation are discussed later.

Integrated Assessment of Future Landuse

Comparison of future landuse propagated a variety of landuse scenarios through an automated spatial model that linked risk surfaces with emergy-based agricultural

benefit. This model produced maps of soil degradation, and provided a single index, the basin mean agricultural benefit ratio (ABR), that defined optimality.

Optimality for landuse planning is a multi-criteria assessment. The goal is not to maximally reduce erosion, but to maximize system productivity while minimizing costs. The ABR, which divides yield (productivity) by erosion (costs), allows conditions of accelerated erosion to persist as long as local yields are proportionally higher (indicating investment/subsidy from other systems in need of the products). For example, subsistence and commercial agriculture exhibited nearly identical erosion rates (surface deflation) but have somewhat different ABR values, with commercial operations (tea, sugarcane) attracting outside resources more effectively than subsistence cropping systems. This has a net beneficial effect on the basin (more emergy per unit cost), and should be actively solicited.

Landuse change scenarios

There is no end to the array of potential landuse scenarios that can be explored using this assessment framework. The nine scenarios compared in this work were not intended to represent the entire variety of potential modifications, simply a sampling of the major options. Particularly for the spatially targeted scenario, additional testing would be informative. The result in this case is considered more the assessment tool (Figure 6-17) than a comprehensive utilization of that tool. In fact, one extension of this tool is for participatory intervention that solicits land management strategies from stakeholders. The ability to systematically compare various stakeholder designs rapidly may be useful for integrating technical recommendations and participatory intervention.

Markov modeling: The first scenarios were spatially stochastic. Markov chain landuse change models are simple to implement, but have serious conceptual limitations. Most critically, there are no constraints on any given pixel changing to any other. This is particularly problematic for sites that remain under forest cover because they are either too steep or too infertile to support active rural landuses. This problem was also observed for the severe degradation landuse class, which was generally confined to the lowlands, but emerged more uniformly in space after Markov chain predictions.

Spatial targeting: Implementation of spatial targeting to allocate low risk landuses to higher risk areas was somewhat complex. Risk classes were delineated, and for each risk class, a separate table of transition probabilities defined. These values were adjusted so that at higher risk, certain landuses were avoided. However, it is not reasonable to select where wetlands and badlands (severe degradation) persist; they are not managed landuses. Therefore, targeted allocation was developed for only the 6 active landuses. The results indicate that this approach was effective; almost identical proportions of each landuse were observed between the baseline scenario (do nothing) and spatially targeted landuse, but location in the basin varied. There is ample potential to explore these scenarios further, adjusting transition not only based on inherent risk, but also on altered overall management strategies (e.g. enhanced commercial agriculture). These explorations are left for further research.

Farm management practices: The implementation of farm management strategies for erosion control is the most commonly proposed strategy for erosion control. This work illustrates the potential for on-farm management. Specifically, the management sensitive component of risk includes decisions about landuse and measures of cover and

cover height. Given the decision to use the land for subsistence agriculture, the potential to ameliorate risk is limited to ground cover, woody cover, annual-to-perennial ratio and ground cover height. In most subsistence agricultural fields, the crops are annuals, and woody biomass is absent. However, ground cover is a strongly significant predictor of risk: increasing cover from 33% to 66% changes the probability of degradation from 0.61 to 0.45. Similarly, for pasture landuse an increase in cover from 50% to 80% changes the degradation probability from 0.88 to 0.67. Clearly, risk is strongly sensitive to site variables that are averaged for large scale spatial assessment.

Scenario comparison

Results indicate that landscape scale degradation advanced dramatically between 1986 and 2001. Using the historic condition (scenario 8) as a benchmark, the change between the two scenes appears even more profound. While it is likely that estimated background degradation prevalence is inaccurate due to long term effects on risk factors designated herein as immutable, that 1986 is closer to the undeveloped condition than to the 2001 condition illustrates the persistent severity and intensity of the erosion problem.

Future landuse in the absence of intervention (2016 – scenario 1) results in ongoing degradation. By 2016 it is estimated that an additional 5% of the basin will be degraded, with the proportion of severely degraded land increasing nearly 50%.

Efforts to intervene at the landscape scale by altering patterns and proportions of landuse appear relatively ineffective according to model results. None of the adjustments to specific landuse transition probabilities (scenarios 2-5) had functionally significant effects of degradation rates or ABR levels (though each made a statistically significant difference, based on variance estimated for scenario 1 and assumed equal for all

scenarios). There were observable and significant differences between these scenarios, but even the most effective (reducing livestock densities) was not able to maintain degradation prevalence at 2001 levels. Reforestation and active badland restoration, assumed possible for this analysis, were marginally less successful interventions.

The final two scenarios without spatial targeting explore the potential of more comprehensive changes in landuse pattern. The first, a combination of the four landuse-specific scenarios with more modest changes in each, was also relatively ineffectual. Only the deeply unrealistic landuse scenario (#7) had a net protective effect, reducing degradation prevalence and raising ABR values from the 2001 condition, in this case returning the basin to near 1986 levels of both.

Spatial targeting of landuse offers limited indication that large-scale management and control of landuse change can improve basin conditions. Without changing proportions of each landuse subsystem (see Figure 6-20), degradation prevalence is slowed by just over 1% between 2001 and 2016, and the basin mean ABR increases from 3.18 to 3.26. While these changes are statistically different, the effect magnitude is minimal, particularly given the needs of the local subsistence farming population.

Landuse recommendations

Based on the landuse forecasting models, there are three recommendations for more effective land management. The first is to reduce cattle grazing densities in the basin lowlands. Reduced densities, reflected by increased transition probability to dense pasture, was the most effective landuse specific change explored. Second, spatial allocation of higher risk landuse (sparse pasture, logged shrublands) away from areas with high inherent degradation risk had a small but significant effect on landuse

degradation prevalence and indices of net benefit. Finally, a substantial portion of risk management will have to be accomplished by changes in on-farm practices. The potential for mitigating erosion risk via within-landuse management is clear, particularly with respect to ground cover maintenance, and presents the most reasonable short term possibility for attenuating the costs of degradation.

A central conclusion of this work is that degradation assessment is feasible over large areas. However, despite the ability to delineate and project risk to various intervention scenarios, little leverage to provide substantial improvements in land degradation were observed. This suggests, perhaps, that the emphasis of further work should be on prevention in other regions of sub-Saharan Africa wherein degradation is not so alarmingly advanced. These results also indicate that anticipating landuse change, and making plans to accommodate future production needs within the context of resource vulnerability is a critical need for these areas. Specifically, efforts to characterize resource vulnerability prior to development and develop landuse plans at the basin scale that integrate these concerns will greatly attenuate the prevalence of degraded lands and offers the best scenario for meeting the resource needs of growing rural populations.

Suggestions for Further Research

Emergy Simulation Modeling for Yields and Uncertainty

Emergy analysis is synoptic in the sense that tabular assessment of systems is done given singular data values. This has two major disadvantages with respect to the kinds of decision support tools developed in this dissertation. First, synoptic yield assessment does not account for variability in production that results from operating on degraded soils, different climatic regimes or different soil types. Second, still more

variance emerges from smaller-scale differences between sites, which can be treated as random variability. This leads to inherent uncertainty that may affect decision makers.

For example, the spectral methods outlined in this work could be applied in a systematic way to yield trials (either observational or experimental) to develop a formal link between degradation and soil functional performance measures and yield. In this way, the true costs of degradation (i.e., including the loss of yield) could be incorporated.

A solution to both problems was addressed in work associated with this dissertation but omitted from this text. Spreadsheet simulation modeling offers a flexible framework to 1) facilitate emergy evaluation along gradients of forcing functions (e.g., rainfall, soil degradation, and crop variety) and 2) overlay Monte Carlo simulation meta-analysis tools to propagate flow and transformity uncertainty through to final estimates of yields and intensity indices. Further work on specifying uncertainty and incorporating simulation modeling into emergy evaluation will benefit individual analyses as well as offer improved information for integrated assessment.

Constrained Landuse Change Modeling

The landuse change models used in this dissertation are excessively simple. There are clear processes and constraints that guide landuse change, and allocating sites to specific landuse subsystems based on stochastic simulation ignores these process considerations. A more realistic modeling framework is offered by cellular automata (CA), wherein each pixel is allocated to a specific landuse in a manner strongly constrained by process rules and inferred spatial dependence structure in the landscape. For example, slopes constrain allocation to subsistence agriculture, and much of the remnant forest cover in the Awach basin is located on steep escarpment faces. Including

probabilistic constraints on pixel allocation would improve model realism and mapping clarity. Given detailed agroecological zone information available for each crop in Kenya, these process constraints could be included in change scenarios relatively easily.

Tools to Support Participatory Decision Making

The models developed herein represent an effort at scientific inquiry about a problem that has important implications for rural populations in the region. A history of failure of technically sound, but prescribed solutions to problems in developing countries has led the development community to adopt a participatory, bottom-up approach to decision-making and natural resource management. While there is evidence to suggest that this approach has favorable effects on stakeholder involvement (Garrity et al. 1997), considerable debate continues about optimality and efficiency of emergent solutions. The consensus is that technical expertise of participating scientists (top-down information) should be formally incorporated into the participatory strategy in a manner that does not prescribe, but rather informs aspects of the decision making process.

The spatial risk assessment tools outlined in this study might offer a bridge between technical solutions and the need for strong institutions to make solutions persist. In particular, the ability to assess landuse plans emerging from stakeholders dialog within a quantitative framework, and provide feedback in the form of maps and summary indices might successfully integrate knowledge. The more flexibility built into the assessment framework with respect to model assumptions, and therefore the more control a decision-making group has over the model, the more likely synergy between the technical information and stakeholder experience and needs is to occur. This dissertation offers initial steps towards this interactive tool, but substantial refinement is necessary.

APPENDIX A
FOOTNOTES TO EMERGY EVALUATION TABLES

These tables provide reference information for energy, material and transformity values reported for national, district and landuse subsystem emergy evaluations. Given first are energy and material flow notes for each scale of evaluation. Given next are transformity values used throughout this dissertation with sources. Finally, a summary of transformity values computed in this study for important products is given.

Table A-1. Notes to the emergy evaluation of Kenya (Table 3-1).

Notes			Source
1	SOLAR ENERGY		
	Cont Shelf Area =	4.02E+10 m^2	Geological World Atlas (1976)
	Land Area =	5.80E+11 m^2	Europa (1998)
	Insolation =	1.83E+02 Kcal/cm^2/yr	Agroecological Data for Africa (1984)
	Albedo =	22%	Agroecological Data for Africa (1984)
	Energy(J) =	3.70E+21 J/yr	
2	RAIN, CHEMICAL POTENTIAL ENERGY		
	Rain (land) =	0.61 m/yr	Corbett 1993
	Rain (shelf) =	0.31 m/yr	(est. 50% of terrestrial rain)
	Evapotrans. =	0.55 m/yr	National Water Master Plan (1992)
	Energy (land) (J)=	1.56E+18 J/yr	
	Energy (shelf) (J)=	6.06E+16 J/yr	
	Total energy (J) =	1.62E+18 J/yr	
3	RUNOFF, GEOPOTENTIAL ENERGY		
	Rainfall =	0.58 m	
	Avg. Elev =	801.37 m	Corbett 1993
	Runoff rate =	10.60%	National Water Master Plan (1992)
	Energy(J) =	2.78E+17 J/yr	
4	WIND ENERGY		
	Energy(J) =	3.39E+18 J/yr	Chipeta (1976)
5	WAVE ENERGY		
	Coast Length=	8.04E+05 m	Corbett 1993
	Effective length =	4.82E+05 m	60% parallel to wave front
	Wave Energy =	2.20E+04 W/m	Average Wave Height = 1.5 m
	Time =	3.15E+07 s/yr	
	Energy(J) =	3.34E+17 J/yr	
6	TIDAL ENERGY		
	Tide Range =	1.89 m	Tide Tables (1995)
	Density =	1.03E+03 kg/m^3	
	Tides/year =	7.62E+02	
	Energy(J) =	5.49E+17 J/yr	Half tidal energy absorbed at shelf
7	EARTH CYCLE		
	Heat flow =	6.28E+01 mW/^2	Pollack et al. (1991)
	Energy (J) =	1.15E+18 J/yr	
8	HYDROELECTRICITY:		
	Kilowatt Hrs/yr =	3.12E+09 KwH/yr (assume 80% load)	UN Energy Yearbook (1998)
	Energy(J) =	1.12E+16 J/yr	

Table A-1. Continued.

Notes			Source
9	GEOTHERMAL ELECTRIC		
	Kilowatt Hrs/Yr=	6.25E+08 KWh/yr	UN Energy Yearbook (1998)
	Energy (J)=	2.25E+15 J	
10	AGRICULTURAL PRODUCTION		
	Production =	1.21E+07 MT	Europa (1998)
	Energy(J) =	1.62E+17 J/yr	80% caloric
11	LIVESTOCK PRODUCTION		
	Production =	2.84E+06 MT	Europa (1998)
	Energy(J) =	1.31E+16 J/yr	20% protein
12	FISHERIES PRODUCTION		
	Fish Catch =	1.78E+05 MT	Europa (1998)
	Energy(J) =	7.47E+14 J/yr	20% protein
13	FUELWOOD PRODUCTION		
	Fuelwood =	1.90E+07 m^3	Europa (1998)
	Energy(J) =	1.72E+17 J/yr	20% waste cellulose
14	CONSTRUCTION MATERIALS (SAND, BALLAST STONE)		
	Cement Use =	1.13E+06 tonnes	Kenya Statistical Abstract (1999)
	Bitumen Usage =	2.40E+04 tonnes	Kenya Statistical Abstract (1999)
	Aggregate Usage =	Cement use x 3 + Bitumen Usage x 12	Construction Ratios
	Aggregate Usage =	3.69E+12 grams	
15	SODA ASH & CRUSHED SODA		
	Consumption =	5.81E+11 g/yr	Kenya Bureau of Mines (1999)
16	MISC. MINING (Fluorspar, Salt, Limestone)		
	Consumption =	1.72E+11 g/yr	Kenya Bureau of Mines (1999)
17	GOLD		
	Consumption =	9.90E+05 g	Kenya Bureau of Mines (1999)
18	PRECIOUS/SEMI-PRECIOUS GEMS		
	Consumption =	4.30E+07 g/yr	Kenya Bureau of Mines (1999)
19	FOREST CLEARING		
	Clearing Rate =	1.70% per year	Kaufman et al. (1997)
	Forest Area =	5.43E+09 m^2	FAO Estimate (1994)
	Biomass =	5.00E+01 kg/m^2	
	Energy =	6.18E+16 J/yr	

Table A-1. Continued

Notes				Source
20	TOPSOIL			
	Soil loss =	2.67E+13 g/yr		After Barber (1982)
	Energy(J) =	1.81E+16 J/yr		
21	OIL DERIVED PRODUCTS			
	Imports =	1.96E+06 MT	Crude Petroleum	Kenya Statistical Abstract (1999)
	=	1.39E+06MT	Refined Petroleum	Kenya Statistical Abstract (1999)
	=	2.40E+04 MT	Petroleum Products	Kenya Statistical Abstract (1999)
	Energy (J) =	8.20E+16 J/yr	Crude Petroleum	
	=	5.80E+16 J/yr	Refined Petroleum	
	=	1.00E+15 J/yr	Petroleum Products	
22	METALS			
	Imports =	3.94E+05 MT/yr	Ferrous Metals	UN (1997)
	=	2.50E+04 MT/yr	Non-Ferrous Metals	UN (1997)
	=	1.39E+04 MT/yr	Structures and Tools	UN (1997)
	Mass (g) =	3.94E+11 g/yr	Ferrous Metals	
	=	2.50E+10 g/yr	Non-Ferrous Metals	
	=	1.39E+10 g/yr	Structures and Tools	
23	MINERALS			
	Imports =	3.94E+04 MT/yr	Cement	UN (1997)
	=	1.68E+04 MT/yr	Clay	UN (1997)
	=	1.24E+04 MT/yr	Glass	UN (1997)
	Mass (g) =	3.94E+10 g/yr	Cement	
	=	1.68E+10 g/yr	Clay	
	=	1.24E+10 g/yr	Glass	
24	FOOD and AGRICULTURAL PRODUCTS			
	Imports =	1.27E+06 MT/yr		Kenya Statistical Abstract (1999)
	Energy (J) =	1.48E+16 J/yr		
25	LIVESTOCK, MEAT, FISH			
	Imports =	2.77E+04 MT/yr		Kenya Statistical Abstract (1999)
	Energy (J) =	1.27E+14 J/yr		
26	PLASTICS & RUBBER			
	Imports =	1.19E+05 MT/yr	Rubber	UN (1997)
	=	1.45E+05 MT/yr	Plastics	
	Energy(J) =	1.19E+11 g/yr	Rubber	
	=	1.45E+11 g/yr	Plastics	
27	CHEMICALS			
	Imports =	1.44E+05 MT/yr	Chemicals & Dyes	UN (1997)
	=	3.87E+05 MT/yr	Fertilizers	

Table A-1. Continued

Notes				Source
	Mass (g) =	1.44E+11 g/yr	Chemicals & Dyes	
	=	3.87E+11 g/yr	Fertilizers	
28	WOOD, PAPER, TEXTILES,LEATHER			
	Imports =	2.17E+04 MT/yr	Wood	Kenya Statistical Abstract (1999)
	=	6.53E+04 MT/yr	Paper	
	=	2.58E+04 MT/yr	Textiles	
	Energy(J) =	3.25E+14 J/yr	Wood	
	=	9.79E+14 J/yr	Paper	
	=	3.87E+14 J/yr	Textiles	
29	MACHINERY, TRANSPORTATION, EQUIPMENT			
	Imports = Mass (g)	4.45E+04 MT/yr		UN (1997)
	=	4.45E+10 g/yr		
30	IMPORTED SERVICES			
	Dollar Value =	2.75E+09 $US		UN (1997)
31	FOOD and AGRICULTURAL PRODUCTS			
	Exports:	9.84E+05 MT/yr		Kenya Statistical Abstract (1999)
	Energy(J) =	1.32E+16 J/yr		
32	LIVESTOCK, MEAT, FISH			
	Exports =	1.01E+05 MT/yr		Kenya Statistical Abstract (1999)
	Energy (J) =	4.66E+14 J/yr		
33	WOOD, PAPER, TEXTILES, LEATHER			
	Exports =	3.44E+05 MT/yr	Wood	Kenya Statistical Abstract (1999)
		3.33E+04 MT/yr	Paper	
		2.13E+04 MT/yr	Textiles	
		5.41E+03 MT/yr	Leather	
	Energy (J) =	4.15E+15 J/yr	Wood	
		4.01E+14 J/yr	Paper	
		2.57E+14 J/yr	Textiles	
		6.53E+13 J/yr	Leather	
34	OIL DERIVED PRODUCTS			
	Exports =	1.97E+06 MT/yr		UN (1997)
	Energy (J) =	1.20E+16 J/yr		
35	METALS			
	Exports =	1.67E+05 MT/yr	Ferrous Metals	UN (1997)
		2.57E+03 MT/yr	Non-Ferrous Metals	
		1.14E+04 MT/yr	Stuctures and Tools	
	Mass (g) =	1.67E+11 g/yr	Ferrous Metals	
		2.57E+09 g/yr	Non-Ferrous Metals	
		1.14E+10 g/yr	Stuctures and Tools	

Table A-1. Continued

Notes				Source
36	MINERALS			
	Exports =	6.90E+05 MT/yr	Cement	Kenya Bureau Mines (1999)
		2.59E+04 MT/yr	Glass	
		4.40E+04 kg/yr	Gold and Gems	
	Mass (g) =	6.90E+11 g/yr	Cement	
		2.59E+10 g/yr	Glass	
		4.40E+07 g/yr	Gold and Gems	
37	CHEMICALS			
	Exports =	7.90E+04 MT/yr		UN (1997)
	Mass (g) =	7.90E+10 g/yr		
38	MACHINERY, TRANSPORTATION, EQUIPMENT			
	Exports =	1.48E+03 MT/yr		UN (1997)
	Mass (g) =	1.48E+09 g/yr		
39	PLASTICS & RUBBER			
	Exports =	4.78E+04 MT/yr	Plastics	UN (1997)
		5.26E+03 MT/yr	Rubber	
	Energy(J) =	4.78E+10 J/yr	Plastics	
		5.26E+09 J/yr	Rubber	
40	SERVICES IN EXPORTS			
	Dollar Value =	2.88E+09 $US		UN (1997)
41	TOURISM			
	Dollar Value =	4.74E+08 $US		Europa (1998)

Table A-2. Emergy Evaluation of Resource Basis for Kisumu District, Kenya (c.2000)

Note	Item	Raw Units	Transformity (sej/unit)	Solar Emergy (E19sej)	EmDollars (E7 1994 US$)
RENEWABLE RESOURCES					
1	Sunlight	5.69E+18 J	1	0.57	0.57
2	Rain, chemical	6.19E+15 J	31000	19.20	19.17
3	Rain, geopotential	3.14E+14 J	47000	1.48	1.47
4	Wind, kinetic energy	2.43E+15 J	2450	0.59	0.59
5	Waves	4.05E+14 J	51000	2.06	2.06
6	Earth Cycle	1.19E+15 J	58000	6.93	6.92
INDIGENOUS RENEWABLE ENERGY					
7	Agriculture Production	5.18E+15 J	see Table B1	10.25	10.23
8	Livestock Products	2.93E+13 J	see Table B1	10.03	10.02
9	Fisheries Production	1.26E+13 J	5.04E+06	6.35	6.34
10	Fuelwood Production	6.69E+14 J	5.86E+04	3.92	3.91
NONRENEWABLE SOURCES FROM WITHIN SYSTEM					
11	Forest Extraction	1.19E+14 J	6.72E+04	0.80	0.80
12	Aggregates and Sand	2.00E+11 g	1.68E+09	3.36	3.35
13	Top Soil	2.01E+14 J	2.35E+05	4.73	4.73
IMPORTS AND OUTSIDE SOURCES					
14	Oil derived products	2.58E+15 J	1.06E+05	27.34	27.29
15	Electric Power	4.02E+14 J	2.69E+05	10.80	10.78
16	Metals	1.30E+10 g	2.99E+09	3.89	3.88
17	Wood and Charcoal	5.84E+15 J	5.86E+04	34.24	34.19
18	Food & ag. products	2.68E+14 J	1.80E+05	4.82	4.82
19	Meat and Milk	3.22E+13 J	3.40E+06	10.96	10.94
20	Fish for Processing	1.93E+13 J	5.04E+06	9.75	9.73
21	Plastics & rubber	8.52E+13 J	3.61E+05	3.08	3.07
22	Textiles & Paper	8.99E+13 J	6.38E+05	5.73	5.72
23	Chemicals	3.45E+09 g	6.38E+08	0.22	0.22
24	Mech.& trans equip.	7.43E+09 g	1.13E+10	8.36	8.35
25	Service in imports	6.21E+07 $	1.26E+13	78.25	78.12
EXPORTS					
26	Food & ag. products	3.75E+13 J	2.00E+05	0.75	0.75
27	Processed Fish	1.61E+13 J	8.47E+06	13.65	13.63
28	Other Processed Foods	9.51E+14 J	3.36E+05	31.97	31.92
29	Furniture	4.20E+10 g	9.30E+08	3.91	3.90
30	Mech. & trans equip.	4.50E+09 g	1.13E+10	5.09	5.08
31	Plastics & rubber	4.56E+13 J	3.61E+05	1.65	1.64
32	Service in exports	6.03E+07 $	1.00E+13	60.39	60.30
33	Tourism	2.20E+06 $	1.00E+13	2.20	2.20

Table A-2. Continued - footnotes to emergy analysis

Note			Source
RENEWABLE RESOURCES			
1 SOLAR ENERGY			
	Lake Area =	5.02E+08 m^2 at 200 m depth.	Kisumu District Dev. Plan (1997)
	Land Area =	6.60E+08 m^2	Kisumu District Dev. Plan (1997)
	Insolation =	1.50E+02 Kcal/cm^2/yr	Agroecological Data for Africa (1984)
	Albedo =	22%	Agroecological Data for Africa (1984)
	Energy(J) =	5.69E+18 J/yr	
2 RAIN, CHEMICAL POTENTIAL ENERGY			
	Rain (land) =	1.36 m/yr	Corbett (1993)
	Rain (lake) =	1.20 m/yr	Corbett (1993)
	Evapotranspiration =	0.99 m/yr	Corbett (1993)
	Energy (land) (J)=	3.22E+15 J/yr	
	Energy (shelf) (J)=	2.98E+15 J/yr	
	Total energy (J) =	6.19E+15 J/yr	
3 RAIN, GEOPOTENTIAL ENERGY			
	Avg. Elev =	1265.00 m	Corbett (1993)
	Runoff rate =	27%	
	Energy(J) =	3.14E+14 J/yr	
4 WIND ENERGY			
	Energy(J) =	2.43E+15 J/yr	Chipeta (1976)
5 WAVE ENERGY			
	Coast Length =	9.87E+04 m	Corbett 1993
	Parallel Comp. =	5.92E+04 m	Assume 60% parallel to wave front
	Front Wave Energy =	2.17E+02 W/m	Average Wave Height = 0.2 m
	Energy(J) =	4.05E+14 J/yr	
7 EARTH CYCLE			
	Heat flow =	1.81E+06 J/m^2	Global Avg Heat Flow (Wylie 1971)
	Energy (J) =	1.19E+15	
INDIGENOUS RENEWABLE ENERGY			
8 AGRICULTURAL PRODUCTION			
	Production =	3.30E+05 MT	District Development Plan (1997)
	Energy(J) =	5.18E+15 J/yr	
9 LIVESTOCK PRODUCTION			
	L'stock Production =	7.00E+03 MT	District Development Plan (1997)
	Energy(J) =	2.93E+13 J/yr	
10 FISHERIES PRODUCTION			
	Fish Catch =	1.51E+03 MT	Ministry of Fisheries (2001)
	Energy(J) =	1.26E+13 J/yr	
11 FUELWOOD PRODUCTION			
	Fuelwood Prod =	1.11E+05 m^3	District Development Plan (1997)
	Energy(J) =	6.69E+14 J/yr	
NONRENEWABLE RESOURCE USE FROM WITHIN KISUMU DISTRICT			
12 FOREST EXTRACTION			
	Harvest =	1.32E+05 m^2	UNEP (1996)
	Energy(J) =	1.19E+14 J/yr	

Table A-2. Continued

Note			Source
13 AGGREGATES AND SAND			
	Production =	2.00E+07 MT/yr	Estimated
	Mass(g) =	2.00E+11 g/yr	
14 TOPSOIL			
	Soil loss =	2.97E+11 g/yr	Barber (1982)
	Energy(J) =	2.01E+14 J/yr	
IMPORTS OF OUTSIDE ENERGY SOURCES			
15 OIL DERIVED PRODUCTS			
	Imports =	6.17E+04 MT	Kenya Pipeline Authority (2001)
	Energy (J) =	2.58E+15 J/yr	
16 ELECTRICITY			
	Kilowatt Hrs/yr =	1.12E+08 kwh	Kenya Power Corporation (2001)
	Energy(J) =	4.02E+14 J/yr	
17 METALS			
	Imports =	1.30E+04 MT/yr	Central Bureau of Statistics (2001)
	Mass (g) =	1.30E+10 g/yyr	
18 WOOD AND CHARCOAL			
	Imports =	3.87E+05 Tons	UNEP Projection (1994)
	Energy (J) =	5.84E+15 J/yr	
19 FOOD and AGRICULTURAL PRODUCTS			
	Imports =	2.29E+04 MT/yr	Central Bureau of Statistics (2001)
	Energy (J) =	2.68E+14 J/yr	
20 MEAT AND MILK			
	Imports =	7.00E+03 MT/yr	Central Bureau of Statistics (2001)
	Energy (J) =	3.22E+13 J/yr	
21 FISH FOR FACTORY PROCESSING			
	Imports =	4.20E+03 MT/yr	Ministry of Fisheries (2001)
	Energy (J) =	1.93E+13 J/yr	
22 PLASTICS & RUBBER			
	Imports =	2.84E+03 MT/yr	Central Bureau of Statistics (2001)
	Energy(J) =	8.52E+13 J	
23 TEXTILES AND PAPER			
	Imports =	3.00E+03 MT/yr	Central Bureau of Statistics (2001)
	Energy(J) =	8.99E+13	
24 CHEMICALS			
	Imports =	3.45E+03 MT/yr	Central Bureau of Statistics (2001)
	Mass (g) =	3.45E+09 g/yr	
25 MACHINERY, TRANSPORTATION, EQUIPMENT			
	Imports =	7.43E+03 MT/yr	Central Bureau of Statistics (2001)
	Mass (g) =	7.43E+09 g/yr	
26 IMPORTED SERVICES			
	Dollar Value =	6.21E+07 $US	Central Bureau of Statistics (2001)

Table A-2. Continued

Note			Source
EXPORTS OF ENERGY, MATERIALS AND SERVICES			
31 AGRICULTURAL PRODUCTS			
	Exports:	3.20E+03 MT/yr	Central Bureau of Statistics (2001)
	Energy(J) =	3.75E+13 J/yr	
32 PROCESSED FISH			
	Exports =	3.50E+03 MT/yr	Ministry of Fisheries (2001)
	Energy (J) =	1.61E+13 J/yr	
33 PROCESSED FOODS			
	Exports =	7.89E+04 MT/yr	Ministry of Trade (2001)
	Energy (J) =	9.51E+14 J/yr	
34 FURNITURE			
	Exports =	4.20E+04 MT/yr	Ministry of Trade (2001)
	Energy (J) =	4.20E+10 g/yr	
35 METALS			
	Exports =	2.01E+04 MT/yr	(UN, 1997)
	Mass (g) =	2.01E+10 g/yr	
36 MINERALS			
	Exports =	3.75E+04 MT/yr	(UN, 1997)
	Mass (g) =	3.75E+10 g/yr	
37 CHEMICALS			
	Exports =	2.09E+05 MT/yr	(UN, 1997)
	Mass (g) =	2.09E+11 g/yr	
38 MACHINERY, TRANSPORTATION, EQUIPMENT			
	Exports =	4.50E+03 MT/yr	(UN, 1997)
	Mass (g) =	4.50E+09 g/yr	
39 PLASTICS & RUBBER			
	Exports =	1.52E+03 MT/yr	Ministry of Trade (2001)
	Energy(J) =	4.56E+13	
40 SERVICES IN EXPORTS			
	Dollar Value =	2.33E+08 $US	(UN, 1997)
30 TOURISM			
	Dollar Value =	2.20E+06 $US	District Development Plan (1997) Estimate

Table A-3. Emergy evaluation of resource basis for Kericho District, Kenya (c.2000)

Note	Item	Raw Units	Transformity (sej/unit)	Solar Emergy (E19 sej)	EmDollars (E6 US$)
RENEWABLE RESOURCES					
1	Sunlight	1.23E+19 J	1	1.23	1.03
2	Rain, chemical	1.43E+16 J	31000	44.20	37.05
3	Rain, geopotential	3.67E+15 J	47000	17.25	14.46
4	Wind, kinetic energy	1.34E+16 J	2450	3.29	2.75
5	Earth Cycle	4.55E+15 J	58000	26.40	22.13
INDIGENOUS RENEWABLE ENERGY					
6	Agriculture Production	1.14E+16 J	see Table B1	39.58	33.18
7	Livestock Production	1.41E+14 J	see Table B1	33.39	27.99
8	Fuelwood Production	4.19E+15 J	3.09E+04	12.92	10.83
NONRENEWABLE SOURCES FROM WITHIN SYSTEM					
9	Forest Extraction	6.65E+15 J	6.72E+04	44.66	37.43
10	Sand, Gravel and Ballast	5.90E+10 g	1.61E+09	9.50	7.96
11	Top Soil	2.79E+14 J	2.35E+05	6.57	5.50
IMPORTS AND OUTSIDE SOURCES					
12	Oil derived products	1.54E+15 J	1.06E+05	16.29	13.66
13	Electricity	3.47E+14 J	2.69E+05	9.32	7.82
14	Metals	8.97E+09 g	2.99E+09	2.68	2.25
15	Minerals	3.95E+09 g	1.61E+09	0.64	0.53
16	Food & ag. products	1.35E+14 J	1.80E+05	2.43	2.04
17	Livestock, meat, fish	5.76E+12 J	3.40E+06	1.96	1.64
18	Plastics & rubber	1.09E+14 J	6.60E+04	0.72	0.60
19	Chemicals	3.50E+10 g	6.38E+08	2.23	1.87
20	Wood, paper,textiles	5.33E+13 J	6.38E+05	3.40	2.85
21	Mech.& trans equip.	4.29E+09 g	1.13E+10	4.85	4.06
22	Service in imports	2.77E+07 $	1.26E+13	34.90	29.26
EXPORTS					
23	Tea	5.58E+14 J	5.76E+05	32.12	26.92
24	Milk & Meat	2.07E+13 J	3.40E+06	7.05	5.91
25	Wood and Charcoal	2.67E+15 J	5.86E+04	15.65	13.12
26	Raw Ag. Goods	1.12E+14 J	1.80E+05	2.02	1.70
27	Processed Ag. Goods	3.70E+14 J	3.36E+05	12.44	10.43
28	Service in exports	2.23E+07 $	1.19E+13	26.60	22.30
29	Tourism	4.50E+06 $	1.19E+13	5.37	4.50

Table A-3. Continued (table footnotes)

Note			Source
RENEWABLE RESOURCES			
1 SOLAR ENERGY			
	Lake Area =	0.00E+00 m^2	Kericho District Dev. Plan (1997)
	Land Area =	2.52E+09 m^2	Kericho District Dev. Plan (1997)
	Insolation =	1.50E+02 Kcal/cm^2/yr	Agroecological Data for Africa (1984)
	Albedo =	0.22	Agroecological Data for Africa (1984)
	Energy(J) =	1.23E+19 J/yr	
2 RAIN, CHEMICAL POTENTIAL ENERGY			
	Rain (land) =	1.43 m/yr	Corbett (1993)
	Evapotranspiration =	1.15 m/yr	Corbett (1993)
	Total energy (J) =	1.43E+16 J/yr	
3 RAIN, GEOPOTENTIAL ENERGY			
	Rainfall =	1.43 m	
	Avg. Elev =	1901.00 m	Corbett (1993)
	Runoff rate =	20%	
	Energy(J) =	3.67E+15 J/yr	
4 WIND ENERGY			
	Energy(J) =	1.34E+16 J/yr	Chipeta (1976)
5 EARTH CYCLE			
	Land Area =	2.52E+09 m^2	
	Heat flow =	1.81E+06 J/m^2	Pollack et al. (1991)
	Energy (J) =	4.55E+15	
INDIGENOUS RENEWABLE ENERGY			
6 AGRICULTURAL PRODUCTION			
	Energy(J) =	1.14E+16 J/yr	MoARD (1999)
7 LIVESTOCK PRODUCTION			
	Energy =	1.41E+14 J/yr	MoARD (1999)
8 FUELWOOD PRODUCTION			
	Fuelwood Prod =	28937 ha	MoARD (1999)
	Energy(J) =	4.19E+15	
NONRENEWABLE RESOURCE USE			
9 FOREST EXTRACTION			
	Harvest and Clearing =	1.30% annually	District Development Plan (2001)
	Area Cleared and Harvested =	689 Ha	District Development Plan (2001)
	Biomass =	80 kg/m^2	estimate
	Energy(J) =	6.65E+15 J/yr	
10 SAND, GRAVEL & BALLAST			
	Consumption =	5.90E+04 MT/yr	District Development Plan (2001)
	Mass(g) =	5.90E+10 g/yr	
11 TOPSOIL:			
	Soil loss =	4.12E+11 g/yr	Barber (1982) & MoARD (1999)
	Energy(J) =	2.79E+14 J/yr	

Table A-3. Continued

Note			Source
IMPORTS OF OUTSIDE ENERGY SOURCES			
12 OIL DERIVED PRODUCTS			
	Imports =	6.80E+07 Lts	Kenya Pipeline Authority (2001)
	Energy (J) =	1.54E+15 J/yr	
13 ELECTRICITY			
	Kilowatt Hrs/yr =	9.64E+07 kwh	Kenya Power Corporation (2001)
	Energy(J) =	3.47E+14 J/yr	
14 METALS			
	Imports =	8.97E+03 MT/yr	CBS Kenya (2001)
	Mass (g) =	8.97E+09 g/yyr	
15 MINERALS			
	Imports =	3.95E+03 MT/yr	CBS Kenya (2001)
	Mass (g) =	3.95E+09 g/yr	
16 FOOD and AGRICULTURAL PRODUCTS			
	Imports =	1.15E+04 MT/yr	CBS Kenya (2001)
	Energy (J) =	1.35E+14 J/yr	
17 LIVESTOCK, MEAT, FISH			
	Imports =	1.25E+03 MT/yr	CBS Kenya (2001)
	Energy (J) =	5.76E+12 J/yr	
18 PLASTICS & RUBBER			
	Imports =	3.64E+03 MT/yr	CBS Kenya (2001)
	Energy(J) =	1.09E+14 J/yr	
19 CHEMICALS			
	Imports =	3.50E+04 MT/yr	CBS Kenya (2001)
	Mass (g) =	3.50E+10 g/yr	
20 WOOD, PAPER, TEXTILES, LEATHER			
	Imports =	3.55E+03 MT/yr	CBS Kenya (2001)
	Energy(J) =	5.33E+13 J/yr	
21 MACHINERY, TRANSPORTATION, EQUIPMENT			
	Imports =	4.29E+03 MT/yr	CBS Kenya (2001)
	Mass (g) =	4.29E+09 g/yr	
22 IMPORTED SERVICES			
	Dollar Value =	2.77E+07 $US	CBS Kenya (2001)
EXPORTS OF ENERGY, MATERIALS AND SERVICES			
23 TEA			
	Exports:	2.47E+04 MT/yr	Kenya Tea Dvlp. Authority (2000)
	Energy(J) =	5.58E+14 J/yr	
24 MILK, MEAT			
	Exports =	4.50E+03 MT/yr	Ministry of Agriculture (2001)
	Energy (J) =	2.07E+13 J/yr	
25 WOOD AND CHARCOAL			
	Exports =	1.45E+05 MT/yr	UNEP (1996)
	Energy (J) =	2.67E+15 J/yr	

Table A-3. Continued

Note		Source
26 RAW AGRICULTURAL GOODS		
Exports =	6.10E+03 MT/yr	Kenya Cereal and Produce Board (2000)
Energy (J) =	1.12E+14 J/yr	
27 PROCESSED AGRICULTURAL GOODS		
Exports =	2.01E+04 MT/yr	Kenya Cereal and Produce Board (2000)
Mass (g) =	3.70E+14 g/yr	
28 SERVICES IN EXPORTS		
Dollar Value =	2.23E+07 $US	District Development Plan (2001)
29 TOURISM		
Dollar Value =	4.50E+06 $US	

Table A-4. Emergy evaluation of resource basis for Nyando District, Kenya (c.2000)

Note	Item	Raw Units	Transformity (sej/unit)	Solar Emergy (E19 sej)	EmDollars (E6 1999 US$)
RENEWABLE RESOURCES					
1	Sunlight	7.34E+18 J	1	0.73	0.28
2	Rain, chemical	6.90E+15 J	31000	21.38	8.16
3	Rain, geopotential	1.28E+15 J	47000	6.01	2.29
4	Wind, kinetic energy	5.27E+15 J	2450	1.29	0.49
5	Waves	3.28E+13 J	51000	0.17	0.06
6	Earth Cycle	2.59E+15 J	58000	15.04	5.74
INDIGENOUS RENEWABLE ENERGY					
7	Agriculture Production	8.46E+15 J	see Table B1	11.24	4.29
8	Livestock Products	4.06E+14 J	see Table B1	7.84	2.99
9	Fisheries Production	1.13E+12 J	5.04E+06	0.57	0.22
10	Fuelwood Production	1.46E+15 J	5.86E+04	8.53	3.26
NONRENEWABLE SOURCES FROM WITHIN SYSTEM					
11	Forest Extraction	9.49E+14 J	6.72E+04	6.38	2.44
12	Ballast Rocks	3.37E+09 g	1.61E+09	0.54	0.21
13	Sand Mining	1.83E+10 g	1.61E+09	2.94	1.12
14	Top Soil	5.22E+14 J	2.35E+05	12.27	4.68
IMPORTS AND OUTSIDE SOURCES					
15	Oil derived products	3.73E+14 J	1.06E+05	3.95	1.51
16	Electric Power	7.13E+13 J	2.69E+05	1.92	0.73
17	Metals	1.63E+09 g	2.99E+09	0.49	0.19
18	Wood and Charcoal	9.64E+14 J	5.86E+04	5.65	2.16
19	Food & ag. products	1.03E+14 J	1.80E+05	1.85	0.71
20	Milk and Meat	1.84E+13 J	3.40E+06	6.26	2.39
21	Plastics & rubber	1.34E+13 J	6.60E+04	0.09	0.03
22	Chemicals	3.24E+09 g	6.38E+08	0.21	0.08
23	Textiles, Paper	6.38E+12 J	6.38E+05	0.41	0.16
24	Mechanical Equip.	1.17E+09 g	1.13E+10	1.32	0.50
25	Service in imports	6.13E+06 $	1.28E+13	7.85	2.99
EXPORTS					
26	Sugar (processed)	1.83E+15 J	5.56E+04	10.17	3.88
27	Crops and Livestock	2.72E+13 J	5.00E+05	1.36	0.52
28	Aggregates and Sand	1.56E+10 g	1.61E+09	2.51	0.96
29	Agrochemicals	1.12E+09 g	3.36E+10	3.76	1.44
30	Service in exports	6.30E+06 $	2.62E+13	16.51	6.30

Table A-4. Continued

Note			Source
1 SOLAR ENERGY			
	Lake Area =	6.50E+07 m^2	Kisumu District Dev. Plan (1997)
	Land Area =	1.43E+09 m^2	Kisumu District Dev. Plan (1997)
	Insolation =	1.50E+02 Kcal/cm^2/yr	Agroecological Data for Africa (1984)
	Albedo =	0.22	Agroecological Data for Africa (1984)
	Energy(J) =	7.34E+18 J/yr	
2 RAIN, CHEMICAL POTENTIAL ENERGY			
	Rain (land) =	1.31 m/yr	Corbett (1993)
	Rain (lake) =	1.20 m/yr	Corbett (1993)
	Evapotranspiration =	0.92 m/yr	Corbett (1993)
	Energy (land) (J)=	6.51E+15 J/yr	
	Energy (shelf) (J)=	3.85E+14 J/yr	
	Total energy (J) =	6.90E+15 J/yr	
3 RAIN, GEOPOTENTIAL ENERGY			
	Avg. Elev =	1365.00 m	Corbett (1993)
	Runoff rate =	30%	
	Energy(J) =	1.28E+15 J/yr	
4 WIND ENERGY			
	Energy(J) =	5.27E+15 J/yr	Chipeta (1976)
5 WAVE ENERGY			
	Coast Length (incl. Islands) =	8.00E+03 m	Corbett 1993
	Parallel Comp. =	4.80E+03 m	assumed
	Front Wave Energy =	2.17E+02 W/m	Avg. Wave Height = 0.2 m
	Energy(J) =	3.28E+13 J/yr	
6 EARTH CYCLE			
	Land Area =	1.43E+09 m^2	
	Heat flow =	1.81E+06 J/m^2	Pollack et al. (1991)
	Energy (J) =	2.59E+15	
INDIGENOUS RENEWABLE ENERGY			
7 AGRICULTURAL PRODUCTION			
	Production =	5.95E+05 MT	Ministry of Agriculture (2000)
	Energy(J) =	8.46E+15 J/yr	
8 LIVESTOCK PRODUCTION			
	L'stock Production =	9.70E+04 MT	Ministry of Agriculture (2000)
	Energy(J) =	4.06E+14 J/yr	
9 FISHERIES PRODUCTION:			
	Fish Catch =	1.35E+02 MT	Ministry of Fisheries (2000)
	Energy(J) =	1.13E+12 J/yr	
10 FUELWOOD PRODUCTION			
	Fuelwood Prod =	1.61E+05 m^3	District Development Plan (1997)
	Energy(J) =	1.46E+15 J/yr	

Table A-4. Continued

Notes			Source
NONRENEWABLE RESOURCE USE FROM WITHIN NYANDO DISTRICT			
11 FOREST EXTRACTION			
	Clearing =	1.05E+06 m^2 annually	UNEP (1996)
	Energy(J) =	9.49E+14 J/yr	
12 ROCKS AND AGGREGATE			
	Consumption =	1.27E+03 MT/yr	Estimate
	Energy(J) =	3.37E+09 g/yr	
13 SAND MINING			
	Consumption =	1.83E+04 MT/yr	Estimate
	Energy(J) =	1.83E+10 g/yr	
14 TOPSOIL			
	Soil loss =	7.70E+11 g/yr	This Study
	Energy(J) =	5.22E+14 J/yr	
IMPORTS OF OUTSIDE ENERGY SOURCES			
15 OIL DERIVED PRODUCTS			
	Imports =	8.91E+03 MT	KPA (2001)
	Energy (J) =	3.73E+14 J/yr	
16 ELECTRICITY:			
	Kilowatt Hrs/yr =	1.98E+07 kwh	KPC (2001)
	Energy(J) =	7.13E+13 J/yr	
17 METALS			
	Imports =	1.63E+03 MT/yr	CBS (2001)
	Mass (g) =	1.63E+09 g/yr	
18 WOOD AND CHARCOAL			
	Imports =	6.40E+04 MT/yr	CBS (2001)
	Energy (J) =	9.64E+14 J/yr	
19 FOOD and AGRICULTURAL PRODUCTS			
	Imports =	8.77E+03 MT/yr	CBS (2001)
	Energy (J) =	1.03E+14 J/yr	
20 LIVESTOCK, MEAT, FISH			
	Imports =	4.00E+03 MT/yr	CBS (2001)
	Energy (J) =	1.84E+13 J/yr	
21 PLASTICS & RUBBER			
	Imports =	4.48E+02 MT/yr	CBS (2001)
	Energy(J) =	1.34E+13	
22 CHEMICALS			
	Imports =	3.24E+03 MT/yr	CBS (2001)
	Mass (g) =	3.24E+09 g/yr	
23 WOOD, PAPER, TEXTILES,LEATHER			
	Imports =	4.25E+02 MT/yr	CBS (2001)
	Energy(J) =	6.38E+12 J/yr	
24 MACHINERY, TRANSPORTATION, EQUIPMENT			
	Imports =	1.17E+03 MT/yr	CBS (2001)
	Mass (g) =	1.17E+09 g/yr	

Table A-4. Continued

Notes		Source
25 IMPORTED SERVICES		
Dollar Value =	6.13E+06 $US	Economic Survey (1999)
EXPORTS OF ENERGY, MATERIALS AND SERVICES		
26 SUGAR (PROCESSED AND RAW)		
Exports:	8.09E+04 MT/yr	Kenya Sugar Authority (2000)
Energy(J) =	1.83E+15 J/yr	
27 CROPS AND LIVESTOCK		
Exports =	1.30E+03 MT/yr	Ministry of Agiculture (2000)
Energy (J) =	2.72E+13 J/yr	
28 AGGREGATES AND SAND		
Exports =	1.56E+04 MT/yr	Estimate
Mass (g) =	1.56E+10 g/yr	
29 AGROCHEMICALS		
Exports =	1.12E+03 MT/yr	Ministry of Trade (2001)
Mass (g) =	1.12E+09 g/yr	
30 SERVICES IN EXPORTS		
Dollar Value =	6.30E+06 $US	Economic Survey (1999)

Table A-5. Energy and material flows for Awach River basin subsystem evaluation. All analyses were performed for 1 hectare of production.

	SUBSISTENCE AGRICULTURE			
Note				
1	SUNLIGHT			
		Insolation:	1.75E+02 Kcal/cm2/yr	(Vishner 1954)
		Albedo:	15%	assumed
		Energy (J) :	6.23E+13 J	
2	RAINFALL			
		Rainfall	1100 mm/yr	Jaetzold and Schmidt 1982
		Runoff	9.5%	Kenya Nat'l Water Master Plan 1992
		Energy (J) :	4.47E+10 J	
3	MANURE			
		Application Rate	1.80E+05 g/yr	Jaetzold and Schmidt 1982
		Energy (J) :	4.07E+09 J	
4	NATIVE SEEDS			
		Grams:	1.34E+04 g	Jaetzold and Schmidt 1982
		Energy:	2.24E+08 J	
5	SOIL LOSS			
		Erosion rate =	613.00 g/m2/yr	This Study
		% organic in soil =	3.0%	Assumed
		Energy (J) :	4.16E+09 J	
6	HYBRID SEEDS			
		Grams:	4.66E+04 g	Jaetzold and Schmidt 1982
		Energy:	7.81E+08 J	
		Transformity:	1.73E+05 sej/J	assumed
7	POTASH			
		Mean Annual Use:	47.6 g/ha/yr	Jaetzold and Schmidt 1982
8	PESTICIDES			
		Mean Annual Use:	1476.2 g/ha/yr	Jaetzold and Schmidt 1982
9	PHOSPHATE ROCK			
		Mean Annual Use:	18904.8 g/ha/yr	Jaetzold and Schmidt 1982
10	NITROGEN FERTILIZER			
		Mean Annual Use:	4952.4 g/ha/yr	Jaetzold and Schmidt 1982
11	LABOR			
		Person-days:	1.30E+02	Rommelse 1999
		Annual energy:	1.36E+09	
12	SERVICES			
		$ for nutrient inputs	20.5	Rommelse 1999
		$ for pesticide inputs	5.9	
		$ for seeds (improved)	7.8	
13	YIELDS			
		Dry weight =	2.56E+06 g/ha	Jaetzold and Schmidt 1982
14	ENERGY YIELDS			
		Energy per gram:	1.89E+01 kJ	Rommelse 1999
		Energy Total:	4.85E+10 J	

Table A-5. Continued

COMMERCIAL AGRICULTURE (TEA)

Note				
1	SUNLIGHT			
	Insolation:	1.75E+02	Kcal/cm2/yr	(Vishner 1954)
	Albedo:	15%		assumed
	Energy (J) :	6.23E+13	J	
2	RAINFALL			
	Rainfall	1350	mm/yr	Jaetzold and Schmidt 1982
	Runoff	0.095		Kenya Nat'l Water Master Plan 1992
	Energy (J) :	6.04E+10	J	
3	MANURE			
	Application Rate	0.00E+00	g/yr	Jaetzold and Schmidt 1982
	Energy (J) :	0.00E+00	J	
4	NATIVE SEEDS			
	Grams:	0.00E+00	g	Jaetzold and Schmidt 1982
	Energy:	0.00E+00	J	
5	SOIL LOSS			
	Erosion rate =	736	g/m2/yr	This Study
	% organic in soil =	3.0%		Assumed
	Energy (J) :	4.99E+09	J	
6	HYBRID SEEDS			
	Grams:	1.20E+04	g	Jaetzold and Schmidt 1982
	Energy:	2.01E+08	J	
	Transformity:	1.73E+05	sej/J	assumed
7	POTASH			
	Mean Annual Use:	4978.7	g/ha/yr	Jaetzold and Schmidt 1982
8	PESTICIDES			
	Mean Annual Use:	0.0	g/ha/yr	Jaetzold and Schmidt 1982
9	PHOSPHATE ROCK			
	Mean Annual Use:	7750.0	g/ha/yr	Jaetzold and Schmidt 1982
10	NITROGEN FERTILIZER			
	Mean Annual Use:	43000.0	g/ha/yr	Jaetzold and Schmidt 1982
11	LABOR			
	Person-days:	1.27E+02	d/ha/yr	Rommelse 1999
	Annual energy:	1.33E+09	J/ha/yr	
12	SERVICES			
	$ for nutrient inputs	60.6		Rommelse 1999
	$ for pesticide inputs	0.0		
	$ for seeds (improved)	2.0		
13	YIELDS			
	Dry weight =	5.14E+06	g/ha	Jaetzold and Schmidt 1982
14	ENERGY YIELDS			
	Energy per gram:	1.47E+01	kJ	Rommelse 1999
	Energy Total:	7.53E+10	J	

Table A-5. Continued

COMMERCIAL AGRICULTURE (SUGARCANE)

Note				
1	SUNLIGHT			
	Insolation:	1.75E+02	Kcal/cm2/yr	(Vishner 1954)
	Albedo:	15%		assumed
	Energy (J) :	6.23E+13	J	
2	RAINFALL			
	Rainfall	1350	mm/yr	Jaetzold and Schmidt 1982
	Runoff	0.095		Kenya Nat'l Water Master Plan 1992
	Energy (J) :	6.04E+10	J	
3	MANURE			
	Application Rate	0.00E+00	g/yr	Jaetzold and Schmidt 1982
	Energy (J) :	0.00E+00	J	
4	NATIVE SEEDS			
	Grams:	0.00E+00	g	Jaetzold and Schmidt 1982
	Energy:	0.00E+00	J	
5	SOIL LOSS			
	Erosion rate =	736	g/m2/yr	This Study
	% organic in soil =	3.0%		Assumed
	Energy (J) :	4.99E+09	J	
6	HYBRID SEEDS			
	Grams:	1.67E+05	g	Jaetzold and Schmidt 1982
	Energy:	2.79E+09	J	
	Transformity:	5.45E+03	sej/J	assumed
7	POTASH			
	Mean Annual Use:	0.0	g/ha/yr	Jaetzold and Schmidt 1982
8	PESTICIDES			
	Mean Annual Use:	0.0	g/ha/yr	Jaetzold and Schmidt 1982
9	PHOSPHATE ROCK			
	Mean Annual Use:	0.0	g/ha/yr	Jaetzold and Schmidt 1982
10	NITROGEN FERTILIZER			
	Mean Annual Use:	3142.9	g/ha/yr	Jaetzold and Schmidt 1982
11	LABOR			
	Person-days:	1.27E+02	d/ha/yr	Rommelse 1999
	Annual energy:	1.33E+09	J/ha/yr	
12	SERVICES			
	$ for nutrient inputs	3.0		Rommelse 1999
	$ for pesticide inputs	0.0		
	$ for seeds (improved)	27.8		
13	YIELDS			
	Dry weight =	5.33E+07	g/ha	Jaetzold and Schmidt 1982
14	ENERGY YIELDS			
	Energy per gram:	1.63E+01	kJ	Rommelse 1999
	Energy Total:	8.68E+11	J	

Table A-5. Continued

RANGELAND (LOWLAND COMMUNAL)

Notes				
1	SUNLIGHT			
	Insolation:	1.75E+02	Kcal/cm2/yr	(Vishner 1954)
	Albedo:	15%		assumed
	Energy (J) :	6.23E+13	J	
2	RAINFALL			
	Rainfall	1000	mm/yr	Jaetzold and Schmidt 1982
	Runoff	25%		Kenya Nat'l Water Master Plan 1992
	Energy (J) :	2.96E+10	J	
3	SOIL LOSS			
	Erosion rate =	1443	g/m2/yr	This Study
	% organic in soil =	2.0%		Assumed
	Energy (J) :	6.52E+09	J	
4	MEDICINES			
	Mean Annual Use:	650.0	g/ha/yr	Jaetzold and Schmidt 1982
5	LABOR			
	Person-days:	1.08E+02	d/ha/yr	De Boer et al. 1984
	Annual energy:	7.03E+08	J/ha/yr	
6	SERVICES			
	$ for nutrient inputs	0.0		Rommelse 1999
	$ for pesticide inputs	2.6		
	$ for seeds (improved)	0.0		
7	YIELDS			
	Dry weight (milk) =	4.44E+04	g/ha	Simpson and Evangelou 1984
	Dry weight (meat) =	2.89E+03	g/ha	Simpson and Evangelou 1985
8	ENERGY YIELDS			
	Energy per gram (milk):	3.05E+03	kJ/g	Rommelse 1999
	Energy Total (milk):	1.36E+08	J	
	Energy per gram (meat):	9.24E+00	kJ/g	Rommelse 1999
	Energy Total (meat):	2.67E+07	J	

RANGELAND (HIGHLAND CONSTRAINED)

Notes				
1	SUNLIGHT			
	Insolation:	1.75E+02	Kcal/cm2/yr	(Vishner 1954)
	Albedo:	15%		assumed
	Energy (J) :	6.23E+13	J	
2	RAINFALL			
	Rainfall	1500	mm/yr	Jaetzold and Schmidt 1982
	Runoff	15%		Kenya Nat'l Water Master Plan 1992
	Energy (J) :	6.30E+10	J	

Table A-5. Continued

3	SOIL LOSS			
		Erosion rate =	1222.505698 g/m2/yr	This Study
		% organic in soil =	3.0%	Assumed
		Energy (J) :	8.29E+09 J	
4	MEDICINES			
		Mean Annual Use:	2.50E+03 g/ha/yr	Jaetzold and Schmidt 1982
5	LABOR			
		Person-days:	83.0 d/ha/yr	Rommelse 1999
		Annual energy:	6.72E+08 J/ha/yr	
6	SERVICES			
		$ for nutrient inputs	5.0	Rommelse 1999
		$ for pesticide inputs	10.0	
		$ for seeds (improved)	0.0	
7	YIELDS			
		Dry weight (milk) =	2.33E+05 g/ha	Simpson and Evangelou 1984
		Dry weight (meat) =	7.50E+03 g/ha	Simpson and Evangelou 1985
8	ENERGY YIELDS			
		Energy per gram (milk):	3.05E+03 kJ/g	Rommelse 1999
		Energy Total (milk):	7.12E+08 J	
		Energy per gram (meat):	9.24E+00 kJ/g	Rommelse 1999
		Energy Total (meat):	6.93E+07 J	

FARM FORESTS (WOODLANDS AND WOODLOTS)

Notes

1	SUNLIGHT			
		Insolation:	1.75E+02 Kcal/cm2/yr	(Vishner 1954)
		Albedo:	15%	assumed
		Energy (J) :	6.23E+13 J	
2	RAINFALL			
		Rainfall	1350 mm/yr	Jaetzold and Schmidt 1982
		Runoff	0.095	Kenya Nat'l Water Master Plan 1992
		Energy (J) :	6.04E+10 J	
3	NATIVE SEEDS			
		Grams:	1.50E+05 g	Jaetzold and Schmidt 1982
		Energy:	2.51E+09 J	
4	SOIL LOSS			
		Erosion rate =	267 g/m2/yr	This Study
		% organic in soil =	3.0%	Assumed
		Energy (J) :	1.81E+09 J	
5	LABOR			
		Person-days:	5.00E+01 d/ha/yr	Chavangi and Zimmerman 1987
		Annual energy:	5.23E+08 J/ha/yr	

Table A-5. Continued

6	SERVICES			
	$ for nutrient inputs	0.0		Chavangi and Zimmerman 1987
	$ for pesticide inputs	0.0		
	$ for seeds (improved)	10.0		
7	YIELDS			
	Dry weight =	8.00E+06	g/ha	Chavangi and Zimmerman 1987
8	ENERGY YIELDS			
	Energy per gram:	1.47E+01	kJ	Rommelse 1999
	Energy Total:	1.17E+11	J	

SHRUBLANDS

Notes

1	SUNLIGHT			
	Insolation:	1.75E+02	Kcal/cm2/yr	(Vishner 1954)
	Albedo:	15%		assumed
	Energy (J) :	6.23E+13	J	
2	RAINFALL			
	Rainfall	1350	mm/yr	Jaetzold and Schmidt 1982
	Runoff	0.095		Kenya Nat'l Water Master Plan 1992
	Energy (J) :	6.04E+10	J	
3	NATIVE SEEDS			
	Grams:	0.00E+00	g	Jaetzold and Schmidt 1982
	Energy:	0.00E+00	J	
4	SOIL LOSS			
	Erosion rate =	550	g/m2/yr	This Study
	% organic in soil =	3.0%		Assumed
	Energy (J) :	3.73E+09	J	
5	LABOR			
	Person-days:	4.00E+01	d/ha/yr	Chavangi and Zimmerman 1987
	Annual energy:	4.19E+08	J/ha/yr	
6	SERVICES			
	$ for nutrient inputs	0.0		Chavangi and Zimmerman 1987
	$ for pesticide inputs	0.0		
	$ for seeds (improved)	0.0		
7	YIELDS			
	Dry weight (wood) =	8.00E+06	g/ha	Chavangi and Zimmerman 1987
	Dry weight (charcoal) =	1.14E+06	g/ha	Chavangi and Zimmerman 1988
8	ENERGY YIELDS			
	Energy per gram (wood):	1.47E+01	kJ/g	Rommelse 1999
	Energy Total (wood):	1.17E+11	J	
	Energy per gram (charcoal):	1.47E+01	kJ/g	
	Energy Total (charcoal):	1.67E+10	J	

Table A-6. Transformity values and references for emergy analyses.

Product	Units	Transformity	Source
Sunlight	J	1.00E+00	Definition
Wind	J	2.45E+03	Odum et al. (2000)
Rain, Chemical Potential	J	3.10E+04	Odum et al. (2000)
Runoff, Geopotential	J	4.70E+04	Odum et al. (2000)
Waves	J	5.10E+04	Odum et al. (2000)
Earth Cycle	J	5.80E+04	Odum (2000)
Tides	J	7.39E+04	Odum et al. (2000)
Cassava	J	1.24E+04	this study
Sweet Potatoes	J	1.84E+04	this study
Plantains	J	2.09E+04	this study
Potatoes	J	2.87E+04	this study
Wood	J	3.09E+04	Brown et al. (1992)
Sisal	J	3.37E+04	this study
Tea	J	5.44E+04	this study
Maize	J	6.15E+04	this study
Forest Biomass	J	6.72E+04	Brown et al. (1992)
Grapefruits	J	7.04E+04	Brandt Williams (1999)
Oranges	J	7.04E+04	Brandt Williams (1999)
Pineapples	J	7.04E+04	Brandt Williams (1999)
Sugar Cane	J	8.63E+04	this study
Manure	J	9.25E+04	assumed
Rice	J	9.26E+04	Brown and McClanahan (1992)
Millet	J	1.13E+05	this study
Sorghum	J	1.14E+05	this study
Wheat	J	1.14E+05	Odum et al. (1987)
Coffee	J	1.23E+05	this study
Sugar	J	1.41E+05	this study
Wood Products	J	1.43E+05	Brown et al. (1992)
Pulses	J	1.60E+05	this study
Vegetable Oils	J	2.02E+05	Odum et al. (1983) - coconut oil
Tobacco	J	2.31E+05	this study
Cotton Lint	J	3.22E+05	this study
Cow's Milk	J	3.70E+05	Odum et al. (1983)
Goats Milk	J	3.70E+05	this study
Honey	J	3.70E+05	assumed
Sheep's Milk	J	3.70E+05	this study
Cottonseed	J	3.72E+05	this study
Beverage and Tobacco	J	4.37E+05	Odum (1996)
Vegetables and Fruit	J	4.37E+05	Odum et al. (1987)
Butter	J	2.18E+06	Odum et al. (1983)
Milk and Cream	J	2.18E+06	Odum et al. (1983) - butter
Goat	J	2.86E+06	this study
Mutton and Lamb	J	2.86E+06	Odum et al. (1983)
Animal Fats	J	3.36E+06	this study

Table A-6. Continued.

Product	Units	Transformity	Source
Eggs	J	3.36E+06	assumed
Poultry	J	3.36E+06	Odum et al. (1987)
Crude Fibers and Textiles	J	6.38E+06	Brown et al. (1992)
Beef and Veal	J	6.72E+06	Odum et al. (1983)
Hides, Furs, Skins	J	6.72E+06	this study
Pigs/Pork	J	6.72E+06	this study
Fish and Fish Preparations	J	8.47E+06	Brown et al. (1992) - Tilapia Yield
Leather	J	1.44E+07	Odum et al. (1987)
Crude Petroleum	J	8.90E+04	Odum et al. (1983)
Processed Oil	J	1.06E+05	Odum (1996)
Refined Pertroleum Products	J	1.06E+05	Odum (1996)
Top Soil	J	2.25E+05	this study
Geothermal Electricity	J	2.69E+05	Odum et al. (1983)
Hydroelectricity	J	2.77E+05	Odum (1996)
Books, Maps and Paper	J	3.61E+05	Brown et al. (1992)
Furniture	J	5.86E+05	assumed
Labor	J	1.03E+06	This study
Glass	g	1.08E+07	Haukoos (1994)
Inorganic Chemicals	g	6.38E+08	Brown et al. (1992)
Organic Chemicals	g	6.38E+08	Brown et al. (1992)
Plastics	g	6.38E+08	Brown et al. (1992)
Crude Minerals	g	1.55E+09	Brown et al. (1992)
Cement	g	1.73E+09	Haukoos (1994) - USA w/o services
Clay	g	2.86E+09	Odum (1996)
Iron and Steel	g	2.99E+09	Odum et al. (1983)
Fertilizers Manufacture	g	7.06E+09	Odum et al. (1983) - phosphate fertilizer
Rubber	g	7.22E+09	Odum et al. (1987)
Non-Ferrous Metals	g	2.69E+10	Odum et al. (1983) - for aluminum
Electric Machinery	g	1.13E+11	Odum et al. (1987)
General Industrial Machinery	g	1.13E+11	Odum et al. (1987)
Machines	g	1.13E+11	Odum et al. (1987)
Metal Working Machinery	g	1.13E+11	Odum et al. (1987)
Power Generating Equip.	g	1.13E+11	Odum et al. (1987)
Special Industrial Machines	g	1.13E+11	Odum et al. (1987)
Telecomm. & Sound Equip	g	1.13E+11	Odum et al. (1987)
Vehicles (Road)	g	1.13E+11	Odum et al. (1987)
Metal Stuctures	g	1.35E+11	Haukoos (1996) - structural steel
Tools	g	1.35E+11	Haukoos (1996) - structural steel
Medicines	$	2.08E+12	assumed
Medical and Precision Instruments	$	2.08E+12	assumed
Perfumes/Hygiene Products	$	1.29E+13	assumed
Semi Precious Stones	g	7.39E+13	assumed
Precious Stones	g	1.85E+14	assumed
Gold	g	7.39E+14	Brown et al. (1992)

Table A-7. Summary of transformity assessment for Kenyan agricultural products.

Product	Transformity w/Serv.	Transformity w/o Serv.	EIR	EYR	ELR	ESI	% Renew.	% FCSD
Cassava	2.07E+04	1.43E+04	0.44	3.25	0.81	0.55	38%	31.1%
Sweet Potatoes	3.83E+04	2.10E+04	0.83	2.20	1.44	0.58	32%	22.9%
Cooking Bananas	3.17E+04	2.27E+04	0.40	3.52	0.54	0.73	52%	19.1%
Sugarcane	8.02E+03	6.37E+03	0.29	4.48	0.82	0.35	27%	50.4%
Potatoes	5.54E+04	3.22E+04	0.75	2.33	1.18	0.64	36%	20.8%
Sisal	6.50E+04	3.89E+04	0.67	2.49	1.23	0.55	33%	27.1%
Tea	1.31E+05	9.88E+04	0.84	2.19	2.41	0.35	19%	35.4%
Maize	9.98E+04	6.40E+04	0.98	2.02	1.59	0.62	31%	19.2%
Groundnuts	1.21E+05	7.16E+04	0.70	2.43	1.32	0.53	31%	27.5%
Millet	2.15E+05	1.33E+05	0.62	2.62	1.28	0.48	30%	32.1%
Sorghum	2.10E+05	1.32E+05	0.62	2.61	1.20	0.52	32%	29.8%
Coffee	1.74E+05	1.29E+05	0.91	2.10	1.17	0.77	40%	12.0%
Pyrethrum	2.12E+05	1.44E+05	0.50	3.01	0.73	0.68	46%	21.3%
Beans	2.93E+05	1.81E+05	0.69	2.44	1.18	0.58	35%	24.5%
Tobacco	3.90E+05	2.50E+05	2.75	1.36	7.33	0.37	10%	16.7%
Cotton	4.97E+05	3.56E+05	0.97	2.03	1.79	0.54	28%	23.1%
Lowland Livstock (milk)	4.06E+07	3.77E+07	0.17	6.75	2.04	0.09	33%	52.3%
Highland Livestock (milk)	8.66E+06	7.31E+06	0.27	4.73	1.47	0.18	40%	38.4%
Lowland Livestock (meat)	2.06E+08	1.91E+08	0.17	6.75	2.04	0.09	33%	52.3%
Highland Livestock (meat)	8.90E+07	7.51E+07	0.27	4.73	1.47	0.18	40%	38.4%
Refined Sugar	5.14E+04	4.84E+04	-	-	-	-	-	-
Refined Tea	5.76E+05	5.34E+05	-	-	-	-	-	-

Table A-8. Summary of dynamic simulation model to predict soil component transformities for tropical soils under two ecosystems.

	Savanna		Forest	
	Transformity	Standard Deviation	Transformity	Standard Deviation
Biomass (sej/J)	4.46E+04	1.24E+04	4.56E+04	6.50E+03
Litter (sej/J)	6.24E+04	8.94E+03	6.65E+04	9.90E+03
Soil Org. Matter (sej/J)	2.23E+05	4.04E+04	2.18E+05	3.86E+04
Nutrients (sej/g)	2.60E+10	3.80E+09	2.56E+10	4.29E+09
CEC/Clay (sej/g)	1.34E+10	1.30E+09	1.34E+10	1.88E+09
Soil Structure (sej/J)	5.14E+10	5.79E+10	1.11E+11	1.25E+11

APPENDIX B
SPECTRAL CALIBRATION MODELS

Spectral calibration models for rapid assessment of soil properties are provided in this section. Presented first is a summary of soil properties for the 513 soil samples that comprise the calibration library and a table of functional thresholds for each soil property (after Shepherd and Walsh 2002). For each property for which continuous regressions were developed, a calibration and validation model fit is presented. A table follows that summarizes with root-mean-square error estimates for each quartile of the calibration range, given in raw soil property units. Finally, a summary of soil property values inferred for the Awach basin is given; where binary screening models were used, the proportions of soils meeting the specified screening criteria are given. Screening criteria are designed so that a case (positive classification) indicates a soil with functional impairment.

Table B-1. Soil functional capacity thresholds for local interpretation of soil property observations (adapted from Shepherd and Walsh 2002).

Soil test†	Critical limit‡	Risk indicated
Low pH	<5.5	Strongly acid soils; Al/Mn toxicity
High pH	>7.3	Salinity, sodicity, micronutrient deficiency
Low ECEC	<4.0 $cmol_c\ kg^{-1}$	Low cation retention capacity
High ECEC	>8.0 $cmol_c\ kg^{-1}$	High cation retention capacity
Low EXK	<0.2 $cmol_c\ kg^{-1}$	Plant K-deficiency
High EXK	>0.4 $cmol_c\ kg^{-1}$	No plant response to applied K
Low EXP	<5 mg kg^{-1}	Plant P-deficiency
High EXP	>15 mg kg^{-1}	No plant response to applied P; P loading

† pH in 1:2.5 soil:water suspensions; ECEC = sum of exchangeable acidity and exchangeable cations (unbuffered); $ECEC_{clay}$ = ECEC divided by the clay fraction; EXK = exchangeable K; EXP = bicarbonate extractable P; AMN = anaerobic N mineralization potential. ‡ If the logical condition is met then case is classified as abnormal, else normal.

Table B-2. Summary of functional properties for soils in the spectral library (n=513). Mean, 25th and 75th percentile are given.

	Count	Minimum	25th Percent	Mean	75th Percent	Maximum
pH	513	4.84	5.77	6.63	7.60	9.98
Exch. Ca (cmol/kg)	513	1.19	3.70	15.18	27.10	38.60
Exch. Mg (cmol/kg)	513	0.00	1.15	4.48	8.83	14.30
Exch. K (cmol/kg)	513	0.06	0.18	0.74	1.38	6.23
Exch. P (mg/kg)	513	0.32	1.01	15.28	37.59	328.49
SOC (%)	513	0.11	0.82	1.85	3.86	9.22
Clay (%)	513	5.00	17.00	38.07	64.84	79.32
Sand (%)	513	9.17	16.00	41.36	72.14	93.98
Silt (%)	513	1.00	10.00	21.95	34.00	48.68
Exch. Bases (cmol/kg)	351	1.95	5.36	17.96	33.62	46.16
Exch. CEC (cmol/kg)	351	1.95	5.48	18.03	33.62	46.16
Exch. Na (cmol/kg)	47	0.10	0.40	2.51	3.87	17.70

Note: Exch. Na was determined only for soils with pH greater than 7.5.

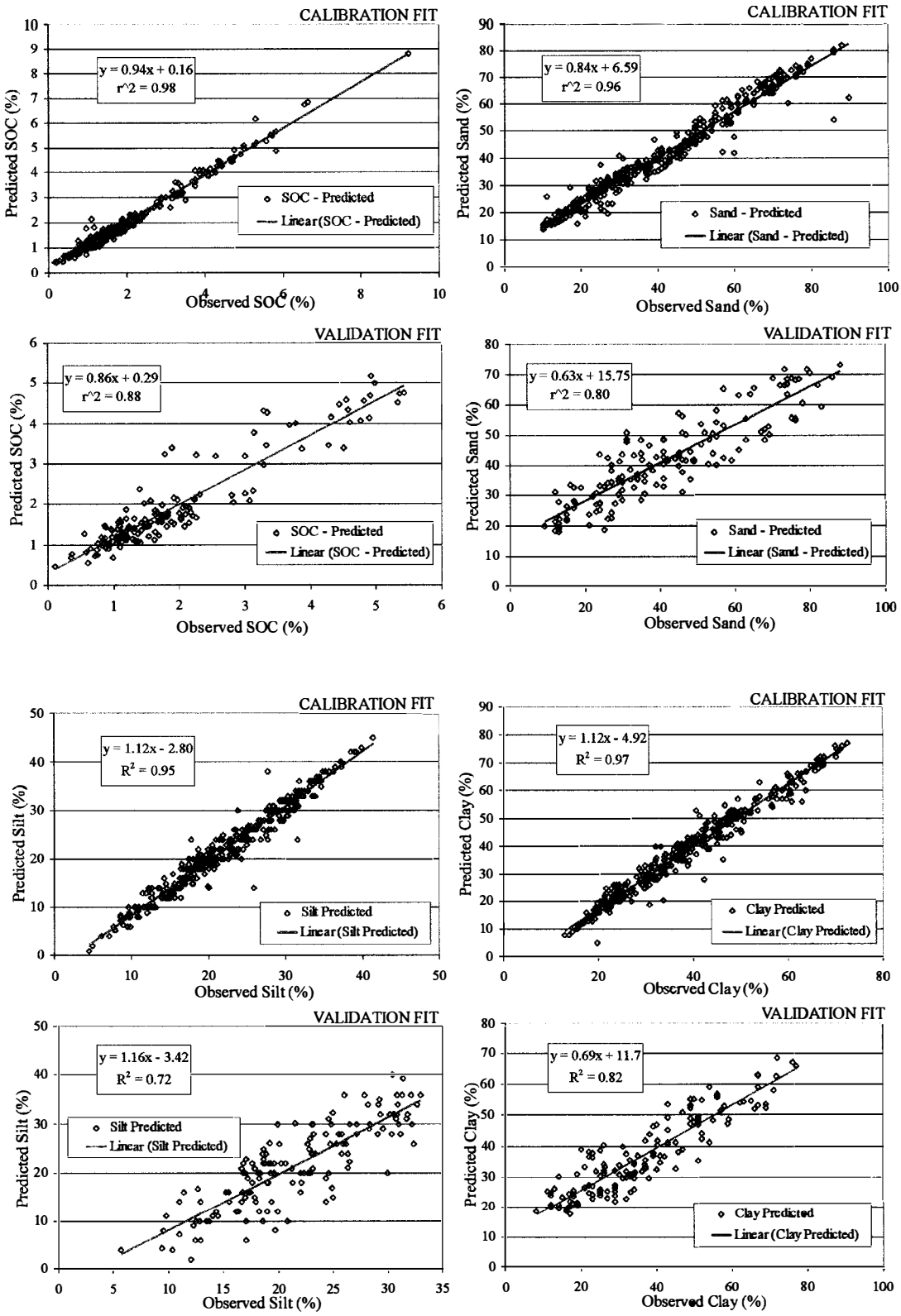

Figure B-1. Regression fits between predicted and observed soil performance criteria based on regression tree models from reflectance spectra. Shown are fits for calibration and holdout validation for SOC, Silt, Sand and Clay content.

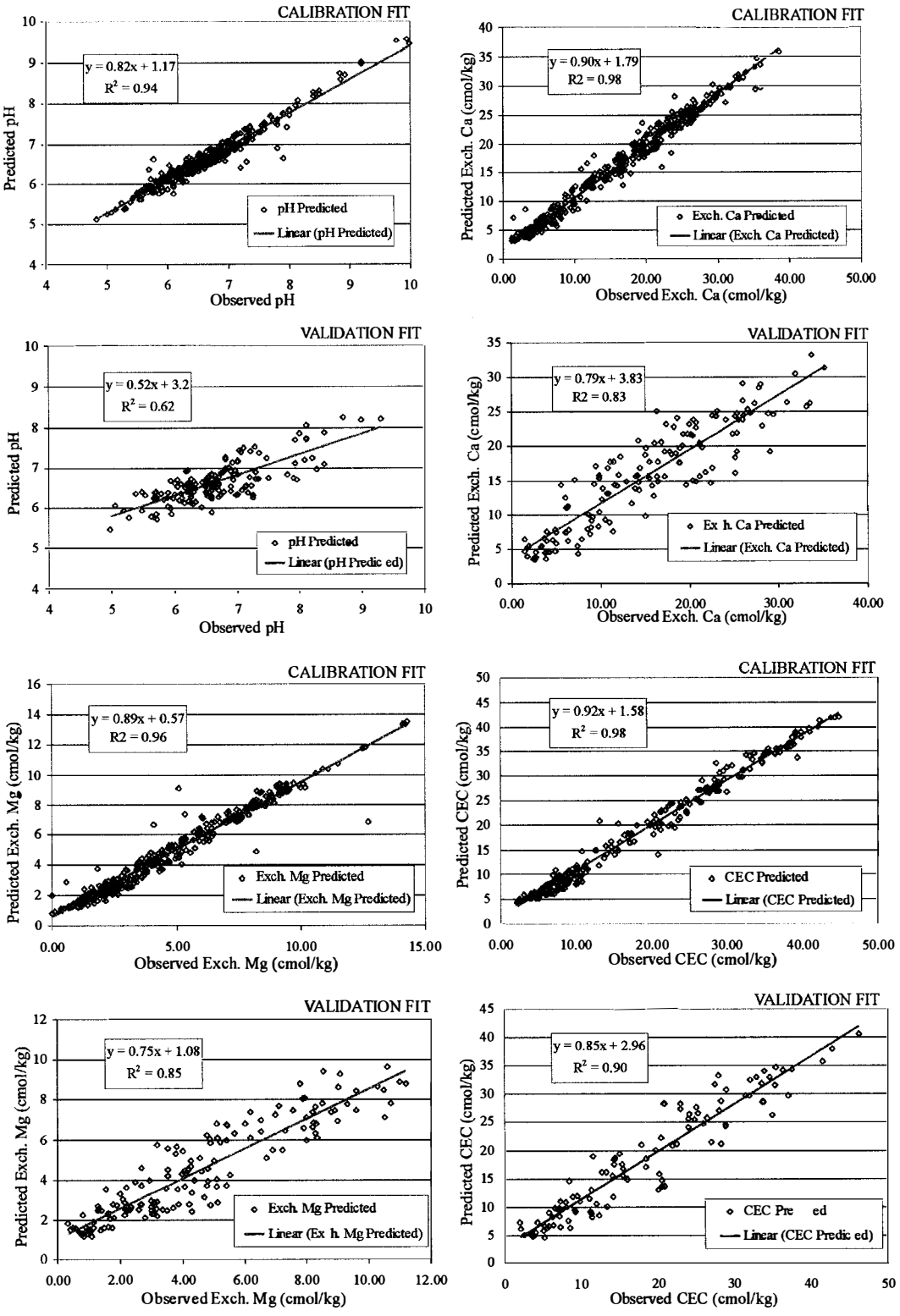

Figure B-2. Regression fits between predicted and observed soil performance criteria based on regression tree models from reflectance spectra. Shown are fits for calibration and holdout validation for pH, cation exchange capacity and exchangeable Ca and Mg.

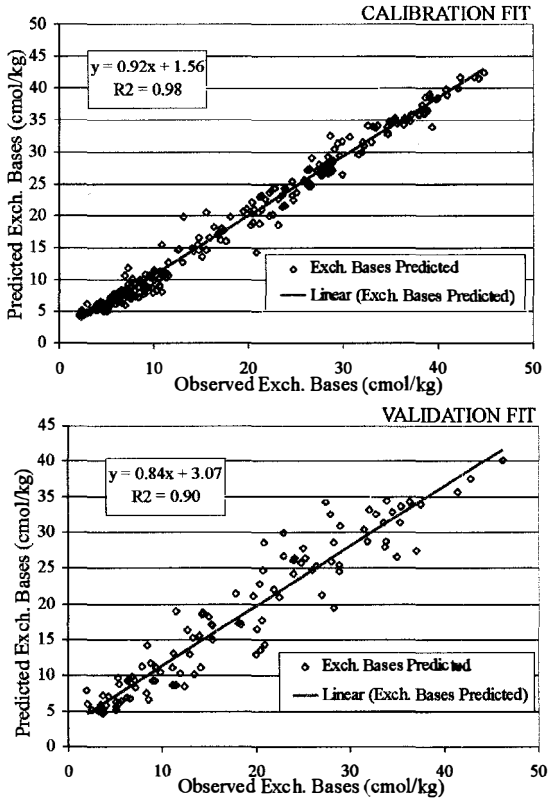

Figure B-3. Regression fits between predicted and observed soil performance based on regression tree models from reflectance spectra. Shown is the fit for calibration and holdout validation for exchangeable bases.

Table B-3. Root mean squared error (RMSE) by quartile for regression tree models in calibration and holdout validation.

	1st Quartile	2nd Quartile	3rd Quartile	4th Quartile
SOC – Calibration (%)	0.24	0.16	0.12	0.22
SOC – Validation (%)	0.29	0.32	0.44	0.56
Sand – Calibration (%)	4.75	3.65	3.15	6.60
Sand – Validation (%)	9.76	8.76	6.47	12.43
Clay – Calibration (%)	3.58	3.43	3.93	3.41
Clay – Validation (%)	9.04	6.50	5.28	8.14
Silt – Calibration (%)	2.02	1.84	2.35	2.11
Silt – Validation (%)	4.03	5.14	5.13	4.25
pH – Calibration	0.23	0.13	0.13	0.27
pH – Validation	0.54	0.29	0.27	0.65
Exch. Mg – Calibration (cmol/kg)	0.63	0.37	0.70	0.83
Exch. Mg – Validation (cmol/kg)	0.89	0.99	1.13	1.42
Exch. Ca – Calibration (cmol/kg)	1.57	1.50	1.53	1.82
Exch. Ca – Validation (cmol/kg)	3.14	3.74	3.47	4.13
CEC – Calibration (cmol/kg)	1.64	1.59	1.72	1.78
CEC – Validation (cmol/kg)	2.43	3.23	4.04	3.93
Exch. Bases – Calibration (cmol/kg)	1.57	1.67	1.74	1.81
Exch. Bases – Validation (cmol/kg)	2.59	3.13	3.79	4.34

Table B-4. Summary of soil properties for Awach basin samples. For properties that were assessed using binary screening models proportions of cases are given.

	Count	Minimum	-1 s.d.	Mean	+ 1 s.d.	Maximum
pH	1260	5.43	6.14	6.65	7.15	8.41
ExCa	1260	4.58	8.67	15.79	22.91	32.24
ExMg	1260	1.59	2.76	4.22	5.68	8.95
SOC	1260	0.75	1.38	2.71	4.05	8.12
Clay (%)	1260	17.54	30.18	38.76	47.34	58.20
Sand (%)	1260	21.57	31.20	37.79	44.37	69.13
Silt (%)	1260	9.83	19.37	23.74	28.11	33.45
ExBases	1260	6.42	10.78	17.32	23.86	33.76
CEC	1260	6.41	11.26	17.73	24.20	36.26

	Count	Proportion Positive
Exch. P (< 5 ppm)	1260	0.56
Exch. K (<0.4 cmol/kg)	1260	0.73
Exch. Na (> 0.4 cmol/kg)	1260	0.31

APPENDIX C
RULE-BASES FOR SATELLITE IMAGE INTERPRETATION

Satellite image interpretation was done using classification trees. Optimal trees were selected based on cross-validation accuracy, and provide a simple set of sequential decision nodes based on reflectance characteristics with which pixels can be classified. These are presented in the following order: binary degradation, ordinal degradation, binary infiltration and landuse. For each, the set of rules that allocate pixels to a specific terminal node are given. For binary degradation, terminal node 1 is degraded and 0 is intact. For ordinal degradation, terminal node 2 is severe degradation, node 1 is moderate degradation and 0 is intact. For binary infiltration class, terminal node 1 indicates a region with < 60 mm/hr infiltration. For landuse, terminal nodes are: 1 = subsistence agriculture, 2 = commercial agriculture, 3 = dense pasture, 4 = sparse pasture, 5 = shrubland, 6 = woodland, 7 = wetland and 8 = severe degradation.

Model Rule Base 1 – Binary Degradation Status

```
/*Terminal Node 1*/
if
(
   B5B4 <= 1.14208
)
{
   terminalNode = -1;
   class = 0;
}

/*Terminal Node 2*/
if
(
   B5B4 > 1.14208 &&
   B5B4 <= 1.396 &&
   B2B1 <= 0.862062 &&
   B5B3 <= 1.81725 &&
   B7B5 <= 0.632407
)
{
   terminalNode = -2;
   class = 0;
}

/*Terminal Node 3*/
if
(
   B5B4 > 1.14208 &&
   B5B4 <= 1.396 &&
   B2B1 <= 0.862062 &&
   B5B3 <= 1.81725 &&
   B7B5 > 0.632407
)
{
   terminalNode = -3;
   class = 1;
}

/*Terminal Node 4*/
if
(
   B5B4 > 1.14208 &&
   B5B4 <= 1.396 &&
   B2B1 <= 0.862062 &&
   B5B3 > 1.81725 &&
   BAND5 <= 100.5 &&
   B3B2 <= 0.874081
)
{
   terminalNode = -4;
   class = 1;
}

/*Terminal Node 5*/
if
(
   B5B4 > 1.14208 &&
   B5B4 <= 1.396 &&
   B5B3 > 1.81725 &&
   BAND5 <= 100.5 &&
   B3B2 > 0.874081 &&
   B2B1 <= 0.840925
)
{
   terminalNode = -5;
   class = 1;
}

/*Terminal Node 6*/
if
(
   B5B4 > 1.14208 &&
   B5B4 <= 1.396 &&
   B5B3 > 1.81725 &&
   BAND5 <= 100.5 &&
   B3B2 > 0.874081 &&
   B2B1 > 0.840925 &&
   B2B1 <= 0.862062
)
{
   terminalNode = -6;
   class = 0;
}

/*Terminal Node 7*/
if
(
   B5B4 > 1.14208 &&
   B5B4 <= 1.396 &&
   B2B1 <= 0.862062 &&
   B5B3 > 1.81725 &&
   BAND5 > 100.5
)
{
   terminalNode = -7;
   class = 0;
}

/*Terminal Node 8*/
if
(
   B5B4 > 1.14208 &&
   B5B4 <= 1.396 &&
   B2B1 > 0.862062 &&
   B7B5 <= 0.553927
)
{
   terminalNode = -8;
   class = 0;
}

/*Terminal Node 9*/
if
(
   B2B1 > 0.862062 &&
   B7B5 > 0.553927 &&
   B5B4 > 1.14208 &&
   B5B4 <= 1.3399
)
{
   terminalNode = -9;
   class = 1;
}

/*Terminal Node 10*/
if
(
   B2B1 > 0.862062 &&
   B7B5 > 0.553927 &&
   B5B4 > 1.3399 &&
   B5B4 <= 1.396
)
{
   terminalNode = -10;
   class = 0;
}

/*Terminal Node 11*/
if
(
   B5B4 > 1.396 &&
   BAND1 <= 78.5 &&
   NDVI <= 0.0703167 &&
   B3B2 <= 0.98373
)
{
   terminalNode = -11;
   class = 0;
}

/*Terminal Node 12*/
if
(
   B5B4 > 1.396 &&
   BAND1 <= 78.5 &&
   NDVI <= 0.0703167 &&
   B3B2 > 0.98373 &&
   B2B1 <= 0.802831
```

```
)
{
   terminalNode = -12;
   class = 0;
}
   .
/*Terminal Node 13*/
if
(
   BAND1 <= 78.5 &&
   NDVI <= 0.0703167 &&
   B3B2 > 0.98373 &&
   B2B1 > 0.802831 &&
   B5B4 > 1.396 &&
   B5B4 <= 1.52697 &&
   BAND3 <= 64.5
)
{
   terminalNode = -13;
   class = 1;
}

/*Terminal Node 14*/
if
(
   BAND1 <= 78.5 &&
   NDVI <= 0.0703167 &&
   B3B2 > 0.98373 &&
   B2B1 > 0.802831 &&
   B5B4 > 1.396 &&
   B5B4 <= 1.52697 &&
   BAND3 > 64.5
)
{
   terminalNode = -14;
   class = 0;
}

/*Terminal Node 15*/
if
(
   BAND1 <= 78.5 &&
   NDVI <= 0.0703167 &&
   B3B2 > 0.98373 &&
   B2B1 > 0.802831 &&
   B5B4 > 1.52697
)
{
   terminalNode = -15;
   class = 1;
}

/*Terminal Node 16*/
if
(
   B5B4 > 1.396 &&
   BAND1 <= 78.5 &&
   NDVI > 0.0703167
)
{
   terminalNode = -16;
   class = 1;
}

/*Terminal Node 17*/
if
(
   B5B4 > 1.396 &&
   BAND1 > 78.5
)
{
   terminalNode = -17;
   class = 1;
}
```

Model Rule Base 2 – Ordinal (Three Catoregory) Degradation Status

```
/*Terminal Node 1*/
if
(
   B5B4 <= 1.21857
)
{
   terminalNode = -1;
   class = 1;
}

/*Terminal Node 2*/
if
(
   B7B5 <= 0.637212 &&
   B2B1 <= 0.870779 &&
   B5B4 > 1.21857 &&
   B5B4 <= 1.28759
)
{
   terminalNode = -2;
   class = 2;
}

/*Terminal Node 3*/
if
(
   B7B5 <= 0.637212 &&
   B2B1 <= 0.870779 &&
   B5B4 > 1.28759 &&
   B5B4 <= 1.48926 &&
   BAND1 <= 72.5
)
{
   terminalNode = -3;
   class = 3;
}

/*Terminal Node 4*/
if
(
   B7B5 <= 0.637212 &&
   B2B1 <= 0.870779 &&
   B5B4 > 1.28759 &&
   B5B4 <= 1.48926 &&
   BAND1 > 72.5
)
{
   terminalNode = -4;
   class = 1;
}

/*Terminal Node 5*/
if
(
   B5B4 > 1.21857 &&
   B5B4 <= 1.48926 &&
   B7B5 <= 0.637212 &&
   B2B1 > 0.870779
)
{
   terminalNode = -5;
   class = 2;
}

/*Terminal Node 6*/
if
(
   B5B4 > 1.21857 &&
   B5B4 <= 1.48926 &&
   B7B5 > 0.637212
)
{
   terminalNode = -6;
   class = 2;
}

/*Terminal Node 7*/
if
(
   B5B4 > 1.48926 &&
   B3B2 <= 1.04445 &&
   B5B3 <= 1.69848 &&
   BAND4 <= 64.5
)
{
   terminalNode = -7;
   class = 2;
}

/*Terminal Node 8*/
if
(
   B5B4 > 1.48926 &&
   B3B2 <= 1.04445 &&
   B5B3 <= 1.69848 &&
   BAND4 > 64.5
)
{
   terminalNode = -8;
   class = 3;
}

/*Terminal Node 9*/
if
(
   B5B4 > 1.48926 &&
   B3B2 <= 1.04445 &&
   B5B3 > 1.69848 &&
   B5B3 <= 1.84687 &&
   B2B1 <= 0.863606
)
{
   terminalNode = -9;
   class = 1;
}

/*Terminal Node 10*/
if
(
   B5B4 > 1.48926 &&
   B3B2 <= 1.04445 &&
   B5B3 > 1.69848 &&
   B5B3 <= 1.84687 &&
   B2B1 > 0.863606
)
{
   terminalNode = -10;
   class = 2;
}

/*Terminal Node 11*/
if
(
   B5B4 > 1.48926 &&
   B3B2 <= 1.04445 &&
   B5B3 > 1.84687
)
{
   terminalNode = -11;
   class = 3;
}

/*Terminal Node 12*/
if
(
   B5B4 > 1.48926 &&
   B3B2 > 1.04445
)
{
   terminalNode = -12;
   class = 3;
}
```

Model Rule Base 3 – Binary Infiltration Status (threshold = 60 mm/hr)

```
/*Terminal Node 1*/
if
(
   BAND1 <= 71.5
)
{
   terminalNode = -1;
   class = 0;
}

/*Terminal Node 2*/
if
(
   BAND1 > 71.5 &&
   ELEV <= 1249
)
{
   terminalNode = -2;
   class = 1;
}

/*Terminal Node 3*/
if
(
   BAND1 > 71.5 &&
   ELEV > 1249 &&
   ELEV <= 1295 &&
   NDVI <= -0.0766979
)
{
   terminalNode = -3;
   class = 1;
}

/*Terminal Node 4*/
if
(
   BAND1 > 71.5 &&
   ELEV > 1249 &&
   ELEV <= 1295 &&
   NDVI > -0.0766979
)
{
   terminalNode = -4;
   class = 0;
}

/*Terminal Node 5*/
if
(
   BAND1 > 71.5 &&
   ELEV > 1295 &&
   SLDN <= 5.25
)
{
   terminalNode = -5;
   class = 1;
}

/*Terminal Node 6*/
if
(
   BAND1 > 71.5 &&
   ELEV > 1295 &&
   SLDN > 5.25 &&
   BAND2 <= 66.5 &&
   B5B4 <= 1.33138
)
{
   terminalNode = -6;
   class = 1;
}

/*Terminal Node 7*/
if
(
   BAND1 > 71.5 &&
   ELEV > 1295 &&
   SLDN > 5.25 &&
   BAND2 <= 66.5 &&
   B5B4 > 1.33138
)
{
   terminalNode = -7;
   class = 0;
}

/*Terminal Node 8*/
if
(
   BAND1 > 71.5 &&
   ELEV > 1295 &&
   SLDN > 5.25 &&
   BAND2 > 66.5
)
{
   terminalNode = -8;
   class = 1;
}
```

Model Rule Base 4 – Landuse (8 classes)

```
/*Terminal Node 1*/
if
(
   B3B2 <= 1.02963 &&
   B5B4 <= 1.12792 &&
   SLDN <= 2.25 &&
   B2B1 <= 0.866169
)
{
   terminalNode = -1;
   class = 3;
}

/*Terminal Node 2*/
if
(
   B3B2 <= 1.02963 &&
   B5B4 <= 1.12792 &&
   SLDN <= 2.25 &&
   B2B1 > 0.866169
)
{
   terminalNode = -2;
   class = 7;
}

/*Terminal Node 3*/
if
(
   B3B2 <= 1.02963 &&
   B5B4 <= 1.12792 &&
   SLDN > 2.25 &&
   ELEV <= 1711.5 &&
   BAND5 <= 83 &&
   NORTH <= 9.969E6
)
{
   terminalNode = -3;
   class = 6;
}

/*Terminal Node 4*/
if
(
   B3B2 <= 1.02963 &&
   B5B4 <= 1.12792 &&
   SLDN > 2.25 &&
   ELEV <= 1711.5 &&
   BAND5 <= 83 &&
   NORTH > 9.969E6
)
{
   terminalNode = -4;
   class = 5;
}

/*Terminal Node 5*/
if
(
   B3B2 <= 1.02963 &&
   B5B4 <= 1.12792 &&
   SLDN > 2.25 &&
   ELEV <= 1711.5 &&
   BAND5 > 83 &&
   BAND1 <= 68.5 &&
   EASTING <= 735916
)
{
   terminalNode = -5;
   class = 3;
}

/*Terminal Node 6*/
if
(
   B3B2 <= 1.02963 &&
   B5B4 <= 1.12792 &&
   SLDN > 2.25 &&
   ELEV <= 1711.5 &&
   BAND5 > 83 &&
   BAND1 <= 68.5 &&
   EASTING > 735916
)
{
   terminalNode = -6;
   class = 6;
}

/*Terminal Node 7*/
if
(
   B3B2 <= 1.02963 &&
   B5B4 <= 1.12792 &&
   SLDN > 2.25 &&
   ELEV <= 1711.5 &&
   BAND5 > 83 &&
   BAND1 > 68.5
)
{
   terminalNode = -7;
   class = 2;
}

/*Terminal Node 8*/
if
(
   B3B2 <= 1.02963 &&
   B5B4 <= 1.12792 &&
   SLDN > 2.25 &&
   ELEV > 1711.5 &&
   B2B1 <= 0.826343
)
{
   terminalNode = -8;
   class = 5;
}

/*Terminal Node 9*/
if
(
   B3B2 <= 1.02963 &&
   SLDN > 2.25 &&
   ELEV > 1711.5 &&
   B2B1 > 0.826343 &&
   B7B5 <= 0.529423 &&
   B5B4 <= 0.690076
)
{
   terminalNode = -9;
   class = 7;
}

/*Terminal Node 10*/
if
(
   SLDN > 2.25 &&
   ELEV > 1711.5 &&
   B2B1 > 0.826343 &&
   B7B5 <= 0.529423 &&
   B5B4 > 0.690076 &&
   B5B4 <= 1.12792 &&
   B3B2 <= 0.874153
)
{
   terminalNode = -10;
   class = 2;
}

/*Terminal Node 11*/
if
(
   SLDN > 2.25 &&
   ELEV > 1711.5 &&
   B2B1 > 0.826343 &&
   B7B5 <= 0.529423 &&
   B5B4 > 0.690076 &&
   B5B4 <= 1.12792 &&
   B3B2 > 0.874153 &&
   B3B2 <= 1.02963
```

```
)
{
   terminalNode = -11;
   class = 3;
}

/*Terminal Node 12*/
if
(
   B3B2 <= 1.02963 &&
   B5B4 <= 1.12792 &&
   SLDN > 2.25 &&
   ELEV > 1711.5 &&
   B2B1 > 0.826343 &&
   B7B5 > 0.529423
)
{
   terminalNode = -12;
   class = 3;
}

/*Terminal Node 13*/
if
(
   B5B4 > 1.12792 &&
   B7B5 <= 0.674608 &&
   B3B2 <= 0.83999
)
{
   terminalNode = -13;
   class = 6;
}

/*Terminal Node 14*/
if
(
   B5B4 > 1.12792 &&
   B7B5 <= 0.674608 &&
   B3B2 > 0.83999 &&
   B3B2 <= 1.02963 &&
   ELEV <= 1160.5
)
{
   terminalNode = -14;
   class = 7;
}

/*Terminal Node 15*/
if
(
   B7B5 <= 0.674608 &&
   B3B2 > 0.83999 &&
   B3B2 <= 1.02963 &&
   BAND7 <= 66.5 &&
   ELEV > 1160.5 &&
   ELEV <= 1367.5 &&
   BAND4 <= 73.5 &&
   NORTH <= 9.9666E6 &&
   B5B4 > 1.12792 &&
   B5B4 <= 1.59016
)
{
   terminalNode = -15;
   class = 3;
}

/*Terminal Node 16*/
if
(
   B7B5 <= 0.674608 &&
   B3B2 > 0.83999 &&
   B3B2 <= 1.02963 &&
   BAND7 <= 66.5 &&
   ELEV > 1160.5 &&
   ELEV <= 1367.5 &&
   BAND4 <= 73.5 &&
   NORTH <= 9.9666E6 &&
   B5B4 > 1.59016
)
{
   terminalNode = -16;
   class = 5;
}

/*Terminal Node 17*/
if
(
   B7B5 <= 0.674608 &&
   B3B2 > 0.83999 &&
   B3B2 <= 1.02963 &&
   BAND7 <= 66.5 &&
   ELEV > 1160.5 &&
   ELEV <= 1367.5 &&
   BAND4 <= 73.5 &&
   NORTH > 9.9666E6 &&
   B5B4 > 1.12792 &&
   B5B4 <= 1.4307
)
{
   terminalNode = -17;
   class = 5;
}

/*Terminal Node 18*/
if
(
   B7B5 <= 0.674608 &&
   B3B2 > 0.83999 &&
   B3B2 <= 1.02963 &&
   BAND7 <= 66.5 &&
   ELEV > 1160.5 &&
   ELEV <= 1367.5 &&
   BAND4 <= 73.5 &&
   NORTH > 9.9666E6 &&
   B5B4 > 1.4307 &&
   B5B3 <= 1.66706
)
{
   terminalNode = -18;
   class = 5;
}

/*Terminal Node 19*/
if
(
   B7B5 <= 0.674608 &&
   B3B2 > 0.83999 &&
   B3B2 <= 1.02963 &&
   BAND7 <= 66.5 &&
   ELEV > 1160.5 &&
   ELEV <= 1367.5 &&
   BAND4 <= 73.5 &&
   NORTH > 9.9666E6 &&
   B5B4 > 1.4307 &&
   B5B3 > 1.66706
)
{
   terminalNode = -19;
   class = 1;
}

/*Terminal Node 20*/
if
(
   B5B4 > 1.12792 &&
   BAND7 <= 66.5 &&
   ELEV > 1160.5 &&
   ELEV <= 1367.5 &&
   BAND4 > 73.5 &&
   B3B2 > 0.83999 &&
   B3B2 <= 0.903698 &&
   B7B5 <= 0.587986 &&
   NORTH <= 9.9696E6
)
{
   terminalNode = -20;
   class = 4;
}

/*Terminal Node 21*/
if
(
   B5B4 > 1.12792 &&
   BAND7 <= 66.5 &&
   ELEV > 1160.5 &&
   ELEV <= 1367.5 &&
   BAND4 > 73.5 &&
   B3B2 > 0.83999 &&
```

```
   B3B2 <= 0.903698 &&
   B7B5 <= 0.587986 &&
   NORTH > 9.9696E6
)
{
   terminalNode = -21;
   class = 3;
}

/*Terminal Node 22*/
if
(
   B5B4 > 1.12792 &&
   BAND7 <= 66.5 &&
   ELEV > 1160.5 &&
   ELEV <= 1367.5 &&
   BAND4 > 73.5 &&
   B3B2 > 0.83999 &&
   B3B2 <= 0.903698 &&
   B7B5 > 0.587986 &&
   B7B5 <= 0.674608
)
{
   terminalNode = -22;
   class = 6;
}

/*Terminal Node 23*/
if
(
   B5B4 > 1.12792 &&
   B7B5 <= 0.674608 &&
   BAND7 <= 66.5 &&
   ELEV > 1160.5 &&
   ELEV <= 1367.5 &&
   BAND4 > 73.5 &&
   B3B2 > 0.903698 &&
   B3B2 <= 1.02963
)
{
   terminalNode = -23;
   class = 3;
}

/*Terminal Node 24*/
if
(
   B5B4 > 1.12792 &&
   B7B5 <= 0.674608 &&
   B3B2 > 0.83999 &&
   B3B2 <= 1.02963 &&
   BAND7 <= 66.5 &&
   B5B3 <= 2.04678 &&
   ELEV > 1367.5 &&
   ELEV <= 1393
)
{
   terminalNode = -24;
   class = 6;
}

/*Terminal Node 25*/
if
(
   B5B4 > 1.12792 &&
   B7B5 <= 0.674608 &&
   B3B2 > 0.83999 &&
   B3B2 <= 1.02963 &&
   BAND7 <= 66.5 &&
   ELEV > 1393 &&
   NORTH <= 9.9674E6 &&
   B5B3 <= 1.80857 &&
   EASTING <= 737866 &&
   NDVI <= 0.204557
)
{
   terminalNode = -25;
   class = 1;
}

/*Terminal Node 26*/
if
(
   B5B4 > 1.12792 &&
   B7B5 <= 0.674608 &&
   B3B2 > 0.83999 &&
   B3B2 <= 1.02963 &&
   BAND7 <= 66.5 &&
   ELEV > 1393 &&
   NORTH <= 9.9674E6 &&
   B5B3 <= 1.80857 &&
   EASTING <= 737866 &&
   NDVI > 0.204557
)
{
   terminalNode = -26;
   class = 2;
}

/*Terminal Node 27*/
if
(
   B5B4 > 1.12792 &&
   B7B5 <= 0.674608 &&
   B3B2 > 0.83999 &&
   B3B2 <= 1.02963 &&
   BAND7 <= 66.5 &&
   ELEV > 1393 &&
   NORTH <= 9.9674E6 &&
   B5B3 <= 1.80857 &&
   EASTING > 737866
)
{
   terminalNode = -27;
   class = 3;
}

/*Terminal Node 28*/
if
(
   B5B4 > 1.12792 &&
   B7B5 <= 0.674608 &&
   B3B2 > 0.83999 &&
   B3B2 <= 1.02963 &&
   BAND7 <= 66.5 &&
   ELEV > 1393 &&
   NORTH <= 9.9673E6 &&
   B5B3 > 1.80857 &&
   B5B3 <= 2.04678 &&
   NDVI <= 0.187452 &&
   EASTING <= 734163
)
{
   terminalNode = -28;
   class = 4;
}

/*Terminal Node 29*/
if
(
   B5B4 > 1.12792 &&
   B7B5 <= 0.674608 &&
   B3B2 > 0.83999 &&
   B3B2 <= 1.02963 &&
   BAND7 <= 66.5 &&
   ELEV > 1393 &&
   NORTH <= 9.9674E6 &&
   B5B3 > 1.80857 &&
   B5B3 <= 2.04678 &&
   NDVI <= 0.187452 &&
   EASTING > 734163
)
{
   terminalNode = -29;
   class = 1;
}

/*Terminal Node 30*/
if
(
   B5B4 > 1.12792 &&
   B7B5 <= 0.674608 &&
   B3B2 > 0.83999 &&
   B3B2 <= 1.02963 &&
   BAND7 <= 66.5 &&
   ELEV > 1393 &&
   NORTH <= 9.9674E6 &&
   B5B3 > 1.80857 &&
```

```
   B5B3 <= 2.04678 &&
   NDVI > 0.187452
)
{
   terminalNode = -30;
   class = 1;
}

/*Terminal Node 31*/
if
(
   B5B4 > 1.12792 &&
   B7B5 <= 0.674608 &&
   B3B2 > 0.83999 &&
   B3B2 <= 1.02963 &&
   BAND7 <= 66.5 &&
   B5B3 <= 2.04678 &&
   ELEV > 1393 &&
   NORTH > 9.9674E6 &&
   B2B1 <= 0.834502
)
{
   terminalNode = -31;
   class = 6;
}

/*Terminal Node 32*/
if
(
   B5B4 > 1.12792 &&
   B3B2 > 0.83999 &&
   B3B2 <= 1.02963 &&
   BAND7 <= 66.5 &&
   B5B3 <= 2.04678 &&
   ELEV > 1393 &&
   NORTH > 9.9674E6 &&
   B2B1 > 0.834502 &&
   B7B5 <= 0.561283
)
{
   terminalNode = -32;
   class = 2;
}

/*Terminal Node 33*/
if
(
   B5B4 > 1.12792 &&
   B3B2 > 0.83999 &&
   B3B2 <= 1.02963 &&
   BAND7 <= 66.5 &&
   B5B3 <= 2.04678 &&
   ELEV > 1393 &&
   NORTH > 9.9674E6 &&
   B2B1 > 0.834502 &&
   B7B5 > 0.561283 &&
   B7B5 <= 0.674608 &&
   BAND3 <= 56.5
)
{
   terminalNode = -33;
   class = 4;
}

/*Terminal Node 34*/
if
(
   B5B4 > 1.12792 &&
   B3B2 > 0.83999 &&
   B3B2 <= 1.02963 &&
   BAND7 <= 66.5 &&
   B5B3 <= 2.04678 &&
   ELEV > 1393 &&
   NORTH > 9.9674E6 &&
   B2B1 > 0.834502 &&
   B7B5 > 0.561283 &&
   B7B5 <= 0.674608 &&
   BAND3 > 56.5
)
{
   terminalNode = -34;
   class = 1;
}

/*Terminal Node 35*/
if
(
   B5B4 > 1.12792 &&
   B7B5 <= 0.674608 &&
   B3B2 > 0.83999 &&
   B3B2 <= 1.02963 &&
   BAND7 <= 66.5 &&
   ELEV > 1367.5 &&
   B5B3 > 2.04678
)
{
   terminalNode = -35;
   class = 3;
}

/*Terminal Node 36*/
if
(
   B5B4 > 1.12792 &&
   B3B2 > 0.83999 &&
   B3B2 <= 1.02963 &&
   ELEV > 1160.5 &&
   BAND7 > 66.5 &&
   B7B5 <= 0.570871
)
{
   terminalNode = -36;
   class = 8;
}

/*Terminal Node 37*/
if
(
   B5B4 > 1.12792 &&
   B3B2 > 0.83999 &&
   B3B2 <= 1.02963 &&
   ELEV > 1160.5 &&
   BAND7 > 66.5 &&
   B7B5 > 0.570871 &&
   B7B5 <= 0.674608 &&
   BAND4 <= 72
)
{
   terminalNode = -37;
   class = 4;
}

/*Terminal Node 38*/
if
(
   B5B4 > 1.12792 &&
   B3B2 > 0.83999 &&
   B3B2 <= 1.02963 &&
   BAND7 > 66.5 &&
   B7B5 > 0.570871 &&
   B7B5 <= 0.674608 &&
   BAND4 > 72 &&
   ELEV > 1160.5 &&
   ELEV <= 1326.5 &&
   EASTING <= 723581
)
{
   terminalNode = -38;
   class = 5;
}

/*Terminal Node 39*/
if
(
   B5B4 > 1.12792 &&
   B3B2 > 0.83999 &&
   B3B2 <= 1.02963 &&
   BAND7 > 66.5 &&
   B7B5 > 0.570871 &&
   B7B5 <= 0.674608 &&
   BAND4 > 72 &&
   ELEV > 1160.5 &&
   ELEV <= 1326.5 &&
   EASTING > 723581
)
{
   terminalNode = -39;
   class = 1;
```

```
}

/*Terminal Node 40*/
if
(
   B5B4 > 1.12792 &&
   B3B2 > 0.83999 &&
   B3B2 <= 1.02963 &&
   BAND7 > 66.5 &&
   B7B5 > 0.570871 &&
   B7B5 <= 0.674608 &&
   BAND4 > 72 &&
   ELEV > 1326.5 &&
   ELEV <= 1523
)
{
   terminalNode = -40;
   class = 3;
}

/*Terminal Node 41*/
if
(
   B5B4 > 1.12792 &&
   B3B2 > 0.83999 &&
   B3B2 <= 1.02963 &&
   BAND7 > 66.5 &&
   B7B5 > 0.570871 &&
   B7B5 <= 0.674608 &&
   BAND4 > 72 &&
   ELEV > 1523
)
{
   terminalNode = -41;
   class = 4;
}

/*Terminal Node 42*/
if
(
   B3B2 <= 1.02963 &&
   B5B4 > 1.12792 &&
   B7B5 > 0.674608
)
{
   terminalNode = -42;
   class = 1;
}

/*Terminal Node 43*/
if
(
   B3B2 > 1.02963 &&
   SLDN <= 2.25 &&
   BAND2 <= 66.5 &&
   EASTING <= 724435
)
{
   terminalNode = -43;
   class = 1;
}

/*Terminal Node 44*/
if
(
   B3B2 > 1.02963 &&
   SLDN <= 2.25 &&
   BAND2 <= 66.5 &&
   EASTING > 724435
)
{
   terminalNode = -44;
   class = 4;
}

/*Terminal Node 45*/
if
(
   SLDN <= 2.25 &&
   BAND2 > 66.5 &&
   BAND7 <= 113.5 &&
   BAND3 <= 75.5 &&
   B3B2 > 1.02963 &&
   B3B2 <= 1.05798
)
{
   terminalNode = -45;
   class = 4;
}

/*Terminal Node 46*/
if
(
   SLDN <= 2.25 &&
   BAND2 > 66.5 &&
   BAND7 <= 113.5 &&
   BAND3 <= 75.5 &&
   B3B2 > 1.05798
)
{
   terminalNode = -46;
   class = 8;
}

/*Terminal Node 47*/
if
(
   B3B2 > 1.02963 &&
   SLDN <= 2.25 &&
   BAND2 > 66.5 &&
   BAND7 <= 113.5 &&
   BAND3 > 75.5
)
{
   terminalNode = -47;
   class = 4;
}

/*Terminal Node 48*/
if
(
   B3B2 > 1.02963 &&
   SLDN <= 2.25 &&
   BAND2 > 66.5 &&
   BAND7 > 113.5
)
{
   terminalNode = -48;
   class = 8;
}

/*Terminal Node 49*/
if
(
   B3B2 > 1.02963 &&
   SLDN > 2.25 &&
   B2B1 <= 0.807765
)
{
   terminalNode = -49;
   class = 1;
}

/*Terminal Node 50*/
if
(
   B3B2 > 1.02963 &&
   SLDN > 2.25 &&
   B2B1 > 0.807765
)
{
   terminalNode = -50;
   class = 8;
}
```

Table C-1. Transition probabilities for Markov-based landuse scenarios.

Scenario 1	From Landuse								
To Landuse	SA	CA	IP	DP	SL	WL	WT	SD	Overall
SA	0.37	0.17	0.22	0.06	0.15	0.15	0.10	0.08	1.30
CA	0.08	0.40	0.06	0.00	0.01	0.03	0.00	0.00	0.58
IP	0.15	0.09	0.29	0.21	0.07	0.07	0.03	0.04	0.95
DP	0.14	0.07	0.19	0.42	0.22	0.08	0.01	0.14	1.28
SL	0.13	0.11	0.07	0.11	0.36	0.25	0.00	0.09	1.11
WL	0.03	0.10	0.11	0.01	0.14	0.39	0.01	0.00	0.78
WT	0.02	0.00	0.00	0.01	0.00	0.00	0.83	0.00	0.87
SD	0.09	0.06	0.05	0.18	0.05	0.04	0.01	0.65	1.14
Overall	1.00	1.00	1.00	1.00	1.00	1.00	1.00	1.00	

Scenario 2	From Landuse								
To Landuse	SA	CA	IP	DP	SL	WL	WT	SD	Overall
SA	0.30	0.07	0.20	0.06	0.14	0.14	0.10	0.08	1.09
CA	0.25	0.75	0.15	0.05	0.05	0.10	0.00	0.00	1.35
IP	0.12	0.04	0.26	0.20	0.06	0.06	0.03	0.04	0.82
DP	0.11	0.03	0.17	0.40	0.22	0.08	0.01	0.14	1.16
SL	0.10	0.04	0.07	0.10	0.34	0.23	0.00	0.09	0.98
WL	0.02	0.04	0.10	0.01	0.13	0.36	0.01	0.00	0.67
WT	0.01	0.00	0.00	0.01	0.00	0.00	0.83	0.00	0.87
SD	0.07	0.03	0.05	0.17	0.05	0.04	0.01	0.65	1.07
Overall	1.00	1.00	1.00	1.00	1.00	1.00	1.00	1.00	

Scenario 3	From Landuse								
To Landuse	SA	CA	IP	DP	SL	WL	WT	SD	Overall
SA	0.34	0.15	0.19	0.06	0.08	0.02	0.10	0.07	1.01
CA	0.07	0.34	0.06	0.00	0.00	0.00	0.00	0.00	0.48
IP	0.14	0.08	0.26	0.20	0.03	0.01	0.03	0.04	0.78
DP	0.13	0.06	0.17	0.39	0.11	0.01	0.01	0.14	1.02
SL	0.19	0.16	0.11	0.16	0.54	0.37	0.01	0.13	1.67
WL	0.05	0.14	0.16	0.01	0.21	0.58	0.01	0.00	1.16
WT	0.02	0.00	0.00	0.01	0.00	0.00	0.83	0.00	0.86
SD	0.08	0.05	0.05	0.17	0.03	0.01	0.01	0.62	1.01
Overall	1.00	1.00	1.00	1.00	1.00	1.00	1.00	1.00	

Scenario 4	From Landuse								
To Landuse	SA	CA	IP	DP	SL	WL	WT	SD	Overall
SA	0.40	0.19	0.22	0.09	0.17	0.15	0.10	0.08	1.39
CA	0.08	0.44	0.06	0.01	0.01	0.03	0.00	0.00	0.63
IP	0.19	0.06	0.40	0.30	0.09	0.09	0.04	0.06	1.23
DP	0.06	0.01	0.09	0.20	0.11	0.04	0.01	0.07	0.58
SL	0.13	0.12	0.07	0.15	0.40	0.25	0.00	0.09	1.22
WL	0.03	0.11	0.11	0.01	0.16	0.39	0.01	0.00	0.81
WT	0.02	0.00	0.00	0.01	0.00	0.00	0.83	0.00	0.87
SD	0.09	0.07	0.05	0.24	0.06	0.04	0.01	0.69	1.26
Overall	1.00	1.00	1.00	1.00	1.00	1.00	1.00	1.00	

Table C-1. Continued

Scenario 5	From Landuse								
To Landuse	SA	CA	IP	DP	SL	WL	WT	SD	Overall
SA	0.37	0.17	0.22	0.06	0.15	0.15	0.10	0.08	1.30
CA	0.08	0.40	0.06	0.00	0.01	0.03	0.00	0.00	0.58
IP	0.15	0.09	0.29	0.21	0.07	0.07	0.03	0.04	0.95
DP	0.14	0.07	0.19	0.42	0.22	0.08	0.01	0.14	1.28
SL	0.17	0.14	0.10	0.20	0.39	0.27	0.01	0.41	1.68
WL	0.03	0.10	0.11	0.01	0.14	0.39	0.01	0.00	0.78
WT	0.02	0.00	0.00	0.01	0.00	0.00	0.83	0.00	0.87
SD	0.04	0.03	0.03	0.09	0.03	0.02	0.01	0.32	0.57
Overall	1.00	1.00	1.00	1.00	1.00	1.00	1.00	1.00	

Scenario 6									
To Landuse	SA	CA	IP	DP	SL	WL	WT	SD	Overall
SA	0.30	0.15	0.17	0.10	0.12	0.12	0.08	0.10	1.14
CA	0.17	0.44	0.12	0.02	0.05	0.07	0.03	0.02	0.92
IP	0.20	0.13	0.39	0.28	0.09	0.09	0.03	0.07	1.28
DP	0.09	0.04	0.09	0.35	0.20	0.06	0.00	0.20	1.04
SL	0.09	0.08	0.06	0.08	0.27	0.19	0.00	0.10	0.87
WL	0.06	0.12	0.13	0.03	0.23	0.45	0.01	0.02	1.05
WT	0.02	0.00	0.00	0.01	0.00	0.00	0.83	0.00	0.87
SD	0.07	0.05	0.04	0.14	0.04	0.03	0.01	0.49	0.85
Overall	1.00	1.00	1.00	1.00	1.00	1.00	1.00	1.00	

Scenario 7	From Landuse								
To Landuse	SA	CA	IP	DP	SL	WL	WT	SD	Overall
SA	0.50	0.25	0.10	0.10	0.00	0.00	0.00	0.00	0.95
CA	0.25	0.50	0.10	0.10	0.00	0.00	0.00	0.00	0.95
IP	0.25	0.25	0.60	0.15	0.25	0.00	0.00	0.00	1.55
DP	0.00	0.00	0.20	0.50	0.10	0.00	0.00	0.25	1.05
SL	0.00	0.00	0.00	0.15	0.50	0.00	0.00	0.50	1.20
WL	0.00	0.00	0.00	0.00	0.15	1.00	0.00	0.00	1.15
WT	0.00	0.00	0.00	0.00	0.00	0.00	1.00	0.00	1.00
SD	0.00	0.00	0.00	0.00	0.00	0.00	0.00	0.25	0.25
Overall	1.00	1.00	1.00	1.00	1.00	1.00	1.00	1.00	

LIST OF REFERENCES

Adinarayana, J., K. Gopal Rao, N. Rami Krishna, P. Venkatachlalam, and J.K. Suri. (1999). A rule-based soil erosion model for a hilly catchment. Catena 37: 309-18.

Agbenin, J.O. and J.T. Goladi. (1997). Carbon, nitrogen and phosphorus dynamics under continuous cultivation as influenced by farmyard manure and inorganic fertilizers in the savanna of northern Nigeria. Agriculture, Ecosystems and Environment 63: 17-24.

Agesti, A. (1990). Categorical Data Analysis. Wiley-Interscience, New York, NY

Aggrawal, R., K.P. Kumar and J.F. Power. (1997). Use of Crop Residue and Manure to conserve water and enhance nutrient availability and peal millet yields in an arid tropical region. Soil and Tillage Research 41: 43-51.

Alfsen, K.H., M.A. DeFranco, S. Glomsrod and T. Johnson. (1996). The cost of soil erosion in Nicaragua. Ecological Economics 16:129-145

Andriesse, W. and B.J.A. van der Pouw. (1985). Reconnaisance Soil Map of the Lake Basin Development Authority Area. Netherlands Soil Survey Institute and Kenya Soil Survey, Nairobi, KENYA

Anonymous. (1994). Kenya Forestry Master Plan Development Programmes. Ministry of Environment and Natural Resources, Nairobi, KENYA

Antrop, M. (1998). Landscape Change: Plan of Chaos? Landscape and Urban Planning 41: 155-61.

Ascough, J.C., C. Baffaut, M.A. Nearing, B.Y. Liu. (1996). The WEPP Watershed Model: I. Hydrology and Erosion. Transactions of the ASAE 40:921-933

Augustin, N.H., R.P. Cummins and D.D. French. (2001). Exploring Spatial Vegetation Dynamics using Logistic Regression and a Multinomial Logit Model. Journal of Applied Ecology 38: 991-1006.

Bak, P. and S. Boettcher. (1997). Self-Organized Criticality and Punctuated Equlibria. Physica D 107: 143-50.

Bandara, J.S., A. Chisholm, A. Ekanayake and S. Jayasuriya. (2001). Environmental costs of soil erosion in Sri Lanka: tax/subsidy policy options. Environmental Modeling and Software 16:497-508

Barber, R.G. (1983). Magnitudes and Sources of Soil Erosion in some Humid and Semi-Arid parts of Kenya and the Significance of Soil Loss Tolerance Values in Soil Conservation in Kenya. Soil and Water Conservation in Kenya: Proceedings of a Second National Workshop, March 1982: Institute for Development Studies, Univ. of Nairobi, Kenya

Batty, M. and P. Longley. (1989). Urban growth and form: scaling, fractal geometry and diffusion-limited aggregation. Environment and Planning A 21:1447-1472

Begon, M., J.L. Harper and C.R. Townsend. (1990). Ecology: Individuals, Populations and Communities. 2nd ed. Boston: Blackwell Scientific Publications.

Bell, J.C., R.L. Cunningham and M.W. Havens. (1994). Soil drainage class probability mapping using a soil-landscape model. Soil Science Society of America Journal 58:464-470

Ben-Dor, E. and A. Banin. (1995). Near infrared analysis (NIRA) as a rapid method to simultaneously evaluate several soil properties. Soil Science Society of America Journal. 59:364–372.

Birnir, B.T., R. Smith and G.E. Merchant. (2001). The Scaling of Fluvial Landscapes. Computers and Geosciences 27: 1189-216.

Biswas, T.D. and S.K. Mukherjee. (2000). Textbook of Soil Science. New Delhi: Tata-McGraw-Hill.

Blackard, J.A. and D.J Dean. (1999). Comparative accuracies of artificial neural networks and discriminant analysis in predicting forest cover types from cartographic variables. Computers and Electronics in Agriculture 24: 131-51.

Boddey, R.M., J.C. de Moraes, B.J.R. Alves and S. Urquiaga. (1997). The contribution of biological nitrogen fixation for the sustainable agricultural systems in the tropics. Soil Biology and Biochemistry 29, no. 5/6: 787-99.

Bojo, J. (1996). The Costs of Land Degradation in Sub-Saharan Africa. Ecological Economics 16: 161-73.

Bolker, B.M., S.J. Pacala and W.J. Parton. (1997). Linear Analysis of Soil Decomposition: Insights from the CENTURY Model. Ecological Applications 8:425-439

Botterweg, P., R. Leek, E. Romstad and A. Vatn. (1998). The EUROSEM-GRIDSEM modeling system for erosion analyses under different natural and economic conditions. Ecological Modeling 108: 115-29.

Bouwer, H. (1986). Intake Rate: Cylinder Infiltrometer. Methods of Soil Analysis, Part 1: Physical and Mineralogical Methods - Agronomy Monograph no. 9. 2nd ed. Madison, WI: American Society of Agronomoy/Soil Science Society of America.

Brady, N.C and R.R. Weil. (2001). The Nature and Properties of Soils. 13th ed. Upper Saddle River, NJ: Prentice Hall.

Brandt-Williams, S. (2001). Handbook of Emergy Evaluation: Folio #4 – Emergy of Florida Agriculture. Center for Environmental Policy, University of Florida, Gainesville, FL

Bridge, S.R.J. and E.A. Johnson. (2000). Geomorphic Principles of Terrain Organization and Vegetation Gradients. Journal of Vegetation Science 11: 57-70.

Brieman, L., J. Friedman, C.J. Stone, and R.A. Olshen. (1984). Classification and regression trees. Chapman & Hall, CRC Press, Boca Raton, FL.

Brooks, K.N., P.F. Ffolliot, H.M. Gregerson and L.F. DeBano. (1997). Hydrology and the Management of Watersheds. 2nd ed. Ames, IA: Iowa State University Press.

Brown, M.T. and T.R. McClanahan. (1996). Emergy Analysis Perspectives of Thailand and Mekong River Dam Proposals. Ecological Modelling 91: 105-30.

Brown, M.T. and S.M. Ulgiati. (1999). Emergy evaluation of the biosphere and natural capital. Ambio 28:486-493

Buenfil, A. (2001). Emergy analysis of water. PhD. Dissertation, University of Florida, Gainesville, FL

Bugaari, H.T., G. Moorhouse and T.J. McNabb. (1998). The Water Hyacinth Problem on Lake Victoria. Aquatics Unlimited internal report. Kampala, UGANDA.

Bujan, A., O.J. Santanatoglia, C. Chagas, M. Massobrio, M. Castiglioni, M. Yanez, H. Ciallella and J. Fernandez. (2003). Soil erosion in a small basin through the use of Cesium-137 technique. Soil and Tillage Research 69:127-137

Buranakarn, V. (1997). Transformity Working Paper. Center for Wetlands, University of Florida, Gainesville, FL

Burrough, P.A. (1989). Fuzzy Mathematical Methods for Soil Survey and Land Evaluation. Journal of Soil Science 40: 477-92.

Calder, I.R., R.L. Hall, H.G. Bastable, H.M. Gunston, O. Shela, A. Chirwa and R. Kafundu. (1995). The impact of land use change on water resources in sub-Saharan Africa: A modeling study of Lake Malawi. Journal of Hydrology 170:123-135

Campbell, D.E. (1999). A Revised Solar Transformity for Tidal Energy Received by the Earth and Dissipated Globally: Implications for Emergy Analysis in Emergy Synthesis: Theory and Applications of the Emergy Methodology, M.T. Brown ed. Center for Environmental Policy, Gainesville, FL

Cassel, D.K. and R. Lal. (1992). Soil physical properties of the tropics: Common beliefs and management constraints. Myths and Science of Soils of the Tropics. SSSA Special Publication #29 R. and P. A. Sanchez eds. Lal, 61-89. Madison, WI: Soil Sci. Soc. of America.

Central Bureau of Statistics. (1999). Statistical Abstract : Republic of Kenya. Nairobi, Kenya: Central Bureau of Statistics.

Chavangi, A.H. and R. Zimmermann. (1987). A Guide to Farm Forestry in Kenya. Ministry of Environment and Natural Resources, Nairobi, KENYA.

Chen, F. (1998). Spatial Analysis of Landuse and Landuse Changes, and Simulation of Soil Erosion in the Oued Laou Watershed, Morocco. PhD Dissertation, University of Georgia, USA.

Chipeta, G.B. (1976). A Study of Wind Power Availability in Kenya. PhD Dissertation, University of Nairobi, KENYA.

Christakos, G. (1998). Spatiotemporal information systems in soil and environmental sciences. Geoderma 85: 141-79.

Christensen, V. (1994). Emergy-based ascendancy. Ecological Modelling 72:129-144

Clark Labs. (2001). The Idrisi Project: Release 2. [Computer program]. Clark University, Worcester, MA

Clark, R.N. (1999). Spectroscopy of rocks and minerals, and principles of spectroscopy. p. 3–52. In Remote sensing for the earth sciences: manual of remote sensing. Vol. 3. N. Rencz (ed.) John Wiley & Sons, New York, NY.

Clarke, K.C. and L.J. Gaydos. (1998). Loose-coupling a cellular automaton model and GIS: long term urban growth prediction for San Francisco and Washington/Baltimore. International Journal of Geographical Information Science 12:699-714

Cohen, M.J. (2001). Dynamic Emergy Simulation of Soil Genesis and Techniques for Estimating Transformity Confidence Envelopes. Proceedings of the Second Biennial Emergy Research Conference, M.T. Brown ed. Center for Environmental Policy, Gainesville, FL

Cohen, M.J., K.D. Shepherd and M.G. Walsh. (submitted 2003). Improved Application of the Universal Soil Loss Equation in a Tropical Watershed.

Connelly, R.D., C.A. Ciesiokola, D.M. Silburn and C. Caroll. (1997). Distributed Parameter Hydrology Model (ANWERS) applied to a range of catchment scales using rainfall simulator data. I-IV Evaluating Infiltration Modeling and Parameter Measurement, Application to Spatially Uniform Catchments, Application to a Spatially Complex Catchment and Pasture Catchment Hydrology. Journal of Hydrology 193, no. 1-4.

Corbett, J.D., S.N. Collis, B.R. Bush, E.I. Muchugu, R.Q. Jeske, R.A. Burton, R.E. Martinez, J.W. White and D.P. Hodson. (1997). Almanac Characterization Tool – Geospatial Database. Blacklands Research Center, Texas Agricultural Experiment Station, Texas A&M University, College Park, Texas, USA

Cook, H.F. and C. Norman. (1996). Targeting agri-environmental policy: an analysis relating to the use of GIS. Land Use Policy 13, no. 3: 217-28.

Crosetto, M.S. Tarantola and A. Saltelli. (2000) . Sensitivity and uncertainty analysis in spatial modelling based on GIS. Agriculture, Ecosystems and Environment 81: 71-9.

Crosson, P.R. (1986). Soil Erosion and Policy Issues. in Agriculture and the Environment. T.T. Phipps, P.R. Crosson and K.A. Price eds. National Center for Food and Agricultural Policy, Resources for the Future, Washington DC, USA

Crul, R.C. (1995). Limnology and Hydrology of Lake Victoria. Dijon, France: UNESCO Publishing.

Daly, H.E. and K.N. Townsend. (1993). Valuing the Earth: Economics, Ecology, Ethics. Cambridge, MA: The MIT Press.

D'Ambrisio, D., S. DiGregorio, S. Gabriele and R. Gaudio. (2001). A cellular automata model for soil erosion by water. Physical Chemistry of Earth B 26:33-39

de Boer, D.H. (2001). Self-organization in Fluvial Landscapes: Sediment Dynamics as an emergent property. Computers and Geosciences 27: 995-1003

de Roo, A.P., J L. Hazelhoff and G.B.M. Heuvelink. (1992). Estimating the Effects of Spatial Variability of Infiltration on the Output of a Distributed Runoff and Soil Erosion Model using Monte Carlo Methods. Hydrological Processes 6: 127-43.

Desmet, P.J.J., and G. Govers. (1996). A GIS procedure for automatically calculating the USLE LS factor on topographically complex landscape units. Journal of Soil and Water Conservation 51:427-433

Dietrich, W.E., C.J. Wilson, D.R. Montgomery and J. McKean. (1993). Analysis of Erosion Thresholds, Channel Networks and Landscape Morphology Using a Digitial Terrain Model. The Journal of Geology 101: 259-78.

Dobos, E. E. Micheli M. F. Baumgardner L. Biehl and T. Helt. (2000). Use of combined digital elevation model and satellite rediometric data for regional soil mapping. Geoderma 97: 367-91.

Doherty, S.J., P.O. Nilsson and H.T. Odum. (2002). Emergy evaluation of forest production and industries in Sweden. Institutionen for Bioenergi, Uppsala, SWEDEN

Drege, H.E. (1995). Erosion and soil productivity in Australia and New Zealand. Land Degradation and Rehabilitation 6:71-78

Dwivedi, R.S., T.R. Sankar, L. Venataratnam, R.L. Karale, S.P. Gawande, K.V.S. Rao, S. Senchaudhary, K.R. Bhaumik and K.K. Mukharjee. (1997). The Inventory and Monitoring of Eroded Lands using Remote Sensing data. International Journal of Remote Sensing 18, no. 1: 107-19.

Edwards, D. (1995). Introduction to Graphical Modeling. Springer-Verlag, New York, NY

Edwards, D. (2000). MIM – A Program for Graphical Modeling version 3.1. [Computer program]. HyperGraph Sofware Inc.

Ehrlich, D., E.F. Lambin and J.P. Malingreau. (1997). Biomass burning and broad-scale land-cover change in western Africa. Remote Sensing of Environment 61:201-209

Ellis, E.A., P.K. Nair, P.E. Linehan, H.W. Beck and C.A. Blanche. (2000). A GIS-Based database management application for agroforestry planning and tree selection. Computers and Electronics in Agriculture 27: 41-55.

Elwell, H.A. (1981). A soil loss estimation technique for Southern Africa. In Soil conservation: problems and prospects, R.P.C Morgan (ed). Wiley, Chichester, UK

Enters, T. (1997). A Framework for the Economic Assessment of Soil Erosion and Soil Conservation. Soil Erosion at Multiple Scales: Principles and Methods for Assessing Causes and Impacts F. W. T. F. Agus and J. Kerr Penning de Vries. Wallingford, UK: CABI Publishing.

Europa Publications. (1998). Europa World Year Book 1997. Europa World Year BookEuropa Publications, Volume II.

Eva, H. and E.F. Lambin. (2000). Fires and land-cover change in the tropics: a remote sensing analysis at the landscape scale. Journal of Biogeography 27:765-776

Food and Agricultural Organization and United Nations (FAO – UN). (1999). FAO Trade and Commerce Yearbook 1998. Rome: United Nations.

Feam, T. (2000). Savitzy-Golay filters. NIR News 6:14-15

Feam, T. (2001). Local or Global? NIR News 12:10-11

Feller, C. and M.H. Beare. (1997). Physical control of soil organic matter in the tropics. Geoderma 79: 69-116.

Fenton, T.E. (1982). Estimating soil erosion by remote sensing techniques in Remote Sensing for Resource Management, C.J. Johnson and J.L. Sanders eds. Soil Conservation Society of America, Madison, WI

Feoli, E., L.G. Vuerich, and Z. Woldu. (2002). Processes of environmental degradation and opportunities for rehabilitation in Adwa, Northern Ethiopia. Landscape Ecology 17:315-325

Fernandes, E.C., M.P.P. Motavilli, C. Castilla and L. Mukurumbira. (1997). Management control of soil organic matter dynamics in tropical land-use systems. Geoderma 79: 49-67.

Fernandes, P., R. Oliver and S. Diatta. (2000). Changes in Organic Matter of a Ferralittic Tropical Soil degraded by Cropping Systems: The Case of Southern Senegal. Arid Soil Research and Rehabilitation 14: 137-50.

Fitz, H.C., E.B. DeBellevue, R. Costanza, R. Boumans, T. Maxwell, L. Wainger and F.H. Sklar. (1996). Development of a general ecosystem model for a range of scales and ecosystems. Ecological Modelling 88: 263-95.

Flamm, R.O. and M.G. Turner. (1994). Alternative model formulations for stochastic simulation of landscape change. Landscape Ecology 9:37-44.

Foley, W.J., A. McIlwee, I. Lawler, L. Aragones, A.P. Woolnough and N. Berding. (1998). Ecological applications of near infrared spectroscopy – a tool for rapid, cost-effective prediction of the composition of plant and animal tissues and aspects of animal performance. Oecologia 116:293-305

Foster, G.R. and L.J. Lane. (1987). User Requirements: USDA – Water Erosion Prediction Project (WEPP). NSERL Report No. 1. USDA-ARS National Soil Erosion Research Lab, West Lafayette, IN

Frohn, R.C. (1998). Remote Sensing for Landscape Ecology: New Metric Indicators for Monitoring, Modeling and Assessment of Ecosystems. Boca Raton, FL: Lewis Publishers.

Gachene, C.K., K.N.J. Jarvis, H. Linner and J.P. Mbuvi. (1997). Soil Erosion Effects on Soil Properties in a Highland Area of Central Kenya. Soil Science Society of America Journal 61: 559-64.

Galvao, L.S., M.A. Pizarro and J.C.N. Epiphanio. (2001). Variations in Reflectance of Tropical Soils: Spectral-Chemical Composition Relationships from AVIRIS data. Remote Sensing of Environment 75: 245-55.

Gan, T.Y., E.N. Dlamini and G.F. Biftu. (1997). Effects of Model complexity and structure, data quality, and objective functions on hydrologic modeling. Journal of Hydrology 192: 81-103.

Garrity, D.P., A. Mercado Jr. and M. Stark. (1997). Building the Smallholder in Successful Natural Resource Management at the Watershed Scale. Soil Erosion at Multiple Scales: Principles and Methods for Assessing Causes and Impacts F. W. T. F. Agus and J. Kerr Penning de Vries. Wallingford, UK: CABI Publishing.

Gavinelli, E., C. Feller, M. Larre-Larrouy, B. Bayce, N. Djegui and J.D. Nzila. (1995). A routine method to study soil organic matter by particle size fractionation:examples for tropical soils. Community Soil Science and Plant Analysis 11:1749-60.

Getahun, A. (1983). The Role of Agroforestry in Soil and Water Conservation in the Tropics. Soil and Water Conservation in Kenya: Proceedings of a Second National Workshop, March 1982: Institute for Development Studies, Univ. of Nairobi, Kenya.

Gijsman, A.J., A. Oberson, H. Tiessen and D.K. Friesen. (1996). Limited Applicability of the CENTURY Model to Highly Weathered Tropical Soils. Agronomy Journal 88: 894-903.

Gillon, D., C. Houssard and R. Joffe. (1999). Using near-infrared reflectance spectroscopy to predict carbon nitrogen and phosphorus content in heterogeneous plant material. Oecologia 118:173-182

Gilruth, P., T.S.E. Marsh and R. Itami. (1995). A Dynamic Spatial Model of Shifting Cultivation in the highlands of Guinea, West Africa. Ecological Modelling 79: 179-97.

Goldschmidt, T., F. Witte and J. Wanink. (1993). Cascading Effects of the Introduced Nile Perch on the Detritivorous/Phytoplanktivorous Species in Sublittoral Areas of Lake Victoria. Conservation Biology 7:686-700

Grabaum, R. and B.C. Meyer. (1998). Multicriteria optimization of landscapes using GIS-based functional assessments. Landscape and Urban Planning 43:21-34

Graef, F. and K. Stahr. (2000). Incidence of soil surface crust types in semi-arid Niger. Soil and Tillage Research 55:213-218

Grove, M. and J. Harbor. (1997). Development and application of a GIS-based model for assessing the long-term hydrologic impacts of land-use change. Abstracts with Programs - Geological Society of America 29:148, 1997

Haan, C.T. (1977). Statistical Methods in Hydrology. Iowa State University Press, Ames, IA

Hall, C.J., D. Lindenberger, R. Kuemmel, T. Kroeger and W. Eichhorn. (2001). The need to reintegrate the natural sciences with economics. Bioscience 51:663-673

Hedeker D. and R.D. Gibbons. (2001). MIXOR Version 2.0. [Computer program]. Discerning Systems, Inc. Chicago, IL

Henderson, T.L., M.F. Baumgardner, D.P. Scott, and D.E. Coster. (1992). High dimensional reflectance analysis of soil organic matter. Soil Science Society of America Journal 56:865-872

Henrot, J. and G. P. Robertson. (1994). Vegetation Removal in Two Soils on the Humid Tropics: Effect on Microbial Biomass. Soil Biology and Biochemistry 26, no. 1: 111-6.

Hilborn, R. and M. Mangel. (1997). The Ecological Detective: Confronting Models with Data. Princeton, NJ: Princeton University Press.

Hill, J. and B. Schutt. (2000). Mapping Complex Patterns of Erosion and Stability in Dry Mediterranean Ecosystems. Remote Sensing of Environment 74: 557-69.

Horton, R.E. (1940). An approach to the physical interpretation on infiltration capacity. Proceedings of the Soil Science Society of America 5:399-417

Howard, D.M., P.J.A. Howard and D.C. Howard. (1995). A Markov model projection of soil organic carbon stores following land use changes. Journal of Environmental Management 45:287-302

Howington, T.M. (1999). A spatial analysis of emergy of an internationally shared drainage basin and the implications for policy decisions. PhD Dissertation, University of Florida. Gainesville FL

Hugget, R.J. (1985). Earth Surface Systems. Berlin, GERMANY: Springer-Verlag.

Hunt, G.R. (1977). Spectral signatures of particulate minerals in the visible and near-infrared. Geophysics 42:501-513

ICRAF. (2000). Improved Land Management in the Lake Victoria Basin – First Report of Progress and Results July 1999 to March 2000. ICRAF Working Paper, Nairobi, KENYA

Itami, R.M. (1994). Simulating spatial dynamics – cellular-automata theory. Landscape and Urban Planning 30:27-47

Jaetzold, R. and H. Schmidt. (1982). Farm Management Handbook of Kenya - Natural Conditions and Farm Management Information, Vol II (West Kenya). Rossdorf, Germany: Ministry of Agriculture, Kenya.

Jensen, J.R. (1996). Introductory digital image processing. Prentice Hall, Upper Saddle River, NJ

Jetten, V., A. de Roo and D. Favis-Mortlock. (1999). Evaluation of Field-Scale and Catchment-Scale Soil Erosion Models. Catena 37: 521-41.

Jetten, V.G., H.T. Riezebos, F. Hoefsloot and J. van Rossum. (1993). Spatial Variability of Infiltration and Related Properties of Tropical Soils. Earth Surface Processes and Landforms 18: 477-88.

Jorgensen. S.J., G. Bendoricchio. (2001). Fundamentals of Ecological Modeling. 3rd ed. Amsterdam, NETHERLANDS: Elsevier.

Kassam, A.H., H.T. van Velthuizen, A.J.B.Mitchell, G.W. Fischer and M.M. Shah. (1991). Agroecological Land Resources Assessment for Agricultural Development Planning: A Case Study of Kenya – Technical Annex 2: Soil Erosion and Productivity. Land and Water Development Division, Rome, ITALY: FAO

Kaufman, L., L.J. Chapman and C.A. Chapman. (1996). The Great Lakes in East African Ecosystems and their Conservation, T.R. McClanahan and T.P. Young eds., Oxford University Press, New York, NY

Kenya Central Bureau of Statistics. (2000). Kenya National Statistical Abstract. Ministry of Finance and Planning, Nairobi, KENYA

Kerr, J. (1997). The Economics of Soil Degradation: From National Policy to Farmers' Needs. Soil Erosion at Multiple Scales: Principles and Methods for Assessing Causes and Impacts F. W. T. F. Agus and J. Kerr Penning de Vries. Wallingford, UK: CABI Publishing.

Khalil, K.I., M. Fahim and F. Hawela. (1997). Soil reflectance as affected by some soil parameters. Egyptian Journal of Soil Science 37:297-310

Kiome, R.M. and M. Stocking. (1995). Rationality of Farmer Perception of Soil Erosion: The Effectiveness of Soil Conservation in Semi-Arid Kenya. Global Environmental Change 5, no. 4: 281-95.

Kipkiyai, J.J., N.K. Karanja, J.Q. Qureshi, P.C. Smithson and P.L. Woomer. (1999). Soil organic matter and nutrient dynamics in a Kenyan nitisol under long-term fertilizer and organic input management. Soil Biology and Biochemistry 31: 1773-82.

Kirkby, M.J. (1980). The Problem. in Soil Erosion M. J. Kirkby and R. P. C. Morgan eds. Chichester, UK: John Wiley and Sons.

Kirkby, M.J., Y. LeBissonais, T.J. Coulhard, J. Daroussin and M.D. McMahon. (2000). The development of land quality indicators for soil degradation by water erosion. Agriculture, Ecosystems and Environment 81:125-135

Koch, M. (2000). Geological controls of land degradation as detected by remote sensing: a case study in Los Monegros, north-east Spain. International Journal of Remote Sensing 21, no. 3: 457-73.

Kooistra, L., R. Wehrens, R.S. Leuven and L.M.C. Buydnes. (1997). Possibilities of visible-near infrared spectroscopy for the assessment of soil contamination in river floodplains. Analytica Chemica 446:97-105

Krishnan, P., D.J. Alexander, B.J. Butler, and J.W. Hummel. (1980). Reflectance technique for predicting soil organic matter. Soil Science Society of America Journal 44:1282-1285

Lagerberg, C. (1999). Emergy Analysis of the Resource Use in Greenhouse Crop Production and of the Resource Basis of the Swedish Economy. PhD Dissertation, Swedish University of Agricultural Sciences, Uppsala, SWEDEN

Lal, R. (1985). Soil erosion and sediment transport research in tropical Africa. Hydrological Sciences Journal 30:239-256

Lal, R. (1994). Global Overview of Soil Erosion. Soil Science Society of America special publication #41, Madison, WI

Lal, R. (1997). Agronomic Consequences of Soil Erosion. Soil Erosion at Multiple Scales: Principles and Methods for Assessing Causes and Impacts F. W. T. F. Agus and J. Kerr Penning de Vries. Wallingford, UK: CABI Publishing.

Lal, R. (1998). Soil erosion impact on agronomic productivity and environment quality. Critical Reviews in Plant Sciences 17:319-464

Lal, R. (1999). Integrated watershed management in the global ecosystem. Special Issue of Soil and Water Conservation. CRC Press, Boca Raton, FL.

Lambert, J.D. (2000). Spatial Transformities for Alachua County, Florida. Emergy Synthesis: Theory and Applications of the Emergy Methodology Gainesville, FL: Department of Envinronmental Engineering Sciences.

Lehman, J.T., R. Mugidde and D.A. Lehman. (1998). Lake Victoria Plankton Ecology: Mixing Depth and Climate Driven Control of Lake Condition in Environmental

Change and Response in East African Lakes. J.T. Lehman (ed). Kluwer Academic Publishers, NETHERLANDS

Leica Geosystems. (2001). ERDAS Imagine v. 8.5. [Computer Program] Leica Geosystems, Heerbrugg, SWITZERLAND

Li, B. (1995). Stability analysis of a non-homogeneous Markovian landscape model. Ecological Modelling 82:247-256

Li, H. and J.F. Reynolds. (1997). Modeling effects of spatial pattern, drought and grazing on rates of rangeland degradation: a combined Markov and cellular automaton approach in Scale in Remote Sensing and GIS, D.A. Quattrochi and M.F. Goodchild eds. Lewis Publishers, Boca Raton, FL

Lindenschmidt, K.E., M. Suhr, M.K. Magumba, R.E. Hecky and F.W.B. Bugenyi. (1998). Loading of Solute and Suspended Solids from Rural Catchment Areas Flowing into Lake Victoria. Water Resources 32:2776-2786

Loehman, E.T. and T.O. Randhir. (1999). Alleviating soil erosion/pollution stock externalities: alternative roles for government. Ecological Economics 30:29-46

Lotka, A.J. (1922). Contribution to the Energetics of Evolution. Proceedings of National Academy of Sciences 8:147-155

Ludwig, B., P.K. Khanna, J. Bauhus and P. Hopmans. (2002). Near infrared spectroscopy of forest soils to determine chemical and biological properties related to soil sustainability. Forest Ecology and Management 171:121-132

Lufafa, A., M.M. Tenywa, M. Isabirye, M.J.G. Majaliwa and P.L. Woomer. (2002). Prediction of soil erosion in a Lake Victoria basin catchment using a GIS-based University Soil Loss model. Agricultural Systems 73:1-12

Luitjen, J.C. (1999). A tool for community-based water resources management in hillside watersheds. PhD. Disseration, University of Florida, Gainesville, FL

Maroko, J. B., R. J. Buresh and P. C. Smithson. (1998). Soil Nitrogen Availability as affected by Fallow-Maize systems on two soils in Kenya. Biology and Fertility of Soils 26: 229-34.

Maroko, J.B., R.J. Buresh and P.C. Smithson. (1999). Soil Phosphorus Fractions in Unfertilized Fallow - Maize Systems in two tropical soils. Soil Science Society of America Journal 63: 320-6.

MathSoft, Inc. (1999). S-Plus 2000: Professional Release 1. [Computer program]. Newer version available from http://www.insightful.com/

Mati, B.M., R.P.C Morgan, F.N. Gichuki, J.N. Quinton, T.R. Brewer and H.P. Liniger. (2000). Assessment of erosion hazard with the USLE and GIS: A case study of the Upper Ewasno Ng'iro North basin on Kenya. JAG 2:78-85

McCune, B. and J.B. Grace. (2002). Analysis of Ecological Communities. MjM Software Design, Gleneden Beach, OR

McCune, B. and M.J. Mefford. (1999). Multivariate Analysis of Ecological Data: PC-ORD v. 4.10. [Computer program]. MjM Software, Gleneden Beach, OR

McLellan, T.M., J.D. Aber, M.E. Martin, J.M. Mellilo and K.J. Nadelhoffer. (1991). Determination of nitrogen, lignin and cellulose content of decomposing leaf material by near infrared spectroscopy. Canadian Journal of Forest Research 21:1684-1688

Meiner, A. (1996). Integration of GIS and a dynamic spatially distributed model for non-point source pollution management. Water Science and Technology 33, no. 4-5: 211-8.

Menz, K. and P. Grist. (1997). Bioeconomic Modeling for Analysing Soil Conservation Policy Issues. Soil Erosion at Multiple Scales: Principles and Methods for Assessing Causes and Impacts F. W. T. F. Agus and J. Kerr Penning de Vries. Wallingford, UK: CABI Publishing.

Mertens, B. and E.F. Lambin. (1997). Spatial modelling of deforestation in southern Camaroon. Applied Geography 17, no. 2: 143-62.

Metternicht, G. (2001). Assessing temporal and spatial changes in salinity using fuzzy logic and GIS: Foundations of an expert system. Ecological Modelling 144: 163-79.

Metternicht, G.I. and A. Fremont. (1998). Estimating Erosion Surface Features by Linear Mixed Modeling. Remote Sensing of Enviroment 64: 254-65.

Meyer, A. and J.A. Martinez-Casasnovas. (1999). Prediction of Existing Gully Erosion in Vineyard Parcels of the NE Spain: A Logistic Modeling Approach. Soil and Tillage Research 50: 319-31.

Miller, S.N., W.G. Kepner, M.H. Mehaffey, M. Hernandez, R.C. Miller, D.C. Goodrich, K.K. Devonald, D.T. Heggem and W.P. Miller. (2002). Integrating landscape

assessment and hydrologic modeling for land cover change analysis. Journal of the American Water Resources Association 38:913-930

Millward, A.A. and J.E. Mersey. (1999). Adapting the RUSLE to model soil erosion potential in a mountainous tropical watershed. Catena 38: 109-29.

Millward, A.A. and J.E. Mersey. (2001). Conservation strategies for effective land management of protected areas using an erosion prediction information system (EPIS). Journal of Environmental Management 61:329-343

Ministry of Water Development, Republic of Kenya. (1992). The Study on the National Water Master Plan : Hydrologic Data, Republic of Kenya/Japan International Cooperation Agency.

Mitsch, W.J. and S.E. Jorgensen. (1989). Ecological Engineering: An Introduction to Ecotechnology. New York, NY: John Wiley and Sons.

Molnar, D.K. and P.Y. Julienne. (1997). Estimation of upland erosion using GIS. Computers and Geosciences 24:183-192

Moore, I.D. and G.J. Burch. (1986). Modeling erosion and deposition: topographic effects. Transactions of the ASAE 29:1624-1630

Moore, I.D., A.K. Turner, J.P. Wilson, S.K. Jenson and L.E. Band. (1993). GIS and land surface-subsurface process modeling. in Environmental Modeling and GIS, M.F. Goodchild, B.O. Parks and L.T. Steyaert eds. Oxford University Press, New York, NY

Morgan, R.P.C. (1995). Soil erosion and conservation. 2nd Ed. Longman Group Limited, Essex, UK

Moussa, R. and C. Bocquillon. (1996). Fractal analyses of tree-like channel networks from a digital elevation model. Journal of Hydrology 187: 157-72.

Mulengera, M.K. and R.W. Payton. (1999). Modification of the productivity index model. Soil and Tillage Research 52:11-19

Murage, E.W., N.K. Karanja, P.C. Smithson and P.L. Woomer. (2000). Diagnostic indicators of soil quality in productive and non-productive smallholders' fields of Kenya's Central Highlands. Agriculture, Ecosystems, and Environment 79: 1-8.

Nagle, G.N., T.J. Fahey and J.P. Lassoie. (1999). Management of Sedimentation in Tropical Watersheds. Environmental Management 23, no. 4: 441-52.

Nearing, M.A. (1998). Why Soil Erosion Models Over-predict small soil losses and under-predict large soil losses. Catena 32: 15-22.

Nearing, M.A., G.R. Foster, L.J. Lane and S.C. Finker. (1989). A process-based soil erosion model for USDA-Water Erosion Prediction Project Technology. Transactions of the ASAE 32:1587-1593

Niehoff, D., U. Fritsch and A. Bronstert. (2002). Land-use impacts on storm runoff generation: scenarios of land-use change and simulation of hydrological response in a meso-scale catchment in SW-Germany. Journal of Hydrology 267:80-93

Oba, G. (1998). Effects of excluding goat herboviry on Acacia tortilis woodlands around pastoralist settlements in northwest Kenya. Acta Oecologia 19, no. 4: 395-404.

Ochumba, P.B.O. (1990). Massive Fish Kills within the Nyanza Gulf of Lake Victoria, Kenya. Hydrobiologia 208: 93-9.

Odum, E.P. (1971). Fundamentals of Ecology. 3rd ed. Philadelphia, PA: W.B. Saunders Company.

Odum, H.T. (1991). Emergy and biogeochemical cycles in Ecological Physical Chemistry: Proceedings of and International Workshop. C. Rossi and E. Tiezzi eds. Elsevier Science Publishers, Amsterdam, NETHERLANDS

Odum, H.T. (1994). Ecological and General Systems: An Introduction to Systems Ecology. 2nd ed. Niwot, Colorado: University Press of Colorado.

Odum, H.T. (1989). Ecological Engineering and Self-Organization. Ecological Engineering: An Introduction to Ecotechnology W. J. and S. E. Jorgensen eds Mitsch. New York, NY: John Wiley and Sons.

Odum, H.T. (1996). Environmental Accounting: EMergy and Environmental Decision Making. New York: John Wiley and Sons, Inc.

Odum, H.T. (2000). Folio #2: Emergy of Global Processes. Handbook of Emergy Evaluation. Center for Environmental Policy, University of Florida, Gainesville, FL.

Odum, H.T. (2000). Simulating Emergy and Materials in Hierarchical Steps. Emergy Synthesis: Theory and Applications of the Emergy MethodologyGainesville, FL: Department of Envinronmental Engineering Sciences.

Odum, H.T. M.T. Brown and S. Brandt-Williams. (2000). Folio #1: Introduction and Global Budget. Handbook of Emergy Evaluation. Center for Environmental Policy, University of Florida, Gainesville, FL.

Odum, H.T., S.J. Doherty, F.N. Scatena and P.A. Kharecha. (2000). Emergy evaluations of reforestation alternatives in Puerto Rico. Forest Science 46:521-530

Odum, H.T and E.C. Odum. (1996). Modeling for All Scales: An Introduction to Systems and Simulation. Gainesville, FL.

Odum. H.T., E.C. Odum and M.T. Brown. (1997). Environment and Society in Florida. Boca Raton, FL: Lewis Publishers.

Odum, H.T. and Nils Peterson. (1996). Simulation and Evaluation with Energy Systems Blocks. Ecological Modelling 93: 155-73.

Oostwoud, D.J. and R. Bryan. (2001). Gully-head erosion processes and semi-arid valley floor of Kenya: A Case Study into Temporal variation and Sediment Budgeting. Earth Surface Processes and Landforms 26: 911-33.

Parton, W., P. Woomer, and A. Martin. (1994). Modeling Soil Organic Matter Dynamics and Plant Productivity in Tropical Ecosystems. In The Biological Management of Tropical Soils Fertility, P. Woomer and M. Swift (eds). Wiley-Sayce, San Francisco CA

Patten, B.C. (1995). Network Integration of Ecological Extremal Principles: Exergy, Emergy, Power, Ascendency, and Indirect Effects. Ecological Modelling 79: 75-84.

Phillips, J.D., P. A. Gares and M.C. Slattery. (1999). Agricultural Soil Redistribution and Landscape Complexity. Landscape Ecology 14: 197-211.

Pickup, G. and V.H. Chewings. (1988). Forecasting patterns of erosion in arid land forms from Landsat MSS data. International Journal of Remote Sensing 9:69-84

Pilotti, M. and B. Bacchi. (1997). Distributed Evaluation of the Contribution of Soil Erosion to the Sediment Yield from a Watershed. Earth Surface Processes and Landforms 22: 1239-51.

Pimentel, D. (1993). World Soil Erosion and Conservation. Cambridge University Press, Cambridge, UK

Pollack, H.N., S.J. Hurter, and J.R. Johnson. (1993) Heat flow from the earth's interior: analysis of the global data set, Reviews of Geophysics 31: 267-280.

Portela, R. (1999). Energy evaluation of large scale development projects : Mato Grosso Natural Resource Management Project, a case study. MS Thesis, University of Florida, Gainesville, FL

Price, K.P. (1993). Detection of soil erosion within Pinyon-Juniper woodlands using Thematic Mapper (TM) data. Remote Sensing of Environment 45: 233-48.

Priya, S. and R. Shibasaki. (2001). National spatial crop yield simulation using GIS-based crop production model. Ecological Modelling 135: 113-29.

Rafaelli, S.G., D.R. Montgomery and H.M. Greenberg. (2001). A Comparison of Thematic Mapping of Erosional Intensity to GIS-Driven process models in an Andean drainage basin. Journal of Hydrology 244: 33-42.

Raikes, P. (1983). Livestock Development and Policy in East Africa. Africana Publishing Company, New York, NY

Reader, J. (1997). Africa: A Biography of a Continent. Penguin Books, London UK

Reeves, J.B., G.W. McCarty, and J.J. Mesinger. (1999). Near infrared reflectance spectroscopy for the analysis of agricultural soils. Journal of Near Infrared Spectroscopy 7:179–193.

Renard, K.G., G.R. Foster, G.A. Weesies and J.P. Porter. (1991). RUSLE: Revised Universal Soil Loss Equation. Journal of Soil and Water Conservation 41:30-33

Renschler, C.S., C. Mannaerts and B. Diekkruger. (1999). Evaluating spatial and temporal variability in soil erosion risk – rainfall erosivity and soil loss ratios in Andalusia, Spain. Catena 34:209-225

Repetto, P.L. (1996). Revised Universal Soil Loss Equation: Estimation at the Landscape Scale using GIS. Masters Thesis, Montana State University, Bozeman, MT

Reusing, M., T. Schneider and U. Ammer. (2000). Modeling soil loss rates in the Ethiopian Highlands by integration of high-resolution MOMS-02/D2 stereo-date in a GIS. International Journal of Remote Sensing 21, no. 9: 1885-96.

Risse, L.M., M.A. Nearing, A.D. Nicks and J.M. Laflen. (1993). Error assessment in the Universal Soil Loss Equation. Soil Science Society of America Journal 57:825-833.

Ritchie, J.C. and G.W. McCarty. (2003). Cesium-137 and soil carbon in a small agricultural watershed. Soil and Tillage Research 69:45-51

Romitelli, M.S. (1997). Emergy Basis of Watersheds. PhD Dissertation, University of Florida. Gainesville FL

Rountree, K.M. (1983). Rainfall Erosivity in Kenya - Some Preliminary Considerations. Soil and Water Conservation in KenyaUniversity of Nairobi: Institute for Development Studies.

Sanchez, P.A. (1973). Properties and Management of Soils in the Tropics. Wiley-Interscience, New York, NY

Sanchez, P.A., C.A. Palm and S.W. Buol. (2003). Fertility capability soil classification: a tool to help assess soil quality in the tropics. Geoderma 1949:1-29

Sanchez, P.A., K.D. Shepherd, M.J. Soule, F.M. Place, R.J. Buresh, A.N. Izac, A.U. Mokwunye, F.R. Kwesiga, C.G. Ndiritu and P.L. Woomer. (1997). Soil Fertility Replenishment in Africa: An Investment in Natural Resource Capital. in Replenishing Soil Fertility in Africa. Soil Science Society of America Special Publication #51, Madison, WI

Scholes, M., C.D. Powlson and G. Tian. (1997). Input control of organic matter dynamics. Geoderma 79: 25-47.

Schoorl, J.M. and A. Veldkamp. (2001). Linking land use and landscape process modelling: a case study for the Alora Region (Spain). Agriculture, Ecosystems and Environment 85: 281-92.

Schroeder, R.A. (1999). Geographies of environmental intervention in Africa. Progress in Human Geography 23, no. 3: 359-78.

Schumann, A.H., R. Funke and G.A. Schultz. (2000). Application of a geographic information system for conceptual rainfall runoff modeling. Journal of Hydrology 240:45-61

Seppelt, R. and A. Voinov. (2002). Optimization methodology for land use patterns using spatially explicit landscape models. Ecological Modelling 151:125-142

Serneels, S. and E.F. Lambin. (2001). Proximate causes of land-use change in Narok District, Kenya: A spatial statistical model. Agriculture, Ecosystems and Environment 85: 65-81.

Shachter, R.D. and D.E. Heckerman. (1987). Thinking Backward for Knowledge Acquisition. Artificial Intelligence 8, no. 3.

Shang, C. and H. Tiessen. (1997). Organic Matter Lability in a Tropical Oxisol: Evidence from Shifting Cultivation, Chemical Oxidation, Particle Size, Density and Magnetic Factionations. Soil Science 162, no. 11: 795-807.

Shang, C. and H. Tiessen. (2000). Carbon Turnover and Carbon-13 Natural Abundance in Organo-Mineral Fractions of a Tropical Dry Forest Soil under Cultivation. Soil Science Society of America Journal 64: 2149-55.

Sharma, T., P.V. Satya Kiran, T.P. Singh, A.V. Trivedi, and R.R. Navalgund. (2001). Hydrologic Response of a watershed to land use changes: a remote sensing and GIS approach. International Journal of Remote Sensing 22, no. 11: 2095-108.

Shepherd, K.D. and M.J. Soule. (1998). Soil Fertility Management in west Kenya: Dynamic Simulation of Productivity, Profitability and Sustainability at Different Resource Endowment Levels. Agriculture, Ecosystems and Environment 71: 131-45.

Shepherd, K.D. and M.G. Walsh. (2002). Development of reflectance spectral libraries for characterization of soil properties. Soil Science Society of America Journal. 66:988-998

Siciliano, R. and F. Mola. (2000). Multivariate data analysis and modeling through classification and regression trees. Computational Statistics and Data Analysis 32: 285-301.

Simpson, J.R. and P. Evangelou eds. (1984). Livestock Development in Sub-Saharan Africa: Constraints, Prospects, Policy. Westview Press Boulder, CO

Sklar, F.H. and R. Costanza. (1990). The Development of Dynamic Spatial Models for Landscape Ecology: A Review and Prognosis. Quantitative Methods in Landscape Ecology M. G. and R. H. Gardner eds Turner. New York, NY: Springer.

Smaling, E. (1993). An Agro-Ecological Framework for Integrated Nutrient Management with Special Reference to Kenya. Waginingen: Landbouwuniversiteit te Wageningen. NETHERLANDS

Solomon, D., J. Lehmann and W. Zech. (2000). Land-use effects of soil organic matter properties of chromic luvisols in semi-arid northern Tanzania: carbon, nitrogen, lignin and carbohydrates. Agriculture, Ecosystems and Environment 78: 203-13.

Soule, M.J. and K.D. Shepherd. (2000). An Ecological and Economic Analysis of Phosphorus Replenishment for Vihiga Division, western Kenya. Agricultural Systems 64: 83-98.

Steinberg, D., and P. Colla. (1997). CART—Classification and regression trees. [Computer program]. Salford Systems, San Diego, CA.

Stocking, M. (1995). Soil Erosion in Developing Countries: Where Geomorphology Fears to Tread! Catena 25: 253-67.

Stolte, J., C.J. Ritsema and A.P.J. DeRoo. (1997). Effects of crust and cracks on simulated catchment discharge and soil loss. Journal of Hydrology 195: 279-290

Stoorvogel, J.J. and E.M.A Smaling. (1990). Assessment of soil nutrient depletion in Sub-Saharan Africa: 1983-2000 – Volume 1: Main Report. The Winand Staring Center, Wageningen, NETHERLANDS

Sudduth, K.A., and J.W. Hummel. (1993). Soil organic matter, CEC and moisture sensing with a portable NIR spectrophotometer. Transactions of the ASAE 36:185–193.

Sullivan, M., J.J. Warwick and S.W. Tyler. (1996). Quantifying and delineating spatial variations of surface infiltration in a small watershed. Journal of Hydrology 181:149-168

Survey of Kenya (1978). Belgut and Nyakach 1:50,000 topographic quadrangle maps. Ministry of Finance and Planning, Nairobi, KENYA

Sutherland, R.A. and R.B. Bryan. (1991). Sediment budgeting: A case study in the Katiorin drainage basin, Kenya. Earth Surface Processes and Landforms 16:383-398

Swallow, B.M., M.G. Walsh, F. Mugo, C. Ong, K. Shepherd, F. Place, A.Awiti, M. Hai, D. Ombalo, O. Ochieng, L. Mwarasomba, N. Muhia, D. Nyantika, M. Cohen, D. Mungai, J. Wangila, F. Mbote, J. Kiara and A. Eriksson. (2002). Improved land management in the Lake Victoria basin: Annual Technical Report July 2000 to June 2001. ICRAF Working Paper, Nairobi, KENYA

Swenson, J.J. and J. Franklin. (2000). The effects of future urban development on habitat fragmentation in the Santa Monica Mountains. Landscape and Urban Planning 55:79-93

Thomas, D.B. and W.M. Senga eds. (1983). Soil and Water Conservation in Kenya: Proceedings of a Second National Workshop. Institute of Development Studies, Nairobi, KENYA

Thomas, R.W. and R.J. Huggett. (1980). Modeling in Geography: A Mathematical Approach. Barnes and Noble Books, Totowa, NJ

Thompson, J. and J.N. Pretty. (1996). Sustainability Indicators and Soil Conservation: A Participatory Impact Study and Self-Evaluation of the Catchment Approach in the Ministry of Agriculture, Kenya. Journal of Soil and Water Conservation July-August: 265-73.

Tiessen, H.E. Cuevas and P. Chacon. (1994). The Role of Soil Organic Matter in Sustaining Soil Fertility. Nature 371: 783-5.

Tiffen, M., M. Mortimore and F. Gichuki. (1994). More People Less Erosion: environmental recovery in Kenya. John Wiley, Chichester NY.

Tilley, D.R. (1999). Emergy Basis of Forest Systems. PhD Dissertation, University of Florida. Gainesville FL

Turmbore, S. (2000). Age of Soil Organic Matter and Soil Respiration: Radiocarbon Constraints on Belowground Dynamics. Ecological Applications 10, no. 2: 399-411.

Turner, M.G. and R.H. Gardner (eds). (1990). Quantitative Methods in Landscape Ecology. New York, NY: Springer.

Ulgiati, S.M. and M.T. Brown. (1998). Monitoring patterns of sustainability of natural and man-made ecosystems. Ecological Modelling 108:23-36

Ulgiati, S., M.T. Brown, S. Bastianoni and N. Marchettini. (1995). Emergy-based Indices and Ratios to Evaluate the Sustainable Use of Resources. Ecological Engineering 5: 519-31.

Ulgiati, S., H.T. Odum and S. Bastianoni. (1994). Emergy Use, Environmental Loading and Sustainability: An Emergy Analysis of Italy. Ecological Modelling 73:215-68.

United Nations. (1996). Energy Statistics Yearbook 1996. United Nations.

United Nations Dept. of Economic and Social Affairs - Statistics Division. (1999). International Trade Statistics Yearbook 1997. New York.

United States Department of Commerce–National Oceanic & Atmospheric Administration. (1994). Tide Tables 1995 - Central and Western Pacific Ocean and Indian Ocean. Tide Table - High and Low Water PredictionsNOAA.

Urban, D.L. (2002). Classification and Regression Trees in Analysis of Ecological Communities, B. McCune and J.B. Grace, MjM Software Design, Gleneden Beach, OR

Uri, N.D. (2001). The Environmental Implications of Soil Erosion in the United States. Environmental Monitoring and Assessment 66:293-312

van Noordwijk, M., M. van Roode, E.L. McCallie and B. Lusiana. (1997). Erosion and Sedimentation as Multiscale Fractal Processes: Implications for Models, Experiments and the Real World. Soil Erosion at Multiple Scales: Principles and Methods for Assessing Causes and Impacts F. W. T. F. Agus and J. Kerr Penning de Vries. Wallingford, UK: CABI Publishing.

van Oost, K., G. Govers and P. Desmet. (2000). Evaluating the effects of changes in landscape structure on soil erosion by water and tillage. Landscape Ecology 15: 577-89.

Van Rompaey, A.J.J. and G. Govers. (2002). Data quality and model complexity for regional scale soil erosion prediction. International Journal of Geographical Information Science 16:663-680

Veldkamp A. and E.F. Lambin. (2001). Predicting land-use change. Agriculture, Ecosystems and Environment 85:1-6

Venables, W.N. and B.D. Ripley. (1999). Modern Applied Statistics with S-Plus. Springer Texts in Statistics and Computing, New York, NY

Verburg, P.H., G.H.J. De Koning, K. Kok, A. Veldkamp, and J. Bouma. (1999). A spatial explicit allocation procedure for modelling the pattern of land use change based upon actual land use. Ecological Modelling 45:16-41

Villa, F. and R. Costanza. (2000). Design of multi-paradigm integrating modelling tools for ecological research. Environmental Modelling and Software 15: 169-77.

Walpole, S.C. and J.A. Sinden. (1997). BCA and GIS: Integration of economic and environmental indicators to aid land management decision. Ecological Economics 23:45-57

Walsh, S.J., D.R. Butler and G.P. Malanson. (1998). An overview of scale, pattern, process relationships in geomorphology: a remote sensing and GIS perspective. Geomorphology 21: 183-205.

Weller, D.E., T.E. Jordan and D.L. Correl. (1998). Heuristic Models for Material Discharge from Landscapes with Riparian Buffers. Ecological Applications 8, no. 4: 1156-69.

West, T.O. and M.K. Wali. (2002). Modeling regional carbon dynamics and soil erosion in disturbed and rehabilitated ecosystems as affects by landuse change and climate. Water, Air and Soil Pollution 138:141-164

Wielemaker, W.G. and H.W. Boxem. (1982). Soils of the Kisii Area. Kenya Soil Survey, Ministry of Agriculture, Nairobi, KENYA

Williams, J.R., P.T. Dyke, and C.A. Jones. (1983). EPIC – a model for assessing the effects of erosion on soil productivity in The Third International Conference on State of the Art in Ecological Modelling. Elsevier, Amsterdam, NETHERLANDS

Willams, S.B. (1999). Evaluation of watershed control of two Central Florida lakes: Newnans Lake and Lake Weir. PhD Dissertation, University of Florida. Gainesville FL

Wilson, J.P. and J.C. Gallant. (1996). EROS: A Grid-Based Program for Estimating Spatially-Distributed Erosion Indices. Computers and Geosciences 22: 707-12.

Wischmeier W.H. and D.D. Smith. (1978). Predicting rainfall erosion losses: a guide to conservation planning. USDA Agricultural Handbook No. 537, Washington DC

World Bank. (1996). African Development Indicators. World Bank, Washington, DC.

Zech, W., N. Senesi, G. Guggenberger, K. Kaiser, J. Lehmann, T.M. Miano, A. Miltner and G. Schroth. (1997). Factors controlling humification and mineralization of soil organic matter in the tropics. Geoderma 79: 117-61.

Zhu, T.X., L.E. Band and R.A. Vetessey. (1999). Continuous Modeling of Intermittent Stormflows on a Semi-Arid Agricultural Catchment. Journal of Hydrology 226: 11-29.

Ziegler, A.D., R.A. Sutherland and T.W. Giambelluca. (2001). Accelertation of Horton overland flow and erosion by footpaths in an upland agricultural watershed in northern Thailand. Geomorphology 41:249-262

Zobisch, M. A. (1993). Erosion Susceptibility and Soil Loss on Grazing Lands in some Semi-Arid and Subhumid Locations of Eastern Kenya. J. Soil and Water Conservation 48, no. 5: 445-8.

Zobisch, M.A., C. Richter, B. Heiligteig and R. Schlott. (1995). Nutrient Losses from Cropland in the Central Highlands of Kenya due to surface runoff and soil erosion. Soil and Tillage Research 33: 109-16.

BIOGRAPHICAL SKETCH

Matthew Jarumi Cohen was born in Zaria, Nigeria on December 17, 1973. Matt has a Bachelor of Science degree with distinction in engineering and a concentration in environmental science from Swarthmore College. He earned his Master of Engineering in Environmental Engineering Sciences with a concentration in Systems Ecology at the University of Florida in 1999. He was awarded the CDM Fellowship, and received research awards from ICRAF, USDA and USAID for his doctoral research. The research was done in collaboration with the International Center for Research in Agroforestry (ICRAF) in Kisumu, Kenya. His ongoing research interests include integrated emergy-based decision support, watershed-scale empirical characterization using digital imagery and reflectance spectroscopy, and systems/spatial modeling.

I certify that I have read this study and that in my opinion it conforms to acceptable standards of scholarly presentation and is fully adequate, in scope and quality, as a dissertation for the degree of Doctor of Philosophy.

Mark T. Brown, Chair
Associate Professor of Environmental Engineering Sciences

I certify that I have read this study and that in my opinion it conforms to acceptable standards of scholarly presentation and is fully adequate, in scope and quality, as a dissertation for the degree of Doctor of Philosophy.

William R. Wise
Associate Professor of Environmental Engineering Sciences

I certify that I have read this study and that in my opinion it conforms to acceptable standards of scholarly presentation and is fully adequate, in scope and quality, as a dissertation for the degree of Doctor of Philosophy.

Thomas L. Crisman
Professor of Environmental Engineering Sciences

I certify that I have read this study and that in my opinion it conforms to acceptable standards of scholarly presentation and is fully adequate, in scope and quality, as a dissertation for the degree of Doctor of Philosophy.

Michael W. Binford
Professor of Geography

I certify that I have read this study and that in my opinion it conforms to acceptable standards of scholarly presentation and is fully adequate, in scope and quality, as a dissertation for the degree of Doctor of Philosophy.

Keith D. Shepherd
Senior Consultant: Systems Agronomist, Natural Resources Strategies in Policy Programme, International Centre for Research in Agroforestry (ICRAF), Nairobi KENYA

This dissertation was submitted to the Graduate Faculty of the College of Engineering and to the Graduate School and was accepted as partial fulfillment of the requirements for the degree of Doctor of Philosophy.

August, 2003

Pramod P. Khargonekar
Dean, College of Engineering

Winfred M. Phillips
Dean, Graduate School